IL
NUOVO CIMENTO
ORGANO DELLA SOCIETÀ ITALIANA DI FISICA
SOTTO GLI AUSPICI DEL CONSIGLIO NAZIONALE DELLE RICERCHE

VOL. XIV, N. 5 *Serie decima* 1° Dicembre 1959

Analysis of a High Energy Nuclear Interaction in Emulsion Chamber.

S. HASEGAWA

Institute for Nuclear Study - Tokyo

(ricevuto il 9 Febbraio 1959)

Summary. — A high energy jet shower of primary energy exceeding 10^{14} eV found in emulsion chamber is fully analysed. The distribution of the transverse momentum of secondary π^0-mesons is measured and the mean value of 450 MeV/c is obtained. The emission angle dependence of the transverse momentum of decayed γ-rays of π^0-mesons is examined by different two methods, and appreciable change of the transverse momentum by the emission angle can not be found. The angular distributions of both charged secondary and π^0-meson is compared and no noticeable change is found. The cascade shower function in the emulsion chamber in the early stage of the development of the cascade shower is constructed experimentally for the purpose of the energy determination of the decayed γ-ray of the π^0-meson. Finally, the feature of the total structure function with many different γ-ray sources is studied, and, from this analysis, the energy converted to soft component of the jet shower and the average multiplicity of the γ-rays can be determined.

1. – Introduction.

The high energy nuclear collisions have so far been investigated with special regard of the peculiar properties of high energy phenomena and the structure of the nucleon, etc. Since the importance of the transverse momentum of secondary particles of jet showers for the detailed study of the multiple meson

production has been pointed out by J. NISHIMURA (1), much systematic investigations on the high energy jet showers by means of nuclear emulsions have been reported revealing many interesting features of high energy jet showers.

Our preceding paper (2) is the one in which were reported the procedures and results of the extensive co-operative experiment in Japan in 1956 on the observation of high energy jets of the primary energy ranging from 10^{12} eV to 10^{14} eV. The emulsion chambers were specially designed and constructed in order to measure the transverse momentum of π^0-mesons of the jets with high precision. The spectrum of the transverse momentum was studied, and the results were briefly summarized as follows. The spectrum of the transverse momentum has a rather narrow distribution having a maximum at around 400 MeV/c with the width of about 200 MeV/c. No noticeable change of transverse momentum due to the difference of the primary energy or the energy of the emitted π^0-meson can be found, and no appreciable variation of the transverse momentum for the individual shower is found beyond the statistical fluctuations. These experimental results permit us to make many interesting analyses of the detailed dynamics of multiple meson production, such as direct connection of the angular distribution with the energy spectrum of the secondary particles of the jet.

Another extensive study on this line is the one of the Bristol (3) group. They studied jet showers in large emulsion stacks with the traditional method of measurement. The experimental results on π^0-mesons of the Bristol group do not contradict with ours in spite of different experimental methods.

In spite of these analyses, it seems desirable further to study many other problems such as the angular variation of the transverse momentum, the production ratio of neutral pions to charged secondaries, and the difference of the angular distribution of produced π-mesons and other heavy particles.

Another problem is the possible difference (*) between the collision features of the extremely high energy collisions and of the rather low energy region of the primary energy, say from 10^{12} eV to 10^{14} eV, which has been hitherto systematically investigated in the nuclear emulsions.

---

(1) J. NISHIMURA: *Soryushiron Kenkyu* (in Japanese), **12**, 24 (1956); Z. KOBA: *Proc. of the VI-th Rochester Conference* (1956), p. IV-43.

(2) O. MINAKAWA, Y. NISHIMURA, M. TSUZUKI, H. YAMANOUCHI, H. AIZU, H. HASEGAWA, Y. ISHII, S. TOKUNAGA, Y. FUJIMOTO, S. HASEGAWA, J. NISHIMURA, K. NIU, K. NISHIKAWA, K. IMAEDA and M. KAZUNO: *Suppl. Nuovo Cimento*, **11**, 112 (1959).

(3) B. EDWARDS, J. LOSTY, D. H. PERKINS, K. PINKAU and J. REYNOLDS: *Phil. Mag.*, **3**, 237 (1958).

(*) S. N. NIKOL'SKII *et al.*: *Oxford Conference* (1956). They investigated the hard component in the air shower and found some suggestions for the discontinuity of the collision feature at the energy exceeding about 10^{15} eV of the primary energy of the air shower, though the unresolved questions are left.

The high energy event is expected to reveal some such properties more distinctly.

Recently, a few extremely high-energy events exceeding about 10^{14} eV of the primary energy of the jet found in the emulsion stacks have been reported by many groups ([4-7]). The analysis of the event for the problems that are mentioned above seems rather unsatisfactory. In these analyses, the energy determination of γ-rays from π^0-mesons is made by the use of the relation of the opening angle of the electron pairs and by the cascade shower in the very beginning stage of its development, thus the precision does not seem to be enough. If the multiplicity of the secondary particles was very large, as is expected if we let go highest energy event further, the difficulty for the clear research of the secondary particles of the jet on the problem above mentioned seems to be very deep-rooted. The emulsion chamber specially designed seems to offer a very promising clue for the research of the extremely high energy nuclear collisions as shown in the following.

A high energy nuclear collision, the event S.H.1, was found in our emulsion chamber. This is the nuclear collision of an incident high energy proton exceeding 10^{14} eV on the carbon target. The usual half-angle method and the method of the energy balance used by the Bristol group in the statistical manner fix the primary energy of the jet to about $2 \cdot 10^{14}$ eV.

Because of the high energy and a large multiplicity of the secondaries of the event S.H.1, the systematic study of the details of the jet is possible.

The angular distributions of both the charged secondaries and π^0-mesons are studied. What especially attracts our attention is whether there exists any difference between the angular distribution of these particles or not. The energy determinations of π^0-mesons and the decayed γ-rays of π^0-mesons are made by a similar device as in our previous paper ([2]), and the spectrum of the transverse momentum of π^0-mesons is obtained. The spectrum is similar to that of our preceding paper, having a mean value of about 450 MeV/c, and no appreciable angular variation is found for the transverse momentum of π^0-mesons. The production ratio of neutral pions to charged secondaries and it's angular variation is studied.

Finally, in the Appendix II, the feature of the structure function of the cascade shower with many γ-ray sources is studied; and from this analysis the

---

([4]) P. H. Fowler: *Seventh Rochester Conf. on High Energy Nuclear Physics* (1957).

([5]) P. Ciok, M. Danysz, J. Gierula, A. Jurak, M. Miesowicz, J. Pernegr, J. Vrana and W. Wolter: *Nuovo Cimento*, **6**, 1409 (1957).

([6]) I. M. Gramenitskii, G. B. Zhdanov, E. A. Zamchalova and M. N. Scherbakova: *Journ. Exper. Theor. Phys.*, **5**, 763 (1957).

([7]) S. Tokunaga and K. Nichikawa: private communication. We are much indebted to them for sending us their experimental data before publications.

3815

energy converted to these π^0-mesons is estimated to be $(0.8 \div 1.6) \cdot 10^{13}$ eV, which is consistent with that obtained by another method. This method is similar to that used for the analysis of the structure of the soft component of air showers and seems to be applicable to the energy determination of high energy jet showers.

2. – Analysis of the event.

2·1. *Description of the event.* – The event S.H.1 was found in the course of general shower scanning in the emulsion plates just beneath the third lead plate in the type *B* chamber. The chamber is made of two parts and each part consists of 7 carbon plates 8 mm thick and 3 lead plates 5 mm thick with 200 μm G-5 emulsion plates under every carbon and lead plate. In Fig. 1, the details of this chamber are shown together with the position and a schematical picture of this event. A large nuclear interaction occurred in the third carbon plate, and many tracks of the secondary

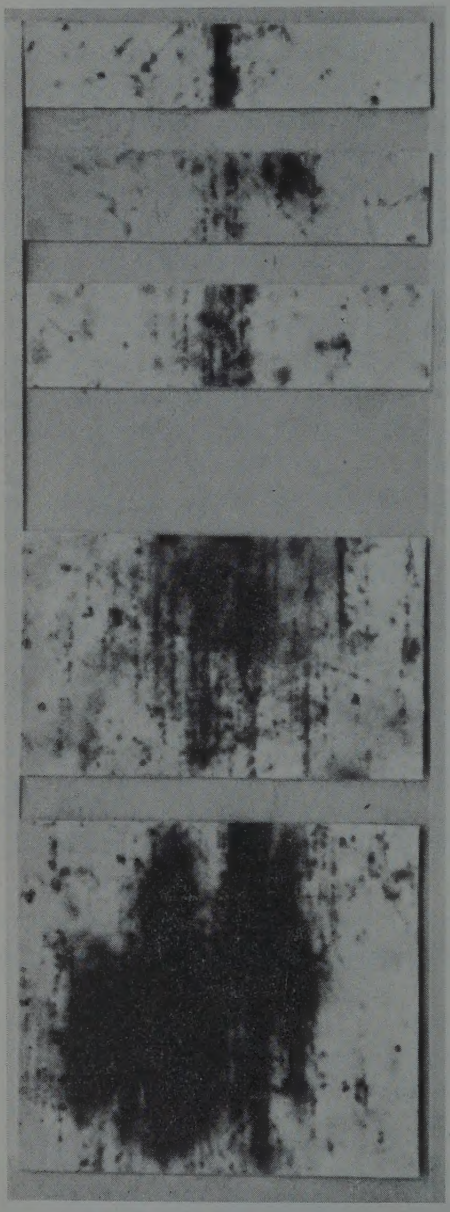

Fig. 1. – The emulsion chamber and the schematic picture of the event S.H.1.

particles are observed in the emulsion plate just below. This bundle of tracks of secondary particles can be followed in successive emulsion plates, and the zenith angle of the shower axis is found to be about 20 degrees. The γ-rays start to develop into the cascade shower in the lead plates after passing the carbon plates and the empty space without materialization. 20 separate cascade cores are observed under the last lead plate, where the shower contains as a whole about two hundred tracks.

In the lower carbon plates under three lead plates, the cascade showers developed by separate γ-rays begin to suffer angular divergence and mix up with each other so that the showers do not show a clear multicore structure, and they bear some resemblance to the structure of an extensive air shower.

In the following section, the results obtained from these different kinds of observation are discussed.

2·2. *The primary particle of the jet and the angular distribution of the charged secondaries.* – 44 tracks of the charged secondaries are followed in the first three emulsion plates placed between the carbon plates. Among these thirteen are emitted in a very collimated forward cone of about $5 \cdot 10^{-4}$ radian, so that they can not be well separated in the first two emulsion plates. They are separated only in the third emulsion plate, just 2.45 cm away from the origin of the jet containing 13 tracks.

Some secondaries emitted in the wide diffuse cone are unlikely to be observed

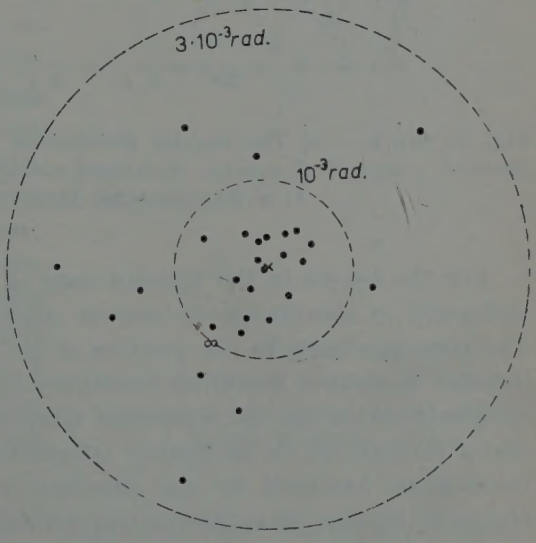

Fig. 2. – The target diagram of 37 tracks of charged secondary particles in the forward cone. • charged secondary; ∞ electron pair; × centre of gravity of the charged particle for the forward cone.

because their tracks are hard to be distinguished without ambiguity from the general background.

From the following-through of the above 44 secondary tracks in successive emulsions, the position of the origin of the jet can be determined within a precision of 1 mm. The primary particle is searched for in the corresponding region of the plate just above, and the possibility of a primary particle being a heavy nucleus is excluded.

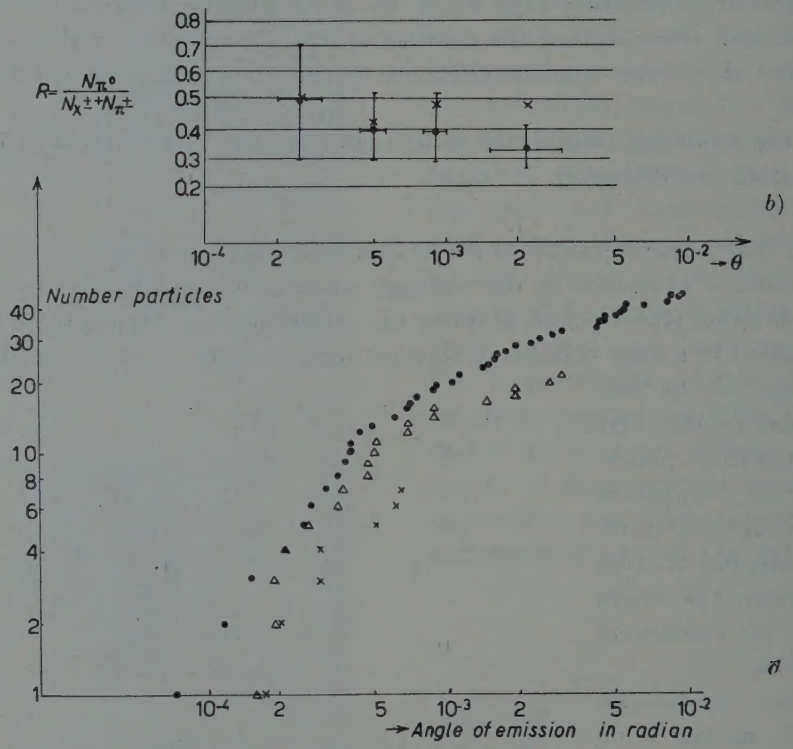

Fig. 3*a* and *b*. – *a*) The angular distribution of charged secondaries, π^0-mesons and decayed γ-rays of π^0-mesons. ● charged secondaries; × π^0-mesons; △ decayed γ-rays. *b*) ● Experimental data; × corrected value.

For the tracks in the forward cone of angle $* \cdot 10^{-2}$ radian, there is no ambiguity in identifying the shower tracks from general background tracks. The correspondence in the position of the tracks is examined plate by plate in order to observe a possible secondary interaction in the carbon plates, and no identification for the secondary interaction is observed. In the emulsion plates themselves, no secondary interaction is found either. The secondary interactions produced by the particles in the diffuse cone are hard to be observed, because these interactions will take place at low energy and if they

exist, the secondary particles diverge and can not be distinguished from other general background.

The possibility of the occurrence of the secondary jet in their passing through the carbon plates of 1.7 cm is estimated as 0.056 assuming the interaction mean free path of the high energy nucleon and pion as 60 g/cm². Thus the above negative result does not show a contradiction with this expectation.

One electron pair is found to originate in the second carbon plate. The angular distribution is obtained from the target diagram of the shower tracks assuming their centre of gravity as the shower axis. In Fig. 2, and Fig. 3, the target diagram and the angular distribution of the secondary charged particles are shown. The forward collimated region of the angular distribution seems to fit the type of the spectrum $1/\theta \cdot \theta \mathrm{d}\theta$, which is discussed in our previous analysis ([8]).

2·3. *The secondary π^0-mesons and the decayed γ-rays from the π^0-mesons.*

2·3.1. Energy determination of γ-rays and π^0-mesons. – The γ-rays from the secondary π^0-mesons start to develop the cascade multiplication in the lead layers. In the cascade showers 20 cores are observed, most of which have energy exceeding about $5 \cdot 10^{10}$ eV. The cores of lower energy are likely to be missed because they are diffuse and will be at a large distance from the centre. The probability of penetration of γ-rays in three lead plates without materialization is evaluated in this case at about 7%, so that most of the high energy γ-rays of the π^0-mesons are materialized and only few will escape observation. Since the γ-rays pass through the carbon plates and the empty space before their materialization in the lead plates, the spacial separation between the cores is larger than the dimension of the cores. The target diagram of each 20 γ-ray core is constructed, and in Fig. 4 the diagram just beneath the third lead plate 6.7 cm apart from the origin

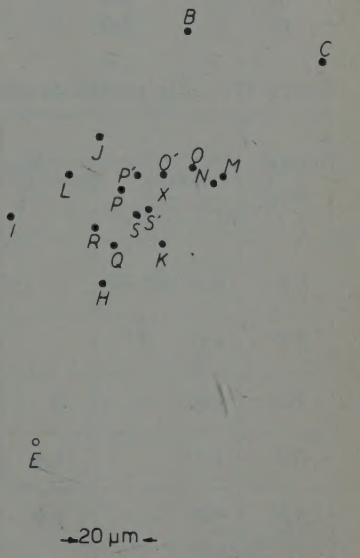

Fig. 4. – Target diagram of decayed γ-rays at 6.7 cm from the jet origin. × Energy weighted centre.

([8]) S. HASEGAWA, J. NISHIMURA and Y. NISHIMURA: *Nuovo Cimento*, **6**, 979 (1957).

TABLE I. – *Energy of γ-rays determined from cascade shower and value of transverse momentum.*

γ-ray	Energy (10^{11} eV)	Distance from the shower axis (μm)	Angle (rad)	$P_{T\gamma}$ (10^8 eV/c)
A	1.0	180	$28 \cdot 10^{-4}$	2.80
B	3.0	100	15.5	4.65
C	0.4	130	20	0.80
D	0.7	360	56	3.92
E	0.9	130	20	1.80
H	3.0	60	9.4	2.82
I	3.0	60	9.4	2.82
J	3.0	45	7.1	2.13
K	5.0	23	3.6	1.80
L	5.0	45	7.1	3.55
M	2.0	45	7.0	1.40
N	10.0	32	5.0	5.00
O	5.0	30	4.3	2.15
O'	7.0	17	2.6	1.82
P	6.0	14	2.2	1.32
P'	6.0	12	1.8	1.08
S	(3.0)	10	1.5	2.25
S'	(3.0)	12	1.8	2.70
R	2.0	30	4.7	0.94
Q	3.0	24	37.5	1.13

TABLE II. – *The reliable coupling of $\pi^0 \to 2\gamma$ decay and the value of transverse momentum.*

Coupling	Energy	$n = \frac{E_{\gamma_2}}{E_{\gamma_1}}$	r_{obs} (μm)	r_{exp} (μm)	$\frac{r_{obs}}{r_{exp}}$	R_μ (from the shower axis)	Angle (rad)	$P_{T\pi^0}$ (MeV/c)
SS'	$3.0 \cdot 10^{12}$ eV		11			11	$1.65 \cdot 10^{-4}$	480
PP'	3.0		12			12	1.8	540
MN	1.5	5	13	20	0.65	35	5.2	750
OO'	1.1	1.4	18	16	1.05	20	3.0	300
RK	0.5	2.5	38	27	1.40	20	3.0	150
QH	0.45	1.0	42	32	1.30	50	75	340
JL	0.7	1.7	32	25	1.25	47	73	510

The average value of the transverse momentum of produced π^0-mesons, $\overline{P}_{T\pi^0}$, is calculated as 440 MeV/c.

of the jet is presented. The test of convergency of the direction of each γ-core to the jet origin is studied examining their position in two different plates, and 19 γ-rays out of 20 are confirmed as the ones from the primary jet. The energy of each γ-ray is determined by counting the number of cascade electrons within a circle of certain radius from the centre of the core and comparing it with the theoretical transition curves. The theoretical curve is obtained by the cascade shower theory without Landau approximation (9), and furthermore it is calibrated experimentally comparing with the value of the track length of some cascade showers of known energy found in our emulsion chambers. (See Appendix I). There are only three cascade units of lead for our shower, so that all of the cascade cores remain still at the early stage of their development. The effect of the fluctuation in shower development is known to be quite large at the early stage of the development, so the error of our energy determination is estimated at about a factor 2. The results are shown in Table I.

Another check for the energy determination of the γ-rays is made by using the kinematical relation between the energy and the opening angle of π^0-2γ decay. The relation is expressed by

$$(1) \quad \theta_{2\gamma} = \frac{\gamma}{L} = \frac{m_{\pi_0} C^2}{\sqrt{E_{\gamma 1} E_{\gamma 2}}} = \frac{m_{\pi_0} C^2}{E_{\pi_0}} \left(\sqrt{n} + \frac{1}{\sqrt{n}} \right),$$

where $n = E_{\gamma 1}/E_{\gamma 2}$, r is the separation between two corresponding cascade showers measured in the last emulsion

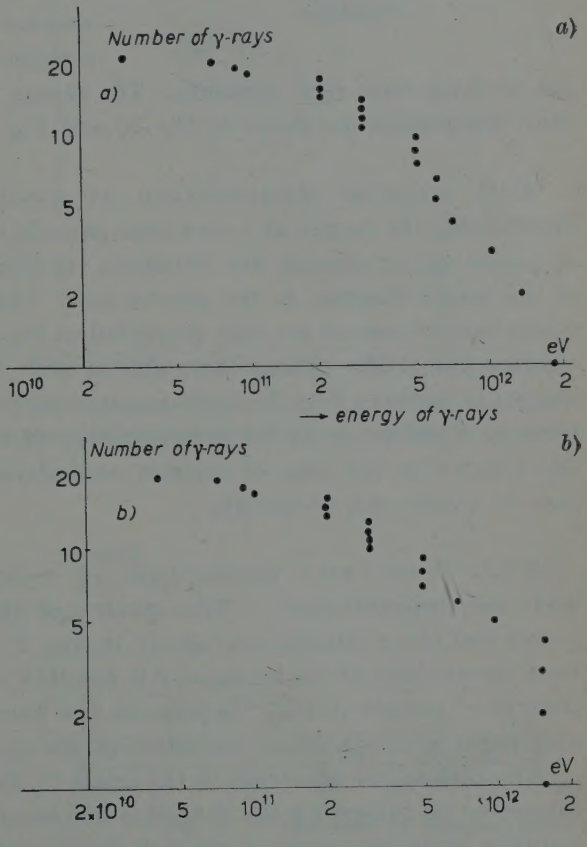

Fig. 5. – Integral energy spectrum of the γ-rays. *a*) Determination of energy by the cascade shower. *b*) Determination of energy by the possible coupling into π^0-mesons.

(9) See reference (2); K. KAMATA and J. NISHIMURA: *Suppl. Progr. Theor. Phys.*, **6**, (1958).

plate, and L is the distance from the point of the jet to this plate. $\theta_{2\gamma}$ is the opening angle of the decayed γ-rays of a π^0-meson.

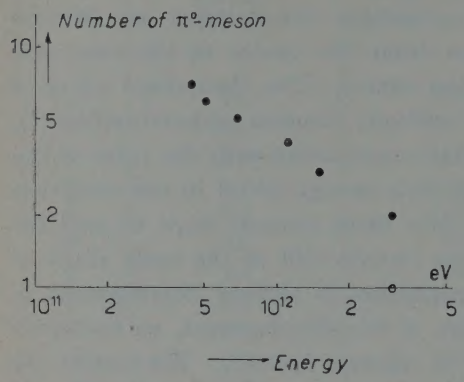

Fig. 6. – Integral energy spectrum of π^0-mesons.

Using the observed values of L, $E_{\gamma 1}$, and $E_{\gamma 2}$, the separation, r, is estimated from this formula (1). The ratio of the calculated separation, r_{calc}, to the observed one, r_{obs}, is the measure of the possible coupling. In Table II, the most reliable couplings are listed. The result is good enough to conclude that there is no miscoupling. The cascade showers S, S' and P, P' have the highest energy cores, and the couplings SS' and PP' are the most reliable ones. 14 γ-rays out of 20 γ-rays are thus coupled into 7 π^0-mesons. For other γ-rays, belonging to a rather diffuse cone, the coupling can not be made with such certainty. The energy spectra of γ-rays and π^0-mesons thus determined are shown in Fig. 5, and Fig. 6 respectively.

2·3.2. Angular distribution of γ-rays and π^0-mesons. – After determining the energy of γ-rays from cascade showers the angular distribution of γ-rays and π^0-mesons are obtained, regarding the energy weighted centre of the target diagram as the shower axis. The angular distributions of both γ-rays and π^0-mesons are also presented in Fig. 3. Comparison of the angular distribution of the charged secondaries with that of the soft component of the jet is made in Fig. 3. Both angular distributions appear similar, though there is a difference in the determination of the shower axis, weighted with the number in the case of charged secondaries and with the energy in the case of γ-rays and π^0-mesons.

2·3.3. Transverse momentum of γ-rays and π^0-mesons and its angular dependence. – The spectra of the transverse momenta of the γ-rays and the π^0-mesons are shown in Fig. 7. The mean value of the transverse momentum of the π^0-mesons is 450 MeV/c. The dashed line of the spectrum of π^0-mesons in Fig. 7 represents the normalized spectrum of our preceding paper after statistical correction of the shower axis of the jets.

The lack of the spectrum in the small P_T value of γ-rays, however, is considered to be caused by the detection efficiency for the cascade shower of our emulsion chamber, because the flat distribution from nearly zero energy for the decayed γ-rays of fast π^0-mesons is predicted by the kinematical relation of the π^0-2γ decay. We next test the angular variation of the transverse

momentum. The relation between the transverse momentum of the γ-rays and their production angles is shown in Fig. 8. No noticeable change can be found within the limits of the error of measurement. For the test of the angular variation of the transverse momentum we can further consider the following analysis. If the transverse momentum of the γ-rays is independent from the angle, and the relation $\theta = \bar{P}_{T\gamma}/P$ holds statistically, the angle and the energy of the γ-rays are inversely proportional. Then the slope of the spectrum of one jet with turned-over scale must coincide with that of the other. The result of this test is shown in Fig. 8. Both spectra agree well within the limits of the errors

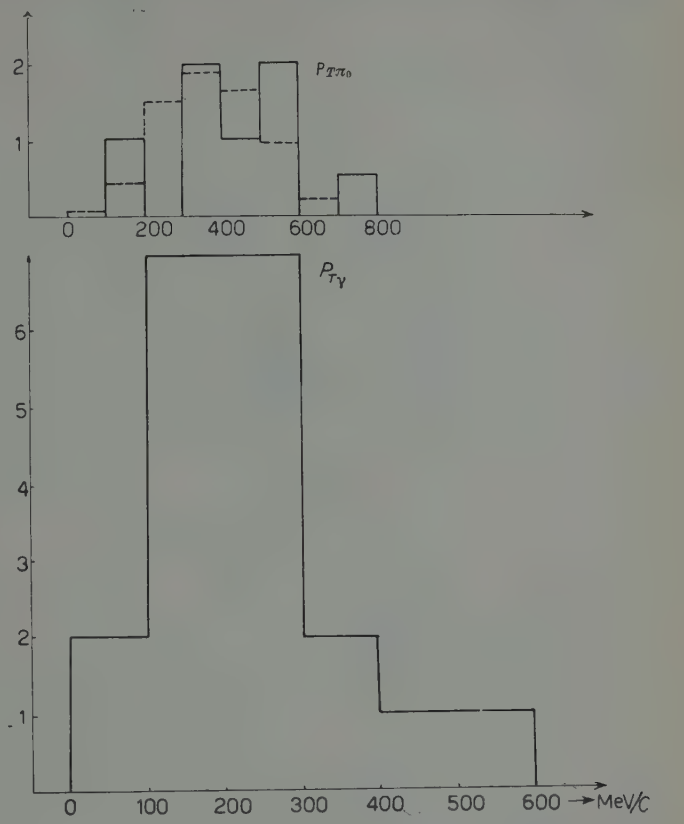

Fig. 7. – Distributions of $P_{T\pi_0}$ and $P_{T\gamma}$ $P_{T\pi^0}$ dashed line represent the normalized experimental data of our previous paper.

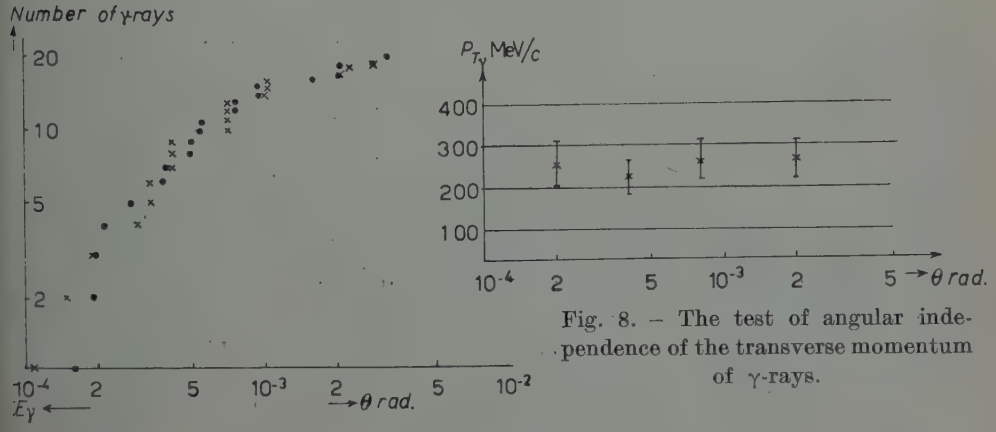

Fig. 8. – The test of angular independence of the transverse momentum of γ-rays.

of measurement. This fact confirms also the independence of the transverse momentum from the angle.

2·3.4. Production ratio of neutral pion to charged secondaries and its angular variation. – The angular variation of the ratio of the produced π^0-meson to the charged secondaries is investigated in the intervals of small angle regions, as shown in Fig. 4. Both the experimental and the corrected values, with the detection efficiency of the emulsion chamber taken into consideration, are plotted. No appreciable angular variation is found. This means that the angular distribution of π^0-mesons seems to be similar to that of heavy particles other than π^0-mesons. The conclusion, however, must be drawn after better statistics will be available.

The experimental value of the ratio of charged secondaries to neutral pions without any correction inside the region of the angle of $7\cdot10^{-4}$ radian, where $(1/\theta)\theta\,\mathrm{d}\theta$ for the spectrum of angular distribution of both kinds of particles seems to hold, is

$$R = \frac{N_{\pi^0}}{N_{\chi^\pm} \pm N_{\pi^\pm}} = 0.44 \pm 0.09 .$$

Comparison with the data obtained by other groups will be made later.

2·4. *Energy estimation of the primary particles.* – From the target diagram and the angular distribution of the charged secondaries, it is estimated that the half-angle of this jet is about $3\cdot10^{-3}$ radian, containing 30 tracks, though the ones which diverge in the very diffuse cone are not all picked up. In an usual half-angle method, assuming the forward-backward symmetry in the centre of mass system of the produced particles in a nucleon-nucleus collision, the primary energy of this event is estimated at about $E_0 \simeq 2\cdot10^{14}$ eV.

Next we consider the energy balance from the knowledge of the secondary particles. The total energy converted to π-meson component is $4.8\cdot10^{13}$ eV if we assume the charge independence of the π-meson. The residual energy is considered to be converted into heavy particles other than pions. From the angular distributions of both the charged secondaries and the soft component of the jet, two or three particles from the top end of the angular distribution of the charged particles are considered to be other particles than pions. This is also derived from the charge-neutral ratio in the forward collimated region as stated in the preceding section. We use the transverse momentum 1.8 BeV/c for these particles, as the Bristol group did and we take into account the same energy of neutral particles, and then we get the energy for these particles as 8.10^{13} eV $\sim 10^{14}$ eV.

Thus the following relation holds

$$E_0' = E_0 - E_{\pi^{\pm,0}} - E_{K^{\pm,0}} = 7\cdot10^{13}\ \mathrm{eV} \sim 5\cdot10^{13}\ \mathrm{eV} .$$

This amount of energy can be considered to be either the energy of the survivor of the incident nucleon or the incorrect estimation of E_0.

Another method of energy balance is the one used by the Bristol group. In our case the energies converted to $\pi^{\pm,0}$ and $X^{\pm,0}$ are,

$$E_{\pi^0} = 1.6 \cdot 10^{13} \text{ eV},$$

$$E_{\pi^\pm} = \sum P_{T\pi}/\theta_i = 3.1 \cdot 10^{13} \text{ eV},$$

and

$$E_{\chi^{\pm,0}} = \sum \bar{P}_T \chi^{\pm,0}/\theta_i = 1.3 \cdot 10^{14} \text{ eV},$$

where 20% of the particles from the top end of the angular distribution are considered to be heavy particles which have the average transverse momentum $\bar{P}_{T\chi^{\pm,0}} \simeq 1.8$ GeV/c. $\bar{P}_{T\pi}$ is the transverse momentum of the π-meson and is adopted as 400 MeV/c, the same as the π^0-mesons in reference [2]. Thus the total energy is given as,

$$E_{\pi^{\pm,0}} + E_{\chi^{\pm,0}} = 1.77 \cdot 10^{14} \text{ eV}.$$

This seems to give a rather good energy balance, but a great difficulty arises with respect to the experimental results of the angular distribution of the secondary particles. A clear conclusion, however, for this problem can not be derived from this single event.

3. – Discussions and summary.

A high energy jet shower, the event S.H.1, is fully analyzed, and the experimental results are summarized as follows.

3·1. *The angular distributions of the secondary particles.* – The angular distribution and the multiplicity of the charged secondaries of the jets have so far been studied most frequently in nuclear emulsions. As well known, the angular distribution and the multiplicity of the high energy jet fluctuate from event to event being followed by the so-called inelasticity of the event. The systematic study, however, of the angular distribution of the jet has been made specially in the smallest angle region of the spectrum [8]. The angular distribution in this small angle region is interesting and important in the dynamical study of the multiple meson production. First, because the highest energy part of the produced particles is contained in this region and well represents the characteristic features of the meson production in nucleon-nucleon collisions as

shown in the tunnel model or in the composite model ([10-12]). Secondly, because the shape of the angular distribution is approximately invariant under the Lorentz transformation from the Laboratory system to the centre of mass system.

The $(1/\theta)\cdot\theta\,\mathrm{d}\theta$ angular distribution was confirmed. This event shows this type of angular distribution of the charged secondaries in the smallest angle region, in spite of its high energy exceeding the energy region of the jets analysed in our previous paper, say from 10^{12} eV to several times 10^{13} eV. The high energy α-primary jets of the Warsaw group ([5]) and the Soviet group ([6]) also show $(1/\theta)\cdot\theta\,\mathrm{d}\theta$ angular distribution in the forward cone. On the other hand, the Bristol group found this distribution statistically in the collected charged secondaries.

Another kind of problem arises in the difference of the angular distribution between the π-meson and the heavy particles other than π-mesons, that is the examination of the angular variation of the production ratio of π^0-mesons to that of charged secondaries. This problem is of importance because of what it comprizes in connection with the detailed study of high energy nuclear collisions, and is studied in the emulsion chamber just by comparing the angular distribution of the π^0-mesons and the charged secondaries. As shown in Section 2·3, the angular distribution of both kinds of particles has almost the same shape in the smallest angle region.

3·2. *Transverse momentum.* – In our preceding paper, the spectrum of the transverse momentum has been obtained using about 20 jet showers of primary energy ranging from several times 10^{12} eV to about 10^{14} eV. In this primary energy range, a possible dependence of the transverse momentum on either the primary energy or on the energy of π^0-mesons was investigated in statistical manner. Furthermore, a possible difference in the distribution of the transverse momentum in each individual shower was also examined. This event is a good sample for these studies because of the considerable high energy and the high multiplicity of the event. A systematic study is possible in this single event. The average value of the transverse momentum of the π^0-meson is about 450 MeV/c, and the spectrum of the transverse momentum is the same as the one in our preceding paper within the limits of statistical fluctuation.

Another important examination is a possible dependence of the transverse momentum on the emission angle of the π^0-mesons, and it is made in this event using γ-rays in the small angle ranges. The results show no appreciable change

---

([10]) F. C. Roesler and C. B. A. McCusker: *Nuovo Cimento*, **10**, 127 (1953).
([11]) G. Cocconi: *Phys. Rev.*, **93**, 1107 (1954).
([12]) Y. Terashima: *Progr. Theor. Phys.*, **13**, 1 (1955).

with respect to the angle of emission. This was examined also in this event using both the spectrum of energy and the angular distribution of γ-rays, as stated in the preceding Section, and is shown in Fig. 8. These results are very important for the study of many dynamical properties of the jet.

3·3. *Energy spectrum of secondary π^0-mesons.* – As in Fig. 5, and Fig. 6, the shape of the energy spectrum of γ-rays and π^0-mesons is approximately represented by $(1/E^2)\,\mathrm{d}E$. The result coincides with that derived using the angular distribution of π^0-mesons, $(1/\theta)\cdot\theta\,\mathrm{d}\theta$ and the angle independence of the transverse momentum. This spectrum is also confirmed by the Bristol group.

3·4. *Angular distribution of the energy flow converted to π^0-mesons.* – The $(1/\theta^2)\cdot\theta\,\mathrm{d}\theta$ distribution seems to fit the experimental curve, and this is the direct conclusion from the angular distribution of π^0-mesons, $(1/\theta)\cdot\theta\,\mathrm{d}\theta$, and the angle independence of the transverse momentum, that is $E \propto \mathrm{const}/\theta$.

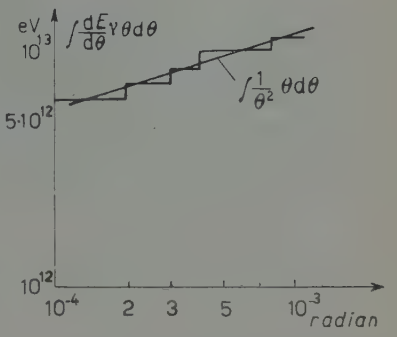

Fig. 9. – Angular distribution of the energy flow converted into π^0-mesons.

3·5. *Production ratio of neutral pion to charged secondary.* – The determination for this ratio is of importance of its implications with respect to the heavy meson production at high energy, and it has deep connection with the nucleon structure and the collision feature. This has been studied by many groups on the event of primary energy ranging from $*\cdot10^{11}$ eV to $*\cdot10^{13}$ eV in the emulsion stacks ([13-16]). The most extensive research of this ratio is that of the Bristol group ([3]). They measured this ratio by the method which has been widely used in ordinary emulsion stacks, that is by comparing the relative numbers of charged shower particles with electron pairs. They found $R = 0.40 \pm 0.04$ in the research of the inner cone of the jet showers.

Furthermore, they divided the events in two groups, in the one are the jets of high multiplicity, $n_s > 22$, and in the other are those of low multi-

([13]) R. R. Daniel, J. H. Davies, J. H. Mulvey and D. H. Perkins: *Phil. Mag.*, **43**, 753 (1952).

([14]) M. Koshiba and M. F. Kaplon: *Phys. Rev.*, **97**, 193 (1955).

([15]) F. A. Brisbout, C. Dahanayake, A. Engler, Y. Fujimoto and D. H. Perkins: *Phil. Mag.*, **1**, 605 (1956).

([16]) A. Debenedetti, C. M. Garelli, L. Tallone and M. Vigone: *Nuovo Cimento*, **4**, 1150 (1956).

plicity $n \leqslant 22$. They conclude that the proportion of heavy particles other than pions tends to be greatest in the events of high multiplicity. This was connected also with the collision feature of the jet, and the high multiplicity events correspond to close collisions, and it is expected to lead to a higher production rate of heavy particles. It is very interesting to study these conclusions on the extremely high energy jets. As for the study of these features the emulsion chamber seems to be very effective, because the discrimination of the number of charged secondaries and of decayed γ-rays of π^0-mesons is clearer in the emulsion chamber than in the usual emulsion stacks for the inner cone of the jet. In this event, in the collimated forward cone, the production ratio is given as $R = 0.44 \pm 0.09$. Ciok *et al.* [5] obtained a rather unusual ratio in the forward cone in their high energy event.

* * *

The author wishes to thank Prof. O. Minakawa for his continuous encouragement. The author is also grateful to Prof. Y. Fujimoto and Prof. J. Nishimura for the kind advice they have given him at all stages of this work. Thanks are also due to the co-operative members of the Japanese emulsion chamber group for the balloon flight of the emulsion chambers and for stimulating discussions.

Appendix I

The experimental construction of the cascade shower curve in the early stage of the development.

The main difficulty for the energy determination of γ-rays and for the identification of the π^0-mesons in this analysis arises from the fact that the transition of each cascade shower can be observed only in the first few cascade units under the lead plates. The precision of the cascade shower theory is best at the shower maximum, but the precision is not good enough in this early stage of the development of the cascade shower owing to the approximation used in the computation. Furthermore, the effect of the fluctuation of the cascade shower is expected to be fairly large in this early stage of the development. Thus the precision of the theoretical curve in the early stage of development is tested, and also the effect of the fluctuation is studied.

The following theoretical relation is the base of the experimental construction of the cascade shower curve, in the approximation $r \ll 1$ cascade unit,

$$\pi\,(E_0, r, t) = \pi(E_0 \cdot r, t)\ [17]\,,$$

---

[17] J. Nishimura and K. Kamata: *Progr. Theor. Phys.*, **7**, 185 (1952).

TABLE III.

Event	core no.	$n\left(=\frac{1}{\cos\theta}\right)$	Visible energy (from the transition curve)	Coupling energy to a π^0-meson	Advised energy	Origin
T.H.1	(1)	1.10	$2 \cdot 10^{11}$ eV	$5.66 \cdot 10^{11}$ eV	$2.8 \cdot 10^{11}$ eV	Carbon
	(2)	1.10	$2 \cdot 10^{11}$ eV		$2.8 \cdot 10^{11}$ eV	
T.H.2	(1)	1.0	$2 \cdot 10^{11}$ eV	$3 \cdot 10^{11}$ eV	$1.2 \cdot 10^{11}$ eV	Carbon
	(2)	1.0	$2 \cdot 10^{11}$ eV		$1.8 \cdot 10^{11}$ eV	
	(3) (*)	1.0			$1 \cdot 10^{11}$ eV	
T.H.3	(1) (*)	1.04	$0.6 \cdot 10^{11}$ eV		$0.6 \cdot 10^{11}$ eV	Carbon
	(2) (*)	1.04	$0.6 \cdot 10^{11}$ eV		$0.6 \cdot 10^{11}$ eV	
T.H.4	(1)	1.04	$2 \cdot 10^{11}$ eV	$2.14 \cdot 10^{11}$ eV	$1.25 \cdot 10^{11}$ eV	Carbon
	(2)	1.04	$1.4 \cdot 10^{11}$ eV		$0.95 \cdot 10^{11}$ eV	
	(3)	1.04	$1 \cdot 10^{11}$ eV	$1 \cdot 10^{11}$ eV	$0.67 \cdot 10^{11}$ eV	
	(4)	1.04	$0.5 \cdot 10^{11}$ eV		$0.33 \cdot 10^{11}$ eV	
	(5)	1.04	$0.8 \cdot 10^{11}$ eV	$0.85 \cdot 10^{11}$ eV	$0.68 \cdot 10^{11}$ eV	
	(9)	1.04	$0.2 \cdot 10^{11}$ eV		$0.17 \cdot 10^{11}$ eV	
1605, NO, 25 (**)					$1 \cdot 10^{12}$ eV	

(*) Energy is determined from the coupling into π^0-meson with γ-rays which are not listed in this Table.

(**) Energy is determined from the track length of the cascade shower.

where $\pi(E_0, r, t)$ gives the total number of electrons within the radius r of the shower developed by a single γ-ray of energy E_0 after passing through t cascade units. Thus the same curve must be expected when the number of electrons is plotted as function of the product $E_0 \cdot r$ at a given depth.

As for the determination of the primary energy of the γ-ray, we adopt the following cascade showers: one is the cascade shower which is to couple into a π^0-meson (this is apparent from the kinematical relation of the decay process of a π-meson into two γ-rays) and the other is the cascade shower whose energy can be determined from the track length of the cascade shower. In the former case the ratio of the energy disparity is computed from the energy ratio obtained from the transition curve of each γ-ray, and this is believed to be the most suitable energy determination of the γ-ray in our case.

Table III is the list of the cascade showers initiated by decayed γ-rays from π^0-mesons in our chamber and of one single γ-ray used in this present process. n represents $1/\cos\theta$, where θ is the angle of declination of the cascade axis to the line perpendicular to the emulsion surface. We use the cascade shower in the range of n from $n=1$ to $n=1.10$, and this means that a precision of about 5% around $n=1.05$ is adopted in the measurement of the path of the cascade shower.

Fig. 10 and Fig. 11 represent the experimental results as well as the theoretical curve without Landau approximation under the 2nd and 3rd lead plates.

The heavy line is the experimentally constructed shower curve, which has been used in the energy determination of the γ-rays in the event S.H.1. In

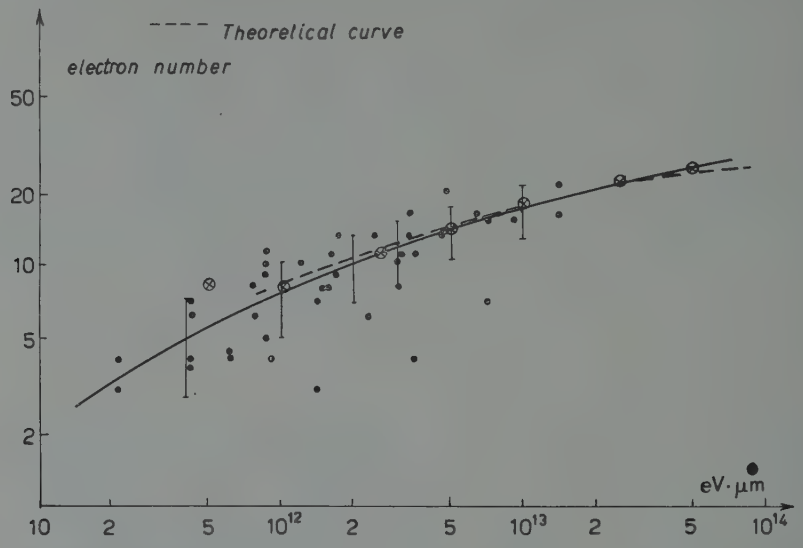

Fig. 10. – Cascade shower curve under two lead plates. T.H.1 ●, T.H.2 ●; T.H.3 ●; T.H.4 ●; 1605 NO 25 ⊗; see Table III.

Fig. 11 the experimental results of Pinkau [18] in 2 cascade units are also plotted. This is because in his data the origin of the path of the cascade

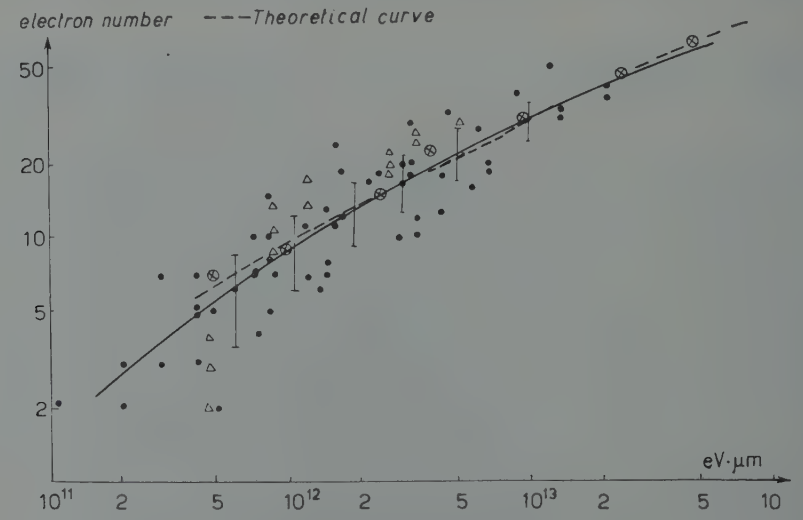

Fig. 11. – Cascade shower curve under three lead plates. T.H.1 ●, T.H.2 ●; T.H.3 ●; T.H.4 ●; 1605 NO 25 ⊗; Pinkau △; see Table III.

[18] K. PINKAU: *Phil. Mag.*, **2**, 1389 (1957).

shower was taken as the top of the electron pair from the γ-rays; and then the comparison must be made with shifted unit in our data. The agreement is rather good.

The rigorous treatment of the problem of the fluctuation in the early stage of development of the cascade shower seems to be impossible by these data. At the first few cascade units, the feature of development with the path of cascade shower changes rapidly depending on where it starts to develop. In our case, the jets occur in the carbon plates settled on the empty space and lead plates. As we can not see distinctly where the electron pair starts, the path of the cascade shower can not be determined clearly. The fluctuation is believed to be Poissonian at the shower maximum ([15]). In Fig. 10 and Fig. 11 the mean square deviation of Poisson fluctuation is presented for comparison. The fluctuation seems rather large beyond the random fluctuation in this system of measurement.

Appendix II

Analysis of the structure function with many γ-ray sources.

In the emulsion plates put between the carbon plates under the lead plates where the cascade showers from decayed γ-rays start to develop, each cascade shower is mixed up owing to the angular divergence in the lead plates and it takes some resemblance to the structure function of the air shower. Many γ-rays of different energies and different distances from the shower axis contribute to the total structure function in accordance with their energies and positions, respectively. In Fig. 12, the structure of the shower under the second carbon plates from the lead plates

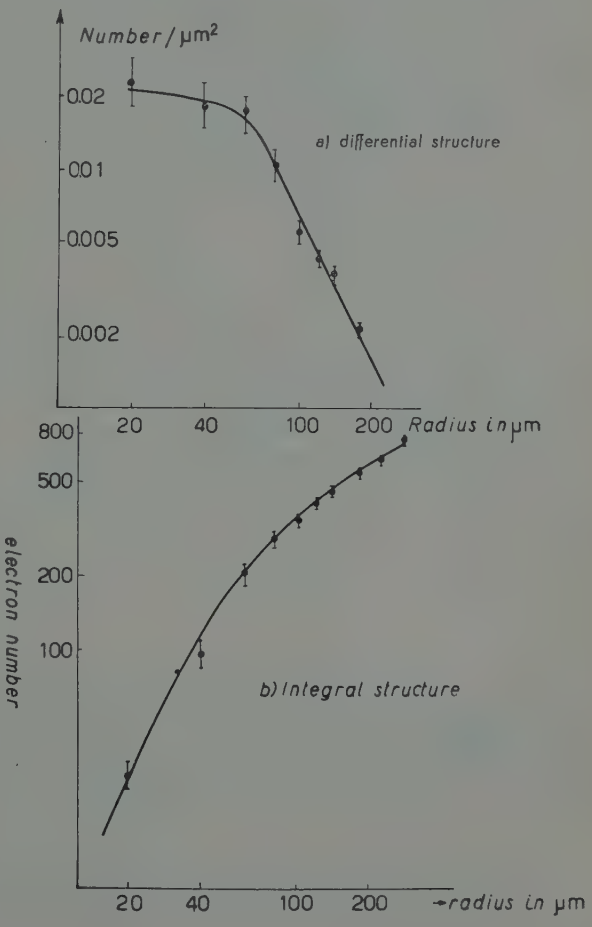

Fig. 12. – Differential and integral structure of mixed γ-rays.

is shown. Both the differential and the integral spectrum are plotted. The flatness of the differential spectrum, according to the r^2 dependence in the integral spectrum, at the core of the total structure function is a characteristic point different from the single cascade shower. The analysis of this structure function is made in the following manner. The total structure function is divided in two parts. The one is the part distant from the shower axis and the other is the part near the core.

i) *Far from the shower axis*, $r \gg r_0$. - The number of electrons within a circle of radius r of the cascade shower of age s started from energy E_0 is given in the cascade theory by

$$f(s, r, E_0) \sim \frac{2\pi}{s} c(s) \left(\frac{E_0 r}{K}\right)^s \quad (13) , \tag{A-II.1}$$

where the notation corresponds to that of Nishimura and Kamata (17).

In the case of jet showers, many γ-rays are produced, thus the structure function is the superposition of individuals of each γ-ray,

$$f'(s, r) = \sum_i \frac{2\pi}{s_i} c(s_i) \left(\frac{E_0 r}{K}\right)^{s_i} . \tag{A-II.2}$$

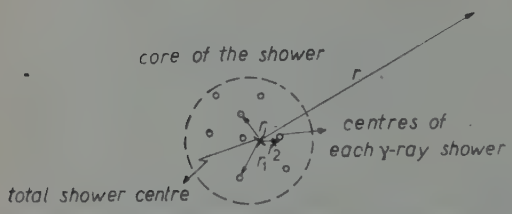

Fig. 13. – Illustration of the Appendix II.

The distance r_i is so small that it is neglected, see Fig. 13. If each shower age s_i approaches to unity that is to the shower maximum, we get information on the total energy, that is $n\langle E_0 \rangle$, with the smallest error, where $n\langle E_0 \rangle$ represents the multiplicity and the average energy of the γ-rays A similar treatment is usually used in the analysis of the behavior of the structure function of the air shower.

ii) *Near the shower axis*, $r \ll r_0$. - The contribution from many γ-rays near the core is represented in differential form by

$$g'(s, r)\, 2\pi r \, \mathrm{d}r = \sum_i C(s_i) \left(\frac{E_{0i} r_i}{K}\right)^{s_i} \frac{1}{r_i^2} 2\pi r \, \mathrm{d}r . \tag{A-II.3}$$

Taking the average transverse momentum of γ-rays to be $\bar{P}_{T\gamma}$, the energy of γ-rays with the lateral displacement r_i from the core can be expressed in the average by,

$$\frac{\bar{P}_{T\gamma}}{\theta_i} = \frac{\bar{P}_{T\gamma}}{r_i/L} = E_{0i} , \tag{A-II.4}$$

where L is the distance from the origin of the jet to the position observed.

Then the total structure function is represented in the integral form as follows,

$$g(s, r) = \frac{(E_{0i})^2}{(L\bar{P}_{T\gamma})^2} \left(\frac{L\bar{P}_{T\gamma}}{K}\right)^s C(s)\,\pi r^2 . \tag{A-II.5}$$

Accordingly, if the relation

$$E_0 R = L\bar{P}_{T\gamma} ,$$

holds, at some distance R from the shower axis, the following relation can be obtained compared with the structure function of the single cascade shower of γ-rays, that is,

$$\frac{2}{s} = \sum (E_{0i})^2 \left(\frac{R}{L\bar{P}_{T\gamma}}\right)^2 . \tag{A-II.6}$$

From these consideration, we get information upon $\sum_i E_{0i}^2$, that is $n\langle E_{0i}^2\rangle$, of the jet, because the other quantities in the formula (A-II.6) are known. Thus, as in the case of air showers, the structure function far from the shower axis gives us information on the total energy of the shower, and the one near the core gives us information on the summation of the square of the energy of each γ-ray. Thus, the ratio n, which is given by the relation

$$n = \frac{(\sum E_{0i})^2}{(\sum E_{0i}^2)} , \tag{A-II.7}$$

tells us information on the average multiplicity of γ-rays of the shower.

TABLE IV.

$\sum E_1$ (known)	$\sum E_1$ (structure function)	$\langle \sum E_1^2 \rangle^{\frac{1}{2}}$ (known)	$\langle \sum E_1^2 \rangle^{\frac{1}{2}}$ (structure function)	n (known)	n (structure function)
$1.61 \cdot 10^{13}$ eV	$(0.8 \sim 1.6) \cdot 10^{13}$ eV (*)	$3.34 \cdot 10^{12}$ eV	$(3.3 \sim 5.5) \cdot 10^{12}$ eV	20	~ 12

(*) Error is estimated at about 30 %.

In the event S.H.1, the shower age of the total shower is approximately $s \sim 0.6$ from the slope of the structure function far from the core. Table IV shows the results obtained by this method. The error listed is due mainly to

---

([19]) L. JÁNOSSY and H. MESSEL: *Proc. Phys. Soc.*, A **63**, 1101 (1950).

its rather younger shower age. The difference by a factor of 2 or more of this results from the directly observed data seems to be rather systematic, because the energy weighted multiplicity is calculated in this case.

This method seems to be fairly powerful for the estimation of the energy and multiplicity of the γ-rays of a jet shower initiated in the lead plates in the emulsion chamber where individual cascade showers initiated by γ-rays are mixed up, and the energy and multiplicity can not be obtained from direct observations.

RIASSUNTO (*)

L'A. esamina dettagliatamente uno sciame di alta energia avente un'energia primaria superiore a 10^{14} eV scoperto in una camera ad emulsione. Misura la distribuzione dell'impulso trasversale dei mesoni π^0 secondari ed ottiene il valore medio di 450 MeV/c. Con due metodi diversi esamina il rapporto fra l'angolo di emissione l'impulso trasversale dei raggi γ di decadimento dei mesoni π^0, ma non trova alcuna variazione dell'impulso trasversale al variare dell'angolo di emissione. Paragona le distribuzioni angolari delle particelle secondarie cariche e dei mesoni π^0 e non trova sensibili differenze. Allo scopo di determinare l'energia dei raggi γ di decadimento dei mesoni π^0, costruisce sperimentalmente la funzione della cascata nella camera ad emulsione nei primi stadi di sviluppo dello sciame. Infine studia l'aspetto della funzione totale della struttura con molte differenti sorgenti di raggi γ, e, con questa analisi, può determinare l'energia convertita nella componente molle dello sciame a cascata e la molteplicità media dei raggi γ.

(*) *Traduzione a cura della Redazione.*

IL NUOVO CIMENTO Vol. XIV, N. 5 1° Dicembre 1959

The Elastic and Inelastic Scattering of 6 and 7 MeV γ-rays from Lead.

S. G. Cohen (*)

Atomic Energy Research Establishment - Harwell

(ricevuto il 25 Maggio 1959)

Summary. — 6 and 7 MeV γ-rays, produced in the $^{19}F(p, \alpha)^{16}O$ reaction at proton energies of 1.5 and 2.9 MeV, respectively, have been scattered from lead, and the spectrum of scattered γ-rays measured at a mean scattering angle of 30°, using a sodium iodide scintillator. Elastic scattering has been observed, particularly for 7 MeV γ-rays for which the average differential cross section at the latter energy is about $5 \cdot 10^{-28}$ cm²/sr. This elastic scattering is probably associated with resonance absorption of the Doppler broadened primary γ-rays. In addition, inelastic scattering of γ-rays leading to excited states of lead nuclei has been observed.

In recent years a number of investigations into the elastic scattering of γ-rays have been carried out (1), particularly, in attempts to show the existence of the Delbrück scattering by the nuclear elecrostatic field, predicted by quantum electrodynamics (2). These attempts have for the most part (3,4) been confined to relatively low energy γ-rays which are available in reasonable

(*) present address: Hebrew University, Jerusalem.

(1) A. M. Bernstein and A. K. Mann: *Phys. Rev.*, **110**, 805 (1958). This article also contains references to other recent experimental work.

(2) J. M. Jauch and F. Rohrlich: *Theory of Photons and Electrons* (Cambridge, Mass., 1955).

(3) See, however, J. Moffat and M. W. Stringfellow: *Phil. Mag.*, **3**, 540 (1958) who measured the small angle scattering of 100 MeV electron bremsstrahlung.

(4) E. G. Fuller and E. Hayward: *Phys. Rev.*, **101**, 692 (1956). These authors measuring the elastic scattering of bremsstrahlung radiation up to 20 MeV for large scattering angles.

intensity from radioactive isotopoes, in particular the 1.33 MeV γ-rays from ^{60}Co and the 2.6 MeV γ-rays from ThC″. In this region of energy, a number of other processes, such as Rayleigh and nuclear Thompson scattering contribute to the total elastic scattering. Since good theoretical estimates of the cross-sections and angular distributions for Delbrück and Rayleigh scattering are not available, it is difficult to interpret the experimental results unambiguously.

This note reports some preliminary observations on the scattering from lead of higher energy γ-rays in the region of 6 and 7 MeV, which are produced moderately intensely in the ^{19}F(p, α)^{16}O reaction. Despite our continued ignorance of what happens at lower energies it seemed worthwhile to extend the experimental study to somewhat higher energies, where the Rayleigh contribution to the elastic scattering would presumably be less, although at these higher energies in heavier nuclei it is to be expected that other processes will also contribute to scattering. Nuclear scattering associated with resonance absorption of the primary γ-rays might play a serious part, especially since the γ-rays near 7 MeV produced in the above reaction are Doppler broadened and since the level density increases rapidly with energy. The γ-rays near 6 MeV are not Doppler broadened, and it is possible that for these γ-rays the nuclear resonance absorption is not large. Another process which one would expect, especially if there is appreciable resonance absorption, is the inelastic scattering of γ-rays, leading to excited states of the scattering nucleus. The study of such a process might be useful for investigating the properties of higher excited states, which can be produced in this way. This has previously been studied only by observing the production of isomeric states of nuclei after excitation by electron bremsstrahlung ([5-7]).

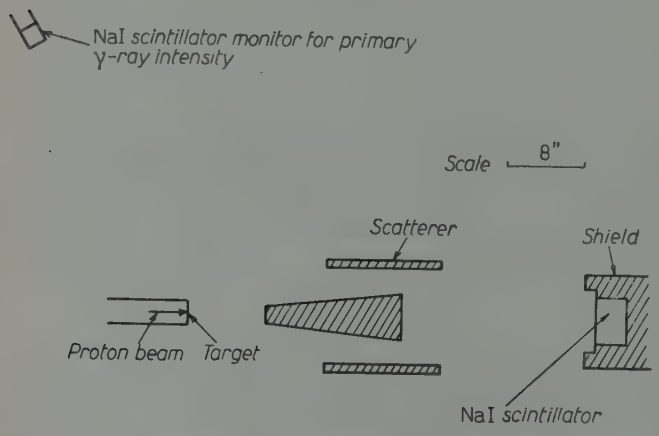

Fig. 1. – Experimental arrangement for detecting scattered γ-rays.

γ-rays from a thick calcium fluoride target, bombarded with protons from the Harwell Van de Graaff were scattered from a large

([5]) A. T. W. Cameron and L. Katz: *Phys. Rev.*, **86**, 608 (1951).
([6]) C. S. Del Rio y Sierra and V. L. Telegdi: *Phys. Rev.*, **90**, 439 (1953).
([7]) J. Goldenberg and L. Katz: *Phys. Rev.*, **90**, 308 (1953).

annular cylinder of lead (mass 60 kg) into a large shielded NaI scintillator (4½ in. diameter, 3 in. thick). The direct radiation was attenuated by a lead cone 14 in. long. Most of the measurements were made in a geometry (Fig. 1) corresponding to a mean scattering angle of 30°. The pulse size distributions in the detector were recorded using a 100 channel analyser down to pulse sizes corresponding to energy lost in the crystal of about 3 MeV. Care was taken to minimize distortion of the spectra by pile-up and to prevent excessive over-leading of the analyser. Counting losses were accurately estimated. The intensity of the primary γ-rays was monitored using a smaller NaI scintillator situated at about 100 cm from the target in a direction making about 120° with the incident proton beam.

Experiments were carried out at two different proton bombarding energies, 1.5 MeV and 2.9 MeV. With the former energy, the most intense γ-ray has an energy of 6.14 MeV, but is accompanied by relatively weak γ-rays at 6.91 and 7.12 MeV. With the higher energy protons, the most intense γ-rays are now 6.91 and 7.12 MeV, these being of approximately equal intensity. For 2.9 MeV protons, the energies of the latter γ-rays are broadened by α-recoil to a full width of about 150 keV in each case ([8]). The life-time of the 6.14 level of ^{16}O is relatively long and in a thick target the broadening due to α-recoil of this γ-ray is negligible.

Fig. 2 and 3 show the pulse size distributions, on a logarithmic scale, of the scattered γ-radiations and the background spectra, obtained at a mean scattering angle of 30° for the two proton

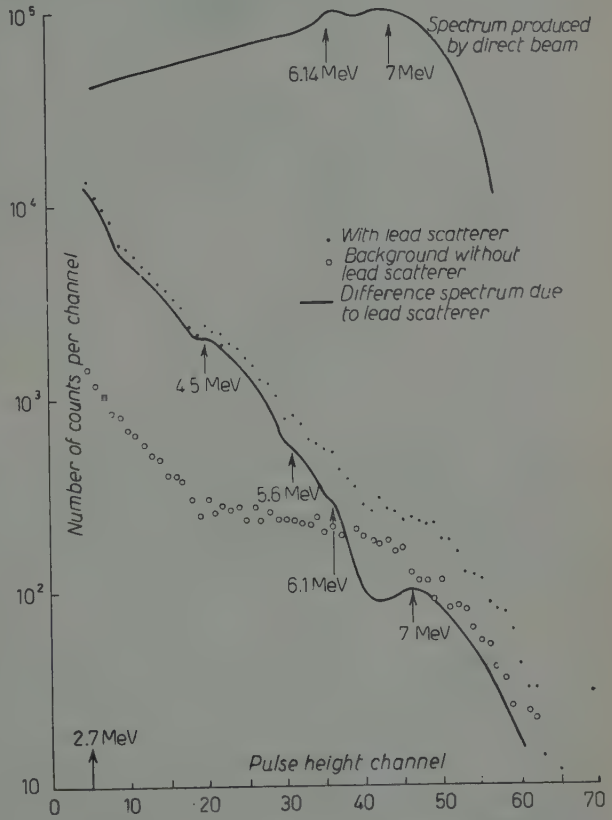

Fig. 2. – Spectrum of γ-rays scattered from lead. Primary γ-rays mostly around 7.0 MeV. Proton energy 2.9 MeV. Mean angle of scattering 30°.

([8]) C. P. SWANN and F. R. METZGER: *Phys. Rev.*, **108**, 982 (1957).

energies. The pulse spectra obtained with the unattenuated primary beam (of reduced intensity) are shown in the figures with the same scale of abscissa. In both figures, there is evidence of scattered radiation, in excess of the background, of energy in the region of the intense components of the primary radiation, and this is presumably the elastic scattering, at least in the case of the 7 MeV primary radiation. This scattering, however, is much more evident for the primary γ-rays near 7 MeV, and remembering the large Doppler-broadening of these γ-rays, suggests that in this case most of the scattering is nuclear elastic scattering associated with nuclear absorption. Approximate estimates for the average differential elastic cross-sections at 7.0 MeV for 30° scattering give the values $5 \cdot 10^{-28}$ cm²/sr. The interpretation of the «bump» at 6.14 MeV in Fig. 3 is less clear, since there is a possibility of scattered radiation of approximately this energy resulting from non-elastic scattering of the relatively weak primary radiation near 7.0 MeV, which appears together with the 6.15 MeV radiation at 1.5 MeV bombarding energy (9). In particular, inelastic scattering to levels at 899 keV in ^{204}Pb and 803 keV in ^{206}Pb would give rise to γ-rays near 6.14 MeV. Using the shape of the scattered spectrum in Fig. 2 in an attempt to correct in a very crude manner for the contribution of non-elastic scattering from higher energy radiation in the region of 6.14 MeV in Fig. 3, it seems probable that not more than half of the excess counts over background in this region are

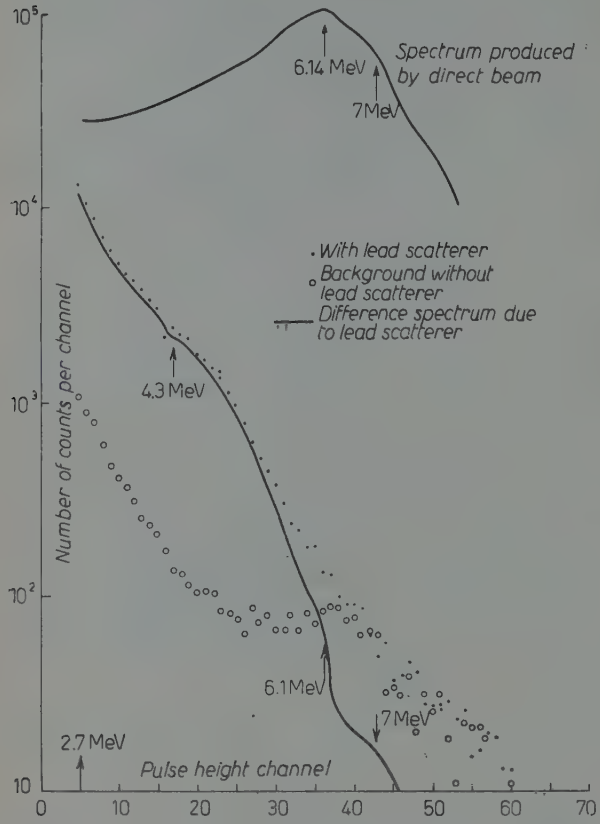

Fig. 3. – Spectrum of γ-rays scattered from lead. Primary γ-rays mostly 6.14 MeV. Proton energy 1.5 MeV. Mean angle of scattering 30°.

(9) C. Y. Chao, A. V. Tollestrup, W. A. Fowler and C. C. Lauritsen: *Phys. Rev.*, **79**, 108 (1950).

attributable to this cause, and one obtains that the differential elastic scattering cross-section for 30° at 6.14 MeV is not less than about $3 \cdot 10^{-29}$ cm²/sr. Unfortunately, our lack of theoretical knowledge of the Rayleigh scattering at this energy precludes at this stage any conclusion concerning the existence of Delbrück scattering at this energy from the experimental results. (The highest energy for which precise calculations exist is 1.33 MeV ([10])). BERNSTEIN and MANN have made a crude extrapolation of these results to 2.6 MeV and obtain an upper limit of about 10^{-28} cm²/sr for the sum of the Rayleigh and Thomson scattering at 30° for lead. One would expect the Rayleigh cross-section at 7 MeV to fall considerably below the value at 6 MeV. A non-negligible contribution to the elastic scattering at this energy might also arise from the nuclear scattering involving distant nuclear levels as virtual intermediate states. This has been estimated by LEVINGER ([11]) to be negligible compared with the Thompson scattering at 2.62 MeV for lead, but might perhaps be comparable with the Thompson scattering at 6 MeV.

Energy of primary γ-rays (MeV)	Energy of scattered γ-rays (MeV)	Approximate energy of excited levels of Pb nuclei produced after inelastic scattering (MeV)
7.0 (average)	7.0	
	6.1	0.9
	5.6?	1.4?
	4.5	2.5

It is seen in Fig. 2 and 3 that below the energies corresponding to elastic scattering the curves rise steeply and eventually pass into the tail of the relatively intense Compton γ-rays, the mean energy of which should be about 2.5 MeV for 7.0 MeV primary γ's. Particularly for primary γ-rays near 7.0 MeV it is seen that the curve for the scattered spectrum has a complicated structure indicating the presence of inelastically scattered γ-rays at various energies. The approximate energies of the excited states produced in this way after inelastic scattering are shown in the accompanying table, as the difference between energy of primary radiation and scattered radiation. Excited states of lead nuclei are known near all these energies. Particularly, strongly excited is a level or group of levels near 2.6 MeV. This may include the well-known 3- state of ^{208}Pb, but may include other levels which seem to

([10]) G. E. BROWN and T. F. MAYERS: *Proc. Roy. Soc.*, A **242**, 89 (1957).
([11]) J. S. LEVINGER: *Phys. Rev.*, **84**, 523 (1951).

exist at about this energy for other lead isotopes ([12]), from experiments on the inelastic scattering of protons.

Because of the complicated structure and poor resolution, it is impossible to resolve the curve into component curves corresponding to pulse spectra of separate γ-rays, and thus to estimate relative intensities. In fact the steepness of the spectrum as a function of energy suggests the presence of a continuum of γ-rays on which the inelastic peaks are superimposed. This continuum, except at energies close to the main Compton γ-rays, cannot be explained away by pile-up or by bremsstrahlung of high energy secondary electrons in the lead. It would seem to be due to the diffuse Compton scattering from bound electrons, particularly K electrons, the high energy Compton scattered γ-rays being produced by scattering from the high momentum components of the electron wave functions. A rough estimate of this effect, extrapolating from theoretical estimates ([13]) is not inconsistent with the experimental results.

The scattered spectrum for primary γ's of 6.14 MeV (Fig. 2) is more featureless, although again it shows indications of some structure corresponding to inelastic scattering. In this case, the interpretation of the energies of the excited states is ambiguous since one cannot say whether the primary γ-rays responsible for the scattering are the relatively stronger 6.14 MeV γ-rays or the weaker 7.0 MeV radiation, for which the cross-section will presumably be greater. It would seem that the steeply falling spectrum produced by the continuum γ-rays as assumed in the previous paragraph masks the peaks corresponding to inelastic scattering, the cross-section for which would indeed be expected to be lower at 6.14 MeV compared to 7 MeV, if, as appears reasonable, the inelastic scattering is particularly evident, when there is resonance absorption of the primary γ-rays.

A short description of work in progress ([14,15]) of a similar nature to that described here, has been brought to the author's attention.

* * *

I would like to thank Dr. E. Bretscher for his hospitality at Harwell during the summer 1958 when this work was done, and to Dr. E. Paul for invaluable encouragement and help.

([12]) B. L. Cohen and S. W. Mosko: *Phys. Rev.*, **106**, 995 (1957); B. L. Cohen and A. G. Rubin: *Phys. Rev.*, **111**, 1568 (1958).

([13]) J. Randles: *Proc. Phys. Soc.*, A **70**, 337 (1957).

([14]) S. A. E. Johansson: *Bull. Am. Phys. Soc.*, **3**, 174 (1958).

([15]) K. Reibel and A. K. Mann: *Bull. Am. Phys. Soc.*, **3**, 174 (1958).

RIASSUNTO (*)

Sono stati diffusi su piombo, dei raggi γ aventi energie di 6 e 7 MeV, raggi prodotti nella reazione $^{19}F(p, \alpha)^{16}O$ con protoni di energie rispettivamente di 1.5 MeV e 2.9 MeV; è stato quindi misurato lo spettro dei raggi γ diffusi sotto un angolo medio di scattering di 30°, con uno scintillatore di ioduro di sodio. È stato osservato in modo particolare lo scattering elastico dei raggi γ di 7 MeV, per i quali la sezione d'urto differenziale media è, a tale energia, di circa $5 \cdot 10^{-28}$ cm²/sr. Questo scattering elastico è associato con ogni probabilità ad un assorbimento per risonanza dei raggi γ primari allargati per effetto Doppler. È stato inoltre osservato lo scattering anelastico di raggi γ che portano a stati eccitati dei nuclei del piombo.

(*) *Traduzione a cura della Redazione.*

The Deceleration of Meteors During Their Passage through the Earth's Atmosphere.

F. Verniani

Istituto di Onde Elettromagnetiche dell'Università - Firenze

(ricevuto il 4 Giugno 1959)

Summary. — The deceleration of meteors is computed theoretically as a function of the characteristic quantities of evaporation, in particular, of velocity. It is shown that for over $\frac{3}{4}$ of all meteors, the deceleration increases until the end of the evaporation, and that, at the point of maximum rate of evaporation, the deceleration, as a first approximation, may be assumed the same for all meteors.

It is known that meteors are particles of very small mass (generally less than a milligram), which enter the earth's atmosphere at high velocities, of the order of a few tens of km/s. They collide violently with the air molecules and evaporate, owing to the heat generated in these collisions, producing an ionized column of high electronic density; moreover, the larger meteors leave also a visible trail.

The theory of meteoric evaporation was primarily elaborated by Herlofson [1]: it is based on the assumption that only single collisions occur between a meteor and air molecules. This assumption is fully justified by the fact that the mean free path of air molecules, at the heights at which meteors usually evaporate (about 100 km), is notably greater than the dimensions of the meteors themselves. Herlofson's theory leads to the following expressions:

$$r = r_0 \exp\left[-\frac{v_0^2 - v^2}{12l}\right], \tag{1}$$

$$p = \frac{2}{3}\varrho g r_0 \cos\chi \cdot \exp\left[-\frac{v_0^2}{12l}\right]\left[E\left(\frac{v_0^2}{12l}\right) - E\left(\frac{v^2}{12l}\right)\right], \tag{2}$$

$$n = \frac{\pi N}{2gHAl}\, p r^2 v^3, \tag{3}$$

---

[1] N. Herlofson: *Phys. Soc. Rep. Progr. Phys.*, **11**, 444 (1948).

where: r = radius of the meteor (assumed spherical);
r_0 = radius of the meteor outside the earth's atmosphere;
v = velocity of the meteor;
v_0 = velocity of the meteor outside the earth's atmosphere;
p = atmospheric pressure;
ϱ = meteoric density;
g = acceleration of gravity;
χ = zenithal angle of the meteor trajectory with respect to the earth;
l = latent heat of vaporization of meteoric matter per unit mass;
$E(x) = \int (e^x/x)\,\mathrm{d}x$, logarithmic integral;
n = rate of meteor evaporation, *i.e.*, number of atoms evaporated from the meteor per unit time;
N = Avogadro's number;
H = scale height;
A = average atomic weight of meteor.

Eqs. (1), (2), (3) are too complicated for practical applications; HERLOFSON has given also some approximate expressions of the same, which hold for $(v_0 - v)/v_0 \ll 1$.

In fact, if $(v_0 - v)/v_0 \ll 1$, we have, with fair accuracy

$$n_{\max} = \frac{4}{9}\frac{N}{HA} M_0 v_0 \cos\chi\,, \tag{4}$$

$$p_{\max} = \frac{8}{3}\varrho g l \frac{r_0}{v_0^2}\cos\chi\,, \tag{5}$$

$$r_{\max} = \tfrac{2}{3} r_0\,, \tag{6}$$

$$n = \frac{9}{4} n_{\max} \frac{p}{p_{\max}}\left(1 - \frac{1}{3}\frac{p}{p_{\max}}\right)^2, \tag{7}$$

where $n_{\max}$ is the maximum rate of evaporation, $p_{\max}$ and $r_{\max}$, the atmospheric pressure and the meteor radius, respectively, at the point of maximum evaporation.

In the present paper, we wish to show, starting from Herlofson's equations, that it is possible to evaluate the deceleration a of meteors during their passage through the earth's upper atmosphere, as a function of the velocity of the meteor, of its radius and of atmospheric pressure (and, hence, of velocity only, through eqs. (1) and (2)). Differentiation of (1) leads to

$$\mathrm{d}v = \frac{6l}{rv}\,\mathrm{d}r. \tag{8}$$

Since the short path of the meteor within the atmosphere may be assumed

to be a straight line ($\chi = \text{constant}$), we readily find

$$a = \frac{6l}{rv} \cdot \frac{\mathrm{d}r}{\mathrm{d}t} . \tag{9}$$

Obviously, a is negative, such being $\mathrm{d}r/\mathrm{d}t$; in the following, it is expedient to denote by a the absolute value of the deceleration, and therefore consider $\mathrm{d}r$ as the absolute value of the radius variation. Following our convention, the decrease of the meteor radius per unit time is related to the rate of evaporation by the expression

$$n \cdot \mathrm{d}t = 4\pi r^2 \, \mathrm{d}r \cdot \varrho \frac{N}{A} . \tag{10}$$

Thus, with the help of (10) and (3), expression (9) turns into

$$a = \frac{3}{4\varrho g H} \frac{v^2}{r} p . \tag{11}$$

Eq. (11) clearly shows that the (negative) acceleration of the meteor increases during the detectable phase of evaporation, *i.e.*, during the time when the meteor can generate an ionized column, whose electronic density is sufficiently high to allow detection by radioelectric means.

In fact, during this phase, v^2 diminishes but slightly, while $1/r$ and especially p, increase in a notable degree. It is possible to prove theoretically that, for the major part of meteors, deceleration increases up to the end of evaporation; in fact, by expressing a as a function of r, through eqs. (1) and (2) we have

$$a = \frac{\cos\chi}{2H} v^2 \exp\left[-\frac{v^2}{12l}\right]\left[E\left(\frac{v_0^2}{12l}\right) - E\left(\frac{v^2}{12l}\right)\right] , \tag{12}$$

and differentiating with respect to v

$$\frac{\mathrm{d}a}{\mathrm{d}r} = \frac{\cos\chi}{H} v \left\{\exp\left[-\frac{v^2}{12l}\right]\left(1 - \frac{v^2}{12l}\right)\left[E\left(\frac{v_0^2}{12l}\right) - E\left(\frac{v^2}{12l}\right)\right] - 1\right\} . \tag{13}$$

This derivative is surely negative until v remains greater than or equal to $\sqrt{12l}$, which corresponds to a value of roughly 9 km/s. It can be shown [2] that about 75 per cent of meteors evaporate completely before being slowed down to such a velocity; therefore, at least $\frac{3}{4}$ of meteors lose speed during evaporation with a steadily increasing deceleration. Through (12) it is also possible

---

[2] F. VERNIANI: *Ric. Scient.*, **29**, 1965 (1959).

to show that, for equal instantaneous velocity, the deceleration of a meteor increases with increasing initial velocity; this result, however, is wholly intuitive.

It is instead interesting to give an approximate expression of (11) to be used when $(v_0 - v)/v_0$ is far below unity, as is precisely the case during the entire appreciable phase of evaporation. By substituting (5) and (6) into (11), and taking into account the fact that at the point of maximum evaporation, the velocity of almost all meteors differs but slightly from the initial velocity v_0, we find that at the point of maximum evaporation the expression for the acceleration a may be written as

$$a_{max} = \frac{3l}{H} \cos \chi \,. \tag{14}$$

Thus, with good approximation, we find that the value of meteor deceleration, at the point of maximum evaporation, is the same for all meteors whose trajectories are equally inclined, regardless of either mass or velocity.

The little variation of scale height with altitude affects only slightly the value of a_{max}.

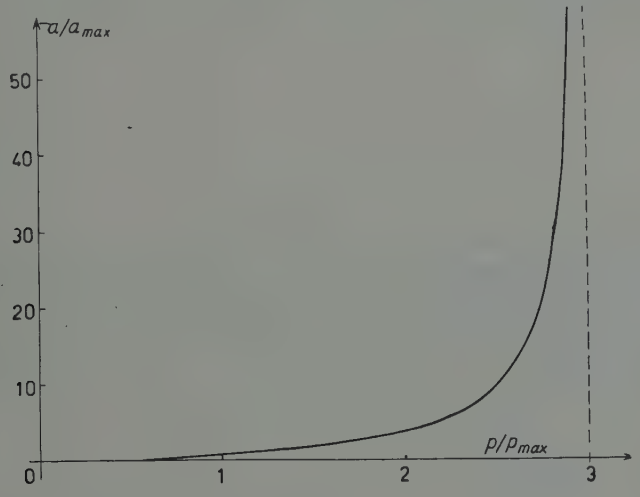

Fig. 1.

Taking into account the fact that by giving l in km²/s² and H in km, the ratio l/H approximates unity, (14) may be written also, as a first approximation, as

$$a_{max} = 3 \cos \chi \quad \text{km/s}^2 \,, \tag{15}$$

Following a procedure similar to the one used by HERLOFSON for deducing eqs. (4), (5), (6), (7), it is possible to give the trend of a as a function of p, during the course of evaporation. We obtain

$$a = \frac{2p}{3p_{\max} - p} a_{\max} . \tag{16}$$

Eq. (16) shows that the trend of $a/a_{\max}$ as a function of $p/p_{\max}$, plotted in Fig. 1, is the same for all meteors, independently of all their characteristics.

We see that the few experimental values of a ([3]) are in good agreement with the theoretical predictions deduced from eqs. (11) and (15). For instance, for $\chi = 30°$, we have for $a_{\max}$ the value 2.6 km/s²; this result is an indirect corroboration of Herlofson's theory on meteoric evaporation.

* * *

I wish to warmly thank Professor NELLO CARRARA for his constant encouragement and helpful advice.

([3]) D. W. R. MCKINLEY: *Astrophys. Journ.*, **113**, 225 (1951).

RIASSUNTO

Viene valutata teoricamente la decelerazione delle meteore in funzione delle grandezze caratteristiche dell'evaporazione, in particolare della velocità. Si prova che per oltre $\frac{3}{4}$ delle meteore la decelerazione aumenta fino al termine dell'evaporazione e che in prima approssimazione la decelerazione nel punto di evaporazione massima è la stessa per tutte le meteore.

IL NUOVO CIMENTO Vol. XIV, N. 5 1° Dicembre 1959

On the Interpretation of the K^--Meson Interaction in Nuclear Emulsion.

U. Kundt, K. Lanius and K. Lewin

Deutsche Akademie der Wissenschaften zu Berlin
Kernphysikalisches Institut Zeuthen - Berlin

(ricevuto il 10 Luglio 1959)

Summary. — Observed frequencies of pions emitted by K^- captures at rest in nuclear emulsion are used for an estimation of the percentage of $1\mathcal{N}$ interactions. It is shown that a value of 20% is an upper limit for the percentage of $2\mathcal{N}$ interactions. Simultaneously it turns out that the capture must occur preferentially at the nuclear surface. We determine a branching ratio for the production of different kinds of hyperons in the $1\mathcal{N}$ interactions.

Introduction.

From a large number of experimental tests on the capture of stopped negative K-mesons in nuclear emulsion and in bubble chambers it has been found that the following two absorption processes take place:

$$K^- + \mathcal{N} \to Y + \pi\,,$$

$$K^- + 2\mathcal{N} \to Y + \mathcal{N}\,.$$

Recently several authors [1-3] investigated K^- captures in emulsion and

[1] European Collaboration: *International Conference on Mesons and Recently Discovered Particles* (Padua-Venice, 1957), II-1; *Annual International Conference on High Energy Physics at CERN* (1958), p. 179.

[2] Y. Eisenberg, W. Koch, M. Nicolić, M. Schneeberger and H. Winzeler: *Nuovo Cimento*, **11**, 351 (1959).

[3] G. B. Chadwick, S. A. Durrani, P. B. Jones, J. W. G. Wignall and D. H. Wilkinson: *Phil. Mag.*, **3**, 1193 (1958).

found that (15÷50)% of all reactions are $2\mathcal{N}$ reactions. This result gives a much higher value for $2\mathcal{N}$ reactions than the formerly assumed one of ~10%. Furthermore EISENBERG *et al.* [2] determined in their work the branching ratio for the $1\mathcal{N}$ reactions. Their results differ strongly from the hydrogen data [4].

In the present work we shall consider the questions of the relative number of captures by light and heavy nuclei, the number of $1\mathcal{N}$ and $2\mathcal{N}$ interactions, and whether the K^- absorptions take place preferentially on the surface of the nucleus or homogeneously throughout the entire nucleus.

1. – Internal energy spectrum of the pions.

The internal energy spectrum for pions produced together with Σ and Λ^0 hyperons has been calculated by several authors (see *e.g.* [2,5,6]). In this work we use the same spectrum as the Berne group [2]. It was calculated under the assumption that the nucleon momentum distribution is a Gaussian with a maximum at 170 MeV/c and that the impulse approximation is valid.

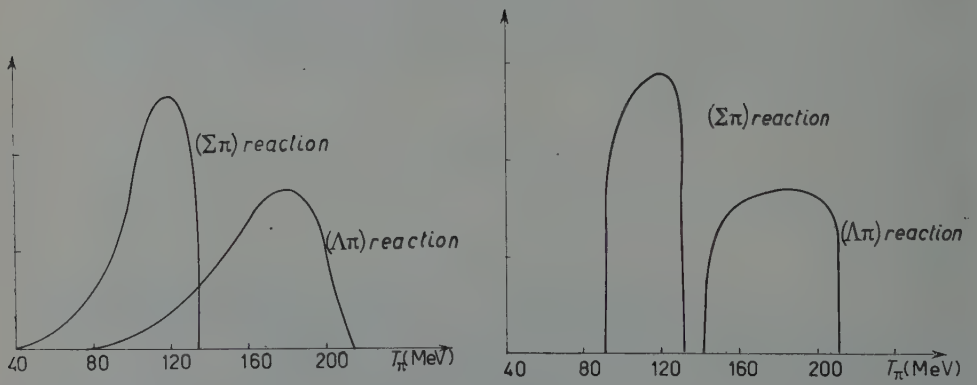

Fig. 1. – Internal energy spectra for the produced pions: *a*) calculated with a Gaussian distribution for the nucleon momentum density (α=170 MeV/c). *b*) Analogous spectra calculated with a Fermi distribution (cut off at 26 MeV).

The used potentials are: $V_\pi = 40$ MeV, $V_Y = 25$ MeV. The sum of the binding and excitation energy (*i.e.* the energy being necessary to remove a nucleon from the nucleus) was taken as 20 MeV [5]. The calculations were along the

---

[4] *International Conference on Mesons and Recently Discovered Particles* (Padua-Venice, 1957), XIX-8.

[5] F. C. GILBERT, C. E. VIOLET and R. S. WHITE: *Phys. Rev.*, **107**, 228 (1957).

same lines as described by GILBERT, VIOLET and WHITE (5). In order to investigate the influence of the shape of the pion spectra, we also have calculated the analogous spectra using a Fermi distribution with a cut-off at 26 MeV for the nucleon momentum. The two sets of curves are shown in Figs. 1*a* and 1*b*.

2. – Pion emission probabilities.

The pion emission probabilities were calculated for the light and heavy nuclei of the emulsion by the same method used in the work of WEBB *et al.* (6) based on the Serber model. The interaction mean free paths for pions in nuclear matter were taken from FRANK, GAMMEL and WATSON (7). It was assumed that 25% of the interacting charged pions were scattered inelastically (8). The radius of the heavy nuclei was taken as 6.36 fermi and the radius of the light nuclei 3.35 fermi. The calculated pion emission probabilities for the two sets of spectra are given in Table I for the surface and homogeneous cases. The results for the spectrum calculated with the Fermi momentum distribution are given in parentheses (*).

TABLE I. – *Pion emission probabilities.*

Kind of reaction	Heavy nuclei		Light nuclei		Weighted mean	
	surface	homogen.	surface	homogen.	surface	homogen.
$\pi\Lambda$	0.67 (0.67)	0.40 (0.37)	0.70 (0.70)	0.48 (0.46)	0.68 (0.67)	0.41 (0.39)
$\pi\Sigma$	0.73 (0.72)	0.52 (0.50)	0.78 (0.78)	0.65 (0.63)	0.74 (0.73)	0.55 (0.53)

Table I shows that the emission probabilities are weakly dependent on the specific shape of the internal energy spectrum. We have also made a similar calculation for $V_\pi = V_Y = 0$ and the results were not significantly different.

(6) F. H. WEBB, E. L. ILOFF, F. H. FEATHERSTON, W. W. CHUPP, G. GOLDHABER and S. GOLDHABER: *Nuovo Cimento*, **8**, 899 (1958).

(7) R. M. FRANK, J. L. GAMMEL and K. M. WATSON: *Phys. Rev.*, **101**, 891 (1956).

(8) G. BERNARDINI, E. T. BOOTH and L. M. LEDERMANN: *Phys. Rev.*, **83**, 1075, 1277 (1951); G. BERNARDINI and F. LÉVY: *Phys. Rev.*, **84**, 610 (1951); G. GOLDHABER and S. GOLDHABER: *Phys. Rev.*, **91**, 467 (1953); A. H. MORRISH: *Phys. Rev.*, **90**, 674 (1953).

(*) Also in the following tables the data calculated with the Fermi momentum distribution are given in parentheses.

3. – $2\mathcal{N}$ interactions.

In our experimental work (9) we have measured the percentages of K^- captures in light and heavy nuclei and the relative frequency of the emitted pions in each of the two groups. Under the assumption of charge independence and with the emission probabilities of charged pions given in Table I we have calculated the numbers of $1\mathcal{N}$ interactions in light and heavy nuclei (Table II). For this calculation we have assumed as a first approximation, that 12% of all $1\mathcal{N}$ interactions belong to the $\Lambda^0\pi$-case (4).

Using the values of Table II we have calcultaed the weighted mean pion emission probabilities given in Table I (*).

TABLE II. – *Percentages of* $1\mathcal{N}$ *interactions.*

	Surface	Homogeneous
Light nuclei	80 (80)	101 (101)
Heavy nuclei	77 (78)	117 (115)

To determine the number of $1\mathcal{N}$ interactions for emulsion nuclei we make use of the fact that pions emitted with energies greater than 100 MeV can originate only in the $\Lambda^0\pi$ case. On the basis of experimental data given in the literature (1,2,6) we have taken the number of charged pions emitted with energies over 100 MeV as (7 ± 1)% of all charged pions emitted. The external spectrum for the $\Lambda^0\pi$ case was calculated with the help of the energy distribution for inelastically scattered pions given by SHAFI and PROWSE (10). The number of pions produced in the $\Lambda^0\pi$ case can then be obtained by using the weighted mean emission probabilities given in Table I. Knowing the percentage of charged pions produced in the $\Lambda^0\pi$-case, the total observed per-

(9) C. GROTE, I. HAUSER, U. KUNDT, K. LANIUS, K. LEWIN, H. W. MEIER and U. KRECKER: *Nuovo Cimento*, **14**, 532 (1959).

(*) For all reactions we had 75% captures in heavy nuclei (9). The above described correction, which takes into account that we consider here only $1\mathcal{N}$ interactions, gives for the surface case 74% and for the homogeneous case 77%. The influence of this variation on our calculations is negligibly small. *E.g.* the weighted mean pion emission probabilities in Table I differ from the corresponding values calculated without correction only by the third decimal.

(10) U. SHAFI and D. J. PROWSE: *International Conference on Mesons and Recently Discovered Particles* (Padua-Venice, 1957), X-2.

centage of K^- captures emitting charged pions, and making use of the weighted emission probabilities in Table I, one can readily calculate the number of charged pions produced. The observed percentage of K^- captures emitting charged pions was taken to be $(39 \pm 2)\%$, *i.e.* the mean from the European collaboration [11] and our value [9]. Under the assumption of charge independence the total number of pions produced is 1.5 times the number of charged pions, which corresponds to the number of $1\mathcal{N}$ interactions. Table III lists the resulting number of $1\mathcal{N}$ interactions.

TABLE III (*). – $1\mathcal{N}$ *interactions.*

Surface capture	$(80 \pm 4)\%$ $[(81 \pm 4)\%]$
Homogeneous capture	$(113 \pm 6)\%$ $[(116 \pm 6)\%]$

(*) Here and in the Tables that follow the errors refer only to the statistical errors in the measured values.

4. – Branching ratio.

Using a procedure similar to that given in the preceding section we can calculate a partial branching ratio for the $1\mathcal{N}$ interactions. For this we used the experimental ratio given by the Berne group [2] for all emitted pions,

$$\frac{\pi^-}{\pi^+} = 3.5 \pm 0.6 \, .$$

We also used the well known relations of the transition probabilities (see Table IV)

$$(f)^2 = \tfrac{1}{2}(g)^2 \, ,$$

$$(a)^2 + (b)^2 + (c)^2 = 2((d)^2 + (e)^2) \, ,$$

$$(b)^2 = (d)^2 \, .$$

In column 1 of Table IV we give the different possible $1\mathcal{N}$ reactions, in column 2 the transition probabilities; column 3 and 4 give the resulting branching ratios for the surface and homogeneous cases normalized to 100. The last column gives the branching ratio calculated from the bubble chamber

(11) EUROPEAN COLLABORATION: *Nuovo Cimento*, **12**, 91 (1959).

data for K^- capture in hydrogen [4]), The K^- captures on neutrons were calculated under the assumption of charge independence, the number of neutrons being taken equal to the number of protons.

TABLE IV. – *Branching ratio for* 1π *interactions* (*normalized to* 100).

Reaction	Matrix element	Surface capture	Homogeneous capture	Hydrogen bubble chamber
(*a*) $K^-+p\to\Sigma^++\pi^-$	$a_1/2+a_0/\sqrt{6}$	44 ± 4 (46 ± 4)	37 ± 4 (41 ± 3)	29 ± 3
(*b*) $K^-+n\to\Sigma^-+\pi^0$	$a_1/\sqrt{2}$			
(*c*) $K^-+p\to\Sigma^-+\pi^+$	$-a_1/2+a_0/\sqrt{6}$	15 ± 2 (15 ± 2)	14 ± 2 (14 ± 2)	30 ± 3
(*d*) $K^-+n\to\Sigma^0+\pi^-$	$-a_1/\sqrt{2}$	29 ± 2 (30 ± 2)	25 ± 2 (27 ± 2)	29 ± 9
(*e*) $K^-+p\to\Sigma^0+\pi^0$	$-a_0/\sqrt{6}$			
(*f*) $K^-+p\to\Lambda^0+\pi^0$	$b_1/\sqrt{2}$	4 ± 1 (3 ± 1)	8 ± 2 (6 ± 1)	4 ± 2
(*g*) $K^-+n\to\Lambda^0+\pi^-$	b_1	8 ± 2 (6 ± 1)	16 ± 3 (12 ± 2)	8 ± 4

5. – Discussion.

From the results in Table III we see that the homogeneous capture of K^--mesons in 1π reactions is in clear contradiction with the experimental data. Because of the number of Σ-hyperons with energies above 60 MeV the number of multinucleon interactions must be greater than 15%. The assumption of different shapes for the internal pion spectra and different values of the pion and hyperon potentials have little influence on the calculated number of 1π interactions and the branching ratio. The results, however, are sensitive to the value of the mean free paths of pions in nuclear matter. In our calculation we used the values given by FRANK *et al.* [7]) for the interaction m.f.p. which are based on the experimental data for the pion-nucleon interaction. These values of the m.f.p. are in good agreement with the experimental values obtained for pion interactions with complex nuclei (see *e.g.* STORK [12])) for the energy involved in the K^- interactions. The results are also not very sensitive to reasonable variations in the percentage of inelastically scattered pions. This means that the value of $\sim 20\%$ 2π-interactions *i.e.* pure surface capture, should be considered as an upper limit.

As seen in Table IV the branching ratio at production in the 1π interactions is not in contradiction with the hydrogen bubble chamber data for the last 4 reaction channels. Our calculations for the branching ratios concerning the first 3 reaction channels are dependent on the exact value of the

[12]) D. H. STORK: *Phys. Rev.*, **93**, 868 (1954).

π^-/π^+ ratio. Within the $3\sqrt{N}$-statistical error of the π^-/π^+ ratio there is agreement between our results and the hydrogen bubble chamber data also for these 3 cases.

The new experimental results ([9,11]) concerning the percentage of emitted pions from K^- captures in emulsion seem to indicate that the used frequency of 7% of emitted pions with energies greater than 100 MeV ([1,2,6]) was to small.

We have not attempted to present a calculated external pion spectrum because of the sensitivity of such a spectrum to several of the parameters employed, especially the π^-/π^+ ratio.

Assuming, that our partial branching ratio for the surface case given in Table IV, is correct within the limits of error, and assuming further that

$$\frac{K^- + p \to \Sigma^- + \pi^-}{K^- + p \to \Sigma^+ + \pi^-} = 1\,, \quad (*)$$

we obtain the complete branching ratio of $1\mathcal{P}$-interactions presented in Table V.

TABLE V.

Interaction	$a_1 \neq 0$ $a_0 = 0$	Rates
$K^- + p \to \Sigma^- + \pi^-$	$(a_1)^2/4$	15
$\to \Sigma^+ + \pi^-$	$(a_1)^2/4$	15
$\to \Sigma^0 + \pi^0$	0	0
$\to \Lambda^0 + \pi^0$	$(b_1)^2/2$	4
$K^- + n \to \Sigma^- + \pi^0$	$(a_1)^2/2$	29
$\to \Sigma^0 + \pi^-$	$(a_1)^2/2$	29
$\to \Lambda^0 + \pi^-$	$(b_1)^2$	8

These values we got assuming pure isospin triplet state interaction ($a_1 \neq 0$, $a_0 = 0$). The mixture state ($a_1 \neq 0$, $a_0 \neq 0$) and the pure singlet state interaction ($a_1 = 0$, $a_0 \neq 0$) can uniquely be excluded, since they are in strong contradiction with the data given in Table IV.

(*) We used tis approximation, because experiments show ([13]) that with increasing relative momentum between K^--meson and nucleon this ratio tends to 1.

([13]) *Annual International Conference on High Energy Physics at CERN* (1958), p. 178.

* * *

We would like to thank Mr. E. MARQUIT for many useful discussions and suggestions.

RIASSUNTO (*)

Le frequenze osservate dei pioni emessi da catture K^- in riposo in emulsioni nucleari vengono usate per stimare la percentuale di interazioni $1\mathcal{N}$. Si dimostra che un valore di 20% è il limite superiore per la percentuale di interazioni $2\mathcal{N}$. Nello stesso tempo risulta che la cattura deve accadere a preferenza sulla superficie nucleare. Si determina anche il rapporto di *branching* per la produzione di diverse specie di iperoni nella interazione $1\mathcal{N}$.

(*) *Traduzione a cura della Redazione.*

IL NUOVO CIMENTO Vol. XIV, N. 5 1° Dicembre 1959

Introduction to Complex Orbital Momenta.

T. Regge

Max-Planck-Institut für Physik und Astrophysik - München (*)

(ricevuto il 18 Luglio 1959)

Summary. — In this paper the orbital momentum j, until now considered as an integer discrete parameter in the radial Schrödinger wave equations, is allowed to take complex values. The purpose of such an enlargement is not purely academic but opens new possibilities in discussing the connection between potentials and scattering amplitudes. In particular it is shown that under reasonable assumptions, fulfilled by most field theoretical potentials, the scattering amplitude at some fixed energy determines the potential uniquely, when it exists. Moreover for special classes of potentials $V(x)$, which are analytically continuable into a function $V(z)$, $z = x+iy$, regular and suitable bounded in $x > 0$, the scattering amplitude has the remarcable property of being continuable for arbitrary negative and large cosine of the scattering angle and therefore for arbitrary large real and positive transmitted momentum. The range of validity of the dispersion relations is therefore much enlarged.

---

1. – In the following we shall choose dimentionless variables, by putting $x = kr$, where r is the distance from the origin, k the wave number (fixed). We can write then Schrödinger's equation as follows:

$$\psi'' - \frac{\lambda^2 - \frac{1}{4}}{x^2}\psi + \psi - U(x)\psi = 0 \,. \tag{1.1}$$

Here λ is a generalized complex orbital momentum; when λ assumes positive half-integer values (hereafter referred to as the physical values) we shall write $\lambda = j + \frac{1}{2}$.

Eq. (1.1) is even in λ. For brevity we shall single out all quantities cor-

(*) Now at the Palmer Physical Laboratory - Princeton, N.J.

responding to $U(x)=0$ with the index ^{0}. We shall also suppose

$$\int_0^\infty x|U(x)|\,dx < Q < \infty, \qquad |x^2U(x)| < M = \text{const.} \tag{1.2}$$

Although much of the theory here developed could be retained under a weaker condition, some interesting results would not hold or would require too lengthy proofs. We list here a set of solutions of (1.1) with the appropriate boundary conditions:

$$\begin{cases} F(\lambda,\eta,x) & x\to\infty & \sim\cos\left(x-\eta-\dfrac{\pi}{4}\right) \\ G(\lambda,x) & x\to\infty & \sim\cos\left(x-\dfrac{\pi}{4}\right) \\ S(\lambda,x) & x\to\infty & \sim\sin\left(x-\dfrac{\pi}{4}\right) \\ \varphi(\lambda,x) & x\to 0 & \sim x^{\lambda+\frac{1}{2}}. \end{cases} \tag{1.3}$$

Clearly:

$$\begin{cases} F(\lambda,0,x)=G(\lambda,x)\,; \qquad F\left(\lambda,\dfrac{\pi}{2},x\right)=S(\lambda,x)\,, \\ F(\lambda,\eta,x)=\cos\eta C(\lambda,x)+\sin\eta\, S(\lambda,x)\,, \\ F(\lambda,\eta,x)=F(-\lambda,\eta,x)\,. \end{cases} \tag{1.4}$$

A slight generalized form of a theorem of Poincaré states that $F(\lambda,\eta,x)$, for fixed η and x, is an entire function of λ. If $U(x)=0(x^{-2+2C})$, $C>0$ (*) small x, then $\varphi(\lambda,x)$ is analytic in $R(\lambda)>-C$ if $C<1$ and in $R(\lambda)>-1$ if $C>1$. Therefore $\varphi(\lambda,x)$ and $\varphi(-\lambda,x)$ have a common domain of analyticity in the strip: $|R(\lambda)|<C$, (<1).

For those values for which $\varphi(\lambda,x)$ exists we must have a relation of the kind:

$$\varphi(\lambda,x)=2\lambda[C(\lambda)S(\lambda,x)-S(\lambda)C(\lambda,x)]\,, \tag{1.5}$$

$C(\lambda)$, $S(\lambda)$ depend on λ only and are analytic in $R(\lambda)>-C(-1)$ with the possible exception of $\lambda=0$, where there may be a simple pole. We shall not

(*) In the following we shall use, when there is no danger of confusion, the same letter C for quite different constants in different formulas.

reproduce here the details of the proofs of all these statements which are mostly by-products of more careful estimates contained in the Appendix.

We now observe that the Wronskian of any two solutions of (1.1) is a constant. We have for instance from the small x limit:

$$\varphi(\lambda, x)\varphi'(-\lambda, x) - \varphi(-\lambda, x)\varphi'(\lambda, x) = -2\lambda = W[\varphi(\lambda, x), \varphi(-\lambda, x)] . \tag{1.6}$$

Similarly:

$$W[C(\lambda, x), S(\lambda, x)] = 1 . \tag{1.7}$$

Introducing (1.5) into (1.6) and using (1.7) we find:

$$C(\lambda) S(-\lambda) - S(\lambda) C(-\lambda) = \frac{1}{2\lambda} . \tag{1.8}$$

This identity is of paramount importance in our theory. From it and (1.5) we can write $C(\lambda, x)$ and $S(\lambda, x)$ in terms of $\varphi(\lambda, x)$ and $\varphi(-\lambda, x)$:

$$\begin{cases} C(\lambda, x) = C(\lambda)\varphi(-\lambda, x) + C(-\lambda)\varphi(\lambda, x) , \\ S(x, \lambda) = S(\lambda)\varphi(-\lambda, x) + S(-\lambda)\varphi(\lambda, x) . \end{cases} \tag{1.9}$$

From (1.9) if $R(\lambda) > 0$ we deduce:

$$C(\lambda) = \lim_{x \to 0} x^{\lambda - \frac{1}{2}} C(\lambda, x) \qquad \text{and similarly for } S(\lambda) .$$

Finally we list here the unperturbed functions:

$$\begin{cases} \varphi^0(\lambda, x) = x^{\frac{1}{2}} \Gamma(\lambda + 1) 2^\lambda J_\lambda(x) , \\ C^0(\lambda, x) = \sqrt{\frac{\pi}{2}}\, x^{\frac{1}{2}} \dfrac{1}{2 \cos(\pi\lambda/2)} [J_\lambda(x) + J_{-\lambda}(x)] , \\ S^0(\lambda, x) = \sqrt{\frac{\pi}{2}}\, x^{\frac{1}{2}} \dfrac{1}{2 \sin(\pi\lambda/2)} [J_\lambda(x) - J_{-\lambda}(x)] , \\ C^0(\lambda) = \sqrt{\dfrac{1}{2\pi}}\, 2^\lambda \sin\dfrac{\pi\lambda}{2}\, \Gamma(\lambda) , \\ S^0(\lambda) = \sqrt{\dfrac{1}{2\pi}}\, 2^\lambda \cos\dfrac{\pi\lambda}{2}\, \Gamma(\lambda) . \end{cases} \tag{1.10}$$

2. – If $\lambda = j + \frac{1}{2}$, $\varphi(\lambda, x)$ is the only solution which satisfies the boundary conditions required for the physical interpretation. The phase δ is defined

then from its asymptotic behaviour at large distances:

$$\text{(2.1)} \qquad \begin{cases} \varphi(\lambda, x) \simeq 2\lambda T(\lambda) \cos\left[x - \dfrac{\pi\lambda}{2} + \delta(\lambda)\right], \\ T^2(\lambda) = C^2(\lambda) + S^2(\lambda). \end{cases}$$

We define $\delta(\lambda)$ through (2.1) also when λ is generally complex. Comparing (2.1) with (1.5) we find:

$$\text{(2.2)} \qquad K(\lambda) = \frac{S(\lambda)}{C(\lambda)} = -\operatorname{ctg}\left[\frac{\pi\lambda}{2} - \delta(\lambda)\right].$$

The so defined $\delta(\lambda)$ will be hereafter referred to as the « interpolation » of the phase-shifts in the physical points. Not all analytic functions which interpolate the phase shifts can be generated by a potential. Some necessary conditions are:

a) $K(\lambda)$ is regular analytic in $R(\lambda) > 0$ with the exception of simple poles.

b) $K(\lambda)$ is an hermitian function, that is $K(\lambda) = [K(\lambda^*)]^* = K^\dagger(\lambda)$. (Clearly this follows from $C(\lambda)$, $S(\lambda)$ being also hermitian), if λ is real then $K(\lambda)$ is also real.

a) and *b*) are by no means sufficient. To see it let us evaluate the integral (see Appendix):

$$\text{(2.3)} \qquad P(\lambda) = \int_0^\infty |\varphi(\lambda, x)|^2 \frac{\mathrm{d}x}{x^2} > 0 \qquad R(\lambda) > 0.$$

(Notice that $P(\lambda)$ is *not* an analytic function of λ!).
The result can be stated as follows:

$$\text{(2.4)} \qquad \begin{cases} P(\lambda) = 2\lambda[C(\lambda)\,S'(\lambda) - C'(\lambda)\,S(\lambda)] = 2\lambda\,T^2(\lambda)\left[\dfrac{\pi}{2} - \delta'\right] > 0\,, \quad \lambda \text{ real} > 0, \\ P(\lambda) = \dfrac{2\lambda^2}{R(\lambda)\,I(\lambda)} \cdot |T^2(\lambda)| \sinh[\pi I(\lambda) - 2I(\delta)] > 0\,, \quad \lambda \text{ complex } K(\lambda) > 0. \end{cases}$$

The following inequalities can be therefore derived:

$$\text{(2.5)} \qquad \begin{cases} c) \quad \dfrac{\mathrm{d}\delta(\lambda)}{\mathrm{d}\lambda} < \dfrac{\pi}{2} \qquad \lambda > 0 \text{ real}, \\ d) \quad I(\lambda)[\pi I(\lambda) - 2I(\delta)] > 0 \qquad I(\lambda) \neq 0. \end{cases}$$

Consider now the function $W(L) = K(\lambda)$, $L = \lambda^2$. The half-plane $R(\lambda) > 0$ is mapped into the whole L plane cut along the negative real axis (cut plane). *a*) ... *d*) can be then translated into properties of $W(L)$

a) $W(L)$ is regular analytic in the cut plane with the exception of simple poles.

b) $W(L) = W^{\dagger}(L)$. In particular W is real if L is real > 0.

c) if L real > 0 then $\mathrm{d}W/\mathrm{d}L > 0$ if the derivative is defined.

d) $W(L)$ is a following function in the sense of WIGNER, that is $I(W)$ and $I(L)$ have always the same sign, moreover W is real only if L is real and it can have poles or zeros only on the real axis.

All these properties agree in characterizing $W(L)$ as Wigner's function of L [1], slightly generalized in the sense that continuous distributions of singularities are admitted on the cut while Wigner's function $R(E)$ was meromorphyc. Cond. *a*) ... *d*) restrict considerably the class of interpolations but they are not yet sufficient since some limitation has still to be imposed on the growth of W or K for large λ. We shall derive them in the next part. We only observe that *c*) implies a limitation also on the physical phase shifts. Indeed let us integrate (2.5) *c*) between $\lambda = j + \frac{1}{2}$ and $\lambda = j + \frac{3}{2}$; we find:

$$\delta_{j+1} - \delta_j < \frac{\pi}{2} . \tag{2.6}$$

This is a weak but simple condition on the phase shifts in order that they may be produced by a potential.

3. – If λ is large we expect the perturbation created by $U(x)$ to decrease so that perturbed functions will eventually approach the unperturbed at ∞. Although this statement is in general true there is a number of cases in which it is grossly false so that great care has to be taken in deriving results along this line. For instance it is not generally true that $\delta(\lambda)$ vanishes in the limit of large λ. We shall see that this holds for real λ only, if no condition is imposed on $U(x)$, being valid along any ray in $\pi/2 \geqslant \arg \lambda \geqslant -\pi/2$ for a very special class of potentials. We shall not bother here with a detailed explanation of how these results are derived. The general procedure is the following. We transform (1.1) into an equivalent Green's integral equation of the Volterra type in which the boundary conditions as already included. Suitable upper bounds are then placed upon the sum of the perturbative expansion using a Titchmarsh's lemma. In the Appendix we show the essential points in our procedure. It must be noted that sometimes the lack of simple formulae for

(1) E. WIGNER and J. NEUMANN: *Annals of Math.*, **59**, 418 (1954).

the Bessel functions of general complex order makes it impossible to derive some limit directly. It is then much better to derive the result, usually a condition on the growth of some analytic function in an angle, on the boundary of the domain and then to extend it in the inside using the Phragmen-Lindeloef theorem or its by-products. Using this technique it is possible to derive some more conditions on the interpolation which we state as follows:

$$\exp[-i\pi\lambda](\exp[2i\,\delta(\lambda)]-1)\to 0\,,\qquad -\frac{\pi}{2}<\arg\lambda\leqslant 0\,. \tag{3.1}$$

We can write it into the equivalent form

$$e)\colon\qquad \begin{cases} \lim\limits_{\lambda\to\infty}[K(\lambda)-K^0(\lambda)]=0\,, & \arg\lambda\neq 0,\\ \delta(\lambda)=O\left(\dfrac{1}{\lambda}\right). & \arg\lambda=0, \end{cases}$$

If $U(x)$ us specialized then we have stronger results.

For instance if $U(x)$ admits some bound of the kind: ($A>0$, $C>0$, $B>1$):

$$U(x)<C\exp[-Ax^B]\,,\qquad x>x_0=\text{const.} \tag{3.2}$$

Then

$$|\ln(K(\lambda)-K^0(\lambda))|<-\left(1-\frac{1}{B}\right)2|\lambda|\ln|\lambda|+0(|\lambda|)\,.$$

This bound is essentially the one derived by CARTER [2] for $\lambda=j+\frac{1}{2}$. If $B=1$, similar bounds of some use can be derived. A second way of restricting $U(x)$, of remarkable interest in connection with dispersion relations, is provided by the theorem:

« Let $U(x)$ admit an analytic continuation $U(z)$, $z=x+iy$, regular in the sector $\arg z<\sigma+\varepsilon<\pi/2$, and such that:

$$\int_0^{\infty e^{i\xi}}|z||\mathrm{d}z||U(z)|<\infty\,,\qquad |\xi|\leqslant\sigma$$

is uniformly bounded within the sector, and moreover $U(z)=0(z^{-2+2\sigma})$, $C>0$,

---

[2] D. S. CARTER: *Thesis*, Princeton; N. KHURI: *Phys. Rev.* **107** 1148 (1957). We have had no opportunity of examining directly CARTER's work and we know of his result only through KHURI's paper.

$\frac{1}{z} \to 0$, in the sector, then:

$$|K(\lambda) - K^0(\lambda)| = O(\exp[-2\sigma I(\lambda)]) . \tag{3.3}$$

Potentials satisfying the conditions of this theorem will be named σ-potentials those which do not 0-potentials. »

The proof of this theorem is based upon the WKB method. Indeed if one takes for granted the first WKB approximation then the above results already follow.

(3.2) and (3.3) are in a way complementary conditions on $U(x)$, indeed the first implies an upper bound on $\delta(\lambda)$ along $\arg\lambda = 0$ and nothing along $\arg\lambda = \pm\pi/2$, the second one works the opposite way. In the derivation of (3.3) it is essential to have $\sigma < \pi/2$, correspondingly it can be proved that a higher value of σ cannot improve the bound. Actually no potential attains:

$$|K(\lambda) - K^0(\lambda)| = O(\exp[-(\pi + \varepsilon)|\lambda|) , \quad \varepsilon > 0, \qquad \arg\lambda = \pm\frac{\pi}{2} . \tag{3.4}$$

This can be seen by applying Carleman's theorem to both sides of (3.4) or using Carlson's theorem on the function $F^+(\lambda)$ defined in Appendix IV. One can include $\pi/2$ in our discussion using the weaker statement that if some potentials is a σ-potential, where σ is any angle $< \pi/2$, then:

$$|K(\lambda) - K^0(\lambda)| = O(\exp[-(\pi - \varepsilon)I(\lambda)]) , \qquad \varepsilon > 0$$

ε can be taken small at will.

Finally we report some limit:

$$\lim_{\lambda\to\infty} \frac{S(\lambda)}{S^0(\lambda)} = \lim_{\lambda\to\infty} \frac{C(\lambda)}{C^0(\lambda)} = 1 \qquad \arg\lambda \neq 0, \qquad R(\lambda) > 0. \tag{3.5}$$

4. – We shall give here a method of construction of $U(x)$ from the interpolation $K(\lambda)$. We sketch here the essential points only without giving detailed proofs of our statements. We wish to point out also that some more research will be needed in order to cast the theory into a fully satisfactory and rigorous form. We believe, however, that this is more properly a mathematician's task and that what we are going to show here is already enough for the physicist's needs.

The starting point is, as in Gel'fand and Levitan's theory [3-5] an integral

---

[3] I. M. Gel'fand and Levitan: *Amer. Math. Soc. Trans.*, Sec. 2.1.250 (1955).
[4] R. Jost and W. Kohn: *Math. Phys. Medd.*, **27**, (9) (1953).
[5] L. D. Faddeev: *Soviet Phys. Dokl. Transl.*, **3**, 747 (1959).

equation of the Volterra type which relates $\varphi(\lambda, x)$ to $\varphi^0(\lambda, x)$ through a kernel which does not depend on λ:

$$\varphi(\lambda, x) = \varphi^0(\lambda, x) + \int_0^x \frac{K(x, y)\,\varphi^0(\lambda, y)}{y^2}\,\mathrm{d}y\,. \tag{4.1}$$

One can justify (4.1) from two points of view. The first is that by virtue of the asymptotic expansion (see Appendix):

$$\varphi(\lambda, x) = x^{\lambda+\frac{1}{2}}(1 + D) \quad \text{where} \quad D < \frac{Qx^2}{C|\lambda|}\,. \tag{4.2}$$

we have the Mellin representation:

$$\varphi(\lambda, x) = x^{\lambda+\frac{1}{2}} + \int_0^x H(x, y)\, y^{\lambda+\frac{1}{2}} \frac{\mathrm{d}y}{y^2}\,, \tag{4.3}$$

and of course a similar for $\varphi^0(\lambda, x)$. It can be shown that the latter can be solved in $x^{\lambda+\frac{1}{2}}$ and if this function is fed into (4.3) then (4.1) follows. The second way will be apparent later. The y^{-2} factor is merely inserted for symmetry.

In considering the functions $\varphi(\lambda, x)$ or $\varphi^0(\lambda, x)$ the natural problem arises whether they can be considered a complete and orthogonal set in the interval $0 \ldots \infty$. This problem has been considered since long by H. Weil and several other mathematicians. The reader will find a fully satisfactory overall view on this subject in [6]. We shall report here the results found with the help of [6]. The $\varphi(\lambda, x)$ are eigenfunctions of the linear operator: $(R(\lambda) \geqslant 0!)$

$$\Omega_x = x^2\left(\frac{\mathrm{d}^2}{\mathrm{d}x^2} + 1 - U(x)\right), \tag{4.4}$$

subjected to the condition of being of class L^2 in $0 \ldots \infty$ if we adopt the norm:

$$(\varphi, \psi) = \int_0^\infty \varphi(x)\,\psi^*(x)\,\frac{\mathrm{d}x}{x^2}\,. \tag{4.5}$$

(It must be clear that under this norm all solutions of (1.1) are L^2 in any interval $H \ldots \infty$). Using the standard terminology we are in the so called

---

[6] E. C. Titchmarsh: *Eigenfunction Expansions*, associated with second order differential equations I, II. (Oxford, 1946).

limit circle case. If no other condition is implied our set is clearly overcomplete and not orthogonal. We must find a subset which satisfies these conditions. This can be accomplished by imposing another boundary condition at ∞, which cannot be square integrability as in quantum mechanics, because it is already satisfied. The new condition is that all eigenfunctions should have the same asymptotic phase μ or, in other words, they must be multiples of $F(\lambda, \mu, x)$. Now there are only two types of choices of λ for this to happen:

$A)$ $R(\lambda) = 0$, we refer to it as the continuum

$B)$ $R(\lambda) > 0$, and $F(\lambda) = C(\lambda) \cos\mu + S(\lambda) \sin\mu = 0$.

In this case

$$F(\lambda, \mu, x) = F(-\lambda)\varphi(\lambda, x)$$

μ is here real and $0 < \mu < \pi$; for each value of μ we have a different expansion. It can be checked that all functions in A, B) satisfy the orthogonality relations:

$$\text{(4.6)} \quad \begin{cases} (F(\lambda, \mu, x),\ F(\lambda', \mu, x)) = 4\pi\,\delta(\lambda' - \lambda'^2)\,F(\lambda)\,F(-\lambda)\lambda\,, \\ \qquad\qquad \text{if} \quad R(\lambda) = 0, \quad R(\lambda') = 0\,, \\ (F(\lambda, \mu, x),\ F(\lambda_n, \mu, x)) = 0 \qquad F(\lambda_n) = 0, \qquad F(\lambda_m) = 0, \\ (F(\lambda_n, \mu, x),\ F(\lambda_m, \mu, x)) = -\,\delta_{nm}\,\dfrac{1}{2\lambda F(\lambda_n, \mu - (\pi/2))\,F'(\lambda_n, \mu)}\,. \end{cases}$$

Moreover there are infinitely many zeros of $F(\lambda)$, all real. We have correspondingly the expansion theorem:

$$\text{(4.7)} \qquad \delta(x - y) = \frac{1}{2i\pi}\int_P \mathrm{d}\lambda\,\frac{\varphi(\lambda, x)}{x}\,\frac{F(\lambda, \mu, y)}{y\,F(\lambda, \mu)}\,.$$

The path P is shown in Fig. 1. This path can be deformed into $R(\lambda) = 0$, and to loops which enclose the zeros of $F(\lambda, \mu)$. From $R(\lambda) = 0$ we have the A terms, from the loops the B terms. Some remarks are needed for (4.7); it is clearly a symbolical formula and statements of the kind: the Dirac function in (4.7) is independent of μ, and so must be the second term, are in general meaningless or false since $\delta(x - y)$ is a distribution in a space whose definition depends on μ. However, under some

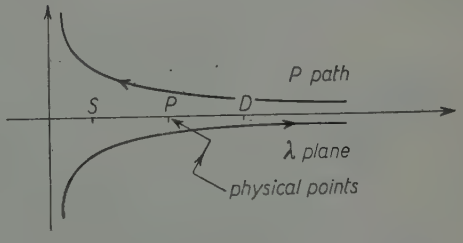

Fig. 1.

conditions, whose exact form will not be stated here, it is true that

$$(4.8) \qquad f(x) = \frac{1}{2\pi i}\int_P \mathrm{d}\lambda\, g(\lambda)\frac{F(\lambda,\mu,x)}{xF(\lambda,\mu)}, \qquad \text{if} \quad g(\lambda) = \int_0^\infty \mathrm{d}x \frac{1}{x}\varphi(\lambda,x) f(x),$$

in particular (4.8) holds if $f(x)$ decreases fast enough. In (4.1) we have always $x > y$; we define $K(x, y)$ also when $y < x$ through the reversed equation:

$$(4.9) \qquad \varphi^0(\lambda, y) = \varphi(\lambda, x) - \int_0^y K(x, y)\varphi(\lambda, x)x^{-2}\,\mathrm{d}x .$$

Under these assumptions we find the following integral representation from (4.9), (4.1) and (4.7):

$$(4.10) \qquad K(x, y) = \frac{1}{2\pi i}\int_P \mathrm{d}\lambda \left[\frac{F^0(\lambda,\mu,x)}{F^0(\lambda,\mu)}\varphi(\lambda, x) - \frac{F(\lambda,\mu,x)}{F(\lambda,\mu)}\varphi^0(\lambda, y)\right].$$

From (4.10) one can verify the differential equation:

$$(4.11) \qquad \Omega_x K(x, y) = \Omega_y K(x, y),$$

(4.1), (4.9) and (4.11) are consistent with (1.1) provided

$$(4.12) \qquad K(x, x) = \frac{x}{2}\int_0^x y\, U(y)\,\mathrm{d}y, \qquad K(x, y) = O(x), \qquad O(y), \qquad x, y \to 0.$$

Conversely (4.11), (4.12) can be used to define $K(x, y)$ as the solution of a certain differential partial equation with appropriate boundary conditions. The so defined $K(x, y)$, if fed into (4.1) generates a function which satisfies (1.1) with the appropriate boundary condition. This is a second way of justifying (4.1). By rewriting (4.10) as follows ($\mu = 0$):

$$(4.13) \qquad K(x, y) = \frac{1}{2\pi i}\int_{-i\infty}^{+i\infty} \mathrm{d}\lambda \left[\frac{C^0(-\lambda)}{C^0(\lambda)} - \frac{C(-\lambda)}{C(\lambda)}\right]\varphi(\lambda, x)\varphi^0(\lambda, y) +$$

$$+ \frac{1}{2\pi i}\int_{\text{loops}} \mathrm{d}\lambda \frac{1}{2\lambda}\left[\frac{1}{C(\lambda)S(\lambda)} - \frac{1}{C^0(\lambda)S^0(\lambda)}\right]\varphi(\lambda, x)\varphi^0(\lambda, y),$$

where the « loops » integral encloses the zeros of $C(\lambda)$ and $C^0(\lambda)$ only, avoiding

those of $S(\lambda)$, $S^0(\lambda)$, and defining $Q(x, y)$ through the same formula where $\varphi(\lambda, x)$ has been replaced everywhere by $\varphi^0(\lambda, x)$ the integral equation follows:

$$K(x, y) = Q(x, y) + \int_0^x K(x, z)\, Q(x, y)\, \frac{dz}{z^2}. \tag{4.14}$$

If $K(x, y)$ is regarded as an unknown in (4.14) this equation is of the Fredholm type. It can be shown that the homogeneous counterpart of (4.14) has no non-trivial solutions and we assume therefore that (4.14) can be always solved under very large conditions. From $Q(x, y)$ we can deduce therefore $K(x, y)$ and $K(x, x)$ in particular. (4.12) yields then $U(x)$. Moreover, $Q(x, y)$ involves $\varphi^0(\lambda, x)$, which is an elementary function, and essentially the ratios $C(-\lambda)/C(\lambda)$, $S(-\lambda)/S(\lambda)$, having noticed from (1.8) that

$$\frac{C(-\lambda)}{C(\lambda)} - \frac{S(-\lambda)}{S(\lambda)} = -\frac{1}{2\lambda\, C(\lambda)\, S(\lambda)}.$$

The knowledge of these ratios implies that of $U(x)$. We are left with the task of connecting them to the interpolation $K(\lambda)$. To carry it out we observe that in virtue of $C(ia) = C(-ia)^*$ and $S(ia) = S(-ia)^*$ these ratios are simply exponential functions of arg $C(ia)$ and arg $S(ia)$. At the same time from (1.8) we know that:

$$K(\lambda) - K(-\lambda) = \frac{1}{2\lambda\, C(\lambda)\, C(-\lambda)}.$$

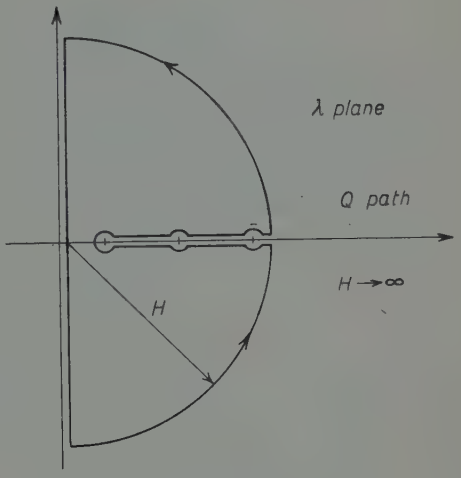

Fig. 2.

We can calculate $\ln|C(\lambda)|$ and similarly $\ln|S(\lambda)|$ from the interpolation. However, owing to (3.5) arg $C(\lambda)/C^0(\lambda)$ and $\ln|C(\lambda)/C^0(\lambda)|$ if $\lambda = ia$ are in some sense conjugate functions if one forgets about the zeros of $C(\lambda)$ and $C^0(\lambda)$. We can still relate them by taking the real and imaginary part of Cauchy's formula:

$$\frac{1}{2\pi i}\int_Q \frac{1}{\lambda - ia - \varepsilon} \ln\frac{C(\lambda)}{C^0(\lambda)}\, d\lambda = \ln\frac{C(ia)}{C^0(ia)}, \qquad \varepsilon > 0 \text{ small.} \tag{4.15}$$

Q means here a path which avoids the branch points of the integrand, as shown in Fig. 2. The result expresses arg C/C_0 as an Hilbert transform of $\ln|C/C_0|$

with an infinite series of additional terms which depend on the location of the branch points, which in turn are perfectly known from $K(\lambda)$. This series converges because the zeros of $C(\lambda)$ and those of $C^0(\lambda)$ tend to be very close when λ is large and to cancel each other. Similarly one proceeds with $S(\lambda)$. We have completed the chain from $K(\lambda)$ up to $U(x)$. The only problem left now is the actual construction of $K(\lambda)$ from the values that it takes at $\lambda = j+\frac{1}{2}$. This problem is still unsolved although we are well on the way to do it. We shall discuss it in the next part.

5. – We shall give here some heuristic arguments on the interpolation problem. Our starting point is Carleman's theorem ([5]):

$$(5.1)\quad \sum_n \left(\frac{1}{h_n}-\frac{h_n}{H^2}\right)\sin\theta_n - \sum_m \left(\frac{1}{k_m}-\frac{k_m}{H^2}\right)\sin\theta_m = \frac{1}{\pi H}\int_{-\pi/2}^{\pi/2} \ln|L(He^{i\theta})|\cos\theta\,\mathrm{d}\theta + \\ + \frac{1}{2\pi}\int_0^H \left(\frac{1}{a^2}-\frac{1}{H^2}\right)\ln|L(ia)L(-ia)|\,\mathrm{d}a + \frac{1}{2}R[L'(0)]\,,$$

$L(\lambda)$ is in this theorem a general analytic function of λ; regular in $R(\lambda)>0$ with the exception of poles in $k_m \exp[i\theta_m]$ and having zeros at $h_n \exp[i\theta_n]$. Suppose now that we have two interpolations of the same set of phase shifts: $K(\lambda)$ and $H(\lambda)$. The difference $K(\lambda)-H(\lambda)$ must have zeros at least in $\lambda = j+\frac{1}{2}$ and poles at most at the poles of $K(\lambda)$ and $H(\lambda)$. (We cannot exclude that $K(\lambda)$ and $H(\lambda)$ coincide elsewhere and that either a new zero arises or two poles coalesce). The poles are distributed with the density 1. Supposing $L(\lambda)=K(\lambda)-H(\lambda)$ the contributions of zeros and poles in (5.1) are nearly opposite and of the order of $\ln H+\text{const}$. Their algebrical sum will tend to a constant limit. What can be said about the contribution of the boundary? For the sake of simplicity let us restrict ourselves to $H(\lambda)=K^0(\lambda)$ so that the problem now is to find a potential (in the following $V^0(x)$) which produces no scattering at a given energy. We have now some very useful estimate of the decrease of $L(\lambda)$ on the boundary. Quite generally $L(\lambda)$ will decrease in such a fashion as to make $Y(H)$ eventually negative and $J(H)$ decreasing. If, however, condition (3.2) is used we see that $Y(H)$ can be made arbitrarily large and negative if H is chosen sufficiently large, so that unless $K(\lambda)=K^0(\lambda)$ we face a contradiction in (5.1). Similarly, if $V^0(x)$ were a σ-potential $J(H)$ could be made arbitrarily large and negative and (5.1) would be again an absurdity. We see therefore that $V^0(x)$ must be a σ-potential which does not decrease faster than any exponential. The usual field theoretical potentials are therefore excluded. These results can be generalized and it can be shown that there is at most one σ-potential which yields a given set of phase shifts at a given energy. In some sense we find unicity in the inversion problem

under rather broad conditions, that is, analiticity requirements in an arbitrarily small angle.

A specific example of $V^0(x)$ can be constructed as follows. We take $H^0(\lambda) = (K^0(\lambda) - 1)/(K^0(\lambda) + 1)$, $H^0(\lambda)$ is again a Wigner's function of λ^2 and it satisfies therefore all the same requirements of $K^0(\lambda)$. It has alternatively zeros and poles in the physical points. If $H(\lambda) = (K(\lambda) - 1)/(K(\lambda) + 1)$ then the ansatz $H(\lambda) = H^0(\lambda) \cdot [1 + (C/(\lambda^2 - \lambda_0^2))]$, where C and λ_0 are constants, still satisfies the correct properties and yields vanishing phases since both $H(\lambda)$ and $H^0(\lambda)$ take the same values at the physical points. λ_0 and C are not entirely arbitrary otherwise $H(\lambda)$ may be somewhere a non-increasing function. Since it is enough here to show the existence of at least two different interpolations we shall be satisfied with one example only which is provided by taking $H^0(\lambda) < 0$ and C small as readily checked. The general problem is still unsolved and we hope to tackle it in a forthcoming paper. In analogy to Bargman's potentials which are solvable for all energies but for a single partial wave it is possible to give potentials which are solvable for all values of the angular momentum at a fixed energy. Since these potentials are a rather academic case we shall deal with them in some future work.

6. – In this part we shall establish some results in the field of dispersion relations. As well-known these relations are statements of analiticity of the scattering amplitude as function of the energy and the transmitted momentum. Although here the energy is kept fixed it is still possible to derive for special classes of potentials enough properties as to guarantee for the existance of such relations. We restrict ourselves to σ-potentials ($\sigma \neq 0$) and moreover we impose some additional condition on $U(x)$ as follows:

$$|U(x)| < C \frac{\exp[-\alpha x]}{x}, \qquad x > x_0. \tag{6.1}$$

Correspondingly, the phase shift will decrease like $\exp[-\alpha' \lambda]$ along the real λ, where $\alpha' = \ln(1 + (\alpha^2/2)) < \alpha$.

Under these conditions we have the following asymptotic estimate:

$$\exp[2i\,\delta(\lambda)] - 1 \sim O(\exp[i(\pi - 2\sigma)\lambda - \alpha'\lambda]), \qquad -\frac{\pi}{2} \leqslant \arg \lambda \leqslant 0\,. \tag{6.2}$$

In these rough extimates we have neglected powers of λ which are not essential in our discussion. (6.2) is very useful if the Legendre expansion of the scattering amplitude:

$$f(z) = f(\cos\theta) = \frac{1}{2i} \sum_{j=0}^{\infty} (2j+1)(\exp[2i\delta_j] - 1)\, P_j(z)\,, \qquad z = \cos\theta, \tag{6.3}$$

is transformed into the integral:

$$f(z) = \frac{1}{2}\int \lambda \, d\lambda \, (\exp[2i\,\delta(\lambda)] - 1) \, \frac{1}{\cos \pi\lambda} \, P_{\lambda-\frac{1}{2}}(-z) \, . \tag{6.4}$$

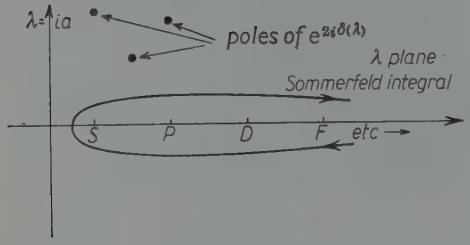

Fig. 3.

This artifice is due to WATSON and it was used by SOMMERFELD (7) in some wave propagation problems. The integration path is shown in Fig. 3. It encloses the zeros of $\cos \pi\lambda$ and avoids the poles of the integrand in the upper quadrant. The important fact about it is that it may converge outside the customary Legendre ellipse. To prove it, one needs an asymptotic expansion of Legendre functions of large order:

$$P_{\lambda-\frac{1}{2}}(z) \sim \frac{1}{\sqrt{2\pi \sin\theta \cdot \lambda}} \exp[\pm i\lambda(\theta - \pi)] \, . \tag{6.5}$$

One must choose the sign which yields the larger result. From (6.5) and (6.2) one sees that it is possible to deform the path in the lower quadrant into $\lambda = ia$, $a < 0$, provided one has $(\theta = \theta_0 + i\theta_1)$

$$\theta_1 < \alpha' \qquad \text{and} \qquad \theta_0 > \pi - 2\sigma \, . \tag{6.6}$$

If the first condition is dropped the lower part of the deformed integral still makes sense but the original expansion diverges. We have to deal now with the upper part where we did not apply immediately the same artifice because of the poles in the integrand. From (6.2) we see that:

$$\exp[2i\,\delta(\lambda)] \to 1 \qquad \text{if} \qquad 0 < -\arg\lambda < \xi_0 \, ,$$

where

$$\operatorname{tg} \xi_0 = \frac{\alpha'}{\pi - 2\sigma} \, .$$

Correspondingly, the same limit holds in $0 < \arg\lambda < \xi_0$.

It follows that within this sector there is at most a finite number of poles

(7) A. SOMMERFELD: *Partielle Differential-Gleichungen der Physik* (Leipzig, 1947), p. 285.

of $\exp[2i\delta(\lambda)]$. The upper part of the path can be deformed along $\arg\lambda = \xi_0$, and the poles in the sector yield a finite sum of residues which are analytic functions (Legendre functions) of z, in the z plane cut along z real > 1.

If we now try to shift the upper path along $\lambda = ia$, $a > 0$ we find that, apart from the contribution of poles, (6.4) still makes sense provided $\theta_0 > 0$ which is included in (6.6). The infinitely many poles yield a converging series if the values of the integral along an arc of arbitrarily large radius A indented in $\lambda = iA$ and $\lambda = A\exp[i\xi_0]$, vanishes for $A \to \infty$. This can be achieved if the condition

$$\theta_1 < \frac{\alpha'}{\pi - 2\sigma}[4(\pi - \sigma) - \theta_0], \tag{6.7}$$

is satisfied. Now particularly interesting are the values $\theta = \pi + i\theta_1$ which correspond to z real < -1 or in the dispersion relation language to $\tau > 2k$, τ being the transmitted momentum and k the wave number, $(x = kr)$. If σ can be taken arbitrarily near to $\pi/2$ then θ_1 may be arbitrarily large and correspondingly there is analyticity in z along the whole negative axis and, for arbitrary large real values of τ.

This result holds in particular for all those potentials which can be included into the formula

$$x\,U(x) = \int_{\alpha}^{\infty} \exp[-px] f(p)\,dp\,, \tag{6.8}$$

Now from the previous literature (see [2,8]) one knows that $f(k, \tau)$ is, for τ fixed real, and an analytic function of k in the whole upper plane $I(k) > 0$ (*) approaching $f_B(\tau)$ (Born approximation) for large k, if $\tau < 2\alpha$. If the latter condition is not satisfied, a domain D arises where analyticity cannot be proved with the usual methods. This domain $D = D(\tau)$ however can be enclosed in a sufficiently large semicircle with center in $k = 0$. Moreover, $f(k, \tau)$ still approaches $f_B(\tau)$ when k is large. We know that $f(k, \tau)$, if k is real, is analytic in a region which in terms of $z = 1 - (\tau^2/2k^2)$ is the sum of the interior of the ellipse of convergence and of the domain defined in (6.7) and the second of (6.6). In particular if k is kept fixed real and $\neq 0$, $f(k, \tau)$ is an analitic function of τ for real arbitrary positive values of τ and in a suitable neighbourhood of them. The same result can be proved with a limiting procedure when $k = 0$. It is remarkable then that analyti-

---

([8]) S. GASIOROWICZ and H. P. NOYES: *Nuovo Cimento*, **10**, 78 (1958).

(*) Bound states will not be considered here. However these can be easily included into the theory.

city follows in the whole $I(k) > 0$ plane. Indeed one can take a semicircle enclosing $D(\tau)$, where $\tau < T =$ constant. Applying Cauchy's theorem to this semicircle we get

$$f(k, T) = \frac{1}{2\pi i} \int_{\hat{C}} \frac{f(k, T)}{h - k} \, \mathrm{d}h \,. \tag{6.9}$$

If $\tau > 2\alpha$ this formula still defines a function, analytic in k and τ, the latter analyticity follows from the fact that all values on the boundary are analytic functions of τ. (6.9) defines a function also within D which must be the analytic continuation of the original function because it coincides with it outside D where is was defined. Take namely k outside $D(\tau)$ but inside the semicircle and split the semicircle into two closed loops, the first enclosing D but not k, the latter k but not $D(\tau)$. The contribution of the first is an analytic function of τ which vanishes if $\tau < 2\alpha$ and therefore always the last just yields the original function. The result follows. The above arguments are standard ideas from the theory of several complex variables. For special potentials one gets still stronger results. Indeed suppose that $|V(z)| < H/z^2$ within and along the boundary of $|\arg z| \leqslant \pi/2$. Let λ^0 be a pole of $\exp[2i\,\delta(\lambda)]$. From the discussion above we know that $R(\lambda^0) > 0$, $I(\lambda^0) > 0$. Moreover $\varphi(\lambda^0, z) \sim C \exp[iz]$ if $z \to \infty$. Also

$$\varphi''(\lambda^0, z) + \varphi(\lambda^0, z) - \frac{\lambda_0^2 - \frac{1}{4}}{z^2} \varphi(\lambda^0, z) - U(z) \varphi(\lambda^0, z) = 0 \,. \tag{6.10}$$

Take now $z = iy$; y real. Then $\varphi \sim C \exp[-y]$ and

$$\ddot{\varphi} - \varphi - \frac{\lambda^{02} - \frac{1}{4}}{y^2} \varphi - U(iy)\varphi = 0 \,, \tag{6.11}$$

the dots now refer to y derivatives. The conjugate reads

$$\ddot{\varphi}^* - \varphi^* - \frac{\lambda^{0*2} - \frac{1}{4}}{y^2} \varphi^* - U(-iy)\varphi^* = 0 \,. \tag{6.12}$$

We multiply now (6.11) by φ^* and subtract (6.12) multiplied by φ. The resulting equation is then integrated between $0 \ldots \infty$. We obtain

$$(\lambda^{02} - \lambda^{0*2}) \int_0^\infty \frac{|\varphi|^2}{y^2} \, \mathrm{d}y = -2i \int_0^\infty I(U(iy)) \, |\varphi|^2 \, \mathrm{d}y \,. \tag{6.13}$$

If $I(U(z))$ is replaced by M/y^2 we obtain

$$R(\lambda^0) I(\lambda^0) < \frac{M}{2} \,. \tag{6.14}$$

This is a restriction on the position on poles: this result enables us to say that only a finite number of poles have $R(\lambda^0) > m+\frac{1}{2}$ where $m+\frac{1}{2}$ is some positive constant. In the Sommerfeld integral one can use $R(\lambda) = m+\frac{1}{2}$ as path, the contribution of the extra poles can be evaluated and yields a finite sum which diverges at most like some power of $-\cos\theta$ or τ when those quantities are large. The contribution of the $R(\lambda) = m+\frac{1}{2}$ path can be best evaluated by using (see App. V) asymptotic expansions of Legendre functions:

$$(6.15)\quad \begin{cases} f(\cos\theta) = \dfrac{1}{2\sqrt{\pi}} \displaystyle\int_{-\infty}^{\infty} \frac{\Gamma(\lambda)}{\Gamma(\lambda+\frac{1}{2})\cos\pi\lambda}\, \zeta\, \mathrm{d}\zeta\, \{\exp[2i\,\delta(\lambda)] - 1\} \cdot \\ \qquad\qquad \cdot \exp[i\zeta\theta_1 + \zeta(\theta_0 - \pi)] \cdot (-2\cos\theta)^m\,, \\ \lambda = m + i\zeta + \frac{1}{2} + \text{contr. extra poles.} \end{cases}$$

This contribution is therefore seen to be growing at most like some power of $-\cos\theta$ or τ when these variables are large in modulus (the cut $\cos\theta$ real > 1 being excluded). The Mandelstam representation can then be derived.

* * *

The author wishes to thank Dr. Symanzik for many suggestions and constant advice. This work was partially supported by the American Air Force.

Appendix I

In order to calculate $P(\lambda)$ we notice that $\varphi(\lambda, x)^* = \varphi(\lambda^*, x)$ and that :

$$(A.1)\qquad \varphi(\lambda, x)\,\varphi''(\lambda^*, x) - \varphi''(\lambda, x)\,\varphi^*(\lambda, x) = \frac{1}{x^2}(\lambda^{*2} - \lambda^2)\,|\varphi(\lambda, x)|^2,$$

or if λ is real:

$$(A.2)\qquad \varphi(\lambda, x)\frac{\partial}{\partial\lambda}\varphi''(\lambda. x) - \varphi''(\lambda, x)\frac{\partial}{\partial\lambda}\varphi(\lambda, x) = \frac{2\lambda}{x^2}\varphi(\lambda, x)^2\,.$$

Integration of these indentities between $0 \ldots \infty$ yields the desired formulas. The asymptotic behaviour of $\varphi(\lambda, x)$ for large x can be obtained through (15) and (1.3).

Appendix II

Most of the bounds used in this paper can be derived from suitable integral equations of the Volterra type and from the following lemma (5):

Lemma: Let $f(x) \geqslant 0$, $g(x) \geqslant 0$ and let $f(x)$ be continuous $g(x)$ integrable in $0 \leqslant x \leqslant X$. Let $f(x) < C + \int_0^x f(t)\, g(t)\, dt$, $0 \leqslant x \leqslant X$. Then $f(x) < C \exp\left(\int_0^x g(t)\mathrm{d}t\right)$ $0 \leqslant x \leqslant X$.

This lemma will be used also in the interval $X \ldots \infty$ with obvious modifications. We list here the integral equations which we have used and the functions which in our derivation correspond to $f(x)$ and $g(x)$.

$$\text{(I)} \qquad \varphi(\lambda, x) = x^{\lambda+1} + \frac{1}{2\lambda}\int_0^x (U(y) - 1)\, \varphi(\lambda, y) \left[\frac{x^{\lambda+1}}{y^\lambda} - \frac{y^{\lambda+1}}{x^\lambda}\right] \mathrm{d}y\,.$$

We have if $R(\lambda) > 0$: $(y < x)$

$$\left|\frac{x^{\lambda+1}}{y^\lambda} - \frac{y^{\lambda+1}}{x^\lambda}\right| < 2\left|\frac{y}{x}\right|^\lambda |x|\,;$$

we take $f(x) = |\varphi(\lambda, x) x^{-\lambda-1}|$ and $g(x) = |U(x) - 1|\,|x|(1/|\lambda|)$: the result is essentially (4.2). A similar bound holds for $\varphi'(\lambda, x)$

$$\text{(II)} \qquad C(\lambda, x) = \cos\left(x - \frac{\pi}{4}\right) + \int_x^\infty \left[\frac{\lambda^2 - \frac{1}{4}}{y^2} + U(y)\right] C(\lambda, y) \sin(y - x)\, \mathrm{d}y;$$

here we replace the sines and cosines with 1 and take $C = 1$, $f(x) = |C(\lambda, x)|$, $g(x) = |((\lambda^2 - \frac{1}{4})/x^2) + U(x)|$. We obtain a result of the form:

$$|C(\lambda, x)| < C \exp\left[\frac{\lambda^2}{x}\right], \qquad \lambda \text{ large.}$$

Similarly we find a corresponding bound on $C'(\lambda, x)$ and on $S(\lambda, x)$ and $S'(\lambda, x)$. Introducing these bounds in the identity:

$$2\lambda\, C(\lambda) = C(\lambda, x)\, \varphi(\lambda, x) - C'(\lambda, x)\, \varphi(\lambda, x)$$

and taking $x = \lambda$ we find

$$\text{(A.3)} \qquad |C(\lambda)| < |\lambda^\lambda C^\lambda|\,,$$

where C is some constant. This bound, although very rough, can be sharpened with the help of Phragmen-Lindeloef's theorem (9):

$$\text{(III)} \qquad C(\lambda, x) = C^0(\lambda, x) + \int_0^\infty U(y)\, C(\lambda, y)[C^0(\lambda, x)\, S^0(\lambda, y) - C^0(\lambda, y)\, S^0(\lambda, x)]\, \mathrm{d}y\,.$$

We consider this equation for $\lambda = ia$ (a real) only, since otherwise no reliable bound on the unperturbed solutions is available. We know from the Poisson integral representation of Bessel functions that:

$$C^0(\lambda, x)\,, \quad S^0(\lambda, x) < E\sqrt{\pi x}\,, \qquad \lambda = ia,$$

where $E > 1$ is a suitable constant.

The bound holds uniformly in x, λ since E does not depend on them. We take $C^0(\lambda, x) = f(x)E\sqrt{\pi x}$, $g(x) = 2xU(x)\pi E^2$ and since $\int_0^\infty x\,|U(x)\,| = Q < \infty$, we have:

$$\text{(A.4)} \qquad C(\lambda, x) < E\sqrt{\pi x}\, \exp[2\pi E^2 Q] = E'\sqrt{\pi}\, x\,,$$

which is of the same type. The same results follows for $S(\lambda, x)$,

$$\text{(IV)} \quad \varphi(\lambda, x) = \varphi^0(\lambda, x) + \frac{1}{2\lambda}\int_0^\infty U(y)\varphi(\lambda, y)[\varphi^0(\lambda, x)\varphi^0(-\lambda, y) - \varphi^0(\lambda, -x)\,\varphi^0(\lambda, y)]\, \mathrm{d}y.$$

As in (III) we suppose $\lambda = ia$. We have the preliminary inequality:

$$\varphi^0(\lambda, x) < F\sqrt{\lambda\pi x} \qquad F \text{ const.}$$

we take then $\varphi(\lambda, x) = f(x)F\sqrt{\lambda\pi x}\, x$ and $g(x) = 2xU(x)\pi F^2$ and as before we derive a bound of the kind:

$$\text{(A.5)} \qquad \varphi(\lambda, x) < F'\sqrt{\lambda\pi x} \qquad F' \text{ is a constant.}$$

From (A.5) and the formula:

$$\text{(A.6)} \qquad C^0(\lambda) + \frac{1}{2\lambda}\int_0^\infty U(x)\, C^0(\lambda, x)\, \varphi(\lambda, x)\, \mathrm{d}x = C(\lambda)\,.$$

we can prove (3.5) along $R(\lambda) = 0$, $a \to \infty$. Indeed if we split the interval of integration in $0 \ldots \sqrt{a}$ and $\sqrt{a} \ldots \infty$ we find the following bound using (A.5):

$$\int_{\sqrt{a}}^\infty U(x)\, C^0(\lambda, x)\, \varphi(\lambda, x)\, \mathrm{d}x < \pi E F' \sqrt{|\lambda|} \int_{\sqrt{|\lambda|}}^\infty x\,|U(x)\,|\, \mathrm{d}x\,.$$

(9) R. P. Boas: *Entire Functions* (New York, 1955).

This part is $o(\sqrt{\lambda})$ and negligible [$C^0(\lambda)$ is $o(\sqrt{\lambda^{-1}})$]. In $0 \ldots \sqrt{a}$ we expand $C^0(\lambda, x)$ following (1.9) and use (4.2). If $0 < x < \sqrt{a}$ from (4.2) we deduce:

$$\varphi(\lambda, x) = x^{\lambda+1}(1 + O(1)) \qquad \lambda \text{ large.}$$

Two terms arise from (A.6):

$$C^0(\lambda) \int_0^{\sqrt{a}} x U(x) (1 + O(1)) ,$$

and

$$C^0(-\lambda) \int_0^{\sqrt{\lambda}} x U(x) x^{2\lambda} (1 + O(1)) \, \mathrm{d}x .$$

Both are negligible. The limit follows. We have shown here the simplest obtainable bounds. A more refined estimate can be derived using the WKB method but we deliver it to the next Appendix.

Appendix III

The WKB method gives fairly simple estimates of the wave function when λ is large but it is difficult to estimate the error when λ and x are simultaneously complex. Fortunately it is enough for our purposes to take $\lambda = ia$ and x complex. In this case, provided a is large enough, there are no turning points if $U(x)$ is a σ-potential. Indeed it is clear that in this case $U(z)$ admits the Cauchy's rapresentation:

$$z U(z) = \frac{1}{2\pi i} \int_{\infty \exp[-i\sigma']}^{\infty \exp[i\sigma']} \frac{z' U(z')}{z - z'} \, \mathrm{d}z' \qquad \sigma' = \sigma + \varepsilon.$$

The integration path is stretched along the two half-lines $+\infty \exp[-i\sigma'] \ldots 0$ and $0 \ldots \infty \exp[i\sigma']$. Now within $|\arg z| \leqslant \sigma$ we have $|z - z'| \geqslant z \sin \varepsilon$ and clearly:

$$|z U(z)| < \frac{M}{|z| \sin \varepsilon} \qquad \text{or} \qquad U(z) < \frac{M}{z^2 \sin \varepsilon} ,$$

were $M = (1/\pi) \int_0^{\infty \exp[i\sigma]} |z| \, |\mathrm{d}z U| \, (z)|$. Similarly

$$U^{(n)}|z| < \frac{M_n}{z^{2+n}}; \qquad M_n \text{ const.}$$

In order to avoid turning points the function $a^2+z^2+z^2U(z)$ must have no zeros in the sector $B\ |\arg z|<\sigma$. Suppose now that there is Z such that $a^2+Z^2U(Z)=-Z^2$. We have $Z^2U(Z)<(M/\sin\varepsilon)=M'$. Now $Z^2=-a^2+pe^{i\xi}$, where $p<M'$ and if a is taken large enough

$$z\sim\pm\left(ia+\frac{p\exp[i\xi]}{2ia}\right)\quad\text{and}\quad\arg z\sim\pm\frac{\pi}{2}.$$

Hence Z will eventually fall out of the sector Σ which will be free of zeros. If we define $s^2(a,z)=a^2+z^2+z^2U(z)$ one can prove with similar arguments that there exists, for sufficiently large a, a constant C such that:

(A.7) $$|s(z)|>Ca \qquad (C \text{ ind. of } a \text{ and } z).$$

It follows that if we defines $\xi(z)$ through the equations:

$$\frac{\mathrm{d}\xi}{\mathrm{d}z}=\frac{S(a,z)}{z},\qquad\lim_{z\to a}(\xi(z)-a\ln z)=0\qquad z\text{ in }\Sigma,$$

$\xi(z)$ is a single valued regular analytic function of z in Σ. In particular

$$\xi^0(z)=a\ln z-a\ln(a+\sqrt{a^2+z^2})+\sqrt{a^2+z^2}-a+a\ln 2a\,.$$

From (A.7) one can prove then

(A.8) $$|\xi(z)-\xi^0(z)|<\frac{H}{a},$$

where H is independent of z and a. All these inequalities require explicitly $|\sigma|<\pi/z$ equality beeing excluded. Let us define also $w(\xi)=\sqrt{s(z)}\cdot\psi(z)$, where $\psi(z)$ is any solution of (1.1). (1.1) transforms then into:

(A.9) $$\frac{\mathrm{d}^2w}{\mathrm{d}\xi^2}+w=-J(z)\,w\,,$$

where

$$J(z)=\frac{1}{4s^2}\left\{\frac{5}{4}\left[z\frac{\mathrm{d}}{\mathrm{d}z}s^2(z)\right]^2+s(z)^2\left[z^2\frac{\mathrm{d}^2}{\mathrm{d}z^2}s^2(z)+zs^2(z)\right]\right\}.$$

Putting then $X(z)=\sqrt{s(z)/az}\,\varphi(\lambda,z)$, we readily derive the integral equation:

(A.10) $$X(z)=\exp[i\xi(z)]-\int_0^z\sin[\xi(z)-\xi(t)]\,s(t)\,X(t)\,s(t)\,\frac{\mathrm{d}t}{t}\,.$$

Take now $X_1(z)=\exp[-i\xi]X(z)$. $X_1(z)$ satisfies:

(A.11) $$X_1(z)=1-\int_R\frac{1-\exp[2i(\xi(z)-\xi(t))]}{2i}\,J(t)\,X_1(t)\,s(t)\,\frac{\mathrm{d}t}{t}\,.$$

We choose a path R of integration such that along it $I(\xi^0(z)) < I(\xi^0(t))$. It can be proved from the formula for $\xi^0(z)$ that $I(\xi^0(t))$ increases along $\arg t = \text{const}$ and decreases along $I(\sqrt{a^2+t^2}) = \text{const}$. Suppose $I(\xi^0(z)) = a\sigma$. A suitable path is then R_I: $\arg t = \sigma$ and the line R_z:

$$I(\sqrt{t^2+a^2}) = I(\sqrt{z^2+a^2}) .$$

With this position

$$|\exp[2i(\xi^0(z) - \xi^0(t))]| < 1 .$$

Consequently from (A.8) we have when a is large:

$$\left|\frac{1-\exp[2i(\xi(z)-\xi(t))]}{2i}\right| < K = \text{const} .$$

R has a corner T where R_1 and R_2 meet. We have $T = O(a)$. We need now some simple bound on $J(t)$. If $0 < t < T$ one can use (A.7), if $t > T$ then $s(t) > C't$ is also needed. Omitting here the details we arrive at the conclusion that:

$$\int_R |J(t)\, s(t)| \frac{\mathrm{d}t}{t} = O(a^{-1}) .$$

The above estimate holds uniformly for all z such that $I(\xi(z)) = a$. It follows from the lemma that on this line Q one has $X_1(z) = O(1)$ uniformly. Also on Q we have:

$$|\varphi(ia, z)| < C\sqrt{z_>}\exp[-a\sigma] ,$$

where C is some constant, $z_>$ the largest between z, a.

Finally from (A. 6) we derive:

$$C(\lambda)\, S^0(\lambda) - C^0(\lambda)\, S(\lambda) = -\frac{1}{4\lambda^2}\int_0^\infty U(z)\, \varphi^0(\lambda, z)\, \varphi(\lambda, z)\, \mathrm{d}z . \tag{A.12}$$

In (A.12) the integration can be carried out along Q and the above found inequality introduced. Dividing both sides by $C(\lambda)\, C^0(\lambda)$ the result follows. More details on this technique can be found in [6].

Appendix IV

We suppose now that λ is large positive. Our starting point is eq. (IV) (Appendix III). We take firstly $x \leqslant \lambda$. From the general theory of Bessel functions it is easy to prove that $\varphi^0(\lambda, x) > 0$ and that for sufficiently large

λ, $\varphi^0(\lambda, x)x^{-M}$, $M > \frac{1}{2}$ is an increasing function. From the identity:

$$G(x, y, \lambda) = \varphi^0(\lambda, x)\varphi^0(-\lambda, y) - \varphi^0(\lambda, y)\varphi^0(-\lambda, x) =$$

$$= 2\lambda\varphi^0(\gamma, x)\varphi^0(\lambda, y)\int_y^\infty \frac{\mathrm{d}z}{\varphi^0(\lambda, z)^2}, \qquad \infty \geqslant y,$$

replacing $\varphi^0(\lambda, z)$ with the smaller quantity $\varphi^0(\lambda, y)(z/y)^M$ we obtain the bound:

$$|G(\lambda, x, y)| < \frac{y}{M - \frac{1}{2}} \frac{\varphi^0(\lambda, x)}{\varphi^0(\lambda, y)}.$$

Putting then $\varphi(\lambda, x) = \zeta(\gamma, x)\varphi^0(\lambda, x)$ we find the inequality:

$$|\zeta(\lambda, x)| < 1 + \int_0^x |y\, U(y)|\, |\zeta(\lambda, y)\, \frac{1}{M - \frac{1}{2}}\, \mathrm{d}y.$$

From the lemma it follows then

$$\varphi(\lambda, x) \sim \varphi^0(\lambda, x)\, O(1)$$

uniformly in $0 < x < \lambda$. Take then the identity (A.6):

$$C(\lambda) = C^0(\lambda) + \frac{1}{2\lambda}\Big[\int_0^\lambda U(x)\, C^0(\lambda, x)\varphi^0(\lambda, x)\, O(1)\, \mathrm{d}x +$$

$$+ \int_\lambda^\infty U(x)\, C^0(\lambda, x)[C(\lambda)\, S(\lambda, x) - S(\lambda)\, C(\lambda, x)]\, \mathrm{d}x\Big].$$

In this formula $C^0(\lambda, x)\varphi^0(\lambda, x) \sim C^0(\lambda)/(\sqrt{1 - (z/\lambda)^2})$ as it can be deduced from the power series or from the asymptotic expansions of Bessel functions. It can be moreover shown from the Schlaefli representation that:

$$\text{(A.14)} \qquad \left|\frac{C^0(\lambda, x)}{\sqrt{x}}\right|, \left|\frac{S^0(\lambda, x)}{\sqrt{x}}\right| < C = \text{constant}, \quad x \geqslant \lambda.$$

From eq. (III) (Appendix II) it follows that the same kind of inequality holds for $C(\lambda, x)$ and $S(\lambda, x)$. We are now in condition to write:

$$C(\lambda)[1 + O(1)] + S(\lambda)\, O(1) = C^0(\lambda)[1 + O(1)]$$

and similarly

$$S(\lambda)[1 + O(1)] + C(\lambda)\, O(1) = S^0(\lambda)[1 + O(1)].$$

It follows:

$$C(\lambda) = C^0(\lambda)[1 + O(1)] + S^0(\lambda)\, O(1) \quad \text{etc.},$$

and

$$\lim_{\lambda \to \infty} \frac{C(\lambda)^2 + S(\lambda)^2}{C^0(\lambda)^2 + S^0(\lambda)^2} = 1 .$$

Probably our estimate here can be ameliorated at the expense of additional complication. It would be also desirable to have a simpler proof. We turn our attention now to (A.12). Putting $C(\lambda)^2 + S(\lambda)^2 = T(\lambda)^2$ we can write it as follows:

$$\sin \delta(\lambda) = \frac{1}{-4\lambda^2} \int_0^\infty U(x) \frac{\varphi^0(\lambda, x)}{T^0(\lambda)} \frac{\varphi(\lambda, x)}{T(\lambda)} \, \mathrm{d}x .$$

If $x > \lambda$ then from the corresponding bounds (A.14) we deduce:

$$|\varphi^0(\lambda, x)| < 2C\lambda T^0(\lambda) \cdot \sqrt{x} ; \qquad |\varphi(\lambda, x)| < 2C' \lambda T(\lambda) \cdot \sqrt{x} ,$$

C, C' being, as usual, two suitable constants. It follows that the contribution to $\sin \delta$ coming from the interval $\lambda \ldots \infty$ is of the order of

$$CC' \int_\lambda^\infty x |U(x)| \, \mathrm{d}x = O(1) .$$

Actually a more elaborate analysis shows that this bound is pessimistic and one has actually $O(\lambda^{-1})$. Between $0 \ldots \lambda$ one has

$$|\varphi(\lambda, x)\, T^{-1}(x)| < H |\varphi^0(\lambda, x)\, T^{0-1}(\lambda)| .$$

This part of the integral is certainly smaller than:

$$\frac{1}{4\lambda^2} H \int_0^\infty |U(x)| \, \frac{\varphi^0(\lambda, x)}{T^0(\lambda)^2} \, \mathrm{d}x .$$

Since $|U(x)| < Mx^{-2}$ from (2.4) we get the upper bound:

$$\frac{H\pi M}{4\lambda} .$$

If $U(x)$ is of the (3.2) type then the above technique yields easily the stated result. It is not clear to us if the above analysis is included in Carter's result in the sense that his bound may hold regardless of λ being not an half-integer.

A few words on the use of the Phragmen-Lindeloef theorem in extending these results to complex λ are also needed.

Take

$$F^+(\lambda) = \frac{C(\lambda) + iS(\lambda)}{C^0(\lambda) + iS^0(\lambda)} = \frac{T(\lambda)}{T^0(\lambda)} \exp[-i\delta(\lambda)] .$$

This function is easily seen to be regular in $R(\lambda) > 0$. We have also $F^+(\lambda) \to 1$ along $\arg \lambda = 0$ and $\arg \lambda = -(\pi/2)$. $F^+(\lambda)$ is also bounded by an exponential function in the intermediate angles and is therefore bounded by a constant. From Montel's theorem the limit holds in all

$$0 > \arg \lambda > -\frac{\pi}{2},$$

$F^+(\lambda)$ has also no zeros in this sector since if $F^-(\lambda)$ is the adjoint function, then:

$$\exp[-2i\delta] = \frac{F^+(\lambda)}{F^-(\lambda)}$$

and also this function would vanish since (F^+, F^-) cannot vanish simultaneously, for also $C(\lambda)$ and $S(\lambda)$ would vanish and also $\varphi(\lambda, x)$ because of (1.5). But

$$|\exp[-2i\,\delta(\lambda)]| = \exp[2I[\delta(\lambda)]] > \exp[\pi I(\lambda)] > 0$$

and the above claim is clearly impossible, Along $\arg \lambda = \pi/2$ one has $|F^+(\lambda)| = O(\exp[\pi(\lambda) - 2\sigma(\lambda)])$. If one applies Carleman's theorem then unless $\sigma = \pi/2$, one has always zeros of F^+ in this sector. The properties of $F^-(\lambda)$ are of course the same of $F^+(\lambda)$ provided one changes $\arg \lambda$ into $-\arg \lambda$. All extensions to complex λ can be carried out with the same technique.

Appendix V

We shall sketch here briefly the low energy limit. The potential will be supposed to decrease exponentially. In this case a simple generalization of known arguments yields the limit:

$$\sin \delta(\lambda) \underset{k \to 0}{\sim} k^{2\lambda} \eta(\lambda), \tag{A.15}$$

where $\eta(\lambda)$ is finite.

This limit follows from (A.12) and from the similar indentity:

$$C(\lambda)\, S^0(-\lambda) - C^0(-\lambda)\, S(\lambda) = \frac{1}{2\lambda} + \frac{1}{4\lambda^2} \int_0^\infty \underset{0}{U}(r)\, r^{-\lambda + \frac{1}{2}}\, \underset{0}{\varphi}(\lambda, r)\, dr = \frac{\alpha(\lambda)}{2\lambda}. \tag{A.16}$$

$\underset{0}{U}(r)$ is here the usual potential and r the distance $(x = kr)$. Also $k^{-2}\underset{0}{U}(r) = U(x)$. $\underset{0}{\varphi}(\lambda, r)$ is that solution of:

$$\underset{0}{\varphi}'' - \frac{\lambda^2 - \frac{1}{4}}{r^2}\, \underset{0}{\varphi} - \underset{0}{U}(r)\, \underset{0}{\varphi} = 0,$$

which behaves like $r^{\lambda + \frac{1}{2}}$ for small r.

(A.12) can be correspondingly written as (k small):

$$C(\lambda)\,S^0(\lambda) - S(\lambda)\,C^0(\lambda) = -\frac{1}{4\lambda^2}\int_0^\infty U(r)\,r^{\lambda+\frac{1}{2}}\varphi(\lambda, r)\,\mathrm{d}r \cdot k^{2\lambda} = \beta(\lambda)\,k^{2\lambda}\,.$$

It follows that if $R(\lambda) > 0$:

$$\tau^{0^2}(\lambda)\,\eta(\lambda) = \frac{\beta(\lambda)}{\alpha(\lambda)}\,, \qquad \frac{\tau(\lambda)}{\tau^0(\lambda)} = \alpha(\lambda)\,.$$

Therefore $\eta(\lambda)$ is a meromorphyc function of λ in $R(\lambda) > 0$. If λ is large $\alpha(x) \to 1$ and $\beta(\lambda)$ becomes in general large. A good approximation to $\varphi(\lambda, r)$ is then simply $r^{\lambda+\frac{1}{2}}$. Also one can show that if $U(r)$ is a σ potential then $T^0(\lambda)^2\,\eta(\lambda) = 0(\exp[-2\sigma|\lambda|])$ for λ large imaginary. Take now Sommerfeld's integral (6.4). In the low energy limit

$$-z = \frac{\tau^2}{2k^2} - 1 \sim \frac{\tau^2}{2k^2}\,,$$

if τ is kept constant. But if $-z$ is large positive then:

$$P_{\lambda-\frac{1}{2}}(-z) \sim \frac{\Gamma(\lambda)\,T^{2\lambda-1}\,k^{1-2\lambda}}{\sqrt{\pi}\,\Gamma(\lambda+\frac{1}{2})}\,.$$

A factor k^{-1} was omitted for simplicity in (6.4). Having care of this factor and others, Sommerfeld's representation takes the limiting form:

$$f(0, \tau) = \frac{1}{\tau}\int_{-i\infty}^{i\infty} \lambda\,\mathrm{d}\lambda\,\frac{\beta(\lambda)}{\alpha(\lambda)}\left(\frac{\tau}{2}\right)^{2\lambda}\frac{\sqrt{\pi}}{\Gamma(\lambda)\,\Gamma(\lambda+\frac{1}{2})\cos\pi\lambda}\,. \tag{A.17}$$

The discussion of this integral in no point is essentially different from the general case already treated in Section 6, and it is actually simpler because it involves the theory of elementary Mellin transforms.

In (A.17) the path avoids the zeros of α. The resulting analiticity domain is the sector $|\arg\tau| < \sigma$ plus the interms of the circle $|\tau| < \alpha$.

RIASSUNTO

Nel presente lavoro viene definita l'interpolazione degli sfasamenti nello scattering da potenziale per valori generalmente complessi del momento orbitale. Tale definizione si presta particolarmente a discutere le proprietà analitiche (tra cui la rappresentazione di Mandelstam) dell'ampiezza di scattering giovandosi all'uopo di un metodo dovuto a Watson sueccessivamente perfezionato da Sommerfeld.

IL NUOVO CIMENTO Vol. XIV, N. 5 1° Dicembre 1959

Study of Antiprotons with Emulsion Technique.

E. Amaldi, G. Baroni, G. Bellettini, C. Castagnoli
M. Ferro-Luzzi and A. Manfredini

Istituto di Fisica dell'Università - Roma
Istituto Nazionale di Fisica Nucleare - Sezione di Roma

(ricevuto il 20 Luglio 1959)

Summary. — In this paper we report the results obtained from the study of 653 antiprotons observed in nuclear emulsions. The cross-sections, averaged over all the nuclei present in the emulsion (G-5) as well as over the $\bar{p}$ energy interval from 10 to 230 MeV ($\overline{T}_{\bar{p}}=150$ MeV), are given for the following processes: inelastic scattering, elastic scattering and annihilation+charge exchange. The statistics are good enough to give the cross-section for annihilation+charge exchange as a function of the kinetic energy of the incident $\bar{p}$. The annihilation process has been studied in detail for antiprotons annihilating in flight as well as at rest. Among other results we obtained the following: the multiplicity and the spectrum of the $\pi^{\pm}$, the number of pions interacting, on the average, inside the emulsion nucleus where the annihilation takes place, the frequency of emission of the $K\overline{K}$ pairs and the energy balance of the various components emitted by the average emulsion nucleus where the annihilation takes place. From these data the total multiplicity of $\pi^{\pm 0}$ for the annihilation of a $\bar{p}$ with an isolated nucleon is deduced, under the assumption of charge-independence. Finally an estimate is given of the ratio Σ_n/Σ_p, where Σ_n and Σ_p are the probabilities for a $\bar{p}$ at rest to annihilate with the neutrons and protons bound in the emulsion nuclei.

1. – Introduction.

In this paper we report the results of the analysis of 653 new annihilation stars and of the corresponding incident $\bar{p}$ tracks observed in emulsions exposed to an antiproton beam of the Bevatron in Berkeley. In discussing

some of the results, we make use of a total of 669 stars observed in this laboratory from the beginning of the study of antiprotons ([1-3]).

Whenever possible, our results are compared to and combined with the results of other experiments: the Antiproton Collaboration Experiment (ACE I) ([2]) and the more recent work of the groups working at Berkeley ([4,5]), Uppsala ([6,7]) Los Alamos ([8]), Oxford ([9]), Saclay ([10]), and Bern ([11]).

In Section **2** we give a few experimental details referring to: exposure of the emulsion stack to the $\bar{p}$ beam, rules applied in following the tracks of the incident $\bar{p}$ and of the particles emitted in the annihilation process, selection criteria adopted in defining the track samples on which certain types of measurements (range, ionization, scattering) were performed systematically, etc.

Section **3** contains the results of the measurements of the various cross-sections for $\bar{p}$ in flight. In the present work the expression « $\bar{p}$ in flight » refers to $\bar{p}$ annihilating with kinetic energy, $T_{\bar{p}}$, larger than 10 MeV and smaller than 230 or 250 MeV; which of these two values should be used, depends on the nature of the problem, since in certain cases it is possible to extend the observations up to the front edge of the stack ($T_{\bar{p}} = 250$ MeV), while in other cases the « identification efficiency » (Section **3**·1.1) becomes very small already at 2 cm from the front edge ($T_{\bar{p}} = 230$ MeV).

([1]) O. CHAMBERLAIN, W. W. CHUPP, G. GOLDHABER, E. SEGRÈ, C. WIEGAND, E. AMALDI, G. BARONI, C. CASTAGNOLI, C. FRANZINETTI and A. MANFREDINI: *Phys. Rev.*, **101**, 909 (1956); *Nuovo Cimento*, **3**, 447 (1956).

([2]) W. H. BARKAS, R. W. BIRGE, W. W. CHUPP, A. G. EKSPONG, G. GOLDHABER, H. H. HECKMAN, D. H. PERKINS, J. SANDWEISS, E. SEGRÈ, F. M. SMITH, D. H. STOCK, L. VAN ROSSUM, E. AMALDI, G. BARONI, C. CASTAGNOLI, C. FRANZINETTI and A. MANFREDINI: *Phys. Rev.*, **105**, 1037 (1957).

([3]) E. AMALDI, C. CASTAGNOLI, M. FERRO-LUZZI, C. FRANZINETTI and A. MANFREDINI: *Nuovo Cimento*, **5**, 1797 (1957).

([4]) O. CHAMBERLAIN, G. GOLDHABER, L. JAUNEAU, T. KALOGEROPOULOS, R. SILBERBERG and E. SEGRÈ: *International Conference on Mesons and Recently Discovered Particles* (Padua-Venice, 22-28 September 1957).

([5]) O. CHAMBERLAIN, G. GOLDHABER, L. JAUNEAU, T. KALOGEROPOULOS, E. SEGRÈ and R. SILBERBERG: *Phys. Rev.*, **113**, 1615 (1959).

([6]) A. G. EKSPONG, S. JOHANSSON and B. E. RONNE: *Nuovo Cimento*, **8**, 84 (1958).

([7]) A. G. EKSPONG and B. E. RONNE: *Nuovo Cimento* **13**, 27 (1959).

([8]) A. H. ARMSTRONG and G. M. FRYE: *Phys. Rev. Lett.*, **1**, 14 (1958) and private communication.

([9]) G. B. CHADWICK and P. B. JONES: *Phil. Mag.* (in press); A. ENGLER, P. B. JONES and J. H. MULVES: in press.

([10]) A. BERTEHLOT, C. CHOQUET, A. DAUDIN, O. GOUSSU and F. LEVY: *Compt. Rend.*, **248**, 94 (1959).

([11]) J. DYER, H. H. HECKMAN, F. M. SMITH, Y. EISENBERG, W. KOCH, M. NIKOLIC, M. SCHNEEBERGER and H. WINZELER. We thank the group of the University of Bern for communicating to us their results on diffraction scattering before publication.

TABLE I. – *Summary of the experimental results on the interaction of $\bar{p}$ in flight with emulsion nuclei.*

Process	λ in cm σ in mb $\sigma_0 = 550$ mb	ACE I [2]		Berkeley+ACE I [5]		Uppsala [7]		Rome		Section
		H excl.	H incl.	H excl.	H incl.	H excl.	H incl.	H excl.	H incl.	
Annihilation+ +charge exchange	λ_a	14.3 ± 3.1	—	—	18.6 ± 2	21.7 ± 1.7	20.8 ± 1.6	18.8 ± 1.0	18.0 ± 0.9	3·1.1
	σ_a/σ_0	2.7 ± 0.6	—	1.9 ± 0.2	—	1.79 ± 0.14	—	2.06 ± 0.11	—	3·1.1
Inelastic scattering	λ_i	~ 150	—	463 ± 200	—	580 ± 240	—	$< 250 \pm 60$	—	3·1.2
	σ_i/σ_0	~ 0.26	—	0.11 ± 0.05	—	0.076 ± 0.020	—	0.155 ± 0.036	—	3·1.2
Total (reaction)	λ_r	13.0 ± 2.7	—	—	—	20.4 ± 1.3	—	17.5 ± 0.9	—	3·1.1
	σ_r/σ_0	3.0 ± 0.6	—	—	—	1.9 ± 0.15	—	2.21 ± 0.12	—	3·1.1
Elastic scattering on H	σ_{eH}	—		71 ± 25		92 ± 28		66 ± 17		3·2
Elastic scattering on nuclei ($\theta > 5°$)	$\sigma_{eN}(\theta > 5°)$	—		—		—		530 ± 70		3·1.2
Followed track length (m)	l	3		17.6		37.3		75.9		
Average kinetic energy of $\bar{p}$ (MeV)	$\langle T_{\bar{p}} \rangle$	140		140		150		150		

The statistical material was sufficiently large to attempt giving the cross-section for annihilation + charge exchange as a function of the kinetic energy $T_{\bar{p}}$ in the interval extending from 10 MeV to 230 MeV.

Some of the more relevant results on the cross-sections, integrated over the entire energy interval, have been collected in Table I where the results obtained in emulsion by other authors are also given for comparison.

Our results refer to a total followed antiproton path of 75.9 m, which is reduced to 62.7 m in all cases where it is impossible to extend the observations to less than 2 cm from the front edge. These values of the investigated path length should be compared to a total path of 55.2 m followed by all other laboratories together. Thus, our data provide the most extended homogeneous piece of information available to-day from emulsion work. By combining our data, whenever possible, with those of other laboratories, one obtains results which are affected by rather small statistical errors.

The agreement between the various groups is generally satisfactory. Only in the case of the inelastic scattering cross-section σ_i we find a value twice larger than the one found by the Berkeley group. Nevertheless, we consider that our result still constitutes a lower limit for σ_i (Section 3·1.2).

The values found by the various groups for the cross-section for elastic collision of $\bar{p}$ against free protons (Hydrogen), are in very good agreement with one another, and can be combined in order to increase the statistical accuracy (Section 3·2). The final result, as well as the partial ones, are in good agreement ([12]) with the result of counters experiments ([13]) as well as with the recent bubble chamber results ([14]), which gave previously a value lower by $(40 \div 50)\%$ ([15]).

The cross-section for elastic collision against nuclei (different from Hydrogen), σ_{eN}, refers to deflections larger than 5°. The scatterings were actually measured down to 1.5° in order to enable comparison between the forward peak arising from the diffraction scattering plus Coulomb interaction and the predictions of various optical models ([16]). In the estimate of σ_{eN} a cut-off angle of 5° was chosen in order to eliminate a large part of these two effects.

Section 4 contains the results on the annihilation stars. These are par-

---

([12]) G. Baroni, G. Bellettini, C. Castagnoli, M. Ferro-Luzzi and A. Manfredini: *Nuovo Cimento* **12**, 564 (1959).

([13]) C. A. Coombes, B. Cork, W. Galbraith, G. R. Lambertson and W. A. Wenzel: *Phys. Rev.*, **112**, 1303 (1958).

([14]) L. Agnew: *Thesis*, UCRL 8785 (1959).

([15]) L. Agnew, T. Elioff, W. B. Fowler, L. Gilly, R. Lander, L. Oswald, W. Powell, E. Segrè, H. Steiner, H. White, C. Wiegand and T. Ypsilantis: *Phys. Rev.*, **110**, 994 (1958).

([16]) G. Baroni, G. Bellettini, C. Castagnoli, M. Ferro-Luzzi and A. Manfredini: *Nuovo Cimento* (in press).

		ACE I [2]	Berkeley + ACE I [5]	Uppsala [7]	Saclay [10]	Oxford [9]	Los Alamos [8]	Rome
Number of annihilation stars	at rest	15	111+15	175 161		175	9	349+ 4 [b]
	in flight	21	74+21	183 179		202	7	304+10 [b]
	combined	36	185+36	358 340	132	377	16	653+14 [b]
$\langle N_{\pi^\pm} \rangle$ (uncorrected for efficiency)	at rest	2.8±0.4	2.50±0.26	2.37±0.11				2.46±0.14
	in flight	2.4±0.4	2.30±0.28	2.26±0.10				2.18±0.13
	combined	2.6±0.3	2.41±0.19					2.32±0.10
e_π (efficiency)		0.9±0.1	0.90±0.10				1.00	0.93±0.03
$\langle E_{\pi^\pm} \rangle$ MeV (uncorrected for inelastic scattering)	at rest		324±21			~ 413 [a]		379±12
	in flight		361±30			~ 400		370±17
	combined	346±20	339±18			~ 407	334±24	375±10
N_{π^+}/N_{π^-} (100 MeV $\geqslant T \geqslant$ 20 MeV)			0.45±0.12	0.66±0.3			~ $\frac{3}{4}$	0.73±0.20
Pairs of $K\bar{K}$ per star			3.5±1.5%		4.5%	10±3%		4±2%
$\langle E_{K\bar{K}} \rangle$ MeV	all stars combined		50±25					55±28
$\langle \sum E_H \rangle$ MeV	at rest		144±15					121±10
	in flight		220±26					173±22
	combined		176±13					145± 9
$\langle N_H \rangle$	at rest		3.33±0.34					3.42±0.19
	in flight		5.09±0.60					4.80±0.40
	combined		4.07±0.31					3.84±0.18
No. of $\bar{p}_\varrho$ per star			2^{+3}_{-2}%	5±2%		3.5±2%		$\leqslant$2.2%

[a] These values have been deduced by us from the histograms given by the authors (private communication).
[b] These 14 events are considered in detail in a previous publication [2].

tially collected in Table II, where the results of other groups are given for comparison. The main differences with respect to previous work are the following: we find a value higher than that of the Berkeley group for the mean energy $\langle E_{\pi^\pm} \rangle$ of the charged pions emitted from annihilation stars due to $\bar{p}$ at rest ($T_{\bar{p}} < 10$ MeV), and a lower value for the average energy of the heavy prongs emitted in each star, $\langle \sum E_H \rangle$.

Section **5** contains a discussion of our data and a comparison with the results of other authors, followed by an analysis of the information available on annihilation stars observed in emulsions. In particular, it contains a discussion of the average energy balance per star, from which it appears that the rather low value of $\langle \sum E_\Pi \rangle$ is reflected by the fact—already noticeable in previous results—that the fraction of the total energy taken off by neutral pions is a bit larger than one half the energy taken off by the charged pions. The same qualitative feature, although reduced, appears in the results obtained by combining the Berkeley and Rome data.

One should notice, however, that the errors affecting the contributions of the π^- and π^0 components are correlated in opposite directions. Furthermore the procedure involved in the derivation of this result is open to some criticism, expecially as regards the computation of the energy U taken off by the evaporation and knock-on nucleons from the observed heavy prong energy (Section **5**·3.). Thus one can conclude that our results on the energy balance are still compatible with the assumption of charge-independence.

One of the most interesting features of the annihilation process of $\bar{p}$, is the average number $\langle N_\pi \rangle$ of pions, of any charge, emitted in the $\bar{p}$-nucleon annihilation. Its value was given as 5.4 ± 0.3 from previous emulsion work ([5]), and as 4.7 ± 0.5 ([14]) or 4.94 ± 0.31 ([17]) from bubble chamber experiments. Because of our rather large value of $\langle E_{\pi^\pm} \rangle$, any type of analysis of our data provides a value of $\langle N_\pi \rangle$ smaller than that found in previous emulsion work. From our data we find (Section **5**·3)

$$(1.1a) \qquad \begin{cases} \langle N_\pi \rangle = 5.10 \pm 0.24 & \text{for annihilations in flight} \\ \langle N_\pi \rangle = 4.60 \pm 0.15 & \text{for annihilations at rest} \\ \langle N_\pi \rangle = 4.82 \pm 0.14 & \text{for all annihilations combined} \end{cases}$$

which should be replaced by

$$(1.1b) \qquad \begin{cases} \langle N_\pi \rangle = 5.12 \pm 0.22 & \text{for annihilations in flight} \\ \langle N_\pi \rangle = 4.77 \pm 0.14 & \text{for annihilations at rest} \\ \langle N_\pi \rangle = 4.92 \pm 0.13 & \text{for all annihilations combined} \end{cases}$$

([17]) N. HOROWITZ, D. MILLER, J. MURRAY and R. TRIPP: UCRL, 8591, in press in *Phys. Rev.*

if the Berkeley and Rome data combined are used. These values are in excellent agreement with the recent bubble chamber results mentioned above.

This conclusion justifies, in our opinion, the use of an analysis procedure of the emulsion data different from that applied in previous works. We adopt the value of $\langle E'_{\pi^\pm} \rangle$ obtained from bubble chamber works as a basic data, and we use it for computing the various quantities relative to the annihilation stars observed in emulsions by means of the equations expressing the conservation of energy and the balance of particles; the results of such a computation are then compared with the corresponding measured values. The agreement between the two sets of values is found to be as good as can be expected. Thus, we may conclude that the main features of the annihilation stars observed in emulsions are fairly well understood and in satisfactory agreement with the data derived from other experimental techniques. Only minor details need further clarification.

The procedure mentioned above involves the determination of the number ν of pions that, on the average, interact with the nucleons of the same nucleus in which the annihilation takes place. Two other methods for determining ν are described in Section 5·4; one is based on the frequency of annihilation stars without any heavy prong, the other on the frequency of the knock-on protons ($T_H \geqslant 30$ MeV) per annihilation star.

The three results are in reasonable agreement, so that they can be averaged together. Thus one obtains:

$$(1.2) \qquad \begin{cases} \nu = 2.24 \pm 0.33 & \text{for annihilations in flight} \\ \nu = 1.34 \pm 0.14 & \text{for annihilations at rest} . \end{cases}$$

From these values of ν one can derive an estimate of the annihilation radius, for the definition of which we refer to Section 5·5. The result found is:

$$(1.3) \qquad \begin{cases} R_a/R = 0.98 \pm 0.03 & \text{for annihilations in flight} \\ R_a/R = 1.06 \pm 0.03 & \text{for annihilations at rest} . \end{cases}$$

From the first of these two values we derive an estimate of the mean free path of $\bar{p}$ inside the emulsion nuclei

$$\lambda_{\bar{p}} = (0.80 \pm 0.15) \cdot 10^{-13} \text{ cm} ,$$

in satisfactory agreement with Fulco's computation [18].

---

[18] J. Fulco: UCRL, 8416 (1958).

Finally, we have attempted an analysis of the annihilation stars produced by $\bar{p}$ at rest, which aims at establishing the ratio $\xi = \Sigma_n/\Sigma_p$ of the probabilities for $\bar{p}$ at rest to annihilate with neutrons and protons bound in emulsion nuclei. The result of such an analysis gives a value of ξ appreciably lower than the neutron-proton ratio in emulsion nuclei ($\xi = 1.2$). This result, however, finds a very simple and natural interpretation by considering the isotopic spin states of the $\bar{p}$-p and $\bar{p}$-n systems.

2. – Details on exposure, track-following and selection criteria.

2·1. *Exposure at the bevatron and beam composition.* – Our stack of 175 Ilford G5-emulsions, 600 μm thick and of (15 × 23.5) cm² area, was exposed to an antiproton-separated beam by our Berkeley colleagues, who supplied us the following data. The magnet system focused on the stack negative particles of momentum $p = (729 \pm 15)$ MeV/c; the exposure corresponded to $3 \cdot 10^{14}$ protons of 6.1 GeV impinging on a Beryllium target 6 in. thick. Under these conditions a flux of about 10 $\bar{p}$ per cm² was expected to be superimposed on a background of tracks at minimum ionization of about 10^5 particles/cm².

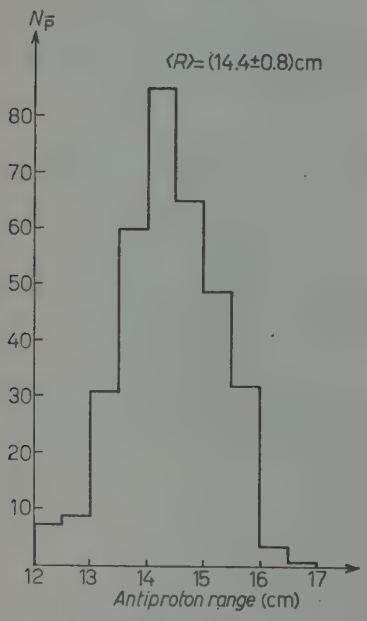

Fig. 1. – Range distribution of $\bar{p}$ annihilating at rest ($T_{\bar{p}} < 10$ MeV).

These estimates agree as much as can be expected with the measured quantities. As we shall see later from range measurements of $\bar{p}$ annihilating at rest (Fig. 1), we found $p = (725 \pm 15)$ MeV/c. After correction for the range straggling ($\Delta R = \pm 3.6$ mm) we deduce an uncertainty in the entrance momentum $\Delta p/p = \pm 1.6\,\%$.

The flux distribution of both background particles and antiprotons over the entrance face of the stack (beam end) is shown in Fig. 2. The curves of constant flux of minimum tracks—due to background particles—show that the beam was well centred on the entrance face of our stack. The beam of antiprotons appears to be slightly displaced horizontally as compared to the beam of background particles.

The angular spread of the beam was measured directly from the direction of minimum tracks at their entrance into the stack, and indirectly from the

direction of all minimum tracks producing stars (due mainly to π^-) observed in a region located a few mm from the front edge. Both methods gave a very strongly peaked angular distribution with a maximum angular spread of $\pm 3°$.

The composition of the beam was determined by measuring: *a*) the density of stars produced by π^- near the front edge of the stack; *b*) the variation with depth in the emulsion of the flux of minimum tracks which, at any depth, remained inside $\pm 3°$ with respect to the mean direction of the incoming

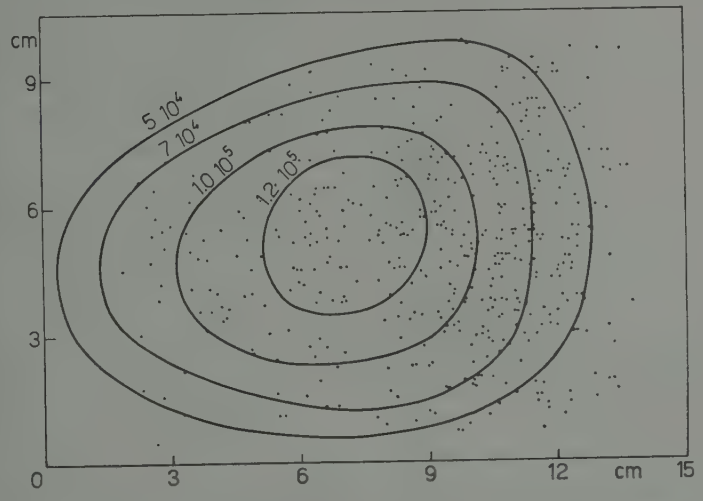

Fig. 2. – Distribution over the leading face of the stack of the points of entrance of the antiprotons, and curves of constant flux of background particles giving tracks of minimum ionization. The number attached to each curve represents the number of particles per cm².

particles at the entrance. From the measurements of type *a*) — after correction for scanning efficiency and using a mean free path of π^- of 700 MeV/c for production of stars in emulsion $\lambda_{star} = 40$ cm ([19]) — we found that the beam had the same composition near the lateral surface as it had along the axis of the stack. A quantitative analysis gave: $\Phi(\pi^-)$ of the order of $(30 \div 40)\%$ and $\Phi(\mu) + \Phi(e)$ of the order of $(70 \div 60)\%$.

From measurements of type *b*) — with a total mean free path of π^- of 700 MeV/c in emulsion $\lambda_{tot} = 30$ cm ([19]), and taking into account a weak transition effect in the first 5 cm of the stack followed by a slow absorption — we deduced

$$\Phi(\pi^-) \simeq (40 \pm 10)\%, \quad \Phi(\mu) \simeq (60 \pm 10)\%, \quad \Phi(e) \simeq 2\%.$$

([19]) A. Barbaro, G. Baroni and C. Castagnoli: *Nuovo Cimento*, **9**, 154 (1958).

These results do not agree with those obtained with the same separated beam by the propane bubble chamber group at Berkeley ([14]): $\Phi(\pi^-) \simeq 10\%$, $\Phi(\mu) \simeq$ $\simeq 87\%$ $\Phi(\mathrm{e}) \simeq 3\%$. The difference between the two results is not relevant for the discussion that follows and could be due to the fact that the two measurements were made at different positions with respect to the beam.

2·2. *Track following and entrance criteria.* – We have adopted the same scanning criteria as the Berkeley group ([5]), except that the scanning was made twice: once along a line at 3 mm from the front edge and a second time along a line at 7 mm. The second scanning was made in order to identify tracks of $\bar{\mathrm{p}}$ which entered the stack so close to the surface between two successive emulsions, as to escape observation at 3 mm.

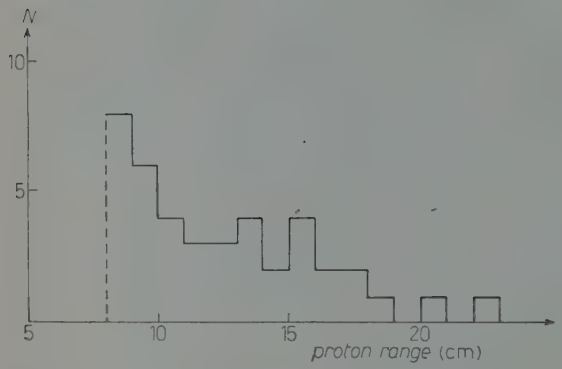

Fig. 3. – Range distribution of particles of protonic mass which stop without giving any star or blob.

The tracks with blob density $1.3 \leqslant b/b_0 \leqslant 1.5$ and entering the stack at an angle $\leqslant 3°$ with respect to the direction of the incident minimum tracks, were followed to their end. The total number of these tracks was 918.

Of these, 390 come to rest, and can be divided into 349 $\bar{\mathrm{p}}$ identified from the presence of an annihilation star and 41 tracks not associated with any

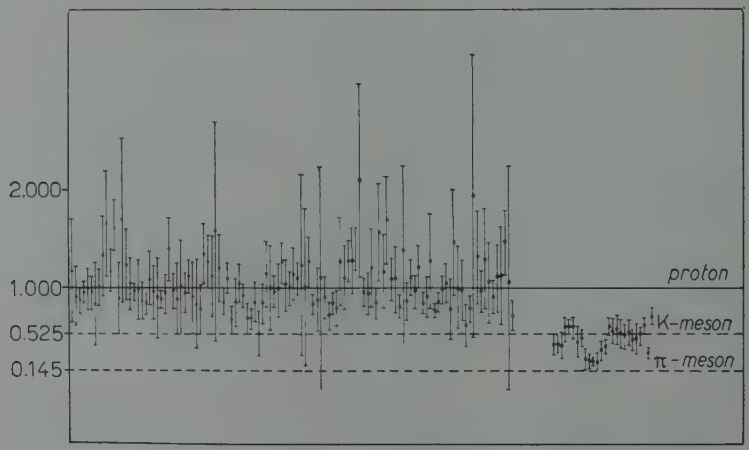

Fig. 4*a*. – Results of mass measurements by means of mean gap length *vs.* range method.

star or blob, which can be interpreted either as $\bar{p}_e$ or as background protons. The range distribution of the $\bar{p}$ at rest is shown in Fig. 1. Fig. 3, similar to Fig. 1, refers to the range distribution of the particles of protonic mass selected according to the entrance criteria and which stop without producing any star or blob (Section 2·3).

The 528 tracks which stop in flight have been studied in order to establish the direction of motion and the mass of the corresponding particles. This was made by measuring the variation of the mean gap-length with the range.

The measurements have actually been made only on those tracks which annihilated between 2 and 7 cm from the front edge. These limits have been chosen for the following reasons. For $\Delta R \leqslant 2$ cm, the variation of ionization of a proton is too small to allow a mass determination; therefore, we decided to leave out of our statistics all the stars found in this range interval. For $\Delta R \geqslant 7$ cm, the tracks due to K^- of the same entrance velocity as $\bar{p}$ are already at the end of their range. Therefore the tracks with $\Delta R \geqslant 7$ cm can be due to $\bar{p}$ or p which, obviously, can not be discriminated by means of mass measurements.

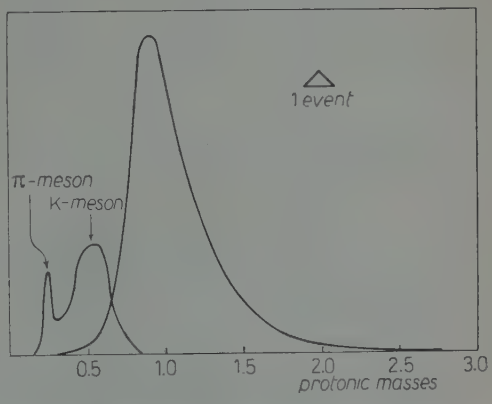

Fig. 4*b*. – Statistical distribution of the results given in Fig. 4*a*. Graph made by means of the method of constant area per event.

TABLE III. – *Number of observed* $\bar{p}$ *annihilations presented in this paper.*

	Events used in the stars statistics		Stars close to emulsion surfaces	
$\bar{p}$	without K-mesons	with K-mesons	$\lvert\Delta z\rvert \leqslant 20\ \mu m$	TOTAL
At rest	327	5	17	349
In flight	284	1	19	304
TOTAL	611	6	36	653

With this procedure we found 112 particles of protonic mass, 22 particles of mass lower than protonic (18 K^- and 4 π^-) and 59 tracks due to particles moving backwards with respect to the beam direction.

Fig. 4*a* and *b* show the results of the mass measurements described above. The inaccuracy of the pion mass, as it appears from these two figures, arises from the uncertainty of the calibration curve.

Table III summarizes the new events presented in this paper.

2·3. *Tracks of protonic mass of uncertain interpretation.* – In this Section we will discuss three classes of events which may be due to antiprotons, but whose interpretation is uncertain; they will be indicated later on as: « Stops in flight », « Possible charge exchange » and « Possible $\bar{p}_\varrho$ ». All these tracks had their end-point at a distance from the lateral surfaces of the emulsions $|\Delta z|$ larger than 20 μm.

2·3.1. Stops in flight. – The first class is that of tracks due to incoming particles of protonic mass which satisfy the entrance criteria and which disappear in flight without giving any secondary track. This class consists of 5 tracks which stop at: $T_{\bar{p}} = 50$, 128, 168, 180 and 186 MeV.

These events may be due to $\bar{p}$ undergoing either charge exchange or an annihilation without emission of charged pions, *i.e.* to the case $N_{\pi^\pm} = 0$ of the class of stars considered in Section 4·1.4 (Table VII).

2·3.2. Possible charge exchange. – The second class of uncertain events is that of stars produced in flight by incoming particles of protonic mass satisfying the entrance criteria, which show a visible energy smaller than the kinetic energy of the $\bar{p}$ at the annihilation point (Table IV).

TABLE IV. – *Tracks of protonic mass of uncertain interpretation because the visible energy of the star is smaller than the kinetic energy of the incoming particle.*

Event number	$T_{\bar{p}}$ (MeV)	$\sum E_H$ (MeV)	N_{EV}	N_{KO}
35	90	44	0	1
491	140	3.3	1	0
503	114	25.2	2	0
519	90	14.0	2	0
558	192	62.6	2	1
560	172	22.5	3	0
564	168	120.5	2	1
574	178	14.5	3	0
657	178	15.9	1	0
665	174	33.5	4	0

The above events could be due either to a charge exchange process or to an annihilation star in which the energy taken off by neutral particles is

exceptionally large due to a fluctuation; they could, however, also be due to background protons.

From the cross-section for charge exchange obtained with counters — (10 ± 3) mb in H at $T_{\bar{p}} = 133$ MeV ([13]); (4 ± 2) mb in other nuclei at $T_{\bar{p}} = 450$ MeV ([20]) — we expect to have, in our sample of annihilations in flight, about (4 ± 1) processes of this type.

All the events of these two classes have been included in the $\bar{p}$ statistics according to the criteria adopted in previous works ([2,4,7]).

2·3.3. Possible $\bar{p}_{\varrho}$. – Finally, the third class of events of uncertain interpretation is defined by the following selection criteria. Among all the tracks which satisfy the entrance criteria specified in Section 2·2 and which come to rest without producing charged prongs, those of protonic mass were selected. Such a sample includes background protons as well as antiprotons of $T_{\bar{p}} \leqslant 10$ MeV which either annihilate without emission of charged prongs or undergo a charge exchange with a nuclear proton ($\bar{p}_{\varrho}$).

Events of this type—if any—must be found mainly in the range interval (14.4 ± 0.8) cm, as shown in Fig. 1. We actually found 7 tracks in this range interval; two of these, however, were interpreted as $\bar{p}$, because one showed a blob and the other an electron at its end.

The other 5 tracks have been plotted in Fig. 3, together with all other tracks due to particles belonging to the same class, so as to verify if a significant statistical accumulation of tracks takes place in the range interval (14.4 ± 0.8) cm. Since no effect of this type is observed, we conclude that these 5 tracks can all be due to background protons and therefore they have not been included in our $\bar{p}$ statistics. One can also state that if $\bar{p}_{\varrho}$ exist, their frequency in emulsion does not exceed the value $(5 + \sqrt{5})/333 = 2.2\%$. This result is in agreement with that of other authors (Table II).

2·4. *Selection criteria adopted in the analysis of star prongs.* – In the analysis of the annihilation stars only part of the corresponding prongs was investigated in detail; the selection was made by adopting, for each particular problem, convenient rules based on the values of the blob density b/b_0 and the dip angle φ. Table V summarizes the various selection criteria to which we shall frequently refer later on; thus, for example, when we mention the tracks of class B we will refer to tracks with $b/b_0 > 1.1$ and a dip angle $\varphi \leqslant 45°$.

([20]) J. Button, T. Elioff, E. Segrè, H. M. Steiner, R. Weingart, C. Wiegand and T. Ypsilantis: *Phys. Rev.*, **108**, 1557 (1957).

TABLE V. – *Selection rules adopted in the investigation of the star prongs.*

$\varphi \leqslant$	$b/b_0 > 1.1$		$b/b_0 < 1.1$	
	Class of events	Used in the study of:	Class of events	Used in the study of:
90°	A	evaporation nucleons, etc.	D	pion multiplicity
45°	B	energy of prongs of stars at rest	—	—
16°	C	energy of prongs of stars in flight	—	—
12°	—	—	E	pion spectrum (scattering)

3. – Antiproton cross-sections.

3·1. *Collision with nuclei.*

3·1.1. Annihilation + charge exchange cross-section with nuclei. – Before presenting our results, it should be noticed that, for the sake of brevity, we will speak here of annihilation cross-section σ_a or annihilation mean free path λ_a; it would be more correct, however, to substitute always the word annihilation with the expression annihilation + charge exchange, because all the events which could be due to processes of the second type (Section 2·3) have been systematically lumped together with the stars certainly due to annihilation processes. It should be added that the charge exchange cross-section represents only $\sim 0.5\%$ of the annihilation cross-section [21].

In order to derive the annihilation cross-section as a function of the $\bar{p}$ energy, we have adopted the following criteria of evaluation of the kinetic energy of the antiproton at the annihilation point.

When the annihilation took place after a range in emulsion smaller than 13 cm, the residual range was evaluated as the difference between the average value of the range of antiprotons annihilating at rest ((14.4 ± 0.8) cm) and the observed range. The error affecting the energy at the annihilation point was computed for each event by taking into account the spread of the ranges given in Fig. 1.

---

[21] E. SEGRÈ: *Annual Review of Nuclear Science*, **8**, 127 (1958).

When the observed range was longer than 13 cm, the residual range was determined from an evaluation of the ionization of the $\bar{p}$ track close to the annihilation point.

Finally, when the residual range was estimated to be smaller than 5 mm, its value was determined by means of the constant sagitta scattering *vs.* range method ([22]).

The annihilation mean free path in emulsion $\lambda_a(T_{\bar{p}})$ was determined at various energy intervals. From these values, the corresponding average annihilation cross-sections were deduced by means of the relation

$$\sigma_a(T_{\bar{p}}) = \frac{\sum_i N_i \sigma_a^{(i)}}{\sum_i N_i} = \frac{1}{\lambda_a \sum_i N_i}, \tag{3.1}$$

where N_i is the number of nuclei of type i per cm^3.

The results obtained by such a procedure are plotted in Fig. 5. The last point on the right (corresponding to $T_{\bar{p}}$ between 210 and 230 MeV) is strongly affected by the fact that the mass determination by the method of the mean gap length variation *vs.* range is at the limit of its sensitivity because of the short range available for these measurements.

This point is clarified by the following considerations. A kind of « efficiency for identification of $\bar{p}$ » can be defined as the ratio of the number of tracks for which a mass determination is actually possible, to the total number of tracks measured in the same range interval. This efficiency turns out to be equal to 1 only for tracks of observed range larger than 4 cm ($T_{\bar{p}} \leqslant 200$ MeV at the annihilation point) and tends to zero at 2 cm from the front edge of the stack. Therefore in this range interval the inaccuracy affecting the efficiency obtained by such a procedure is very large.

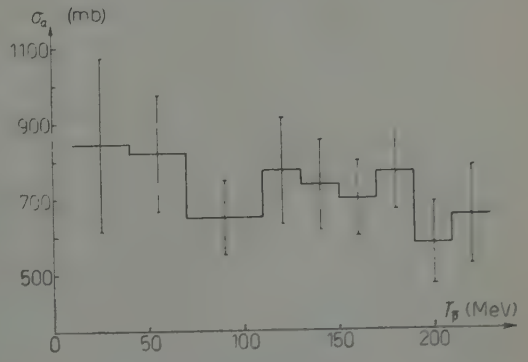

Fig. 5. – The average annihilation cross-section for emulsion nuclei *vs.* $\bar{p}$ kinetic energy: the histogram represents Rome data (283 stars in flight over 62.9 m).

Fig. 6 shows a comparison of our results with those of other authors. The histogram is obtained by combining our results with those of the Berkeley

([22]) G. Baroni, G. Cortini and A. Manfredini: *Nuovo Cimento*, **1**, 473 (1955).

group ([5]); the crosses represent the Uppsala results ([7]). The point on the right represents the results of counter measurements at 450 MeV ([20,21]), averaged over the emulsion composition (Hydrogen included). The curve represents the function

$$\left\langle \left(1 + \frac{V_C}{T_{\bar{p}}}\right) \sigma_a (450 \text{ MeV}) \right\rangle , \tag{3.2}$$

where V_C is the Coulomb potential evaluated at a nuclear radius corresponding to the antiproton cross-section at $T_{\bar{p}} \gg V_C$ ($V_C = 9$ MeV for heavy elements, $V_C = 2.5$ MeV for light elements) ([23,24,5]) and $\langle \sigma_a (450 \text{ MeV}) \rangle = 575$ mb. The symbol $\langle\ \rangle$ means averaging with respect to the emulsion composition.

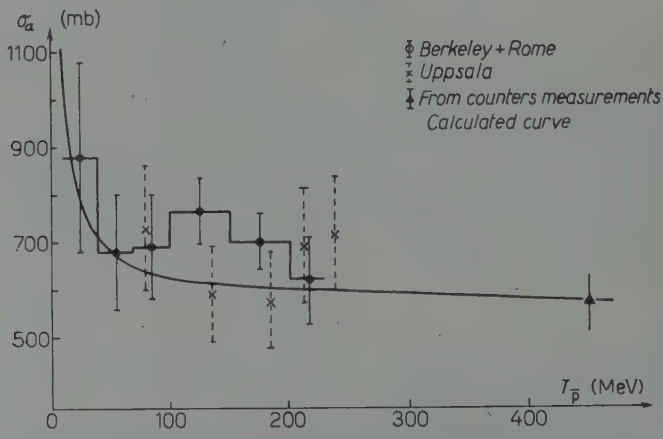

Fig. 6. – The average annihilation cross-section for emulsion nuclei *vs.* $\bar{p}$ kinetic energy: the histogram represents the Berkeley + Rome data, the crosses Uppsala results. The curve, normalized to counter measurements, gives the effect of electrostatic interaction.

An estimate of the annihilation mean free path λ_a averaged over the energy interval extending from 10 MeV to 230 MeV, can be derived directly by noticing that 304 stars have been observed over a total followed path of 62.7 m. The latter value is obtained by disregarding the 2 first cm of path close to the leading edge of the emulsions, where the identification of $\bar{p}$ becomes impossible. Furthermore, according to the remark given above, in this Section, the number of stars should be increased from 304 to 348 so as to take into account the « efficiency of identification of $\bar{p}$ » in the range interval between 2 and 4 cm from the front edge. Thus we obtain

$$\lambda_a = (18.0 \pm 0.9) \text{ cm} . \tag{3.3a}$$

([23]) J. M. Blatt and V. F. Weisskopf: *Theoretical Nuclear Physics* (New York, 1952).

([24]) R. M. Sternheimer: *Phys. Rev.*, **101**, 384 (1956).

If the expected contribution arising from annihilation in Hydrogen is subtracted (16 stars, computed from $\sigma_a(\bar{p}p) = 84$ mb) ([13]) we obtain

(3.3*b*) $$\lambda_a = (18.8 \pm 1.0) \text{ cm} \quad (\text{H excluded}) .$$

From (3.3*b*) we deduce

(3.4) $$\sigma_a/\sigma_0 = 2.06 \pm 0.11 ,$$

where σ_0 is the geometric cross-section defined by

(3.5*a*) $$\sigma_0 = \frac{\sum_i N_i \pi R_i^2}{\sum N_i} = 550 \text{ mb} .$$

The sum is extended over all nuclei present in the emulsion (G-5) excluded Hydrogen, and

(3.5*b*) $$R_i = 1.2 \cdot 10^{-13} A_i^{\frac{1}{3}} \text{ cm} .$$

Combining these results with the value (3.10*b*) of the inelastic scattering cross section, we find

(3.6) $$\sigma_r/\sigma_0 = 2.21 \pm 0.12 ,$$

where

$$\sigma_r = \sigma_a + \sigma_i$$

is the reaction cross-section. The corresponding mean free path in emulsion turns out to be

(3.8) $$\lambda_r = (17.5 \pm 0.9) \text{ cm} .$$

3·1.2. Elastic and inelastic scattering by nuclei. – The diffraction scattering has been measured on 15.0 m of tracks of $\bar{p}$ annihilating at rest. Only the scattering angles projected on the emulsion plane $\alpha \geqslant 1.5°$ have been measured ($T_{\bar{p}}$ varied between 250 and 50 MeV). The results of these measurements are in very good agreement with the results of other authors ([25]). They have already been reported and compared with the diffraction scattering of protons of 125 MeV (26.4 m of path) in a previous paper ([16]) and can be summarized as below. ([26]) The antiproton angular

([25]) G. Goldhaber and J. Sandweiss: *Phys. Rev.*, **110**, 1476 (1958).

([26]) Only recently did we become aware of a similar work going on at the Bern University ([11]).

distribution is much more peaked in the forward direction than that of the protons. This result can be interpreted qualitatively, in the case of protons, as due to destructive interference, between the effects of Coulomb interaction and nuclear forces. The results of computations made by BJORKLUND and FERNBACH (27) by means of an optical model derived from the phase-shifts given by BALL and CHEW (28), do not quite agree with the angular distribution of $\bar{p}$; however, similar computations made by the same authors in the case of protons, appear to deviate even more from the corresponding experimental results.

Apart from the above, rather accurate, measurements, we have recorded all large angle scatterings during the track following of all the antiprotons presented in this paper (75.9 m).

A deflection larger than 5° in projection—without any additional prong—has been observed in 103 cases. The corresponding angles in space were measured carefully. We have computed (Fig. 7) the maximum angle of deflection (in space) versus the residual range of an antiproton scattered elastically by a silver nucleus for which no recoil (not even 1 blob) is visible. Since all the other nuclei in emulsion are lighter than silver, this curve can be interpreted as an upper limit of the angle of deflection due to an elastic collision for which no recoil is visible. For the points which fall below the curve, with an angle of deflection larger than 5° (98 events), the ionization variation taking place at the collision point was measured by means of either the mean gap length or the total gap length method, according to convenience. An event has been taken as an elastic scattering whenever the gap length was found to be the same within the experimental error, before and after the deflection. Thus, we found 88 elastic scatterings over a total path length of 75.9 m.

The efficiency in detecting this type of events was not as high as that obtained in the measurements of the diffraction scattering; therefore, from the present data we can derive only a lower limit for the elastic scattering cross-section against nuclei, namely

$$\sigma_{\bar{p}N}(\theta > 5°) > 300 \text{ mb}, \quad \text{for } 50 \leqslant T_{\bar{p}} \leqslant 250 \text{ MeV}. \tag{3.9a}$$

By estimating the efficiency of detection of the scatterings, we obtain

$$\sigma_{\bar{p}N}(\theta > 5°) \approx (530 \pm 70) \text{ mb}. \tag{3.9b}$$

---

(27) These computations have been kindly made for us by S. FERNBACH and F. BJORKLUND.

(28) J. S. BALL and G. F. CHEW: *Phys. Rev.*, **109**, 1385 (1958).

The events with a variation of the total gap length outside the experimental error have been considered as inelastic scatterings. A detailed discussion of the separation between elastic and inelastic scatterings will be given in a successive paper.

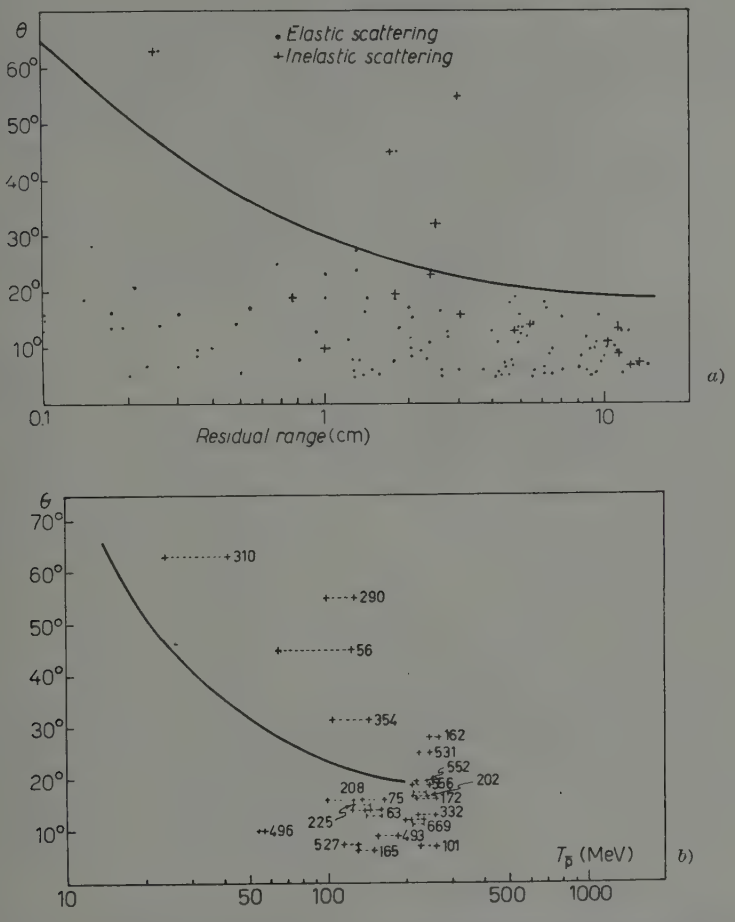

Fig. 7. – Angle of deflection in space versus residual range (*a*) or kinetic energy (*b*). The curve represents elastic collision with a silver nucleus giving minimum visible recoil (1 blob). In Fig. 7*a* elastic scatterings are indicated as dots and inelastic scatterings as crosses. In Fig. 7*b* only inelastic scatterings are given. For each event the kinetic energy before and after the collision is indicated. Event numbers are attached (see Table VI).

This definition differs from that adopted in previous works where an inelastic scattering was defined either by a visible variation of the ionization corresponding to $\Delta T_{\bar{p}}/T_{\bar{p}} \geq 20\%$, or by a visible excitation of the target nucleus. The first criterion is very unsensitive in a wide range of energies of the $\bar{p}$

($75 \leqslant T_{\bar{p}} \leqslant 280$ MeV) where the number of blobs is almost constant. The total gap length or the mean gap length, on the contrary, are very suitable parameters in this energy region. The second criterion does not discriminate against elastic scattering by light nuclei.

With the procedure mentioned above we have found 10 events which should be added to the 5 falling above the curve of Fig. 7, as well as to 8 events showing one or more certain prongs from a point where the total gap length undergoes an appreciable change. Table VI contains the detailed data relative to these 23 events, some of which, however, may be described as quasi-elastic scatterings, *i.e.* as elastic scatterings by nucleons moving in the nucleus due to the Fermi energy.

TABLE VI. – *Inelastic scattering* (*).

Event number	Angle of deflection (in space)	$T_{\bar{p}}$ (MeV)	$\Delta T_{\bar{p}}$ (MeV)	$\frac{\Delta T_{\bar{p}}}{T_{\bar{p}}}$	Remarks
56	45°	125 ± 5	52 ± 5	0.41 ± 0.01	—
63	14°	155 ± 5	15 ± 5	0.09 ± 0.03	—
75	15° 50′	165 ± 5	30 ± 5	0.18 ± 0.03	2 prongs $R = \begin{cases} 31.5\ \mu m \\ 34.3\ \mu m \end{cases}$
101	7°	260 ± 10	30 ± 10	0.11 ± 0.04	—
132	15° 30′	74 ± 3	6 ± 4	0.08 ± 0.05	
162	28°	253 ± 10	25 ± 10	0.10 ± 0.02	1 prong $R = 5.7\ \mu m$
165	7° 20′	150 ± 5	25 ± 10	0.16 ± 0.06	1 prong (p) $R = 410\ \mu m$
172	16° 20′	260 ± 10	40 ± 15	0.15 ± 0.06	1 prong (p) $R = 1100\ \mu m$
202	16° 30′	245 ± 10	25 ± 20	0.10 ± 0.08	1 prong $R = 15.3\ \mu m$
208	16°	130 ± 5	30 ± 5	0.23 ± 0.05	—
225	14°	145 ± 5	20 ± 5	0.14 ± 0.03	—
233	9°	240 ± 10	20 ± 10	0.08 ± 0.04	—
290	55°	130 ± 5	30 ± 5	0.23 ± 0.04	—
308	10°	70 ± 4	8 ± 4	0.11 ± 0.05	—
310	63°	42 ± 2	18 ± 2	0.43 ± 0.05	—
332	13° 30′	260 ± 10	40 ± 10	0.16 ± 0.04	blob
354	32° 15′	145 ± 5	35 ± 10	0.24 ± 0.08	—
493	8° 10′	180 ± 5	25 ± 5	0.14 ± 0.03	1 prong (p) $R = 1510\ \mu m$
527	7° 30′	130 ± 5	15 ± 5	0.11 ± 0.04	electron
531	25° 30′	230 ± 10	20 ± 10	0.09 ± 0.04	2 prongs $R = \begin{cases} 7\ \mu m \\ 8\ \mu m \end{cases}$
552	19° 30′	250 ± 10	35 ± 20	0.14 ± 0.08	—
566	19	250 ± 10	40 ± 20	0.16 ± 0.08	—
669	12 °05′	235 ± 10	15 ± 10	0.06 ± 0.04	1 prong (p) $R = 250\ \mu m$

(*) We thank Dr. G. EKSPONG for a few remarks on the criteria adopted for identifying the inelastic collisions.

After correcting for the geometrical bias arising from the condition that the angle of projecting should be larger than 5°, we find

$$\sigma_i = (73 \pm 13) \text{ mb}, \tag{3.10a}$$

for

$$30 \leqslant T_{\bar{p}} \leqslant 250 \text{ MeV}.$$

If a correction is introduced which takes into account the detection efficiency, we obtain

$$\sigma_i = (85 \pm 20) \text{ mb}. \tag{3.10b}$$

This value is appreciably higher than that given by other authors ([25,7]):

$$\sigma_i = (43 \pm 11) \text{ mb}. \tag{3.11}$$

We believe, however, that our value (3.10*b*) represents a lower limit for σ_i because we have certainly lost some events with $\theta < 5°$ as well as others with a total gap length variation smaller than the statistical accuracy of the measurements: five hundred blobs were counted in each case, both before and after the collision point.

The mean free path in emulsion, corresponding to the cross section (3.10*b*) amounts to

$$\lambda_i = (250 \pm 60) \text{ cm}. \tag{3.12}$$

3·2. *Collision with protons.* – The cross-section for elastic scattering by protons has been already discussed elsewhere ([12]).

Both the angular distribution and the total cross-section obtained from our 15 events were in good agreement with the results of other authors ([29,7]). Combining all these data (Table I) we find ([12])

$$\sigma_e(p\bar{p}) = (71 \pm 13) \text{ mb} \quad \text{for} \quad 50 \leqslant T_{\bar{p}} \leqslant 250 \text{ MeV} \quad (\overline{T}_{\bar{p}} = 150 \text{ MeV}). \tag{3.13}$$

This value, as well as the corresponding angular distribution, agree with Fulco's theoretical results ([30]).

A determination of the cross-section for annihilation of $\bar{p}$ with protons has not been attempted because of the uncertainty involved in the identification of the target nucleus.

([29]) G. Goldhaber, T. Kalogeropoulos and R. Silberberg: *Phys. Rev.*, **110**, 1474 (1958).

([30]) J. Fulco: *Phys. Rev.*, **110**, 784 (1958). J. S. Ball and J. R. Fulco: *Phys. Rev.* **113**, 647 (1959).

4. – Annihilation stars.

4·1. *π-mesons.*

4·1.1. Charged pions multiplicity. – All tracks with $b/b_0 \leqslant 1.1$ arising from annihilation stars have been considered as due to $\pi^{\pm}$ with a small contamination of $K^{\pm}$. The tracks of class B in the case of annihilation at rest and of class C in the case of annihilation in flight (Table V), have been followed for identification. The frequency of stars as a function of the observed multiplicity of charged pions $N_{\pi^{\pm}}$ is given in the upper part of Fig. 8. From these data the average charged pion multiplicities, without efficiency correction, turn out to be

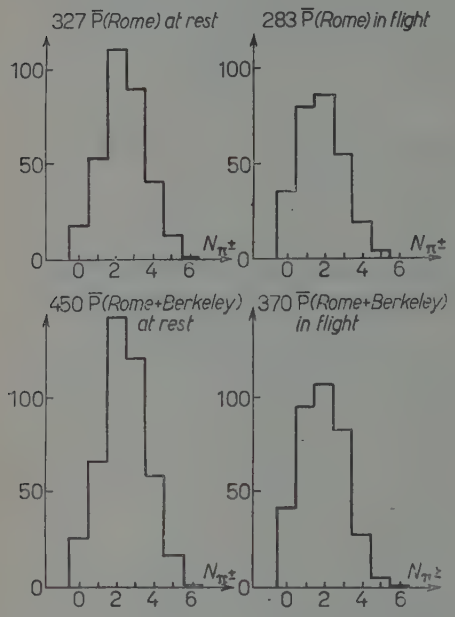

Fig. 8. – Charged pions multiplicity uncorrected for detection efficiency. Upper part Rome data, lower part Rome+Berkeley data combined.

$$(4.1)\quad \begin{cases} \langle N_{\pi^{\pm}} \rangle = 2.18 \pm 0.13 \\ \text{for annihilations in flight} \\ \langle N_{\pi^{\pm}} \rangle = 2.46 \pm 0.14 \\ \text{for annihilations at rest} \\ \langle N_{\pi^{\pm}} \rangle = 2.32 \pm 0.10 \\ \text{for all annihilations combined .} \end{cases}$$

In the lower part of the same figure are given the results obtained by combining the Berkeley ([5]) and Rome data.

By correcting for the efficiency of pion detection (Appendix I) one obtains, from our data

$$(4.2)\quad \begin{cases} \langle N_{\pi^{\pm}} \rangle = 2.34 \pm 0.13 & \text{for annihilations in flight} \\ \langle N_{\pi^{\pm}} \rangle = 2.64 \pm 0.14 & \text{for annihilations at rest} \\ \langle N_{\pi^{\pm}} \rangle = 2.49 \pm 0.10 & \text{for all annihilations combined .} \end{cases}$$

In Section 5·2 we will discuss the value of the total multiplicity $\langle N_{\pi} \rangle = \langle N_{\pi^{\pm 0}} \rangle$; in Section 4·1.4 we will determine a lower limit for the same quantity.

4·1.2. Pion energy spectrum. – Two different procedures have been followed for fast and slow particles.

For tracks of class E (Table V) the $p\beta$ has been determined by multiple scattering on 100 cells per track. All these particles have been assumed to be pions. The effect of distortion has been eliminated on each track by the third difference procedure, applied in the form suggested by SOLNTSEFF ([31]). The validity of this procedure was checked accurately on a conveniently chosen sample of tracks.

All tracks of class B from $\bar{p}$ at rest and of class C from $\bar{p}$ in flight (Table V), have been followed to their end. Whenever a track stopped in the emulsion, the corresponding energy was determined from the range-energy curve ([32]). The results, referred to the total solid angle and corrected for efficiency of pion detection (Appendix I) are given in Fig. 9. Special attention has been paid to the energy region where the results of the two methods overlap.

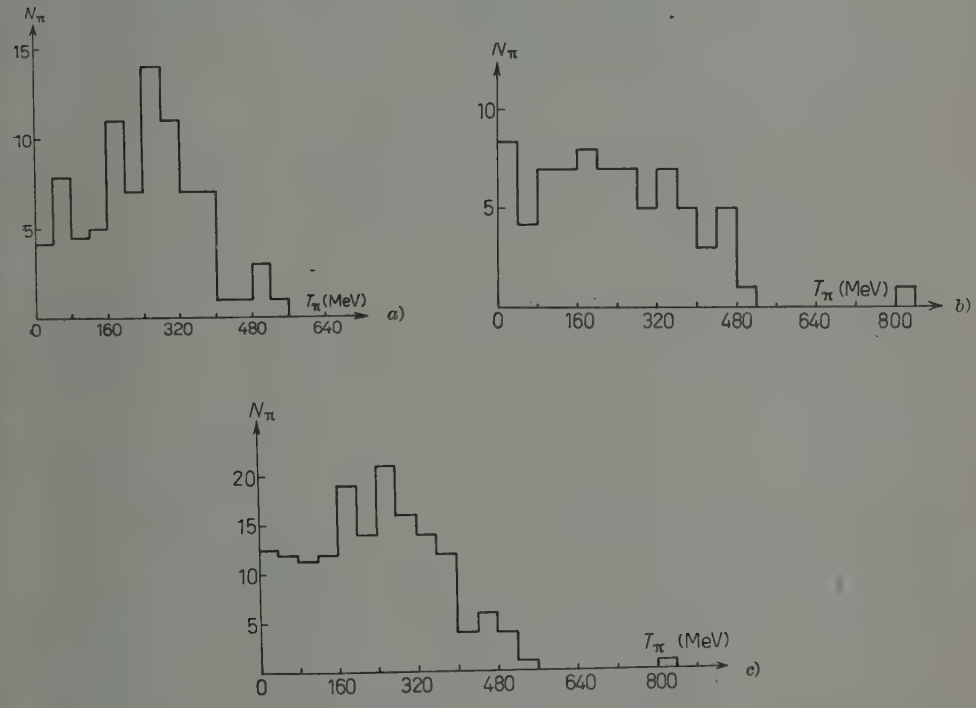

Fig. 9. – Charged pion spectrum: *a*) at rest; *b*) in flight; *c*) all combined.

([31]) N. SOLNTSEFF: *Nucl. Phys.*, **4**, 337 (1957); **6**, 222 (1958).
([32]) W. H. BARKAS: *Nuovo Cimento*, **8**, 201 (1958).

The average pion total energies corresponding to these spectra (not yet corrected for interaction in the nucleus) are

$$(4.3)\qquad \begin{cases} \langle E_{\pi^\pm} \rangle = (370 \pm 17)\ \text{MeV} & \text{for annihilations in flight} \\ \langle E_{\pi^\pm} \rangle = (379 \pm 12)\ \text{MeV} & \text{for annihilations at rest} \\ \langle E_{\pi^\pm} \rangle = (375 \pm 10)\ \text{MeV} & \text{for all annihilations combined .} \end{cases}$$

In the case of $\bar{p}$ at rest, our result is higher than the corresponding Berkeley value (Table II). The difference may be due to various reasons which will be discussed in Section 5·1; as is shown there, the most important cause for systematical error is, in our opinion, the distortion of the emulsion, the correction of which was made in different laboratories by different procedures. This source of error tends to depress the observed value of $\langle E_{\pi^\pm} \rangle$ as compared to the true value, so that we feel inclined to believe that our rather high result is preferable. However, the difference between the results of the two groups, is not much greater than the corresponding statistical errors; therefore it does not appear unjustified to take the averages of the Berkeley and Rome values

$$(4.4)\qquad \begin{cases} \langle E_{\pi^\pm} \rangle = (368 \pm 15)\ \text{MeV} & \text{for annihilations in flight} \\ \langle E_{\pi^\pm} \rangle = (365 \pm 10)\ \text{MeV} & \text{for annihilations at rest} \\ \langle E_{\pi^\pm} \rangle = (366 \pm 9)\ \text{MeV} & \text{for all annihilations combined .} \end{cases}$$

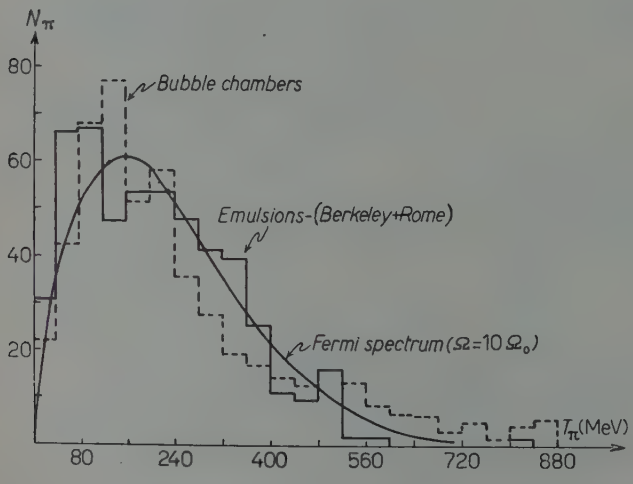

Fig. 10. – Charged pion spectrum: solid histogram Berkeley + Rome data (all combined); dotted histogram bubble chamber data: Horowitz *et al.* + Agnew *et al.* Curve: Fermi's spectrum with $\Omega = 10\,\Omega_0$.

The difference between the values of $\langle E_{\pi^\pm} \rangle$ for $\bar{p}$ at rest and in flight is smaller than the statistical error; therefore we have plotted in Fig. 10 the combined data of Berkeley + Rome (full line histogram).

In the same figure the pion spectrum produced in the annihilation of $\bar{p}$ with Hydrogen (dotted histogram) is given for comparison. This has been obtained by combining the results of Horowitz *et al.* ([17]), who used

a Hydrogen bubble chamber ($21 \leqslant T_{\bar{p}} \leqslant 46$ MeV) with those of AGNEW *et al.* ([14]) who used a propane bubble chamber ($75 \leqslant T_{\bar{p}} \leqslant 200$ MeV).

The corresponding average energy is

$$\langle E'_{\pi^{\pm}} \rangle = (385 \pm 7) \text{ MeV} . \tag{4.5}$$

As can be expected, the spectrum observed in emulsion is slightly shifted towards lower energies as compared to the spectrum observed in Hydrogen. We will come back to this point in Section 5·3.

The curve given in Fig. 10 is Fermi's statistical spectrum computed for $\Omega = 10\,\Omega_0$.

4·1.3. N_{π^+}/N_{π^-} ratio. – As already mentioned in Section 4·1.2 all class B tracks have been followed to their end. Only in a few cases did the particles come out of the stack before stopping. Thus, in the majority of cases, it was possible to decide the sign of the charge by inspecting the track end (decay, star or σ_e). We have found 19 π^+ and 37 π^- whose energy spectrum—not corrected for geometrical bias—is shown in Fig. 11. An influence of the Coulomb barrier is apparent in the figure, since no π^+ was found in the very low energy part of the spectrum.

If we take into consideration only pions of an energy larger than 20 MeV, the influence of the Coulomb barrier should be negligible. With this limitation we find

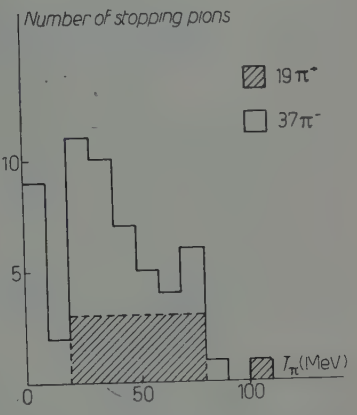

Fig. 11. – Energy distribution of pions with identified charge.

$$\frac{N_{\pi^+}}{N_{\pi^-}} = \frac{19}{26} = 0.73 \pm 0.20 . \tag{4.6a}$$

This value is higher than the one found by other authors (Table II: $20/44 = 0.45 \pm 0.12$ ([5]); $37/56 = 0.66 \pm 0.13$ ([7]); $3/4$ ([8])); however, the differences are not significant because of the large statistical errors. Summing up the data of all laboratories we find

$$\frac{N_{\pi^+}}{N_{\pi^-}} = \frac{81}{130} = 0.61 \pm 0.09 . \tag{4.6b}$$

This result is still slightly lower than the value computed by taking into account: *a*) the neutron-proton ratio in the nuclei of the emulsion (n/p = 1.2); *b*) the fact that in the annihilation with protons the ratio N_{π^+}/N_{π^-} should be

equal to 1, while in the annihilation with neutrons, N_{π^-} should be one unit larger than N_{π^+}.

From the average value

$$\langle N_{\pi^\pm} \rangle = \tfrac{2}{3} \cdot \langle N_{\pi^{\pm 0}} \rangle = \tfrac{2}{3} \cdot (4.77 \pm 0.14) = 3.2 \pm 0.1 \tag{4.7}$$

one derives

$$\left\langle \frac{N_{\pi^+}}{N_{\pi^-}} \right\rangle = \frac{1}{2.2}\left[1 + 1.2\,\frac{1.1}{2.1}\right] = 0.74\,. \tag{4.8}$$

The same value is deduced from the probability of annihilation as a function of the multiplicity of charged pions, using the statistical theory with an equilibrium volume 15 Ω_0 and with the appropriate weight factors originating from spin and isotopic spin of the annihilating nucleons ([2,33]).

If one takes into account the fact that, according to the considerations of Section 5·6, the ratio ξ of the probabilities for a $\bar{p}$ to annihilate with a neutron and a proton is smaller than 1 ($\xi \approx 0.64 \pm 0.26$), from an equation similar to (4.8) follows the value $N_{\pi^+}/N_{\pi^-} \approx 0.8$.

4·1.4. Stars with only minimum tracks. – Table VII shows the data referring to all the stars we have observed without heavy prongs. Part of the stars due to $\bar{p}$ in flight, which do not show a recoil and which have an

TABLE VII. – *Stars without heavy prongs* ($|\Delta z| \geqslant 20\ \mu$m).

Charged pions multiplicity	Stars at rest			Stars in flight		
	Total number of stars	Stars with recoil	Stars with electrons	Total number of stars	Stars with recoil	Stars with electrons
0	2	—	1	5 (a)	—	—
1	3	1	1	4	1	2
2	32	14	10	13	—	2
3	21	9	6	11	3	4
4	15	7	7	5	—	—
5	3	2	—	1	—	—
6	1	1	—	—	—	—
	77	34	25	39	4	8

(a) These 5 events do not include event $\bar{p}$-48 described in Appendix III in which only 2 $K^\pm$ are observed. The energies of the corresponding $\bar{p}$ are given in Sect. 2·3.1.

(33) A. I. NIKOŠOV: *Soviet Physics, JETP*, **3**, 976 (1957).

even number of prongs, may be due to annihilation processes in the Hydrogen present in the emulsion. In the case of stars produced at rest, this process is very improbable since the $\bar{p}$'s tend to be captured in atomic orbits of high Z nuclei.

From the $\bar{p}$-H annihilation cross-section obtained from counter work ($\sigma_a = (84 \pm 13)$ mb at $T_{\bar{p}} = 133$ MeV) ([13,21]) and from a total path length in emulsion of 62.7 m of $\bar{p}$ followed in the region accepted in the present work, one can compute a probable number of annihilations in H (with $\Delta z \geqslant 20$ μm) equal to 14. This value compares satisfactorily with our 21 stars without recoil, without electrons and with an even number of prongs (Table VII): in the same Table appear also 2 stars without recoil but with electrons, and 16 stars with an odd number of prongs.

It may be interesting to notice that the star described in Appendix 3 (in which a K^+K^- pair was observed) belongs to the stars without recoil, without electrons and with an even number of prongs.

The stars which are not due to annihilation in Hydrogen arise from annihilation in nuclei either without absorption of pions, or with absorption of pions accompanied only by neutral evaporation.

Therefore one is tempted to derive an estimate of a lower limit for $\langle N_\pi \rangle$ from the values of $\langle N_{\pi^\pm} \rangle$ deduced from Table VII, on the assumption of charge independence. Thus we obtain

$$(4.9)\quad \begin{cases} \langle N_\pi \rangle = \frac{3}{2}\langle N_{\pi^\pm} \rangle = \frac{3}{2}(2.74 \pm 0.34) = 4.12 \pm 0.57 \text{ for annihilation at rest,} \\ \langle N_\pi \rangle = \frac{3}{2}\langle N_{\pi^\pm} \rangle = \frac{3}{2}(2.25 \pm 0.41) = 3.38 \pm 0.62 \text{ for annihilations in flight.} \end{cases}$$

These values are appreciably lower than those found in Section 5·3. They are also lower than the values found by the Berkeley group through a procedure similar to the one used here ([5]). One should notice, however, that as a result of two opposite effects, the stars without heavy prongs represent a biased sample of low multiplicity. The first effect is due to the increase, with decreasing multiplicity, of the probability that none of the pions produced in the annihilation is absorbed in the nucleus. The second effect is that, by decreasing the multiplicity, the energy of the pions increases, on the average, so as to fall very often above the $(\frac{3}{2}, \frac{3}{2})$ pion-nucleon resonance. One can estimate that the first of these two effects predominates with the result that the values deduced by the procedure given above are expected to provide low values of $\langle N_\pi \rangle$. The fact that $\langle N_\pi \rangle$ turns out to be lower in the case of annihilations in flight —despite the contribution of annihilations with Hydrogen—can be attributed to the annihilation taking place, in this case, deeper in the nucleus (Section 5·5) so that the influence of the first mentioned effect is enhanced.

4·2. *Strange particles.* – Emulsions and bubble chambers give different types of information about the K-mesons emitted in annihilation stars.

While bubble chambers appear to be far superior instruments for the observation of neutral strange particles, the emulsions have a higher efficiency for the detection of charged strange particles of energy small enough to be brought to rest inside the stack. And even when the strange particles emerge from emulsion, their identification is often made possible by scattering and ionization measurements.

Following the tracks with $b/b_0 \geqslant 1.1$ as explained in Section 4·1.2 (class B and C) we have found 3 K mesons which stop in the emulsion and 1 Σ^- which decays in flight. All grey tracks of the corresponding stars have been carefully examined.

In order to identify fast strange particles, an accurate grain or blob counting has been carried out for all the tracks which, from scattering measurements, resulted to have $p\beta > 300$ MeV/c. No case of K-mesons was identified certainly by such a procedure.

Finally 2 more K-mesons were found by examining a star due to a $\bar{p}$ in flight ($\bar{p}$ 48) which showed only 2 gray prongs. These were found to be a K^+ and a K^-, both coming to rest in the emulsion; from the momentum balance it was found that at least 2 π^0 should be emitted in this event.

Table VIII contains all the details of these events.

In conclusion out of 349 stars due to $\bar{p}$ at rest, we have found 3 K-mesons and 1 Σ^-. From these data and taking into account the efficiency for detection of $K^{\pm}$-mesons (Appendix II), we deduce that the production of $K^0\bar{K}^0$, K^+K^-, $K^+\bar{K}^0$ and K^-K^0 occurs in $(4 \pm 2)\%$ of the stars due to $\bar{p}$ at rest.

In Fig. 12 we give the energy distribution of all $K^{\pm}$ observed in emulsions by various groups (Table II). The two curves represent the spectra computed by SANDWEISS [34] for the emission—in the annihilation process— of $2K+1\pi$ and $2K+2\pi$, multiplied by the factor $p(T_k)$ introduced in Appendix II so as to take into account the energy dependence of the experimental bias affecting the detection of $K^{\pm}$.

From the spectra of Sandweiss we obtain an average energy per pair of K particles produced in annihilation stars, of the order of

$$(493 + 200)\cdot 2 = 1390 \text{ MeV} .$$

Thus we can conclude that the production of K-meson pairs corresponds, on the average, to

$$\langle \sum E_{K\bar{K}} \rangle = 1390 \times (4 \pm 2)\cdot 10^{-2} = (55 \pm 28) \text{ MeV} . \tag{4.10}$$

[34] J. SANDWEISS: UCRL, 3577 (1956).

TABLE VIII. – *Strange particles (s. p.) observed in annihilation stars.*

Event number	$T_{\bar{p}}$	Number of s. p.	Observed range (mm)	Kinetic energy (MeV)	Dip angle	Mass (m_e)	Ending	Identity	Parent star					
									N_π	N_H	ΣE_π (MeV)	ΣE_H (MeV)	Total energy of s.p. (MeV)	Visible energy (MeV)
208	0	1	68.48	118	21°	1040 ± 70 (gap-range)	Star at rest with 2 prongs	K^-	2	1	$\geqslant 560$	> 100	611	> 1270
96	0	1	8.48	36	45°	—	Decay with a minimum track [$p\beta = (223 \pm 22)$ MeV/c]	K^+	0	3	—	105	529	634
143	0	1	63.70	105	6°	1230 ± 147 (gap-range)	Star at rest with 3 prongs	K^-	0	2+(1)	—	> 158	598	> 756
462	0	1	57.0	205	45°	3480 ± 1100	Decay in flight with 50 MeV π^-	Σ^-	0	2+(1)	—	> 195	465 (*)	> 659 (*)
48	205	2	*a*) 4.40	24.8	27°	—	Star at rest with 2 prongs	K^-	0	0	—	—	>1057	> 1057
			b) 45.0	45	49°	—	Decay with a minimum track	K^+						

(*) This is obtained as difference of the total energy of the Σ and the rest energy of a nucleon.

We will make use of this value for all stars irrespective of whether they are produced by $\bar{p}$ at rest or in flight.

Two more remarks may be added. The first is that, according to the data of Table VIII, on the average, the number of visible $\pi^{\pm}$ per star with K-mesons is

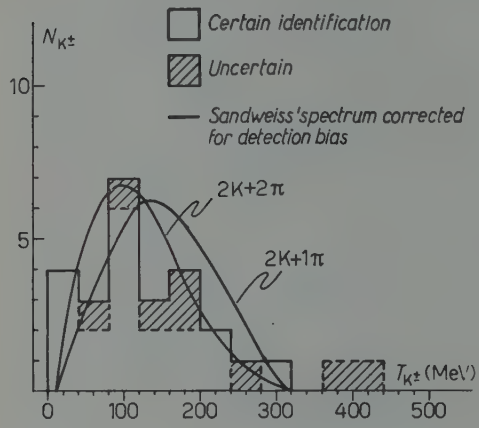

Fig. 12. – The energy distribution of strange particles from annihilation stars: the histogram is obtained by combining the results of all laboratories. The curves are the spectra computed by SANDWEISS corrected for the energy dependence of the detection efficiency.

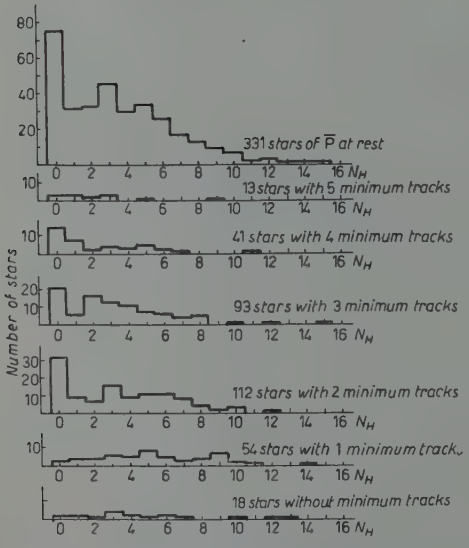

Fig. 13. – Frequency of annihilation stars versus N_H for different values of $N_{\pi^{\pm}}$.

$$\langle N_{\pi^{\pm}} \rangle = 0.4 \pm 0.3 .$$

The second remark refers to the energy of the heavy prongs observed in stars with one or two strange particles. From our data we find

$$(4.11a) \qquad \langle \sum E_H \rangle \geqslant 85 \text{ MeV} ,$$

which should be compared with the value

$$(4.11b) \qquad \langle \sum E_H \rangle \geqslant 105 \text{ MeV} .$$

deduced from the Saclay group results [10] by leaving out of the statistics one uncertain event. The values (4.11) represent lower limits, since not all the heavy prongs emitted in K-stars were measured.

The analysis of these stars cannot be pushed further because the data available are too scanty for determining the corresponding value of $\langle E_{\pi^{\pm}} \rangle$.

4·3. *Nucleons.* – We have limited the investigation of the black star prongs to the case of annihilations at rest.

Following the same rules used in previous works [2,5], we have divided the heavy prongs (H) into knock-on protons (KO: $T_p \geqslant 30$ MeV) and evaporation protons (EV: $T_p < 30$ MeV).

Fig. 13 shows the frequency of annihilation stars due to $\bar{p}$ at rest

as a function of N_H for various values of $N_{\pi^\pm}$. Fig. 14 gives the total number of heavy prongs versus the kinetic energy T_H of both evaporation and knock-on protons. The same data, combined for all values of $N_{\pi^\pm}$, are given in Fig. 15. In these two figures the data have been corrected for both the solid angle actually examined as well as for the finite dimensions of the stack.

Our results show a clear correlation between the number of heavy prongs per star and the multiplicity of charged pions, in agreement with previous works ([2,5]).

Fig. 16 shows the heavy prong differential spectrum from antiproton annihilation stars at rest versus the kinetic energy of the heavy prongs. Our results do not show the change in slope, found by the Berkeley group, at $T_H \sim 100$ MeV.

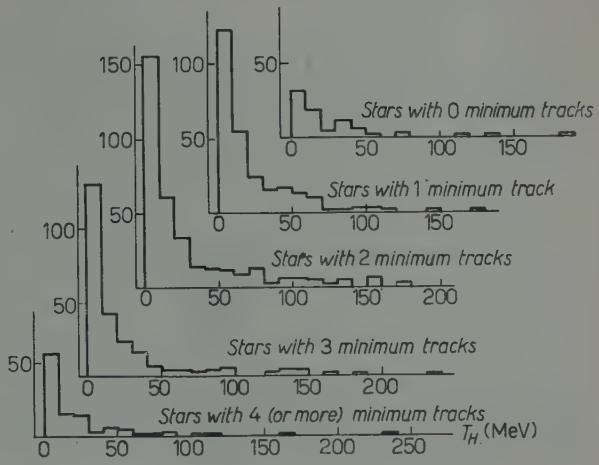

Fig. 14. – The total number of heavy prongs versus kinetic energy T_H for different values of $N_{\pi^\pm}$.

In conclusion, we deduce from our data the following average value of the energy of heavy prongs per star:

$$\langle \sum E_H \rangle = \langle \sum (T_H + 8 \text{ MeV}) \rangle = \begin{cases} (121 \pm 10) \text{ MeV} & \text{for } \bar{p} \text{ at rest} \\ (173 \pm 22) \text{ MeV} & \text{for } \bar{p} \text{ in flight} \\ (145 \pm 9) \text{ MeV} & \text{for } \bar{p} \text{ all combined.} \end{cases} \tag{4.12}$$

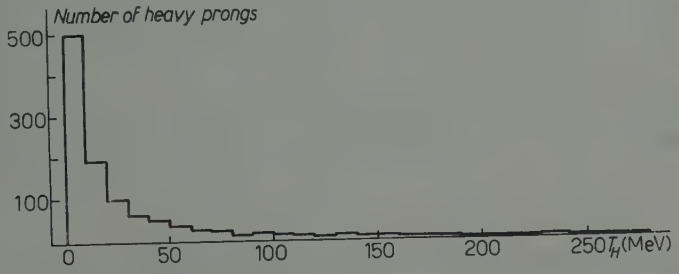

Fig. 15. – The total number of heavy prongs versus kinetic energy T_H, for any value of $N_{\pi^\pm}$.

4·4. *Electrons.* – In all annihilation stars due to $\bar{p}$ at rest a careful research was made for Dalitz pairs.

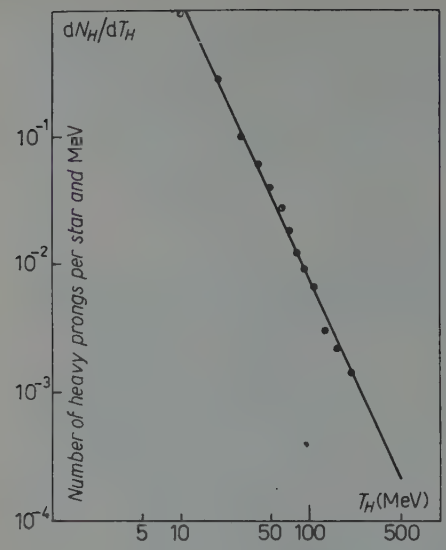

Fig. 16. – Heavy prong spectrum from antiproton annihilation stars at rest *vs.* the energy of heavy prongs T_H.

Over a total number of 192 charged pions we expected to find 5 Dalitz pairs, on the assumption of charge independence and using the known frequency of the Dalitz decay. We have actually observed only two events of this type. In one of these two cases, it was not possible to carry out reliable scattering measurements because of the very large dip angle. In the second case the energy of the two electrons was found to be (15 ± 3) and (22 ± 5) MeV.

We have also studied the electrons associated with annihilation stars due to $\bar{p}$ at rest. Only electrons of energy larger than 15 keV have been taken into consideration.

Table IX shows the observed frequency of stars with 1, 2 and 3 electrons of this type. For comparison we give the corresponding figures in the case of stars produced by the absorption of π^- and K^- ([35]).

TABLE IX. – *Frequency of stars with electrons produced by absorption of* π^-, K^- *and* $\bar{p}$ *in emulsion nuclei.*

Number of electrons, with kinetic energy > 15 MeV, per star	π^- ([34])	K^- ([34])	$\bar{p}$
1	15 %	25 %	26 %
2	4 %	6 %	4 %
3	0	1 %	0
Total . . .	19 %	32 %	30 %

The increase of the number of electrons with the mass of the particle captured in the atomic orbit is roughly what one would expect in the case

([35]) E. B. CHESICK and J. SCHEEP: *Phys. Rev.*, **112**, 1810 (1958); E. H. S. BURHOP: *Auger Effect* (Cambridge, 1952).

of the Auger effect. A quantitative comparison with the theory is, however, very uncertain since an appreciable fraction of the observed electrons arises from γ-ray conversion and β-radioactivity of the residual nucleus.

5. – Analysis and discussion.

5·1. *Comparison with other experimental data.* – A comparison of our experimental results with those of other nuclear emulsion works, is shown in Table II. Unfortunately the details of the Uppsala and Oxford data are not yet available to us and therefore the discussion will mainly refer to the Berkeley and Rome results.

While the agreement is rather satisfactory as a whole, a few comments may be added about the values of the π^+/π^- ratio, and the observed average energy of charged pions $\langle E_{\pi^\pm} \rangle$:

The values of the π^+/π^- ratio obtained by the various authors differ appreciably between them ([4,7]), but the statistical errors are so large that it appears justified to lump together all the data and give as a final result the value 0.61 ± 0.09. It differs from the expected value only slightly more than the statistical error.

The mean energy $\langle E_{\pi^\pm} \rangle$ deduced from the Oxford results is higher than our value, which, in turn, is appreciably higher then the corresponding Berkeley result. The difference between the two latter data appears to be outside the quoted experimental errors.

An incomplete correction for emulsion distorsion would shift the mean energy $\langle E_{\pi^\pm} \rangle$ towards lower values. On the contrary, a higher value of $\langle E_{\pi^\pm} \rangle$ could arise from an uncorrected loss of $\pi^\pm$ of low energy ($b/b_0 > 1.1$).

Finally it should be noticed that the minimum track detection efficiency and the solid angle inside of which the tracks are actually measured may also appreciably influence the value of $\langle E_{\pi^\pm} \rangle$.

Some « a posteriori » information on possible systematic errors affecting the emulsion values of $\langle E_{\pi^\pm} \rangle$, can be deduced by comparing them to the values of $\langle E'_{\pi^\pm} \rangle$, obtained from the annihilations of $\bar{p}$ in H observed in bubble chambers. From the data obtained by Horowitz *et al.* ([17]) with a hydrogen bubble chamber ($21 \leqslant T_{\bar{p}} \leqslant 46$ MeV) one obtains

$$\langle E'_{\pi^\pm} \rangle = (382 \pm 10) \text{ MeV} . \tag{5.1}$$

This value perfectly agrees with the value deduced by Agnew ([14]) from the $\bar{p}$-H annihilations observed in a propane bubble chamber

$$\langle E'_{\pi^\pm} \rangle = (389 \pm 10) \text{ MeV} \quad \text{for } \langle \overline{T}_{\bar{p}} \rangle = 80 \text{ MeV} . \tag{5.2}$$

Combining the spectra obtained by these two groups, one obtains the dotted hystogram of Fig. 10; the corresponding average pion energy is given by (4,5).

Assuming that the measurements in bubble chamber are not affected by systematical errors, the corresponding value of $\langle E'_{\pi^\pm} \rangle$ can be considered as an upper limit for the values of $\langle E_{\pi^\pm} \rangle$ in nuclear emulsion. Then our result appears to be slightly high; it should be noticed, however, that inside one experimental error there is enough room for the correction arising from the energy loss due to inelastic scatterings undergone by the charged pions in emerging from an emulsion nucleus.

5·2. *Energy balance.* – We can now impose the energy balance to the annihilation process in order to establish what fraction of the total energy release W is taken off by neutral pions. Following the same procedure used in previous works, we compute the fraction of the total energy W which is observed in the $\pi^\pm$ component

$$\frac{\langle \sum E_{\pi^\pm} \rangle}{W} = \frac{e_\pi^{-1} \langle N_\pi \rangle \langle E_{\pi^\pm} \rangle}{W} . \tag{5.4}$$

The total energy available is given by

$$W = (2 m_p c^2 - 8) \text{ MeV} = 1868 \text{ MeV} , \tag{5.5a}$$

for $\bar{\text{p}}$ at rest, and by

$$W = (2 m_p c^2 + T_{\bar{p}} - 8) \text{ MeV} = 2018 \text{ MeV} , \tag{5.5b}$$

for $\bar{\text{p}}$ annihilating in flight with an average kinetic energy $\bar{T}_{\bar{p}} = 150$ MeV.

The energy taken off by the nucleons —*i.e.* by the evaporation+knock-on *protons and neutrons*—can be computed by means of the empirical relation ([5,36])

$$U = h \langle \sum E_H \rangle , \tag{5.6a}$$

where

$$h = 2.7 . \tag{5.6b}$$

The energy spent in strange particle production has already been estimated in Section 4·2 (Eq. (4.10)). The fraction

$$1 - \frac{\langle \sum E_{\pi^\pm} \rangle + U + \langle \sum E_{K\bar{K}} \rangle}{W} . \tag{5.7}$$

is taken off by neutral pions and possibly by other neutral particles.

([36]) T. KALOGEROPOULOS: UCRL, 8677 (1959).

The results of such an analysis are shown in Fig. 17 where the results of the Berkeley group and those of the Rome and Berkeley groups combined, are also given for comparison.

Fig. 17. – Energy balance in annihilation stars observed in emulsion.

Our results differ from those of the Berkeley group, mainly because of the lower values that we find for $\langle \sum E_H \rangle$ (Section 5·1). The difference may be due only in minor part to the fact that in our case the average kinetic energy of the $\bar{p}$'s producing the stars analysed for the heavy prongs is $\bar{T}_{\bar{p}} = 114$ MeV, while in the Berkeley case is $\bar{T}_{\bar{p}} = 140$ MeV. According to our data, the neutral particles take off an energy larger than one half that taken off by the $\pi^{\pm}$ component. A similar indication was already noticeable in Ber-

keley's results. It is difficult to state at present to what extent this result may be attributed to experimental errors or to an actual feature of the annihilation of $\bar{p}$ in emulsion nuclei. Apart from some criticism that can be raised about the use of eq. (5.6) (Section 5·3), one has to keep in mind that the error affecting the neutral particles component is correlated in opposite direction to the errors on the other components, in particular to that of the $\pi^{\pm}$ component.

Thus one can conclude that our results are still compatible with the assumption of charge independence.

5·3. *Pion multiplicity and average number of pions interacting in an emulsion nucleus.* – The determination of the pion multiplicity $\langle N_{\pi} \rangle$ in $\bar{p}$ annihilating with a nucleon and of the average number ν of pions interacting per star produced by the annihilation of a $\bar{p}$ in an emulsion nucleus, has been made in previous works by a set of equations expressing the energy and particles balance. These equations contain a few coefficients taken from the analysis of stars produced by charged pions the values of which are open to some criticism. The determination of the set of values of the unknown parameters is made by the « best fit method » to the experimental data ([2,5,36]).

By applying this procedure to our new data, a value of the multiplicity $\langle N_{\pi} \rangle$ is found which is appreciably lower than that deduced from previous emulsion work. This can be easily recognized from the following remarks.

The result of the best fit procedure essentially consists of an increase of the observed energy $\langle E_{\pi^{\pm}} \rangle$ by roughly 15 MeV; this increase represents the correction for the energy lost by the charged pions through scatterings by the nucleons of the nucleus where the annihilation took place. Once the corrected average energy per charged pion

$$\langle E'_{\pi^{\pm}} \rangle = (\langle E_{\pi^{\pm}} \rangle + 15 \pm 5) \text{ MeV} \tag{5.8}$$

is known, one can deduce the average total pion multiplicity

$$\langle N_{\pi} \rangle = \frac{W - \langle \sum E_{KK'} \rangle}{\langle E'_{\pi^{\pm}} \rangle} . \tag{5.9}$$

on the assumption of charge independence, *i.e.*

$$\langle E'_{\pi^{+}} \rangle = \langle E'_{\pi^{-}} \rangle = \langle E'_{\pi^{0}} \rangle = \langle E'_{\pi^{\pm}} \rangle .$$

In Table X the second column shows the values of $\langle N_{\pi} \rangle$ obtained by introducing our results (4.3) into (5.8) and (5.9); in the third column the calcu-

lation has been done using the Berkeley+Rome combined data, (4.4), instead of (4.3).

TABLE X. — $\langle N_\pi \rangle$ *values.*

$\bar{p}$	Rome	Berkeley+Rome [5]	Bubble chambers [17,14]
in flight	5.10 ± 0.24	5.12 ± 0.22	5.10 ± 0.12
at rest	4.60 ± 0.15	4.77 ± 0.14	4.72 ± 0.11
combined	4.82 ± 0.14	4.92 ± 0.13	4.89 ± 0.12

It may be noticed that the values of the third column are practically identical to those deduced from $\bar{p}$-H annihilations observed in bubble chambers which are given in the fourth column of Table X. They have been obtained by introducing the value (4.5) into (5.9).

If we denote by a the fraction of the interacting pions which are absorbed in an emulsion nucleus ([2,5]) we have

$$\langle N_\pi \rangle = \frac{1}{e_\pi} \frac{N_{\pi^{0\pm}}}{N_{\pi^\pm}} \langle N_{\pi^\pm} \rangle + av \,, \tag{5.11a}$$

which, for $e_\pi = 0.93 \pm 0.03$, $N_{\pi^{0\pm}}/N_{\pi^\pm} = \frac{3}{2}$ and $\langle N_{\pi^\pm} \rangle = 2.46 \pm 0.14$ gives

$$\langle N_\pi \rangle = 3.97 \pm 0.26 + av \qquad \text{(for } \bar{p} \text{ at rest)}. \tag{5.11b}$$

Introducing into Eq. (5.11b) the values of $\langle N_\pi \rangle$ given in the fourth column of Table X, we deduce

$$av = 0.75 \pm 0.27 \qquad \text{(for } \bar{p} \text{ at rest)}, \tag{5.12}$$

which, with [5]

$$a = 0.75 \pm 0.03 \tag{5.13}$$

gives finally

$$v = 1.00 \pm 0.36 \qquad \text{(for } \bar{p} \text{ at rest)}. \tag{5.14}$$

The values (5.10), (5.13), (5.14) of $\langle N_\pi \rangle$, a and v can now be tested by computing

$$U = v\{\langle E'_\pi \rangle + w_0 - (1-a)E_0\} \,, \tag{5.15}$$

$$\langle E_{\pi^\pm} \rangle = \frac{\{(\langle E'_\pi \rangle - w)(\langle N_\pi \rangle - v) + (1-a)vE_0\}}{\langle N_\pi \rangle - av} \,, \tag{5.16}$$

where $w_0 \approx (15 \pm 6)$ and $w \simeq (5 \pm 2)$ MeV are two correction terms arising from the energy dependence of the pion-nucleon interaction, and $E_0 = (215 \pm 15)$ MeV is the final average total energy of pions scattered inelastically by nucleons ([5]).

Once U is known, the value of $\langle \sum E_H \rangle$ can be deduced by means of Eq. (5.6).

Table XI shows the results of such a computation for our stars at rest, in flight and all combined. The agreement between the computed and the measured values of $\langle \sum E_H \rangle$ and $\langle E_{\pi\pm} \rangle$ is satisfactory for $\bar{p}$ at rest, while for $\bar{p}$ in flight the computed value of $\langle \sum E_H \rangle$ is much higher than the corresponding measured value. The discrepancy is probably due to the use of eq. (5.15), (5.16) which involves the assumption that $\langle \sum E_H \rangle$ is proportional to ν.

TABLE XI. – *Summary of the results of the analysis of the annihilation stars.*

		At rest	In flight	Combined
$\langle N_\pi \rangle$		4.72 ± 0.11	5.10 ± 0.12	4.89 ± 0.12
ν		1.00 ± 0.36	2.11 ± 0.32	1.52 ± 0.27
$\langle \sum E_H \rangle$ (MeV)	comp.	128 ± 46	269 ± 47	194 ± 34
	meas.	121 ± 10	173 ± 22	145 ± 9
$E_{\pi\pm}$ (MeV)	comp.	369 ± 8	354 ± 18	362 ± 5
	meas.	379 ± 12	370 ± 17	375 ± 10

From the results of METROPOLIS *et al.* ([37]) it may be gathered, for example, that two knock-on protons of 100 MeV each, produced in the same emulsion nucleus, give a number of visible prongs 1.3 times the one produced by a single proton of the same energy.

Therefore we may conclude that our emulsion data are in satisfactory agreement with the value of the multiplicity deduced from bubble chamber work and they show that, on the average, the number of pions interacting in emulsion nuclei is equal to 1 pion per star ($\pm 36\%$) for $\bar{p}$ at rest and equal to 2 pions per star ($\pm 15\%$) for $\bar{p}$ in flight. For all stars combined we have

$$\nu = 1.52 \pm 0.27 .$$

([37]) N. METROPOLIS, R. BIVIUS, R. STORM, J. M. MILLER, G. FRIEDLANDER and A. TURKEVICH: *Phys. Rev.*, **110**, 204 (1958).

5·4. *Other estimates of the number ν of interacting pions per star.* – In this Section we will describe two other estimates of the average number of pions interacting per star in the same nucleus where the annihilation took place. The first method is based on the consideration of the frequency of « white stars » *i.e.* of stars without heavy prongs but with only minimum and gray tracks. In the form adopted here this procedure will actually provide a lower limit for the ν values.

The second procedure is based on the frequency of knock-on protons.

The results of these two methods are given by eq. (5.21), (5.23) and (5.24) which should be compared to the data given in Table X of the previous Section. By averaging these three results we obtain

(5.17*a*) $\qquad \nu = 1.34 \pm 0.14$ for annihilations at rest,

(5.17*b*) $\qquad \nu = 2.24 \pm 0.33$ for annihilations in flight,

where the errors represent the external standard deviations.

5·4.1. Determination of ν from the frequency of « white stars ». – A determination of ν can be made by considering the frequency of stars without heavy prongs (white stars). This procedure has not been used before, owing to the limited statistics available.

The probability of observing N_w white stars out of a total number of stars of any type, N_{stars}, is given by

(5.18) $$\frac{N_w}{N_{\text{stars}}} = \eta^{\langle N_\pi \rangle} + \varphi_{\text{H}} + \varphi_{\text{n}} ,$$

where φ_{H} is the contribution to white stars arising from annihilation in Hydrogen, φ_{n} the probability of observing an annihilation star produced in an emulsion nucleus different from H in which all heavy particles, EV+KO, are neutrons, and η the probability that one of the pions produced in the annihilation does not undergo any interaction. The first term on the right of eq. (5.18) is written on the assumption that no correlation exists between the absorption probability of one, two or more pions (Appendix IV). The quantity η is bound to ν and $\langle N_\pi \rangle$ by the relation

(5.19) $$\eta = 1 - \frac{\nu}{\langle N_\pi \rangle} .$$

In the case of $\bar{\text{p}}$ annihilations in flight, we have $N_w/N_{\text{stars}} = 39/283 = 0.14 \pm 0.02$ from which we should subtract the Hydrogen contribution (Section 4·1.4) $\varphi_{\text{H}} = 14/283 = 0.050 \pm 0.013$. Introducing these data into

eq. (5.18) and neglecting φ_n, we obtain

$$1 - \eta \geqslant 0.38 \pm 0.04 . \tag{5.20}$$

From (5.20) and (5.19) we deduce

$$\nu \geqslant 1.94 \pm 0.19 \quad \text{for annihilations in flight.} \tag{5.21}$$

In the case of annihilations at rest we have $N_w/N_{stars} = 77/337 = 0.23 \pm 0.03$, $\varphi_H = 0$; neglecting again φ_n we obtain

$$1 - \eta \geqslant 0.27 \pm 0.02 \tag{5.22}$$

$$\nu \geqslant 1.29 \pm 0.09 \quad \text{for annihilations at rest.} \tag{5.23}$$

5·4.2. Determination of ν from the frequency of knock-on protons. – According to the current picture of the annihilation process in heavy nuclei, the pions and the strange particles emitted in the primary act produce secondary nucleons through their interaction with the surrounding nuclear matter. These nucleons, in turn, interact with other nucleons so that only part of them emerge from the nucleus with an energy large enough to be considered as knock-ons, according to our definition ($T_H \geqslant 30$ MeV). The other nucleons, as well as their secondaries, constitute the evaporation nucleons. This picture shows that from the number of knock-ons observed per star it is possible to derive an estimate of the average number of pions interacting within the emulsion nucleus where the annihilation takes place.

In the rough scheme described below we have neglected the certainly not large contribution arising from the interaction of strange particles with the surrounding nucleons. Therefore only two processes have been considered: the absorption and the scattering of pions.

It is well known that the absorption of pions within a nucleus takes place mainly through a quasi-deuteron system ([38-40]). The result of this process is the production of two fast nucleons: 2 protons in the case of π^+, 2 neutrons in the case of π^-, and 1 proton and 1 neutron in the case of π^0-absorption.

The actual computation of the number of knock-ons per star was made by taking into consideration: *a*) the multiplicity of the various charge states of the pions; according to eq. (4.8) $n_{\pi^+} = 0.29$, $n_{\pi^-} = 0.38$, $n_{\pi^0} = 0.33$; *b*) the

---

([38]) K. A. Bruckner, R. Serber and K. Watson: *Phys. Rev.*, **81**, 575 (1951).
([39]) V. De Sabata, E. Manaresi and G. Puppi: *Nuovo Cimento*, **10**, 1704 (1953).
([40]) A. Minguzzi and A. Minguzzi-Ranzi: *Nuovo Cimento*, **10**, 1100 (1958).

fact that the absorption cross-section of π^0 is one half that of charged pions; *c*) the experimental results on the probability of observing knock-on protons from the absorption of π^- at rest ([39]) and in flight ([38]) and of π^+ in flight ([40]); *d*) the scattering cross-section of pions by nucleons and, finally; *e*) the spectrum of the annihilation pions.

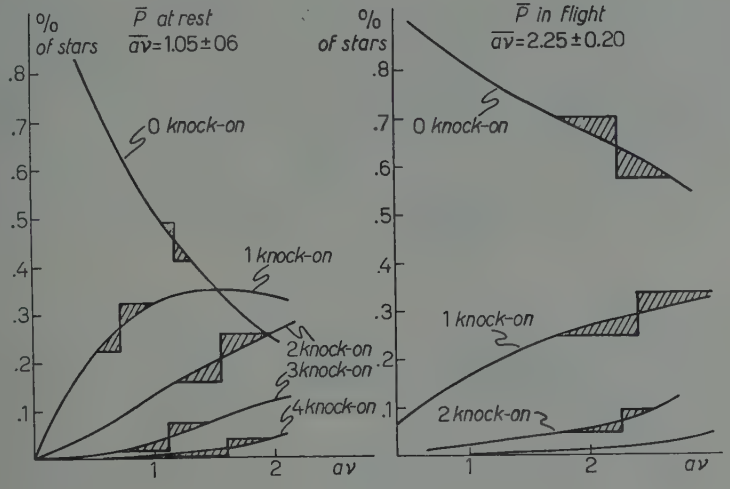

Fig. 18. – Frequency of annihilation stars *vs.* *av*.

The results are presented in the form of graphs (Fig. 18) giving, as a function of *av*, the frequency of annihilation stars with 0, 1, 2, ... knock-on protons. By comparison with the experimental results (Table XII) we obtain:

(5.24*b*) $\qquad av = 2.25 \pm 0.20$ for annihilations in flight,

(5.24*a*) $\qquad av = 1.05 \pm 0.06$ for annihilations at rest.

TABLE XII. – *Observed frequency of annihilation stars with* N_{KO} *knock-on protons.*

N_{KO}	$\bar{p}$ at rest (solid angle = .71 π)	$\bar{p}$ in flight (solid angle = .29 π)
0	.54 ± .04	.63 ± .07
1	.29 ± .03	.29 ± .05
2	.13 ± .02	.07 ± .02
3	.03 ± .01	.01 ± .01
4	.01 ± .01	—

Taking for a the value (5.13), we deduce

$$(5.25) \qquad \begin{cases} \nu \sim 3.0 \pm 0.3 & \text{for annihilations in flight,} \\ \nu = 1.4 \pm 0.1 & \text{for annihilations at rest.} \end{cases}$$

The value obtained by this procedure for $\bar{p}$ in flight is uncertain far beyond the indicated statistical error, because, as it appears from Table XI, the solid angle over which the measurement of the knock-on protons were actually made, was very small. This circumstance affects in a rather complicated way the observed frequency of stars with 0, 1, 2, ... knock-on protons.

With this remark in mind, we may conclude that the results (5.25) do not disagree too much with those of the other methods presented in Sections 5·3 and 5·4.1.

5·5. *The annihilation radius.* – Since the annihilation of an antiproton takes place on the surface of the nucleus, one can define an annihilation radius R_a as the average distance from the centre of the nucleus to the point where the process takes place. This radius should be interpreted differently according to whether the annihilating $\bar{p}$ is in flight or at rest. For $\bar{p}$ in flight, one can use an over-simplified picture, which is approximately correct only when the wave-length of the incident $\bar{p}$ is short as compared to the radius R of the target nucleus. Under these conditions, the annihilation radius R_a can be described as the average distance from the centre of the nucleus to the point where the $\bar{p}$ can penetrate before annihilating.

For $\bar{p}$ at rest, one can still define an annihilation radius R_a; in this case, however, the annihilation takes place from an atomic orbit. Therefore the annihilation radius will be determined by the overlap integral of the square of the antiproton wave function in the atomic state from which the annihilation takes place, and the nuclear density distribution.

An estimate of R_a has been made in previous works ([5,36]) using the value of the average number ν of pions per star interacting with the nucleons of the average emulsion nucleus.

Here we follow the same procedure, starting from the values of ν (5.17) obtained by averaging the results of three independent determinations. By making use of Kalogeropoulos curves ([36])—which give $1 - \eta$ *vs.* R_a/R— we obtain

$$(5.26) \qquad \begin{cases} R_a/R = 0.98 \pm 0.03 & \text{for annihilations in flight,} \\ R_a/R = 1.06 \pm 0.03 & \text{for annihilations at rest.} \end{cases}$$

According to the above remark, we can deduce from the value of R_a/R obtained from $\bar{p}$ in flight, the average penetration of a $\bar{p}$ in emulsion nuclei. Using again Kalogeropoulos curves ([36]), we get

$$D = (1.1 \pm 0.2)\cdot 10^{25} \text{ nucleons/cm}^2 . \tag{5.27a}$$

This value does not include the effect of elastic scattering of the incident $\bar{p}$ by the nucleons in the nucleus. However, in view of the roughness of the model, we do not deem necessary to correct this value for the contribution of the elastic scattering.

The value (5.27*a*) can be transformed into a length once the density of nuclear matter is known; if we agree to adopt for the density of nuclear matter the value

$$\varrho_0 = \frac{A}{\frac{4}{3}\pi r_0^3 A} = \frac{3}{4\pi r_0^3} ,$$

with $r_0 = 1.2\cdot 10^{-13}$ cm, we obtain

$$\lambda_{\bar{p}} = \frac{D}{\varrho_0} = (0.8 \pm 0.15)\cdot 10^{-13} \text{ cm} , \tag{5.27b}$$

which fairly agrees with the value computed by Fulco ([41]) for $T_{\bar{p}} = 150$ MeV: $\lambda_{\bar{p}} = 0.7\cdot 10^{-13}$ cm.

5·6. *Ratio of the probabilities of annihilation of* $\bar{p}$ *at rest with neutrons and protons bound in emulsion nuclei.* – Some information on the ratio of the probabilities of annihilation of antiprotons with neutrons and protons bound in emulsion can be derived from an analysis of the frequency of stars with given numbers of charged pions. The procedure described below is expected to give correct results only in the limiting case of very weak absorption of the annihilation pions within the nucleus where the annihilation took place. Therefore, we can hope that the method will provide a rough—but not uncorrect—result when applied to the annihilation of $\bar{p}$ at rest, while we should expect that it will fail in the case of $\bar{p}$ in flight.

Let us call O_r the frequency of stars produced in emulsion by $\bar{p}$ (at rest) which show r-charged pions tracks.

For even r, one can write

$$O_r = \mu_p^r \alpha_r^r + \mu_p^{r+2} \alpha_{r+2}^r + \mu_p^{r+4} \alpha_{r+4}^r + \ldots + \mu_n^{r+1} \alpha_{r+1}^r + \mu_n^{r+3} \alpha_{r+3}^r + \ldots . \tag{5.28}$$

A similar expression with the subscripts p and n exchanged, holds for odd r.

([41]) J. R. Fulco: *Phys. Rev.*, **114**, 374 (1959).

In eq. (5.28) μ_p^r (μ_n^r) means the probability for a $\bar{p}$ of annihilating with a proton (neutron) with emission of r charged pions, so that

$$(5.29) \qquad \sum_{r=0,\,2,\,4,\,6,\ldots} \mu_p^r = \frac{\Sigma_p}{\Sigma_p + \Sigma_n}, \qquad \sum_{r=1,\,3,\,5,\ldots} \mu_n^r = \frac{\Sigma_n}{\Sigma_p + \Sigma_n},$$

where Σ_p and Σ_n are the probabilities of annihilation of an antiproton with protons and neutrons bound in emulsion nuclei respectively. The coefficients α_k^r represent the probability that out of k charged pions emitted in an annihilation process, r are not absorbed while the remaining $(k - r)$ are absorbed in the same nucleus at the border of which the annihilation took place. Its value depends, in a rather complicated way, on various details of the particular annihilation process considered; in particular it depends on the number of neutral pions accompanying the k charged pions.

A first estimate of α_k^r can be obtained by neglecting any type of correlation. This means that a probability of absorption ε is assigned to each charged pion independently of its energy and of what happens to the other pions emitted simultaneously. On this oversimplified assumption we have

$$(5.30) \qquad \alpha_k^r = \binom{k}{r}(1-\varepsilon)^r \varepsilon^{k-r}.$$

From the discussion appearing at the beginning of Appendix IV, one may conclude that Eq. (5.30) constitutes a rough but not uncorrect description of the actual situation. Thus, as long as the correlation between the absorption of two or more pions can be neglected, all the coefficients α_k^r are expressed in terms of a single adjustable parameter ε, the value of which can be evaluated as shown in Appendix IV.

Then, the set of eq. (5.28) can be solved with respect to μ_p^r and μ_n^r and the ratio Σ_n/Σ_p can be deduced by means of Eq. (5.29).

Table XIII refers to annihilation stars due to $\bar{p}$ at rest; it contains the

TABLE XIII. – *Frequency of stars with a given number of charged pions* ($\bar{p}$ *at rest*).

r	O_r observed	O_r corrected	μ_r $\varepsilon = 0.16$ $e_\pi = 0.93$
0	0.05	0.06	0.004
1	0.16	0,15	0.03
2	0.34	0.35	0.33
3	0.28	0.25	0.27
4	0.13	0.15	0.22
5	0.04	0.04	0.10
6	0.003	0.004	0.014

measured values of O_r, as well as the values of the same quantities, corrected as explained in Appendix IV. Column 4 of the same table contains the values of μ_p^r and μ_n^r as they result for $\varepsilon = 0.16$; the choice of this value is justified in Appendix IV. The ratio $\xi = \Sigma_n/\Sigma_p$ is plotted *vs.* e_π for a few values of ε in Fig. 18. This figure shows that, for our value of $e_\pi = 0.93 \pm 0.03$ the ratio $\xi = 0.64 \pm 0.26$ is appreciably smaller than the n/p = 1.2 ratio valid on the average for the emulsion nuclei. One could add that, since the annihilation of $\bar{p}$ at rest takes place mainly in Br and Ag, the effective n/p ratio is still larger.

The same computation applied to the Berkeley data with $e_\pi = 0.90$ and $\varepsilon = 0.18$ gives $\xi = 0.55 \pm 1.27$.

A confirmation of this result is certainly desirable, by repeating the experiment in emulsion with a better statistics, or better by making it in deuterium. One can notice, however, that various interpretations can be envisaged which make use of the fact that the $\bar{p}$-p system is a mixture of $T=1$ and $T=0$ states whereas the $\bar{p}$-n system is a pure $T=1$ state. Then a low value of ξ could arise, for example, from the fact that the matrix element of the annihilation process is appreciably larger in the $T=0$ state than in the $T=1$ state.

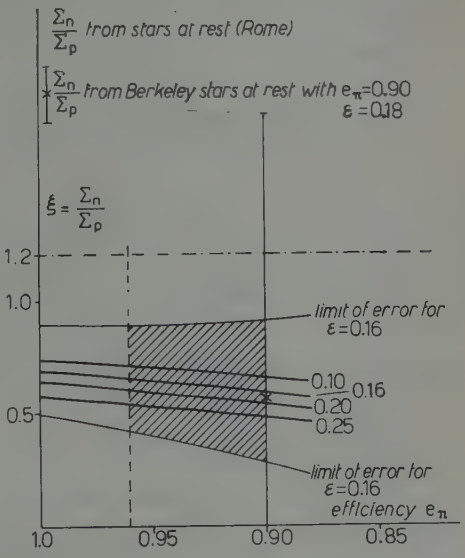

Fig. 19. – $\xi = \Sigma_n/\Sigma_p$ versus e_π for various values of ε.

Another possible interpretation could be based on the fact that, if the $\bar{p}$-nucleon annihilation interaction decreases rapidly by increasing the angular momentum of their relative motion, the annihilation would take place mainly from S and P states of the relative motion of the p —in an atomic orbit— and a nucleon—in a nuclear state. In the case of S and P states there are twice as many allowed transitions for the $\bar{p}$-p than for the $\bar{p}$-n system ([42]).

The application of the same procedure to the annihilation in flight, gives unreliable results, because the value of ε is so high that in the set of equations (5.28) the terms arising from pion absorption, become the most important part of the μ_p^r, μ_n^r.

From the values of μ_p^r and μ_n^r obtained above, one can deduce the multiplicities of charged pions for annihilation of a $\bar{p}$ at rest with a proton and a

([42]) T. D. LEE and C. N. YANG: *Nuovo Cimento*, **3**, 749 (1956).

neutron bound in emulsion nuclei; these turn out to be both equal to the expected value (4.7) inside one experimental error.

* * *

We express our gratitude to Dr. J. LOFGREN, for help in arranging the use of the Bevatron, and to Professors E. SEGRÈ, O. CHAMBERLAIN, and G. GOLDHABER for their precious assistance in planning and carrying out the exposure of our stack.

We also wish to thank the observers who have taken upon themselves the heavy burden of scanning the emulsions.

APPENDIX I

Efficiency of detection of minimum tracks ($\pi^{\pm}$).

The determination of the detection efficiency of tracks at minimum in annihilation stars e_π is rather delicate and has been made by the various groups using different procedures. Some authors have taken $e_\pi = 1$, while others use $e_\pi = 0.90 \pm 0.10$. Since e_π greatly depends on the conditions of exposure and scanning of the stack and on the training of the observers, we felt a direct determination was desirable.

We have adopted the following procedure: the efficiency e_π is written as the product of two factors

$$e_\pi = e_s \cdot e_p ,$$

where the first factor e_s reflects the actual conditions of the « detection system » *i.e.*: *a*) emulsion properties (as for example sensitivity, inhomogeneities), processing (as for example, the number of blobs per unit length of the tracks at minimum), transparency of the emulsion, development gradient, fog, etc., *b*) background of minimum tracks, *c*) optics and *d*) geometry. The second factor e_p represents the effect of the scanning loss by individual observers. The factor e_s has been determined from the observation of $\mu^+ \to e^+$ decays; in this case the observer knows that each μ^+ coming to rest is associated with a fast electron and therefore has a personal efficiency $e_p = 1$ with the result that

$$e_\pi = e_s \geqslant 0.99 .$$

A conservative estimate of the « confusion sphere » at the centre of an annihilation star with many prongs, reduces the value of e_s to 0.98. Surface effects have been avoided by neglecting all stars having their centre situated at less than 20 μm from both air and glass surfaces.

The factor e_p should be taken into account in the case of annihilation stars, because the number of minimum tracks varies in different cases from zero to six. Its estimate was computed, as usual, by comparing the results obtained by two independent observers for the same sample of annihilation stars. The optics was 55×, 12× with a Koristka R4 microscope.

Thus we found $e_p = 0.95 \pm 0.02$ which, combined with the previous determination of e_s, gives

$$e_\pi = 0.93 \pm 0.03 .$$

Appendix II

Efficiency of detection of K-mesons.

In order to establish the percentage of annihilation stars in which K-mesons are produced, it is necessary to estimate the detection efficiency e_K of these particles. Apart from the usual geometrical correction arising from the solid angle in which the tracks have been followed or measured, other factors intervene in the expression of e_K:

1) The contribution of $K^0\overline{K}^0$ pairs (16%) or of K^-K^0 pairs in which the K^- is absorbed in the nucleus (8%).

2) The loss due to K^- which stop in the emulsion without producing a star (K_ϱ^-; 14%).

3) The loss due to K-mesons interacting in flight after a range short enough to prevent them from being distinguished from π^-. This correction has been neglected in our rather rough estimate.

4) The dependence of the efficiency on the K-meson energy T_K, $p(T_K)$. We have estimated this efficiency by taking $p(T_K) = 1$ for K-mesons of an energy between 10 MeV and 120 MeV, $p(T_K) = 0$ for $T_K \leqslant 10$ MeV, and $p(T_K)$ decreasing linearly from 1 to 0 for T_K increasing from 120 MeV to 300 MeV. Then $p(T_K)$ has been multiplied by the spectra given by Sandweiss [34] for the K-mesons emitted in annihilation stars for the two cases of emission of $2\,K + 1\,\pi$ and $2\,K + 2\,\pi$. By integration over all the spectrum and by averaging between these two cases we find a detection efficiency due to this effect which equals 0.65 ± 0.15.

Combining this value with the factors mentioned under 1) and 2) we obtain $e_K \approx 0.3$.

Appendix III

Description of stars with K-mesons.

$\bar{p}$–48 – The star is produced by a $\bar{p}$ in flight of $T_{\bar{p}} \approx 205$ MeV which has previously undergone an elastic scattering by H. In the annihilation process $2\,K^\pm$ are emitted. The K^-, after a range of 4.40 mm, comes

to rest and produces a 2 prongs star: the first is a 22.4 MeV proton, the second is a minimum track which emerges from the stack.

After a range of 5.64 cm the K^+ undergoes a deflection of 16°30′; at the collision point we observe a 4.5 μm long prong. This fact can arise either from a collision with a free H or from an inelastic collision with a nucleus. After this interaction, the K^+ crosses 6.38 mm with a dip-angle of $\sim 83°$ and then decays, probably at rest, emitting a particle which produces a track at minimum. If the deflection is assumed to be due to an elastic scattering by H, we deduce $T_K \sim 45$ MeV for its energy at the time of emission from the annihilation star; then we find that the unbalanced moment $[\boldsymbol{p}_{\bar{p}} - (\boldsymbol{p}_{K^+} + \boldsymbol{p}_{K^-})] = 500$ MeV/c can not be balanced with a single π^0.

The same conclusion is reached if the deflection of the K-meson is interpreted as being due to an interaction with a nucleus.

$\bar{p}$–96 – The K-meson is accompanied by a 44 MeV KO proton and 2 evaporation prongs of 13.6 and 23.0 MeV energy, assuming that they are protons.

p–143 – The K^- is accompanied by a well established 52 MeV proton, a probable proton of $T_p > 90$ MeV and a gray track which produces a star after a 3 cm range. The track which produces the star has a dip angle too large ($\varphi = 54°$) to allow its identification.

p–208 – The star consists of a K-meson, 2 tracks at minimum and a gray track with a 47° dip angle, which emerges from the stack after 2.6 cm of observed range. Because of the large dip-angle it is impossible to decide whether it is due to a proton or to a K-meson.

$\bar{p}$–462 – The star shows four prongs: one is a Σ^- which, after 5.7 cm of range, decays in flight emitting a 50 MeV π^- (3 prong π^--star). From gap measurements we can estimate the initial kinetic energy of the Σ^- to be about 205 MeV. Of the other three prongs of the $\bar{p}$-star, two are certainly protons ($T_p = 47$ and 132 MeV), the third has a dip-angle too large for any measurement and emerges from the stack after 2 cm of visible range..

Appendix IV

Details on the procedure for determining $\xi = \Sigma_n/\Sigma_p$.

In connection with the discussion appearing in Section 5, we notice that the use of eq. (5.30) is justified by the fact that the correlation between the absorption probabilities of two or more pions is expected to be large merely in the case of annihilation processes in which only two charged pions are emitted, while it is already strongly reduced in the case of 3 charged pions. If we neglect the possible existence of pion-pion interactions, the correlation arises only from conservation theorems which, already in the case of 3 particles, leave a relatively large number of degrees of freedom.

The correlation is further reduced by the presence of neutral pions; in addition, the thermal motion of the nucleons in the nucleus gives a contribution in the same direction.

In conclusion, eq. (5.30) is expected to constitute a rough but not uncorrect representation of the actual situation in all cases, excepting that of the emission of two charged pions unaccompanied by any neutral pion; this type of event contributes—very little ([43])—only to μ_p^r.

Thus we felt entitled to compute the coefficients by means of eq. (5.30) for given values of ε (see below).

Before solving the set of eq. (5.28) with respect to μ_p^r and μ_n^r a few corrections should be made to the frequencies O_r actually measured. One is a geometrical correction due to the fact that the gray prongs have been followed only when their dip angle φ was $\leqslant 45°$ (Section 4·1.1). It was made by starting from the frequency of the gray tracks, observed in each class of stars of a given total number of charged pions. The results are given in column 3 of Table XIII. A second correction is due to the efficiency in observing minimum tracks, the value of which is given in Appendix I. A third correction due to charge exchange processes undergone by the charged pions in crossing the nucleus, is partially deleted by the charge exchange undergone by neutral pions. The residual effect is in the sense of decreasing the number of charged pions and therefore its correction can be embodied in the absorption process by a corresponding increase of ε.

A fourth correction is required by the production of charged secondary pions from pions emitted in the annihilation process with an energy larger than 250 MeV. This can be made by taking into account the results of Blau and Caulton ([44]) who found that the production of charged secondaries by π^+ of 500 MeV in emulsion takes place in 1 to 3% of the absorption processes. This correction results in a reduction of 2% of our total multiplicity.

Finally, we notice that the quantity ε which should be introduced in Eq. (5.30) is expected to be of the order of $(15 \div 20)\%$ as may be recognized from the following two independent arguments. The first is based on the results of the emulsion analysis, given in Section 5·3. With the usual notation we may write

$$\varepsilon = \frac{av}{\langle N_\pi \rangle} = \frac{0.75 \times 1.34}{4.6} \approx 0.22 \pm 0.03 .$$

The second argument makes use of bubble chamber and emulsion data; from the value of $\langle N_{\pi\pm} \rangle$ obtained by averaging the results of bubble chamber works

$$\langle N_{\pi\pm} \rangle_H = 3.07 \pm 0.18 \ ([17]) ; \qquad \langle N_{\pi\pm} \rangle_H = 3.21 \pm 0.12 \ ([14])$$

([43]) So far no event has been reported, even in hydrogen bubble chamber, of annihilation processes in which two charged pions are emitted with opposite momenta and a total energy equal to $2\, m_p c^2$.

The evidence is based on the analysis of two prong stars observed by Agnew *et al.* ([14]) in propane bubble chamber (54 events) and by Horowitz *et al.* ([17]) in liquid hydrogen bubble chamber (33 events).

([44]) M. Blau and M. Caulton: *Phys. Rev.*, **96**, 150 (1954).

we deduce

$$\varepsilon = \frac{\langle N_{\pi\pm}\rangle_{\mathrm{H}} - \langle N_{\pi\pm}\rangle_{\mathrm{em}}}{\langle N_{\pi\pm}\rangle_{\mathrm{H}}} = 0.16 \pm 0.05 .$$

RIASSUNTO

In questo lavoro vengono riportati i risultati ottenuti dallo studio di 653 antiprotoni osservati in emulsioni nucleari. Vengono date le sezioni d'urto mediate su tutti i nuclei presenti nell'emulsione (G-5) e nell'intervallo di energia cinetica del $\overline{\mathrm{p}}$ fra 10 e 230 MeV ($T_{\overline{\mathrm{p}}} = 150$ MeV) per i seguenti processi: urto inelastico, urto elastico, annichilazione+scambio di carica. Per questo ultimo processo è stato possibile dare anche la dipendenza della sezione d'urto dall'energia del $\overline{\mathrm{p}}$. Il processo di annichilazione è stato studiato in dettaglio per le stelle prodotte da $\overline{\mathrm{p}}$ sia in volo che in quiete. Fra i vari risultati di questo studio ricordiamo: la molteplicità e lo spettro dei $\pi^{\pm}$, il numero dei pioni che interagiscono in media entro il nucleo di emulsione in cui ha luogo l'annichilazione, la frequenza con cui viene emessa una coppia di $\mathrm{K}\overline{\mathrm{K}}$ e il bilancio energetico delle varie componenti emesse dal nucleo medio di emulsione in cui ha luogo l'annichilazione. Da questi dati viene dedotta, sotto l'ipotesi della validità dell'indipendenza dalla carica, la molteplicità totale dei $\pi^{\pm 0}$ per il processo di annichilazione di un $\overline{\mathrm{p}}$ con un nucleone isolato. Viene data infine una stima del rapporto $\Sigma_{\mathrm{n}}/\Sigma_{\mathrm{p}}$, dove Σ_{n} e Σ_{p} sono le probabilità di annichilazione di un $\overline{\mathrm{p}}$ in quiete rispettivamente con un neutrone e un protone legato nel nucleo medio dell'emulsione.

IL NUOVO CIMENTO Vol. XIV, N. 5 1° Dicembre 1959

K-Hyperon Production Threshold Phenomena (*) (**).

L. Fonda (***) and R. G. Newton

Physics Department, Indiana University - Bloomington, Ind.

(ricevuto il 25 Luglio 1959)

Summary. — The energy dependence of pion proton scattering and K-meson hyperon production cross sections is studied on the basis of a simple model. It is found that the threshold effects can be big enough to be experimentally detectable for the purpose of determining relative hyperon and K-meson parities.

1. – Introduction.

Energy anomalies at thresholds for hyperon production provide us with instances where the « Wigner cusps » [1] may be of considerable experimental importance. The most promising of these effects is that in the Λ-K associated production near the threshold for the production of Σ-hyperons. That the relative ΛΣ parity may be experimentally determined by observing the energy dependence of the reaction $\pi^- + p \to \Lambda + K^0$ or of $\gamma + p \to \Lambda + K^+$ in the vicinity of the threshold where the Σ-K associated production becomes possible was first suggested by Adair [2] and independently by Baz and Okun' [3]. The physics involved is the following (***).

(*) Supported in part by the National Science Foundation.

(**) A preliminary report of this work was presented at the Spring Meeting of the American Physical Society, Washington D.C., April 30 - May 2, 1959.

(***) On leave of absence from the University of Trieste, Italy.

(1) E. P. Wigner: *Phys. Rev.*, **73**, 1002 (1948).

(2) R. K. Adair: *Phys. Rev.*, **111**, 632 (1958).

(3) A. N. Baz' and L. B. Okun': *Sov. Phys. J.E.T.P.*, **8**, 526 (1959); *Žurn. Éksper. Teor. Fiz.*, **35**, 757 (1958).

(***) The following is a condensation of the general argument given in ref. (4); see also ref. (5-7).

(4) R. G. Newton: *Phys. Rev.*, **114**, 1611 (1959).

(5) R. G. Newton: *Ann. Phys.*, **4**, 29 (1958).

(6) L. Fonda: *Nuovo Cimento*, **13**, 956 (1959).

(7) A. I. Baz: *Sov. Phys. J.E.T.P.*, **6**, 709 (1958); *Žurn. Éksper. Teor. Fiz.*, **33**, 923 (1959).

Owing to the fact that the ΣK S-wave production cross-section starts with an infinite slope at threshold, all other cross-sections for processes connected by non-vanishing S-matrix elements to that ΣK S-wave can be expected to have infinite energy derivatives there also. Consequently there will be a « cusp » or « rounded step » in the ΛK production cross-section at the ΣK production threshold, and it will appear in the ΛK S-wave if the ΛΣ parity is even, in the ΛK P-wave if it is odd. Observation of the energy dependence of the ΛK angular distribution in the vicinity of the ΣK threshold may therefore lead to an unambiguous determination of the relative ΛΣ parity. Moreover, if an anomaly at the ΣK production threshold is found in the ΛK production S-wave then only a Σ spin of $\frac{1}{2}$ is compatible with a K spin of zero and a Λ spin of $\frac{1}{2}$.

Similarly, there will be a cusp or rounded step in the pion proton elastic scattering at the thresholds for ΛK and ΣK production and they will appear in the S or P-wave depending on the respective parities $P_{\Lambda K\pi}$ and $P_{\Sigma K\pi}$ (*).

The present paper is a study of these threshold effects. Our purpose is to see if, on the basis of a simple model, one could expect the phenomena in question to be big enough for experimental detection. It is clear from quite general considerations [4], and was pointed out particularly by Baz and Okun' [3], that the size of the effect in the ΛK production cross-section is largely determined by the size of the cross-section for ΣK production by ΛK collisions near threshold. That however leads to no simple explicit statement about the « size of the cusp » in its over-all shape and therefore its experimental observability. Furthermore, we want to determine how strongly the threshold effects depend on the parameters in the model chosen.

We shall investigate all four of the possible relative parity cases for the (πp), (ΛK) and (ΣK) systems. Since the (ΛK) system, however, is in a $T=\frac{1}{2}$ isotopic spin state, only that state has all three systems coupled. Hence we are interested in the (πp) and (ΣK) systems in the $T=\frac{1}{2}$ state only. The $T=\frac{3}{2}$ states of the latter systems are coupled separately to one another, thus producing another cusp or rounded step in the πp scattering at the ΣK production threshold. We shall leave that simpler problem aside.

Assuming, as we shall, that the spins of the Λ and Σ are $\frac{1}{2}$ and that of the K is zero, only the $J=\frac{1}{2}$ state contains the S-wave of the newly produced channel. Therefore only the partial cross-sections referring to that state exhibit threshold anomalies. We shall consequently confine ourselves to the $J=\frac{1}{2}$ state and then talk about S and P waves only.

The fact that we are looking at the $T=\frac{1}{2}$, $J=\frac{1}{2}$ state only, makes it difficult, of course, to compare numbers to experiments. The experimental data we

(*) The ΛK production threshold lies at 762 MeV and the ΣK production threshold at 892 MeV pion laboratory energy.

want to fit lie at the end of our cross-section curves, at 910 to 960 MeV pion laboratory energy. What is known are the ΛK production S and P-waves at 910 and 960 MeV ([8]), the ΣK production S-wave (P-wave small) at 960 MeV ([8]) and the total πp elastic scattering cross-section at 950 MeV ([9]). We considered these data as upper limits for our purposes and made generous allowances for the other states present.

Further restrictions in the model we chose are the neglect of all electromagnetic effects including the $\Sigma^0 - \Sigma^-$ and $K^0 - K^+$ mass difference (*), and of the multiple production of pions. The inclusion of multiple pion production may very well appreciably alter the absolute cross-sections obtained. However, there is no good reason to expect that it would very much change the relative size of the threshold effects we are interested in. The problem we are studying is therefore that of three coupled channels: no. 1, the (π-p) channel; no. 2, the (ΛK) channel; no. 3, the (ΣK) channel; each in the $T = \frac{1}{2}$, $J = \frac{1}{2}$ state.

2. – Model and calculation.

The model we want to describe the coupling of the three two-particle systems (πp), (ΛK) and (ΣK) in the center of mass frame, should be simple enough for ready calculations and yet contain the essential elements that lead to the threshold effects we are looking for. At the same time we want to work a little closer to the customary picture of « forces » than, for example, simply writing down an R-matrix. We therefore chose a potential description in a Schrödinger-type equation. Each channel, of course, satisfies a separate wave equation with a different mass and energy. The three equations are coupled by given functions of the relative distance which we refer to as the production potentials (**). There are, then the three ordinary potentials, $V_{11} = V(\pi p \to \pi p)$, $V_{22} = V(\Lambda K \to \Lambda K)$, $V_{33} = V(\Sigma K \to \Sigma K)$, and the three pro-

([8]) F. Eisler, R. Plano, A. Prodell, N. Samios, M. Schwartz, J. Steinberger, P. Bassi, V. Borelli, G. Puppi, H. Tanaka, P. Waloschek, V. Zoboli, M. Conversi, P. Franzini, I. Mannelli, R. Santangelo and V. Silvestrini: *Nuovo Cimento*, **10**, 468 (1958).

([9]) A. R. Erwin and J. K. Kopp: *Phys. Rev.*, **109**, 1364 (1958).

(*) Since the (ΣK) channel of strangeness zero and total charge zero consists either of $\Sigma^- + K^+$ or of $\Sigma^0 + K^0$, the two mass differences almost cancel; according to ref. ([10]), $M_{\Sigma^-} - M_{\Sigma^0} \approx 6$ MeV, and according to ref. ([11]), $M_{K^0} - M_{K^+} \approx 5$ MeV.

(**) For a general discussion of such systems of equations for several channels, see ref. ([5,6]).

([10]) W. H. Barkas and A. H. Rosenfeld: *University of California Rad. Lab., Report* 8030 (1958).

([11]) F. S. Crawford, M. Cresti, M. L. Good, M. L. Stevenson and H. K. Ticho: *Phys. Rev. Lett.*, **2**, 112 (1959).

duction potentials $V_{21}=V(\pi p \to \Lambda K)$, $V_{31}=V(\pi p \to \Sigma K)$, and $V_{32}=V(\Lambda K \to \Sigma K)$. Since we shall neglect possible spin dependence, the three production potentials, as well as the diagonal ones, must be real and those for reciprocal reactions must be equal due to time reversal invariance. We combine all of them into one real symmetric 3×3 potential matrix.

A further word is necessary concerning the equation to be used. Since the ΣK production threshold lies at a pion laboratory energy of about 892 MeV, which is not only high with respect to the pion rest mass but comparable to the proton mass, neither relativistic nor recoil effects can be neglected. Even the simple pion nucleon scattering alone therefore confronts us with a relativistic two body problem. A simple potential description then certainly no longer suffices. If nevertheless we simulate the real physics by an « effective » potential, we still have a relatively complicated free Hamiltonian, *i.e.*, the sum of the two free particle relativistic energies. Such an equation would be rather difficult to solve even for the simplest potentials. We therefore contented ourselves with introducing the « potential » into the equation after it has been converted into a second order differential equation (*). In other words, the equations (**)

$$W=(p^2+m_{i>}^2)^{\frac{1}{2}}+(p^2+m_{i<}^2)^{\frac{1}{2}}, \qquad i=1,2,3 \tag{1}$$

for each channel are squared twice and then lead to the equations

$$p^2=\frac{(W^2-m_{i>}^2-m_{i<}^2)^2-4m_{i>}^2m_{i<}^2}{4W^2}, \qquad i=1,2,3.$$

If we convert them into wave equations at this stage we have second order differential equations of the Schrödinger type. We then add a potential term $2V\mu$, where μ has the dimensions of a mass, and have a manageable model.

The equations are

$$-\tfrac{1}{2}\mu_i^{-1}\nabla^2\psi_i+\sum_{j=1}^{3}V_{ij}\psi_j=\varepsilon_i\psi_i \qquad i=1,2,3, \tag{2}$$

where

$$\varepsilon_i=\frac{(W^2-m_{i>}^2-m_{i<}^2)^2-4m_{i>}^2m_{i<}^2}{8\mu_iW^2}\equiv\frac{k_i^2}{2\mu_i}. \tag{3}$$

The only remaining question is what should μ_i be. In the non-relativistic case, of course, μ_i is the reduced mass in the i-th channel. There is, however, one difficulty.

(*) See the Appendix for a discussion of the relation between the two equations.
(**) We use natural units, *i.e.*, $\hbar=c=1$.

We can derive a unitary S-matrix from (2). The numbers μ_i and k_i will enter in it as though k_i/μ_i were the relative velocity in the i-th channel. On the other hand, if we derive the form of the unitary S-matrix from the asymptotic requirement of conservation of energy relativistically, then the ratio of outgoing and incoming *relativistic* relative velocities enters, which is the ratio of two k_i/μ_i with μ_i equal to the reduced *energy*:

$$\mu_i = \frac{(k_i^2 + m_{i>}^2)^{\frac{1}{2}} \cdot (k_i^2 + m_{i<}^2)^{\frac{1}{2}}}{(k_i^2 + m_{i>}^2)^{\frac{1}{2}} + (k_i^2 + m_{i<}^2)^{\frac{1}{2}}} . \tag{4}$$

We therefore took these values of μ_i rather than the reduced masses (*).

Equations (2) are not meant to be anything but a simple easily manageable model which may simulate the real physics within a relatively narrow energy interval. They will certainly break down at low energies, since they contain no mechanism for excluding the negative energy solutions when the total energy W gets low enough. When the sum of the masses in one channel is smaller than the difference of the masses in another, they lead to an unphysical threshold at low energies (see Appendix for a more detailed discussion). In the present case there is no reason to believe that they cannot reproduce all the essential features experimentally observed.

For simplicity we may write (2) in matrix form:

$$-\tfrac{1}{2}M^{-1}\nabla^2\psi + V\psi = \varepsilon\psi = \tfrac{1}{2}K^2M^{-1}\psi , \tag{5}$$

where V is the 3×3 potential matrix, ε and K are the diagonal matrices with elements ε_i and k_i given by (3), M is the diagonal matrix whose elements are (4), and ψ is a 3×3 matrix wave function whose rows indicate the three channel components and whose columns differ by their boundary conditions, *i.e.*, the first column has an incoming wave only in the πp channel, the second only in the ΛK channel, the third only in the ΣK channel (**).

Equation (5) is analyzed in terms of partial waves just like the ordinary Schrödinger equation. We assume that V is invariant under rotations. If the intrinsic parities in the three channels are equal, then V will therefore couple only equal orbital angular momenta; if the three parities are not all equal, it will couple the $l = J - \frac{1}{2}$ state of one parity to the $l' = J + \frac{1}{2}$ state of the

(*) Owing to the structure of (2), there is a simple correspondence between any two choices of μ_i. From the solution of an equation with one set of μ_i and potentials V_{ij} one can immediately obtain that of an equation with μ_i' and $V_{ij}' = V_{ij}(\mu_i/\mu_i')^{\frac{1}{2}}(\mu_j/\mu_j')^{\frac{1}{2}}$. Since the μ_i given by (4) are energy dependent and the reduced masses are not, a description with (4) and energy independent potentials corresponds to one with reduced masses and *energy dependent* potentials, and viceversa.

(**) Our notation differs from that in ref. [5]) by transposition of all matrices.

other. Hence the radial equations for the $J=\frac{1}{2}$ state are

$$-\tfrac{1}{2}M^{-1}\psi'' + V\psi + r^{-2}P\psi = \tfrac{1}{2}K^2M^{-1}\psi\,, \tag{6}$$

where P is a diagonal matrix with a one for the channels in the P-state and a zero for those in the S-state. In other words the equation for the pion proton S-wave has

$$P = \begin{cases} \begin{pmatrix} 0 & 0 & 0 \\ 0 & 0 & 0 \\ 0 & 0 & 0 \end{pmatrix}, \text{ if } P_{\Lambda\Sigma} = +1\,, \quad P_{\Lambda K\pi} = -1\,, \\ \begin{pmatrix} 0 & 0 & 0 \\ 0 & 1 & 0 \\ 0 & 0 & 1 \end{pmatrix}, \text{ if } P_{\Lambda\Sigma} = +1\,, \quad P_{\Lambda K\pi} = +1\,, \\ \begin{pmatrix} 0 & 0 & 0 \\ 0 & 0 & 0 \\ 0 & 0 & 1 \end{pmatrix}, \text{ if } P_{\Lambda\Sigma} = -1\,, \quad P_{\Lambda K\pi} = -1\,, \\ \begin{pmatrix} 0 & 0 & 0 \\ 0 & 1 & 0 \\ 0 & 0 & 0 \end{pmatrix}, \text{ if } P_{\Lambda\Sigma} = -1\,, \quad P_{\Lambda K\pi} = +1\,, \end{cases}$$

while the equations for the pion proton P-wave are obtained by subtracting the above P from the unit matrix.

The type of potential we choose in (6) is a square well and for the sake of simplicity we take the radii of all the elements to be the same. In other words, for $r<a$ the matrix V is a constant and for $r>a$ it vanishes. We then have seven parameters at our disposal: the common radius a, the three diagonal potential depths, and the three production potential strengths.

If the parities are all the same so that P is a multiple of the unit matrix, then eq. (6) can be solved explicitly and the S-matrix is calculated in a straightforward manner. If the parities are not all the same, an explicit solution is no longer possible. We then calculate the « inside » solution as a power series in the radial distance. It is readily seen that the expansion is of the form

$$\psi(r) = \sum_{n=0}^{\infty} r^{2n+1}(b_n + rc_n)\,,$$

where the matrix coefficients b_n and c_n satisfy the recursion relations

$$(7)\qquad \begin{cases} b_n = b_{n-1}(2\sqrt{M} - K^2)\left[\dfrac{1-P}{2n(2n+1)} + \dfrac{P}{(2n+2)(2n-1)}\right], \\ c_n = c_{n-1}(2\sqrt{M} - K^2)\left[\dfrac{1-P}{(2n+1)(2n+2)} + \dfrac{P}{2n(2n+3)}\right]. \end{cases}$$

This function is then fitted in the usual manner to the « outside » solution and the S-matrix is obtained from the asymptotic form.

The scattering and production amplitude matrix for total angular momentum J, leading from the orbital angular momentum component l of the incident beam in the β channel of total spin j and spin z-component ν, and travelling in the z-direction, to the orbital angular momentum component l' of the outgoing wave in the γ channel of spin j' and spin z-component ν', seen in the direction $\boldsymbol{k}'$ is

$$\Theta^{(J)}_{\beta lj\nu,\,\gamma l'j'\nu'}(\boldsymbol{k}') = i^{l-l'+1}\left[\pi(2l+1)\right]^{\frac{1}{2}} k_\beta^{-1} Y_{l'}^{\nu-\nu'}(\boldsymbol{k}') \cdot \\ \cdot C_{lj}(J, \nu;\, 0, \nu)\, C_{l'j'}(J, \nu;\, \nu-\nu', \nu')\, T^{(J)}_{\beta lj,\,\gamma l'j'},$$

where the C's are the Clebsch-Gordan coefficients and $T = 1 - S$. From this we obtain the integrated partial cross-sections for our case:

$$\sigma^{(l')}(\beta \to \gamma) = \frac{1}{2}\sum_{\nu\nu'}\int \mathrm{d}\Omega' \,|\, \Theta^{(\frac{1}{2})}_{\beta l\frac{1}{2}\nu,\,\gamma l'\frac{1}{2}\nu'}(\boldsymbol{k}')\,|^2,$$

where $J = \frac{1}{2}$ is understood. If the intrinsic parities of the incoming and outgoing channels are equal, then

$$\sigma^{(0)}(\beta \to \gamma) = \pi k_\beta^{-2}\,|\, T_{\beta 0,\gamma 0}\,|^2,$$

$$\sigma^{(1)}(\beta \to \gamma) = \tfrac{3}{2}\pi k_\beta^{-2}\,|\, T_{\beta 1,\gamma 1}\,|^2,$$

and if they are unequal

$$\sigma^{(0)}(\beta \to \gamma) = \pi k_\beta^{-2}\,|\, T_{\beta 1,\gamma 0}\,|^2,$$

$$\sigma^{(1)}(\beta \to \gamma) = \tfrac{1}{2}\pi k_\beta^{-2}\,|\, T_{\beta 0,\gamma 1}\,|^2.$$

The actual computation of the cross-sections was done with an IBM 650 electronic computer. We shall present three different sets of potentials for each of the four parity cases. Since the experimental data even in the form

of limitations exist at best for six of the cross-sections at about 960 MeV pion laboratory energy, we have more parameters than points and hence an infinity of fits. The twelve sets of curves are to be considered simply as examples of what variations are possible within the sparse experimental limits.

There are two additional points we want to illustrate in passing. One is the possibility, if the threshold cusp for example in the ΛK production at the ΣK production threshold is reasonably large, of obtaining from it the production cross-section for Σ's by ΛK collisions. The other point is the possibility of obtaining, for example, the total cross-section for ΣK collisions near zero energy from the ΣK production cross-section curve. Assuming that multiple pion production is negligible, this total cross-section must equal the sum of those for pion proton and ΛK production (since the elastic scattering at zero energy is finite), both of which can be obtained also by reciprocity from other observations (the first directly from the ΣK production by πp collisions and the second indirectly as described above). A comparison of the results will then give a measure of the multiple pion production. A similar argument applies, of course, to obtaining the total ΛK collision cross-section near zero energy.

The possibility of obtaining the $\Lambda + K \to \Sigma + K$ production cross-section near threshold follows directly from the general equation (14) of ref. [4]. If we apply it to the present case, using cross-sections integrated over angles, then we obtain

$$(8) \qquad \left(\frac{\partial}{\partial k_{\Sigma K}} \sigma_{\pi p \to \Lambda K}\Big|_a\right)^2 + \left(\frac{\partial}{\partial |k_{\Sigma K}|} \sigma_{\pi p \to \Lambda K}\Big|_b\right)^2 = \\ = \pi^{-1}(k_{\Sigma K}^{-1}\sigma_{\pi p \to \Sigma K})(k_{\Sigma K}\sigma_{\Sigma K \to \Lambda K})(\sigma_{\pi p \to \Lambda K}).$$

The notation on the left hand side refers to the derivative of the entire cross-section for $\pi + p \to \Lambda + K$, evaluated once as the ΣK threshold is approached from above, and once, from below; on the right hand side each parenthesis refers to the limit at the ΣK threshold. The states referred to in the subscripts on the right hand side must all agree; that is to say, since in $\sigma_{\Sigma K \to \Lambda K}$ at threshold only the $J = \frac{1}{2}$ state enters, all three cross-sections refer only to $J = \frac{1}{2}$; since the ΛK system is in a $T = \frac{1}{2}$ state, only the $T = \frac{1}{2}$ partial cross-section is meant by $\sigma_{\pi p \to \Sigma K}$; since, depending on the relative $\Lambda\Sigma$ parity, it is either the S or the P state in the ΛK system which is produced in $\Sigma + K \to \Lambda + K$ near zero energy, it is the same S or P state, respectively, which is meant in the final state in $\sigma_{\pi p \to \Lambda K}$; finally on similar grounds, it is the S or P state in the πp system which enters both cross-sections on the right, depending on the relative parity $P_{\Lambda K \pi}$. Hence we can obtain the $\Lambda + K \to \Sigma + K$ cross-section near threshold from (8) only if we know the $J = \frac{1}{2}$ and $T = \frac{1}{2}$ partial cross-sections on the right, as well as the left hand side. If only the sum of the cross-sections

for $J, T = \frac{1}{2}, \frac{3}{2}$ is known, we may obtain upper limits on the $\Lambda + K \to \Sigma + K$ cross-section.

The total ΣK collision cross-section near zero energy is obtained from eq. (16) of ref. (4):

$$k_{\Sigma K}^{-1} \sigma_{\pi p \to \Sigma K} \approx (k_{\Sigma K}^{-1} \sigma_{\pi p \to \Sigma K}) \left[1 - \frac{k_{\Sigma K}}{2\pi} (k_{\Sigma K} \sigma_{\Sigma K}^{\text{total}}) \right], \tag{9}$$

where the parentheses on the right hand side again indicate the values at threshold. One can therefore obtain $\sigma_{\Sigma K}^{\text{total}}$ from the slope and intercept of the curve of $k_{\Sigma K}^{-1} \sigma_{\pi p \to \Sigma K}$ near $k_{\Sigma K} = 0$.

3. – Discussion.

First a remark on the potentials. It is clear that all physical results are invariant under a simultaneous sign change of all off-diagonal potentials. A simultaneous sign change of any two off-diagonal potentials is also of no physical consequence. We may therefore fix the sign of two of them to be always positive. We are giving our results in terms of positive $V(\pi p \to \Lambda K)$ and $V(\pi p \to \Sigma K)$.

Whenever in the following the pion proton elastic cross-sections are uninteresting, *i.e.*, exhibit no marked structure, they are not shown. Table I gives their values for each case at 950 MeV pion laboratory energy (*). The $\pi + p \to \Sigma + K$ production P_1-wave below 960 MeV is in many cases too small to be visible on our scale. In those cases we have not included it in the graphs. Table I also lists the value of the $\Lambda + K \to \Sigma + K$ cross-section at 910 MeV for the purpose of correlation with the size of the ΣK threshold effects. It is to be noticed that there is no clear correlation between the sizes of the potential $V(\Lambda K \to \Sigma K)$ and of the cross-section $\sigma_{\Lambda K \to \Sigma K}$. In Table II we list the values of $k_{\pi p}$, $|k_{\Lambda K}|$ and $|k_{\Sigma K}|$ in the region of interest for the purpose of easy determination of what constitutes a « large » or a « small » cross-section.

In most cases the graphs speak for themselves. We may simply add a few comments.

In comparing cases *A* and *C*, notice that the anomaly is bigger in *C* than in *A* in spite of the smaller $V(\Lambda K \to \Sigma K)$ in the former. There is a marked difference in radii for the two cases. Case *B* has a small cusp despite a large $V(\Lambda K \to \Sigma K)$. The ΛK *S*-wave is accidentally rising very slowly.

(*) All our results are given in terms of the pion laboratory energy. For that it is merely necessary to express the C.M. energy W in (3) in terms of the pion laboratory kinetic energy E_{lab}^{π}:

$$W^2 = (m_\pi + m_p)^2 + 2 m_p E_{\text{lab}}^{\pi} .$$

TABLE I. – *The various cases considered in the text. Listed are the relative parities, the well radius, the potential depths, the pion proton partial S and P_1 elastic scattering cross-section at* 950 MeV *pion laboratory energy, and the partial* $l = 0$ ΣK *production cross-section by* ΛK *collisions at* 85 MeV *C.M. kinetic energy* ($k_{\Lambda K} = 1.24 \cdot 10^{13}$ cm^{-1}).

	$P_{\Lambda\Sigma}=+1$, $P_{\Lambda K\pi}=-1$			$P_{\Lambda\Sigma}=+1$, $P_{\Lambda K\pi}=+1$			$P_{\Lambda\Sigma}=-1$, $P_{\Lambda K\pi}=+1$			$P_{\Lambda\Sigma}=-1$, $P_{\Lambda K\pi}=-1$		
	A	*B*	*C*	*D*	*E*	*F*	*G*	*H*	*I*	*J*	*K*	*L*
a (in 10^{-13} cm)	.575	.75	.75	.6	.55	.5	.7	.65	.8	.9	.7	.7
$V(\pi p \to \pi p)$ (in MeV)	100	— 100	— 100	400	200	200	— 200	— 200	100	— 100	— 200	— 300
$V(\pi p \to \Lambda K)$	225	175	175	500	200	300	100	50	125	75	40	150
$V(\pi p \to \Sigma K)$	100	200	200	50	200	300	100	400	150	50	50	50
$V(\Lambda K \to \Lambda K)$	200	— 200	0	1100	— 350	— 300	— 100	— 200	— 50	100	100	— 400
$V(\Lambda K \to \Sigma K)$	— 800	500	150	— 400	— 300	— 300	200	600	550	— 100	— 500	500
$V(\Sigma K \to \Sigma K)$	50	50	50	0	— 200	— 400	— 400	900	300	50	50	100
$\sigma^{(0)}_{\pi p \to \pi p}$ (at 950 MeV, in mb)	1.57	3.29	4.21	3.49	.62	.12	3.03	6.48	.67	1.66	3.34	4.99
$\sigma^{(1)}_{\pi p \to \pi p}$ (at 950 MeV, in mb)	~ 0	1.38	1.68	.21	.30	.35	1.76	1.67	.35	2.25	1.51	3.88
$\sigma^{(0)}_{\Lambda K \to \Sigma K}$ (at 85 MeV C.M., in mb)	1.74	2.03	5.53	2.24	8.19	10.42	.85	.30	18.17	.28	8.67	10.77

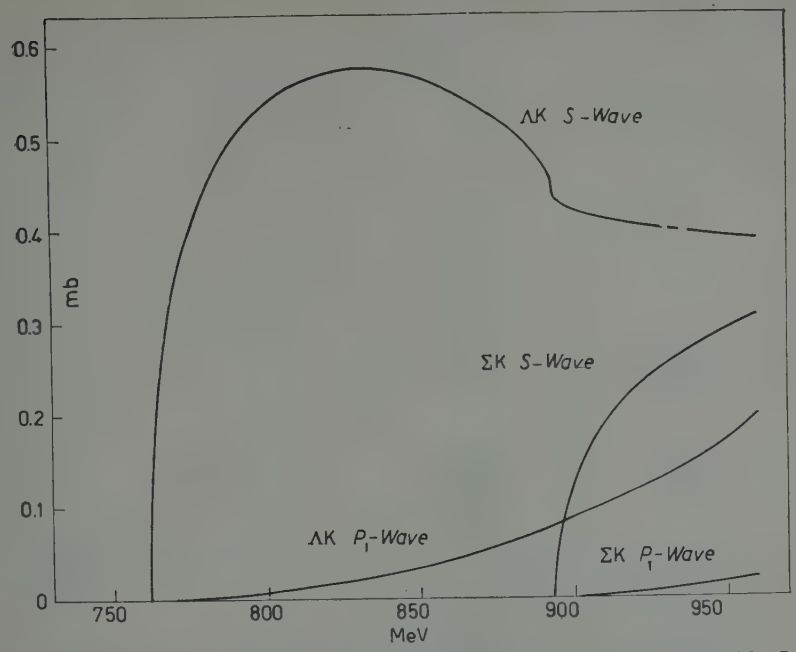

Fig. 1. – ΛK and ΣK partial production cross sections for case *A* (see Table I) against pion laboratory energy.

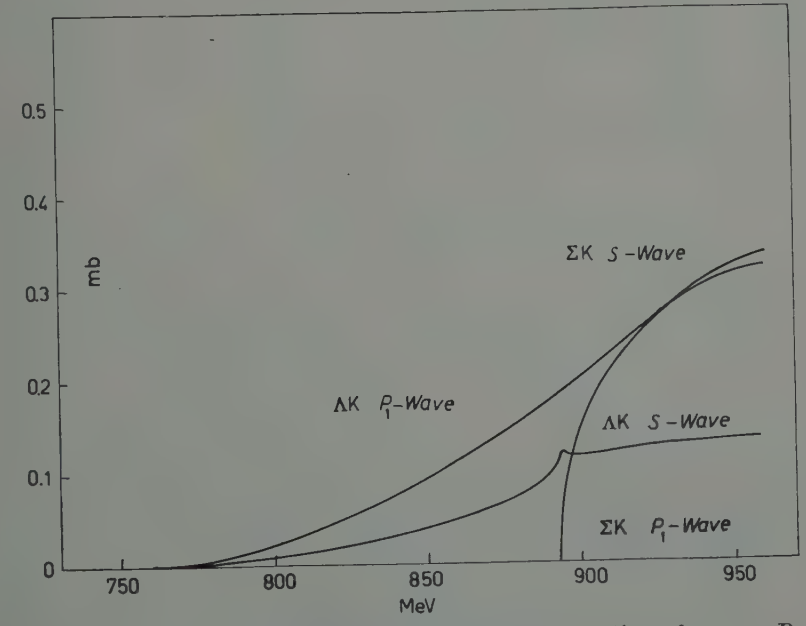

Fig. 2. – ΛK and ΣK partial production cross sections for case *B*.

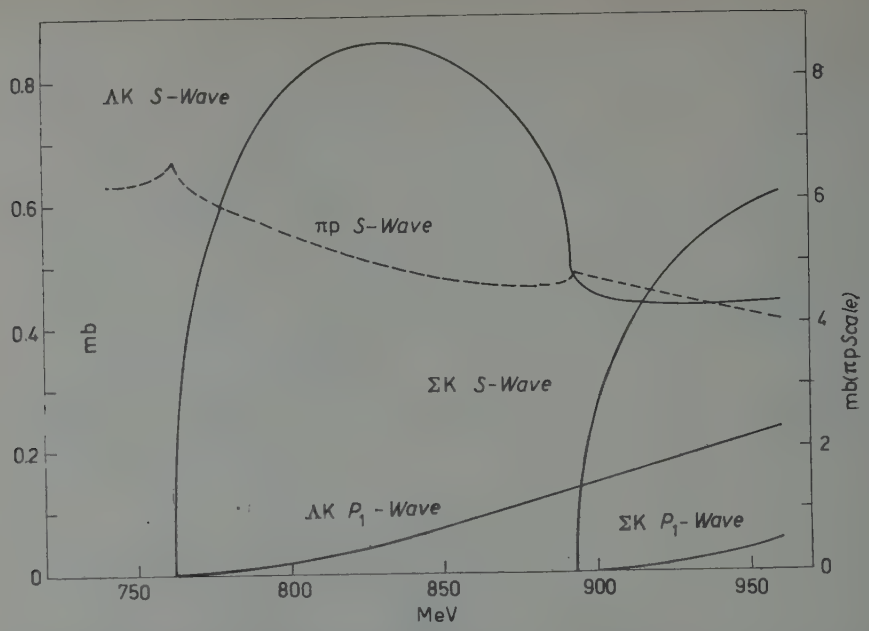

Fig. 3. – ΛK and ΣK partial production cross sections for case C; the partial pion proton elastic scattering cross section for $l=0$ is given by the dashed line and refers to a different scale indicated on the right.

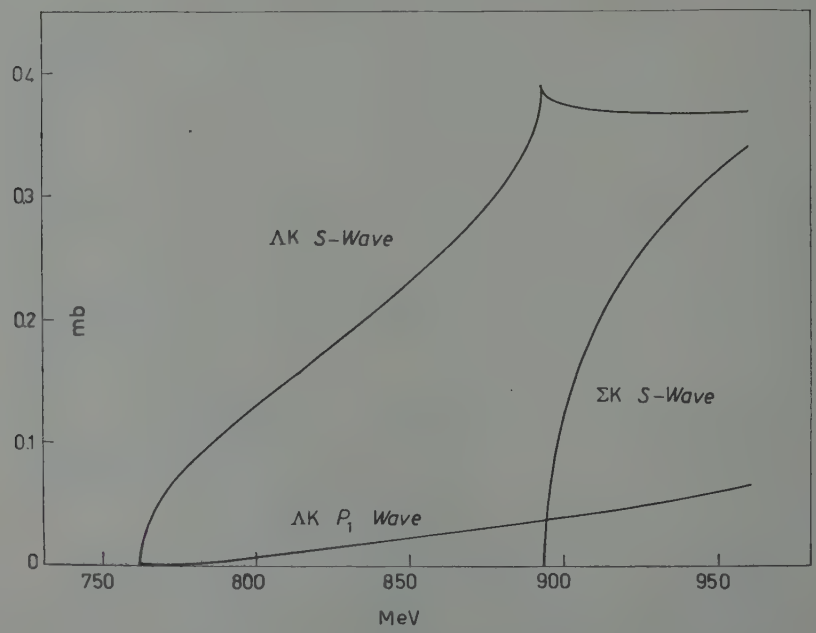

Fig. 4. – ΛK and ΣK partial production cross sections for case D. The ΣK P_1-wave is too small to be visible.

TABLE II. – *Absolute values of the wave numbers in the three channels at various pion laboratory energies.*

E^{π}_{lab} (MeV)	$k_{\pi p}$ (10^{13} cm^{-1})	$\lvert k_{\Lambda K}\rvert$ (10^{13} cm^{-1})	$\lvert k_{\Sigma K}\rvert$ (10^{13} cm^{-1})
960	3.01	1.44	.822
950	2.99	1.40	.758
930	2.96	1.33	.610
910	2.92	1.24	.413
895	2.89	1.18	.143
894	2.89	1.17	.103
893	2.89	1.17	.0236
892	2.89	1.16	.0971
891	2.88	1.16	.139
890	2.88	1.16	.172
885	2.87	1.13	.282
880	2.86	1.11	.359
860	2.83	1.01	.572
840	2.79	.901	.725
820	2.75	.776	.849
800	2.71	.629	.957
780	2.67	.434	1.05
770	2.65	.293	1.10
764	2.63	.155	1.12
762	2.63	.0599	1.13
761	2.63	.0816	1.14
759	2.62	.165	1.15
750	2.61	.345	1.18
740	2.59	.471	1.22
710	2.52	.725	1.33
650	2.39	1.06	1.53
600	2.28	1.27	1.67

Case *D*, Fig. 5, shows a sizeble *downward* cusp in the pion proton scattering P_1-wave at the ΣK threshold. The effect at the ΛK production threshold is *not* a downward cusp, as the insert shows. It follows at once from the mechanism that produces the infinite derivative at the upper side of the threshold by conservation of flux ([4]), that above the *first* threshold the derivative must be negative ([5]). In cases *E* and *F* (see Fig. 7 and 8), which differ mainly in the size of the potential $V(\Sigma K \to \Sigma K)$, there is a resonance in the pion proton elastic P_1-wave just below the threshold for the ΛK channel. In both cases the diagonal potentials are too weak to bind the ΛK and ΣK systems by themselves. The coupled ΛK and ΣK systems, uncoupled from the pion proton channel, however, presumably have a bound state of small binding energy in these cases. Notice the sharp rise of the ΛK production cross-section in both cases near threshold (Fig. 6 and 8) owing to these resonances. The

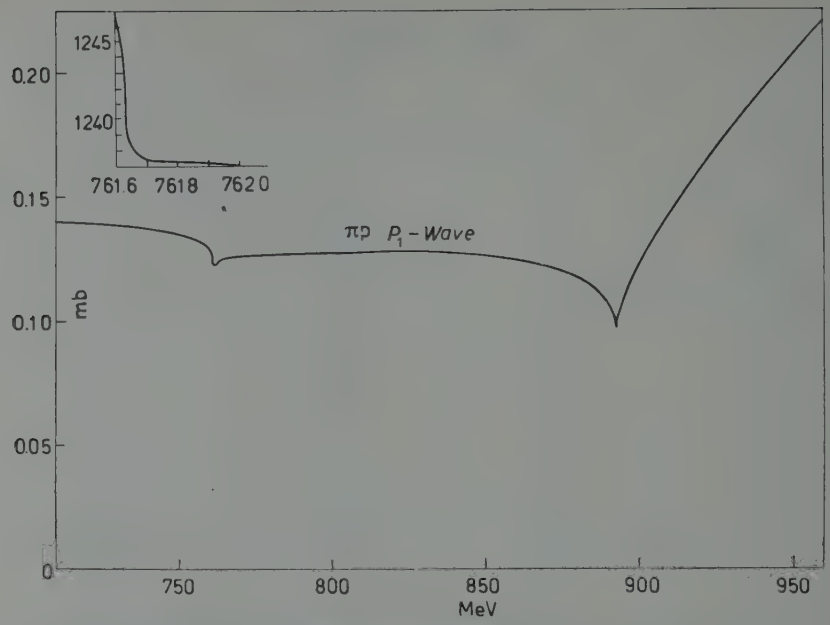

Fig. 5. – Pion proton partial P_1 elastic scattering cross section for case D. The insert shows the detail at the ΛK production threshold.

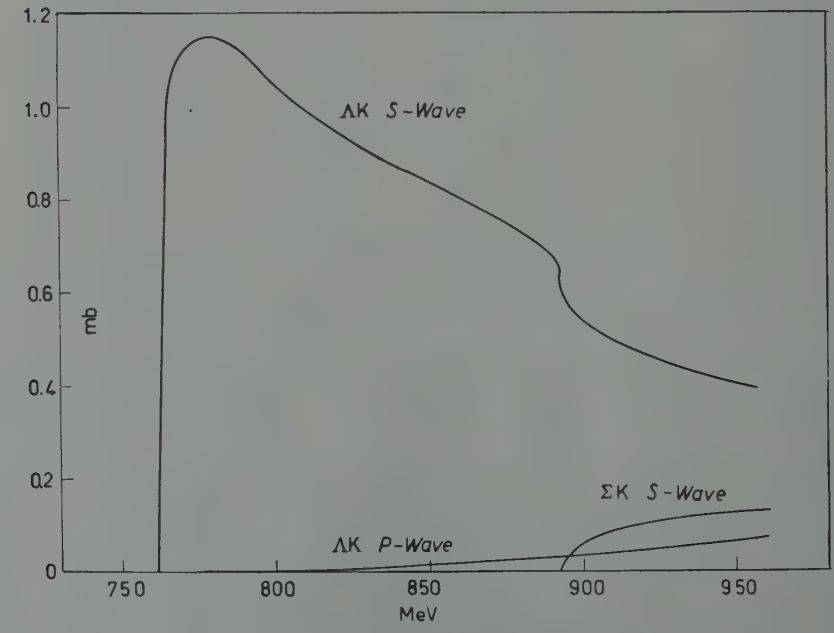

Fig. 6. – ΛK and ΣK partial production cross sections for case E; the ΣK P_1 wave is too small to be visible.

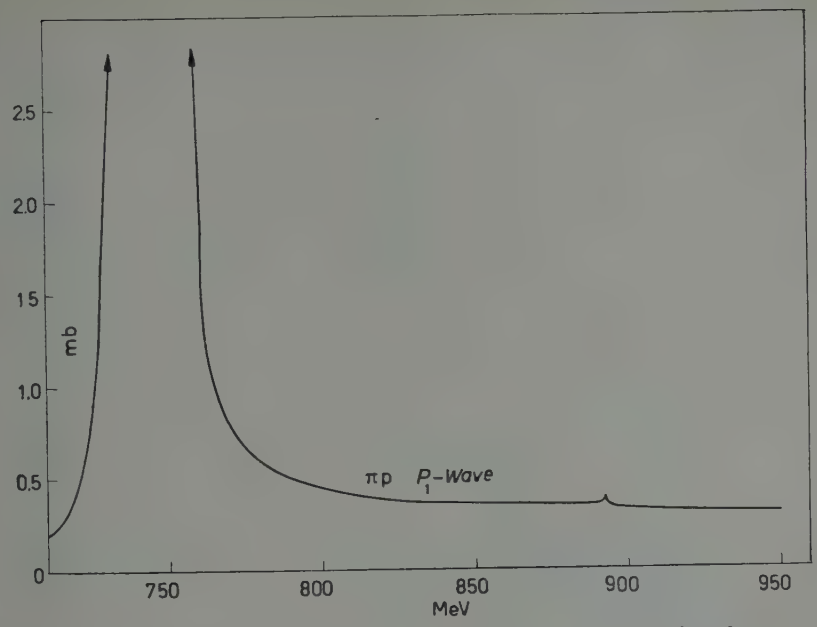

Fig. 7. – Pion proton partial P_1 elastic scattering cross section for case E.

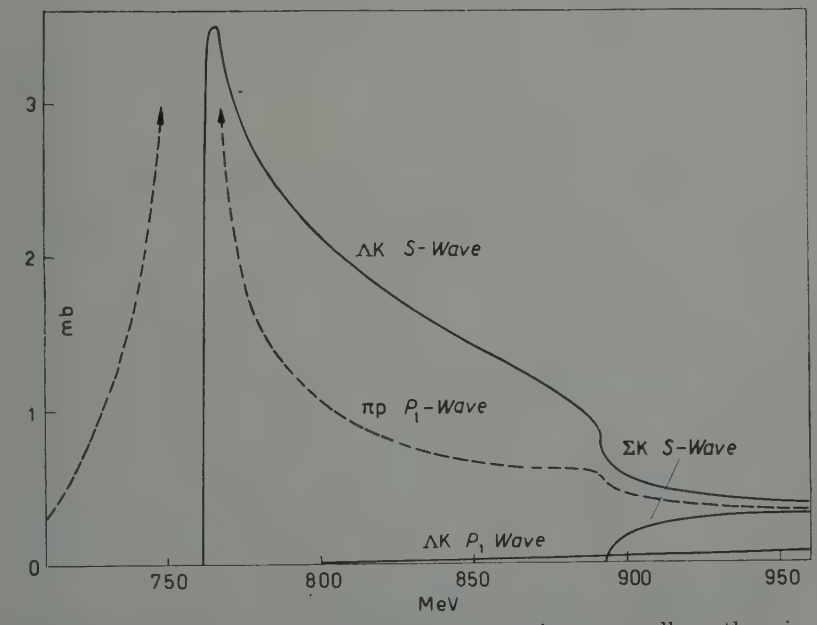

Fig. 8. – ΛK and ΣK partial production cross sections as well as the pion proton partial P_1 elastic scattering cross section for case F. The ΣK P_1 wave is too small to be visible.

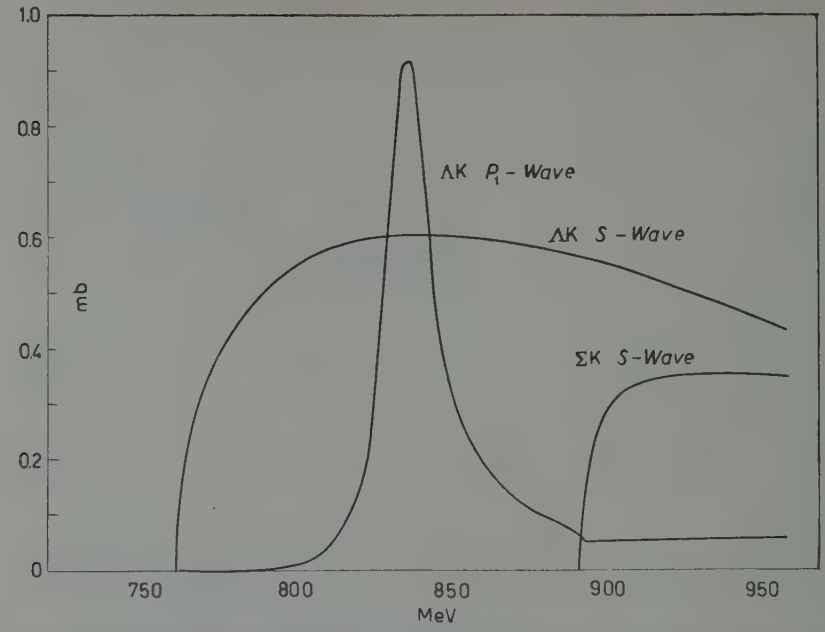

Fig. 9. – ΛK and ΣK partial production cross sections for case G. The ΣK P_1 wave is too small to be visible.

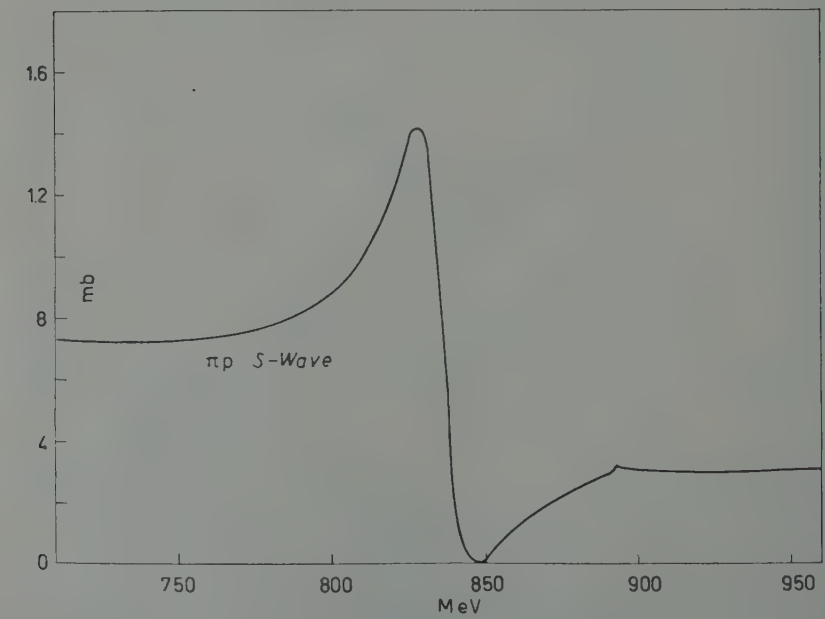

Fig. 10. – Pion proton partial elastic scattering cross section, $l=0$, for case G.

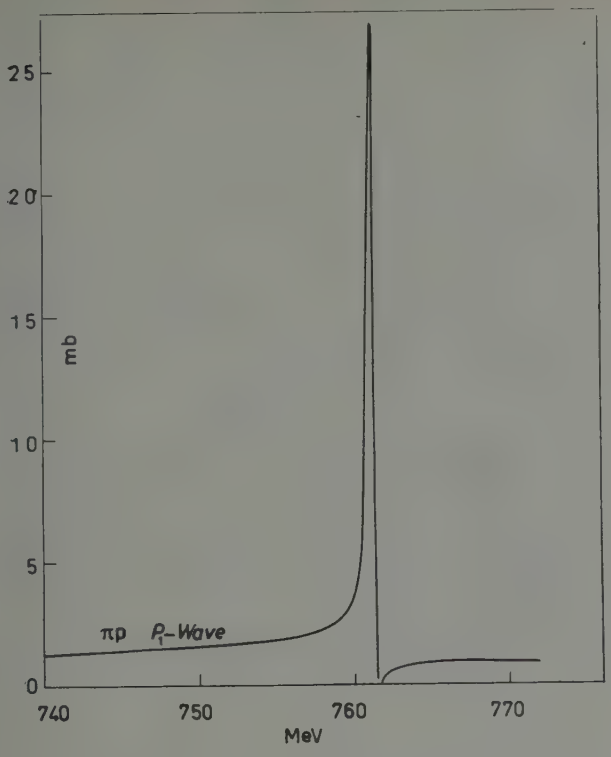

Fig. 11. – Pion proton partial P_1 elastic scattering cross section for case H.

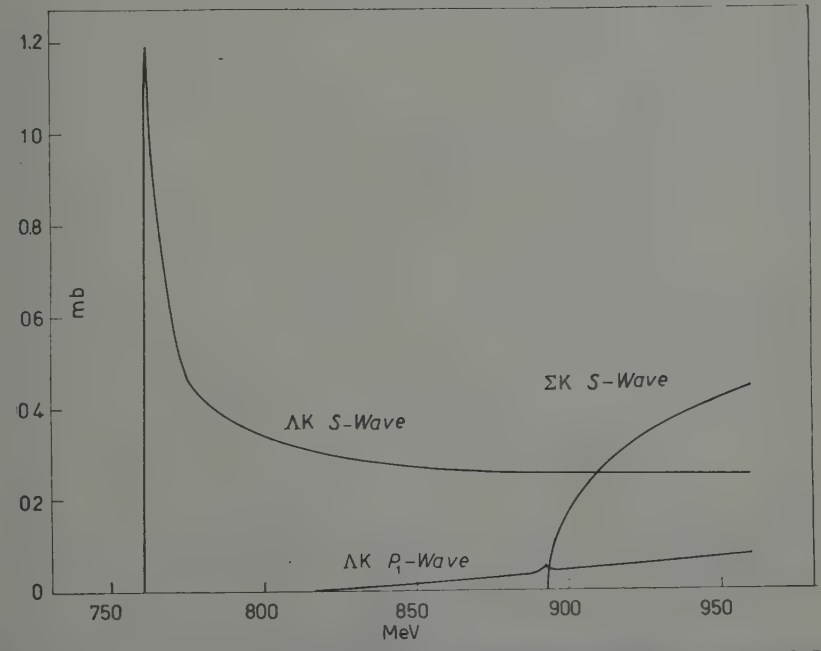

Fig. 12. – ΛK and ΣK partial production cross sections for case H. The ΣK P_1 wave is too small to be visible.

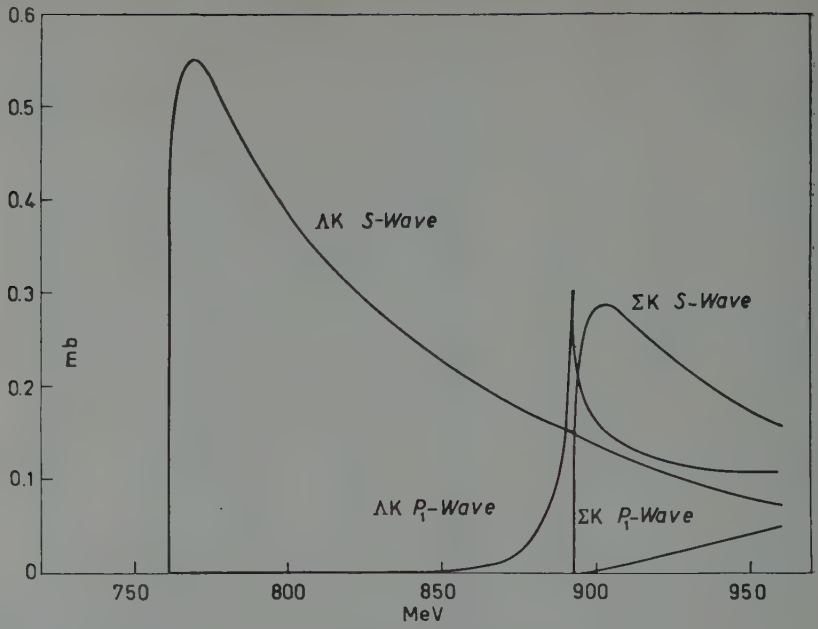

Fig. 13. – ΛK and ΣK partial production cross sections for case *I*.

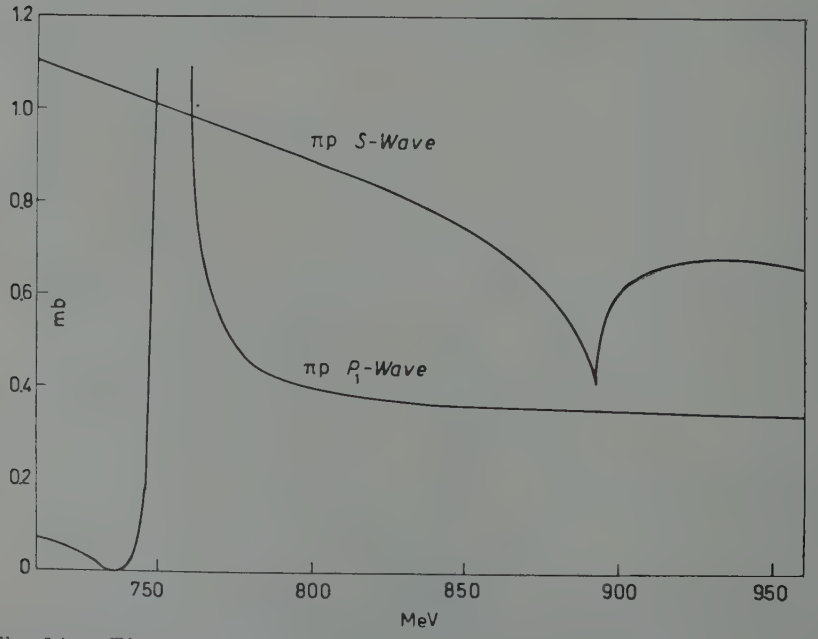

Fig. 14. – Pion proton partial elastic scattering cross sections for case *I*.

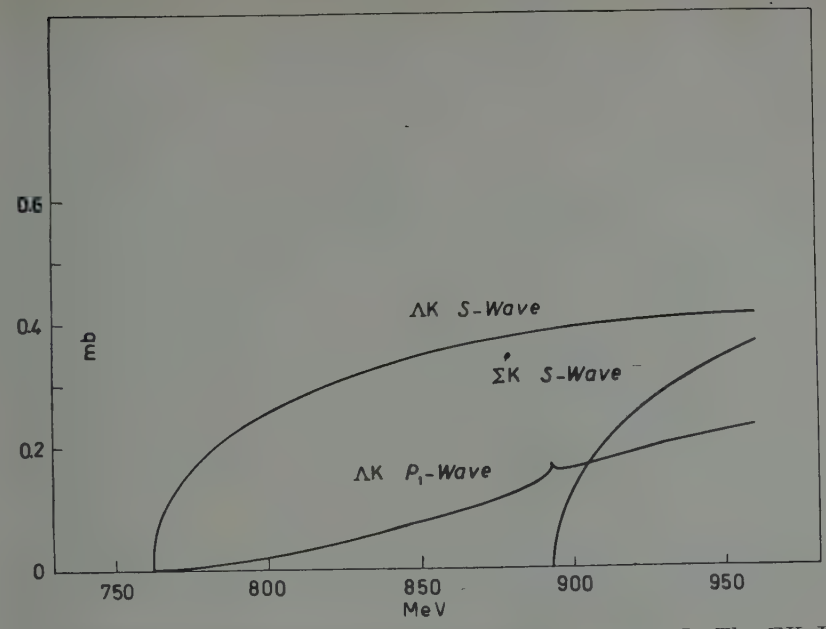

Fig. 15. – ΛK and ΣK partial production cross sections for case J. The ΣK P_1 wave is too small to be visible.

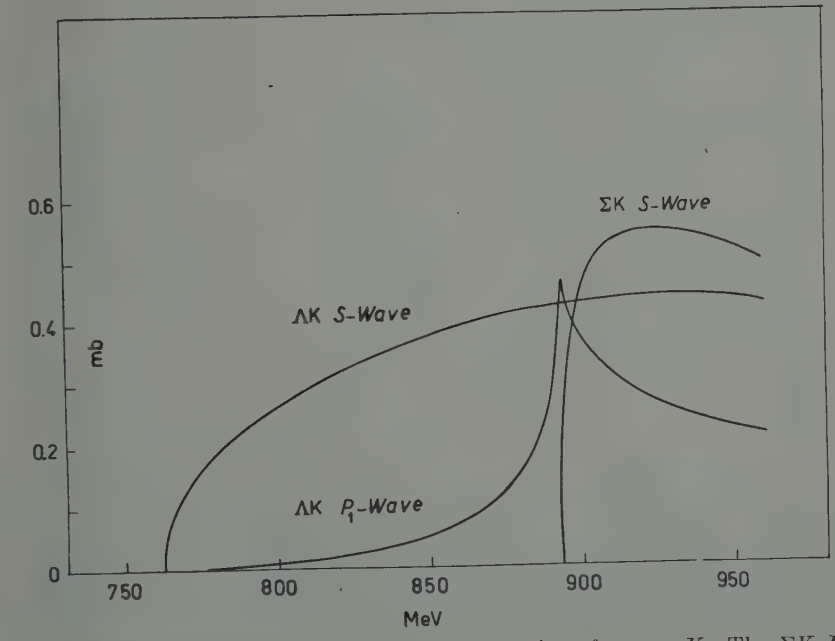

Fig. 16. – ΛK and ΣK partial production cross sections for case K. The ΣK P_1 wave is too small to be visible.

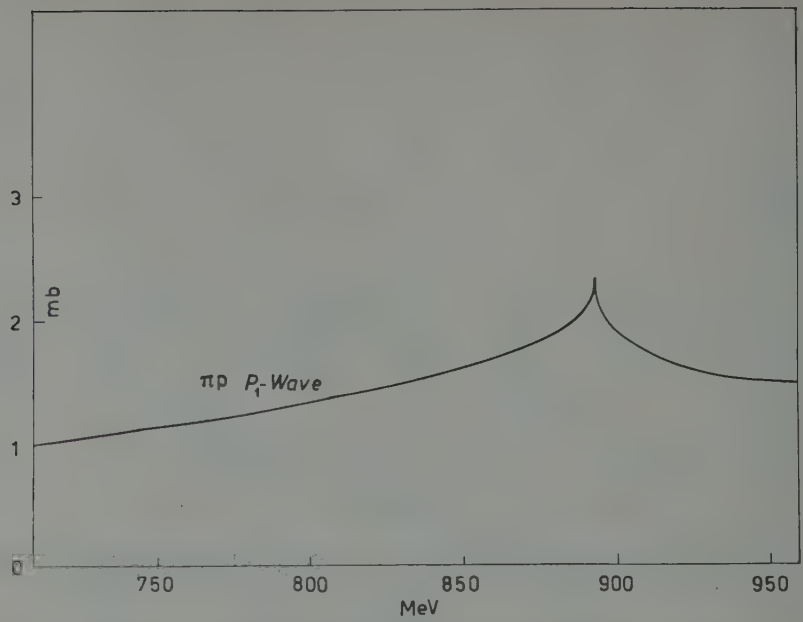

Fig. 17. – Pion proton partial P_1 elastic scattering cross section for case K.

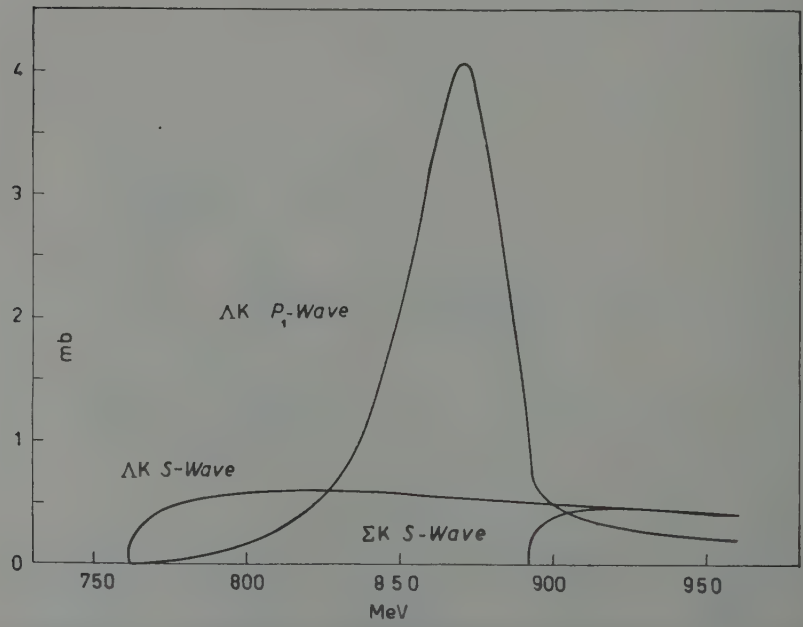

Fig. 18. – ΛK and ΣK partial production cross sections for case L. The ΣK P_1 wave is too small to be visible.

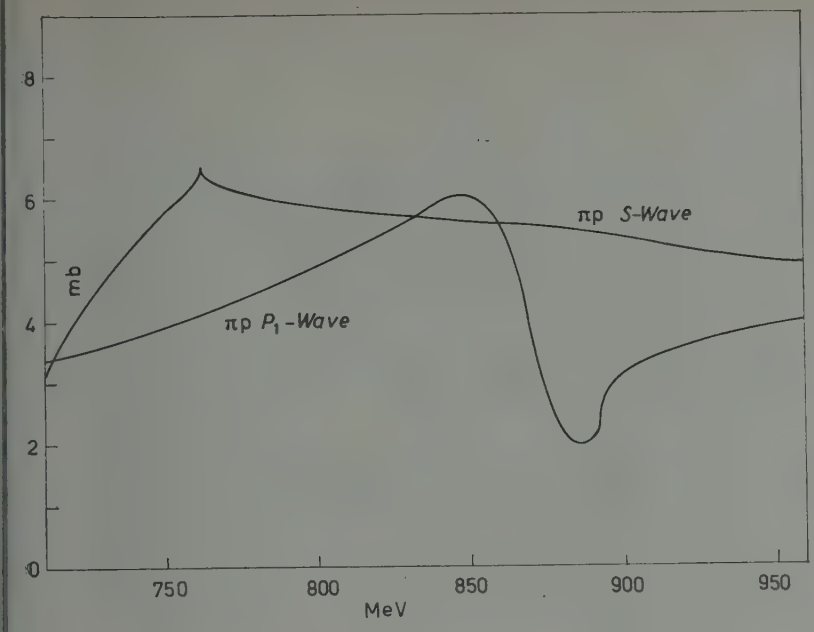

Fig. 19. – Pion proton partial elastic scattering cross sections for case L.

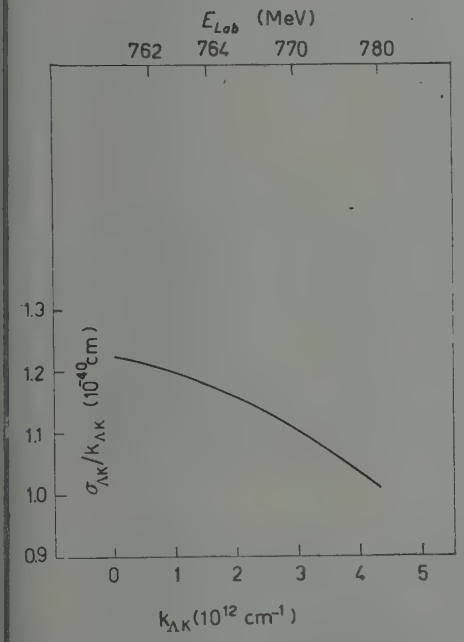

Fig. 20. – The ΛK production cross section divided by $k_{\Lambda K}$ plotted against $k_{\Lambda K}$ near threshold for case A. The corresponding pion laboratory energy is given in the upper scale.

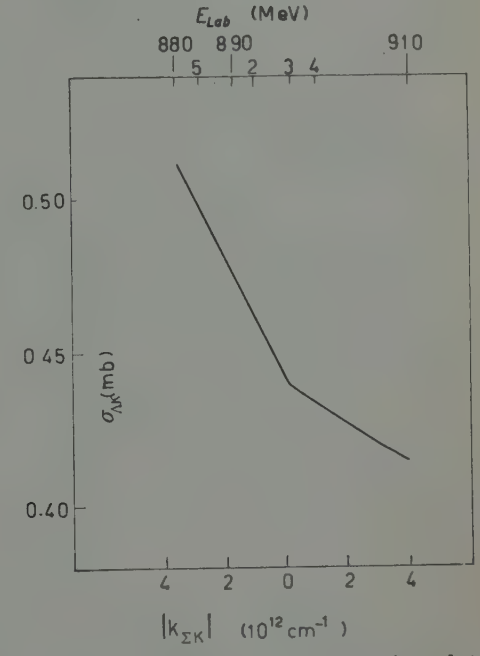

Fig. 21. – ΛK production cross section plotted against $|k_{\Sigma K}|$ near the ΣK threshold. The corresponding pion laboratory energy is given in the upper scale. The scale on the left refers only to the partial cross section for $l=0$; adding the P_1 wave does not alter the shape of the curve.

mechanism for that is, of course, quite different from the familiar resonance near zero energy in an *elastic* cross-section if there is a weakly bound state in the same channel (*).

Cases A to F all had equal parities for the Λ and Σ hyperons. The following cases are those of unequal parities for those two particles.

Case G has a resonance in the pion proton S-wave (Fig. 10) and in the ΛK P_1-wave (Fig. 9) owing to a bound state at 850 MeV of 24 MeV binding energy in the ΣK system. The maxima in the elastic pion proton scattering and in the ΛK production are shifted relative to each other, with the ΛK maximum closer to the bound state. Case H has a sharp resonance (Fig. 11) just below the ΛK threshold and a concomitant very sharp rise in the ΛK production near threshold (Fig. 12) in spite of the fact that the diagonal $V(\Lambda K \to \Lambda K)$ potential does not bind. In case I is a similar but less sharp effect, although the $V(\Lambda K \to \Lambda K)$ is much too weak to bind. The cusps in the ΛK P_1-wave (Fig. 13) and in the πp S-wave (downward; see Fig. 14) are quite marked. Notice that case I has a relatively large radius, $a = 0.8 \cdot 10^{-13}$ cm.

Case J shows very small cusps at the ΣK threshold (see Fig. 15; the πp wave is not shown). Case K, with a smaller radius and a bigger $V(\Lambda K \to \Sigma K)$ has rather large cusps in the ΛK P_1-wave (Fig. 16) and in the πp P_1-wave (Fig. 17). In case L the threshold effects are dominated by a resonance below the ΣK threshold but considerably above the ΛK threshold. This resonance is produced in spite of the fact that the diagonal potential $V(\Sigma K \to \Sigma K)$ is repulsive (**).

Fig. 20 shows the ΛK production cross-section divided by $k_{\Lambda K}$ near $k_{\Lambda K} = 0$ as a function of $k_{\Lambda K}$ for case A. Its curvature is small over a considerable range of pion laboratory energy so that the total ΛK collision cross-section could be obtained from an equation like (9). Nevertheless it must be recognized that the errors introduced by experimental uncertainties in a curve like Fig. 20 are very large.

Fig. 21 shows the ΛK production S-wave on both sides of the ΣK threshold as a function of $|k_{\Sigma K}|$ for case A. The lines being very nearly straight over appreciable pion laboratory energies, use of eq. (8) is practically quite feasible in this case.

* * *

The authors are indebted to Professors R. B. CURTIS and M. H. ROSS for some fruitful conversations and to the Indiana University Research Computing Center for the use of their facilities.

(*) For a detailed discussion of such a phenomenon see ref. (12).

(12) L. FONDA and R. G. NEWTON: *Ann. Phys.*, to be published.

(**) See ref. (12) for an explanation.

APPENDIX

This appendix constitutes a more detailed analysis of the break down of eq. (2) at low energies.

It is clear that a more proper way of treating our relativistic two body problem would have been to start from eq. (1) and after having converted it into a wave equation, to introduce into it a potential matrix V:

$$[(p^2+m_{i>}^2)^{\frac{1}{2}}+(p^2+m_{i<}^2)^{\frac{1}{2}}-W]\psi_i=-\sum_j V_{ij}\psi_j\,. \tag{A.1}$$

Since this equation still neglects retardation effects it is, of course, not really correct; but it has more reality than (2).

The integral equation corresponding to eq. (A.1) and the outgoing wave boundary condition is

$$\psi_i=\varphi_i-\mathcal{G}_i^{(+)}\sum_j V_{ij}\psi_j\,, \tag{A.2}$$

where the Green's function $\mathcal{G}_i^{(+)}$ is given by ($\varepsilon>0$):

$$\mathcal{G}_i^{(+)}(W,|\boldsymbol{r}-\boldsymbol{r}'|)=\frac{-i}{(2\pi)^2|\boldsymbol{r}-\boldsymbol{r}'|}\int_{-\infty}^{+\infty}\mathrm{d}p\,\frac{p\exp[ip|\boldsymbol{r}-\boldsymbol{r}'|]}{(p^2+m_{i>}^2)^{\frac{1}{2}}+(p^2+m_{i<}^2)^{\frac{1}{2}}-W-i\varepsilon}\,. \tag{A.3}$$

The integral is carried out on that sheet of the Riemann surface of the integrand where, on the real axis, the square roots are both positive. The integrand in (A.3) has branch points on the imaginary axis as well as a simple pole in the upper half plane. After adding two quarter circles in the upper half plane at infinity to the path of integration, the integral therefore naturally splits into the sum of two integrals:

$$\mathcal{G}_i^{(+)}=\mathcal{G}_i^{(1)}+\mathcal{G}_i^{(2)}, \tag{A.4}$$

where $\mathcal{G}_i^{(1)}$ is the integral over the contour $C_i^{(1)}$ in Fig. 22 enclosing the pole P_i of the integrand in (A.3), and $\mathcal{G}_i^{(2)}$ is the integral over the contour $C_i^{(2)}$ around the branch lines.

$\mathcal{G}_i^{(1)}$ is easily calculated:

$$\mathcal{G}_i^{(1)}=\frac{\exp[ik_i|\boldsymbol{r}-\boldsymbol{r}'|]}{2\pi|\boldsymbol{r}-\boldsymbol{r}'|}\mu_i\,, \tag{A.5}$$

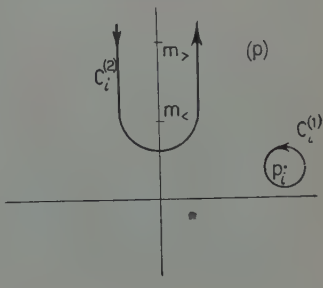

Fig. 22. – Contours of integration in the p-plane for eq. (A.4).

with k_i and μ_i defined by (3) and (4). We note that $\mathcal{G}_i^{(1)}$ is just the proper Green's function required for solving eq. (2). $\mathcal{G}_i^{(2)}$ cannot be evaluated in closed form; it vanishes asymptotically for large r *exponentially*, essentially like $\exp[-m_{i<}|\boldsymbol{r}-\boldsymbol{r}'|]$.

Fig. 23 shows the path described by the pole P_i as W decreases. When $W<m_{i>}+m_{i<}$, P_i moves along the right of the positive imaginary axis, the i-th channel now being closed. When W becomes less than $(m_{i>}^2-m_{i<}^2)^{\frac{1}{2}}$, the pole moves across a branch line onto another sheet of the Riemann surface, where on the real axis $(p^2+m_{i<}^2)^{\frac{1}{2}}$ is negative. From then on there is no residue contribution to the Green's function $\mathcal{G}_i^{(+)}$, which will be given by:

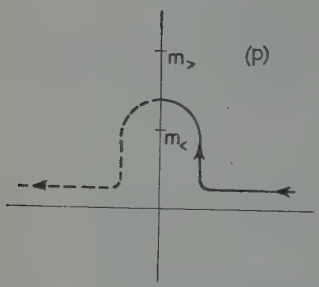

Fig. 23. – The path described by the pole of the integrand in (A.3) as the total energy W decreases. The dashed line represents the continuation on another sheet of the Riemann surface.

$$\text{(A.6)} \qquad \mathcal{G}_i^{(+)}=\mathcal{G}_i^{(2)}. \qquad \text{for } W<(m_{i>}^2-m_{i<}^2)^{\frac{1}{2}}.$$

This shows the most essential difference between eqs. (A.1) and (2). The latter contains no mechanism for avoiding a negative energy for the lighter pairtcle when $W<(m_{i>}^2-m_{i<}^2)^{\frac{1}{2}}$. When $W<m_{i>}-m_{i<}$ eq. (2) leads to an outgoing wave in the i-th channel and hence to an unphysical threshold. Eq. (A.1), on the contrary, automatically excludes negative energy effects and the unphysical outgoing wave.

Asymptotically as either r or W goes to infinity, the Green's function for eq. (A.1) equals the Green's function for eq. (2) since then $\mathcal{G}_i^{(2)}$ vanishes relative to $\mathcal{G}_i^{(1)}$ (except in the energy region where $\mathcal{G}_i^{(1)}$ vanishes identically).

Operation of (A.1) by $[\mathcal{G}_i^{(1)}]^{-1}=(p^2/2\mu_i)-\varepsilon_i$ on the left leads to an equation of the type (2):

$$\text{(A.7)} \qquad \left(\frac{p^2}{2\mu_i}-\varepsilon_i\right)\psi_i=-\sum_j V_{ij}\,\psi_j-\left(\frac{p^2}{2\mu_i}-\varepsilon_i\right)\mathcal{G}_i^{(2)}\sum_j V_{ij}\,\psi_j\,,$$

with an equivalent «potential» term on the right hand side which is both non local and energy dependent (the first term on the right hand side will be absent for all i for which $W<(m_{i>}^2-m_{i<}^2)^{\frac{1}{2}}$).

RIASSUNTO

In questo lavoro è stato eseguito lo studio delle sezioni d'urto di scattering pione-protone e di produzione mesone K-iperone in funzione dell'energia del pione incidente. Dato che gli effetti di soglia risultano cospicui per molti dei casi considerati, esiste la possibilità di determinare sperimentalmente le relative parità $P_{\Lambda\Sigma}$ e $P_{\Lambda K\pi}$.

IL NUOVO CIMENTO Vol. XIV, N. 5 1° Dicembre 1959

Relativistic Deuteron Wave Function. - I (*).

M. Gourdin

Ecole Normale Supérieure - Paris
Faculté des Sciences - Bordeaux

J. Tran Thanh Van

Ecole Normale Supérieure - Paris

(ricevuto il 26 Luglio 1959)

Résumé. — Nous étudions le problème du deutéron à partir de l'équation d'onde relativiste de Bethe et Salpeter. Il est possible, après certaines approximations, de calculer la constante de couplage correspondant à l'énergie de liaison mesurée expérimentalement et de donner une forme explicite numérique pour la fonction d'onde dans l'espace des énergies-impulsions. La transformée de Fourier de cette fonction d'onde, prise à la limite des temps égaux, est comparée avec la fonction d'onde non relativiste de Hulthén généralement utilisée pour représenter le deutéron. Les corrections relativistes produisent un effet répulsif analogue à celui d'un coeur dur, et ce résultat rejoint celui déjà trouvé dans le problème de la diffusion nucléon-nucléon antérieurement traité.

1. – Introduction.

The determination of a deuteron wave function is intrinsicly connected to that of nuclear forces. We inversely can obtain some information of this last problem by a phenomenological knowledge of the deuteron structure from scattering experiments. This first point only is sufficient to justify this paper.

Moreover, the deuteron is one of the most interesting and most convenient targets to study the scattering of a charged particle (electron, proton, meson π,

(*) Supported in part by the United States Air Force through the European Office, Air Research and Development Command.

meson K) by a neutron. But the degree of accuracy of the results depends in certain cases on a precise determination of a deuteron wave function. For example, in the electron deuterium scattering at high energy, it is necessary to take into account relativistic effects in the deuteron and we shall apply our results to this particular problem.

The Schrödinger equation permits to calculate a non-relativistic wave function, the Hulthén wave function, that is sufficient for the scattering problems at low energies. In order to evaluate relativistic corrections to the Hulthén wave function, we think that the best method consists in treating covariantly the problem with a relativistic wave equation for the two-body problem: the Bethe and Salpeter equation (1).

Many authors have considered this approach. But it was a very important progress when WICK (2) showed the possibility to continuate analytically the wave function $\chi(x)$ or equivalently its Fourier transform $\psi(p)$ for purely imaginary values of relative time (or relative energy). The four variables x_1, x_2, x_3, x_4 (or p_1, p_2, p_3, p_4) are now real and play a symmetrical part in a four-dimensional euclidean space. It is mathematically of great advantage and the calculations are so much simpler. WICK (2), CUTKOSKY (3) and SCARF (4) treat the problem of a bound state of two spinless particles interacting by a scalar meson field in the ladder approximation.

Our purpose is to take up again the calculation with a method already used for the scattering problem (5). In an euclidian energy-momentum space we can employ a partial wave expansion with four dimensional hyperspherical harmonics. After the angular integration is carried out, we obtain an infinite set of coupled homogeneous integral equations for one-dimensional radial wave functions. Some approximations are permitted by the form of the interaction kernel in the ladder approximation, and it is possible to give an explicit numerical expression for the deuteron wave function.

In this first paper, we are only interested by the academic problem of a spinless deuteron. The interaction is scalar and the ground state is an S state only. This simplified case permits to test the various methods used to determine the coupling constant where the binding energy has its experimental value. We obtain the wave function in the energy-momentum space and, by Fourier transformation, in the configuration space. The equal time limit of the S wave function is to compare with the non-relativistic Hulthén wave function. We

---

(1) E. E. SALPETER and H. A. BETHE: *Phys. Rev.*, **84**, 1232 (1951).
(2) G. C. WICK: *Phys. Rev.*, **96**, 1124 (1954).
(3) R. E. CUTKOSKY: *Phys. Rev.*, **96**, 1135 (1954).
(4) T. L. SCARF: *Phys. Rev.*, **100**, 913 (1956).
(5) M. GOURDIN: *Thesis* to be published in the *Annales de Physique* (1959); *Nuovo Cimento*, **7**, 338 (1958), referred to as G in the following.

observe a repulsive effect due to relativistic corrections and this corroborates, as in the scattering case, the existence of a hard core.

2. – The radial equation.

2·1. *Infinite system of integral equations.* – In the bound state case, the Bethe and Salpeter equation is an homogeneous integral equation for the wave function $\Phi(p)$ in a four-dimensional space. After Wick's transformation on the relative energy momentum variable p (6), this equation may be written as (7):

$$\Phi(\boldsymbol{p}) = \frac{\alpha}{(p^2 + M^2 + (P^2/4))^2 - P^2 p_4^2} \int W(\boldsymbol{p}, \boldsymbol{p}') \Phi(\boldsymbol{p}') \, \mathrm{d}\boldsymbol{p}' , \tag{1}$$

α is proportional to the coupling constant g^2, p and P are respectively the relative and total energy momentum four-vectors. The kernel function $W(\boldsymbol{p}, \boldsymbol{p}')$ describes the interactions between the two nucleons; we assume, for simplicity, that it is invariant by rotation in the 4-dimensional euclidian space of $\boldsymbol{p}$.

Let us first expand the wave function $\Phi(\boldsymbol{p})$ and the interaction kernel $W(p, p')$ in hyperspherical harmonics (8)

$$\Phi(\boldsymbol{p}) = \sum_{n=0}^{\infty} \sum_{l=0}^{n} A(p, l, n) \mathscr{Y}_{ln}^{0}(\Omega_p) , \tag{2}$$

$$W(\boldsymbol{p}, \boldsymbol{p}') = \sum_{n=0}^{\infty} \sum_{l=0}^{n} \Delta_n(p, p') \mathscr{Y}_{ln}^{0}(\Omega_p) \mathscr{Y}_{ln}^{0}(\Omega_{p'}) . \tag{3}$$

Ω_p corresponds to the set of polar angles θ, φ and β of p. The azimutal quantum number m (corresponding to φ) can be zero in a cylindrical symmetric problem. The integration over θ is immediately performed because of the orthogonality of the spherical harmonics and conservation of the orbital angular momentum l. The situation is different for the third angle β and the third quantum number n. The external propagators for the nucleons depend on $p_4 = p \cos\beta$ and it is convenient to define an auxiliary function $E(p, l, n, n')$ by

$$E(p, l, n, n') = \int_0^{\infty} \frac{\mathscr{C}_l^n(\beta) \mathscr{C}_l^{n'}(\beta)}{(p^2 + M^2 + (P^2/4))^2 - p^2 P^2 \cos^2\beta} \sin^2\beta \, \mathrm{d}\beta . \tag{4}$$

---

(6) We remind that for the bound state wave function, the analytic continuation to imaginary values of the total energy P_0 is not necessary. See references (2) and (5).

(7) Compare with equation (2.1), p. 342 in G.

(8) See G, Appendix I.

The function $\mathscr{C}_l^n(\beta)$ is essentially a Gegenbauer polynomial normalized to unity.

The quantum number n has no physical interpretation; it is not a constant of motion but the parity of n and n' must be the same; the existence of an equal time limit for the wave function in the configuration space implies that $(-1)^l = (-1)^n$.

We hereafter use, instead of n, the number q as determined from $n = l + 2q$.

Finally, for each value of the orbital angular momentum l, the radial wave functions $A(p; l, q)$ are solutions of an infinite set of coupled integral equations:

$$A(p; l, q) = \alpha \sum_{q'=0}^{\infty} E(p; l, q, q') \int_0^{\infty} \Delta_{l+2q'}(p, p') A(p'; l, q') p'^3 \, \mathrm{d}p \, . \tag{5}$$

2·2. *Calculation of* $E(p; l, q, q')$. – To evaluate the function $E(p; l, q, q')$ we use the Poisson formula as for the corresponding scattering problem [9]. The result is the following:

$$E(p; l, q, q') = \frac{\pi}{(p^2 + M^2 + (P^2/4))\left[(p^2 + M^2 + (P^2/4))^2 - p^2 P^2\right]^{\frac{1}{2}}} \sum_{-\infty}^{+\infty} C_s(l; q, q') h^{|s|}(p) \, .$$

The $C_s(l; q, q')$ are the Fourier coefficients of the product of two normalized Gegenbauer polynomials

$$\mathscr{C}_l^{l+2q}(\beta) \mathscr{C}_l^{l+2q'}(\beta) \sin^2 \beta \, \mathrm{d}\beta = \sum_{-\infty}^{+\infty} C_s(l; q, q') \exp\left[2is\beta\right] .$$

The function $h(p)$ given by

$$h(p) = \frac{(p^2 + M^2 + (P^2/4)) - \left[(p^2 + M^2 + (P^2/4))^2 - p^2 P^2\right]^{\frac{1}{2}}}{(p^2 + M^2 + (P^2/4)) + \left[(p^2 + M^2 + (P^2/4))^2 - p^2 P^2\right]^{\frac{1}{2}}} , \tag{6}$$

for real values of p and imaginary values of P satisfies the inequalities:

$$-1 < h(p) \leqslant 0 \, .$$

2·3. *The S-state.* – For the particular $l = 0$ case we immediately obtain [10] the coefficients $C_s(0; q, q')$ and consequently the function $E(p, 0, q, q')$:

$$E(p; 0, q, q') = \frac{2}{(p^2 + M^2 + (P^2/4))^2 \left\{(p^2 + M^2 + (P^2/4)) + \left[(p^2 + M^2 + (P^2/4))^2 - p^2 P^2\right]^{\frac{1}{2}}\right\}} \sum_{|q'-q|}^{q'+q} h^s(p) \, .$$

[9] See G, Section 2·1.

[10] See G: *Thesis*, Appendix VII.

We now use the reference system where the total momentum is zero. The only non-vanishing component of P is the rest mass

$$(P = (0, 0, 0, iM_D) .$$

Next, it is more interesting to consider the binding energy B of the deuteron $B = 2M - M_D$. The small experimental value $B = 2.23$ MeV permits to neglect $\gamma^2 = MB$ in regard to M_D^2.

With the notation $A_q(p)$ for the S components of the wave function, we have to solve the following equations:

$$(7) \qquad A_q(p) = \frac{2\alpha}{(p^2+\gamma^2)\{(p^2+\gamma^2) + [(p^2+\gamma^2)^2 + 4p^2M^2]^{\frac{1}{2}}\}} \sum_{q'=0}^{\infty} \sum_{s=|q'-q|}^{s=q'+q} h^s(p) \cdot \cdot \int_0^{\infty} \Delta_{2q'}(p, p') A_{q'}(p') p'^3 \, dp' .$$

3. – Resolution of the integral equations.

We cannot generally give an exact solution for the infinite set of equations (7). It is necessary to accept some approximations which depend essentially on the explicit form of the kernel functions.

As in the scattering problem, we restrict ourselves to the ladder approximation. It is the infinite iteration of the elementary process corresponding to the exchange of a virtual meson during a small time interval between the two nucleons. We immediately obtain ([11]):

$$(8) \qquad \Delta_{2q}(p, p') = \frac{8\pi^2}{2q+1} \left(\frac{1}{S+D}\right)^2 \left(\frac{S-D}{S+D}\right)^{2q} .$$

S and D are two symmetrical functions of p and p' given by

$$S(p, p') = [(p+p')^2 + \mu^2]^{\frac{1}{2}} , \qquad D(p, p') = [(p-p')^2 + \mu^2]^{\frac{1}{2}} ,$$

where μ is the π-meson mass or possibly a phenomenological parameter.

([11]) See G, Appendix VI.

3·1. *Separation of the equations.* – All the approximations one can make are intimately related to the behaviour of the kernels $\Delta_{2q}(p, p')$ and of the auxiliary function $h(p)$.

Let us first rewrite equation (8) in the form:

$$\Delta_{2q}(p, p') = \Delta_0(p, p') \frac{1}{2q+1} \left(\frac{S-D}{S+D}\right)^{2q},$$

we can immediately see the fast decrease of the interaction when q increases. Consequently any component $A_q(p)$ is only strongly coupled with components $A_{q'}(p)$ corresponding to the small values of q and in a first approximation with $A_0(p)$.

We now consider the integral equation satisfied by $A_0(p)$:

$$A_0(p) = \alpha L(p) \sum_{q'=0}^{\infty} h^{q'}(p) \int_0^{\infty} \Delta_{2q'}(p, p') A_{q'}(p') p'^3 \, dp', \tag{9}$$

where

$$L(p) = 2(p^2+\gamma^2)^{-1}\{(p^2+\gamma^2) + [(p^2+\gamma^2)^2 + 4p^2M^2]^{\frac{1}{2}}\}^{-1}.$$

On the other hand, the function $h(p)$ goes rapidly to zero when $p \to 0$ and $p \to \infty$ and is, in modulus, bounded by unity. Neglecting the coupling between $A_0(p)$ and the other components $A_q(p)$ for these two reasons, we approximate equation (9) by an integral equation for $A_0(p)$:

$$A_0(p) = \alpha L(p) \int_0^{\infty} \Delta_0(p, p') A_0(p') p'^3 dp'. \tag{10}$$

In a similar way we retain for the other components their coupling with $A_0(p)$ only. Once Equation (10) has been solved for $A_0(p)$, the $A_q(p)$ components are given by:

$$A_q(p) \simeq h^q(p) A_0(p). \tag{11}$$

However it is possible to evaluate the error made by replacing the exact equation (9) by an approximate equation (10). Taking the form (11) for $A_q(p)$ and replacing in equation (9) one obtains for $A_0(p)$ an integral equation of type (10) but with a new kernel. It is convenient to write this kernel as the

product of the old kernel $\Delta_0(p, p')$ by a function $\delta(p, p')$. We then obtain the result:

$$\delta(p, p') = 1 + \frac{1}{3} h(p)h(p') \left(\frac{S-D}{S+D}\right)^2 + \ldots + \frac{1}{(2q+1)} h^q(p)h^q(p') \left(\frac{S-D}{S+D}\right)^{2q} + \ldots ,$$

and after summation:

$$\delta(p, p') = \frac{1}{2X(p, p')} \log \frac{1+X(p, p')}{1-X(p, p')} ,$$

where

$$X(p, p') = [h(p)h(p')]^{\frac{1}{2}} \left(\frac{S-D}{S+D}\right) .$$

It can be easily seen that $\delta(p, p')$ is a slowly varying function very close to one and $A_0(p)$ can be reasonably considered as solution of the integral equation (10).

3·2. *Determination of the coupling constant* α. – To transform equation (10) into an integral equation with symmetric kernel we define a new unknown function $F(p)$ and a new kernel:

$$F(p) = p^{\frac{3}{2}} L^{-\frac{1}{2}}(p) A_0(p)$$

$$K(p, p') = p^{\frac{3}{2}} L^{\frac{1}{2}}(p) \Delta_0(p, p') L^{\frac{1}{2}}(p') p'^{\frac{3}{2}}$$

and we have to solve the equation

$$F(p) = \alpha \int_0^\infty K(p, p') F(p') \, \mathrm{d}p' , \tag{12}$$

the kernel of which is symmetric.

We know the binding energy—or in equivalent way the parameter γ^2—and the problem of determining the coupling constant α reduces to the research of the eigenvalue of a symmetric kernel $K(p, p')$. We know from the Hilbert-Schmidt theorem that such a kernel has at least one eigenvalue and this eigenvalue is real.

Together with the eigenvalue α it is important to calculate the corresponding eigenfunction. Unfortunately this problem appears more difficult and we begin with a direct determination of α using two methods: the trace of the kernel and the Fredholm determinant.

Let us define the iterated kernels by the recurrence relationship:

$$K_1(p, p') = K(p, p') , \qquad K_m(p, p') = \int_0^\infty K_{m-n}(p, p'') K_n(p'', p') \, \mathrm{d}p'' ,$$

where n is any integer less than m.

The trace of the kernels are given by the integral:

$$T_m = \int_0^\infty K_m(p, p) \, \mathrm{d}p . \qquad m = 1, 2, \ldots .$$

It is possible to find the smallest eigenvalue knowing the trace of the kernel. For sufficiently large m, one can show that:

$$\alpha = \lim_{m \to \infty} \left(\frac{1}{T_{2m}} \right)^{1/2m} \qquad \text{or} \qquad \alpha = \lim_{m \to \infty} \left(\frac{T_{2m}}{T_{2m+2}} \right)^{\frac{1}{2}} .$$

Setting $m = 1$ therein, we obtain the following value of α [12]:

$$\frac{\alpha_T}{\mu^2} = 0.59 . \tag{13}$$

We now use a second method to determine α. It is well known that equation (12) has no solution except $F(p) = 0$ unless Fredholm's determinant $D(\alpha)$ is zero. This latter can be expanded in powers series of α

$$D(\alpha) = \sum_0^\infty \frac{(-\alpha)^n}{n!} \int_0^\infty \ldots \int_0^\infty \begin{vmatrix} K(p_1, p_1) K(p_1, p_2) \ldots K(p_1, p_n) \\ K(p_2, p_1) K(p_2, p_2) \ldots K(p_2, p_n) \\ \cdot \qquad\qquad\qquad \cdot \\ \cdot \qquad\qquad\qquad \cdot \\ K(p_n, p_1) K(p_n, p_2) \ldots K(p_n, p_n) \end{vmatrix} \mathrm{d}p_1 \, \mathrm{d}p_2 \ldots \mathrm{d}p_n .$$

The coefficient of α^n is a function of T_1, T_2, ..., T_n defined above as the traces of the kernels,

$$D(\alpha) = \sum_0^\infty \frac{(-\alpha)^n}{n!} C_n . \tag{14}$$

[12] It is very important to take into account the binding energy of the deuteron because the small values of p are very important in the calculation of the integrals. Putting $\gamma^2 = 0$ we obtain $\alpha_T/\mu^2 = 0.39$.

To determine the C_n we can use a recurrence relationship:

$$C_{n+1} = \sum_{m=0}^{n} (-1)^{n-m} \frac{n!}{m!} T_{m+1-m} C_m .$$

In particular we obtain:

$$C_0 = 1 , \qquad C_1 = T_1 , \qquad C_2 = T_1^2 - T_2 .$$

We have performed the calculation of α by limiting the series (13) to first and second order terms in α. The results are an underestimate and an overestimate value for the coupling constant:

$$0.43 < \alpha/\mu^2 < 0.68 \tag{15}$$

in agreement with the result (13).

We shall next use an iteration method of the integral equation (10) in order to calculate the eigenfunction $F(p)$ explicitly. This also gives a possible determination of α.

It seems to be natural to compare these values with the corresponding one for the scattering problem. After some approximations to solve the homogeneous integral equation, we adjust α to reproduce the experimental neutron-proton scattering length ([13]). This yields: $\alpha_D/\mu^2 = 0.375$.

We shall conclude that coupling constants of the same order of magnitude (a factor 1.5 cannot be significant) permit to account for both bound state and scattering state at low energies for the neutron-proton system. This result will be extended to the case on two Dirac particles.

3·3. *Determination of the wave function* $A_0(p)$. – To calculate explicitly the eigenfunction we use Kellog's method of iteration for the equation (10). If we remark that $L(p)$ is rapidly decreasing, it is convenient to put

$$A_0(p) = L(p) f(p) .$$

The new unknown function $f(p)$ satisfies the following equation

$$f(p) = \alpha \int_0^\infty \Delta_0(p, p') p'^3 L(p') f(p') \, dp' , \tag{16}$$

([13]) The cruder approximation is certainly to replace the exact kernel—in the ladder approximation—by an approximate separable kernel. See G.

and is related to $F(p)$ by

$$F(p) = p^{\frac{3}{2}} L^{\frac{1}{2}}(p) f(p) . \tag{17}$$

Let us take a trial function $f_1(p) = (p^2+1)^{-1}$ (in units $\hbar = c = \mu = 1$) and construct the following sequence:

$$f_2(p) = \int_0^\infty \Delta_0(p, p') p'^3 L(p') f_1(p') \, \mathrm{d}p' ,$$

$$f_n(p) = \int_0^\infty \Delta_0(p, p') p'^3 L(p') f_{n-1}(p') \, \mathrm{d}p' .$$

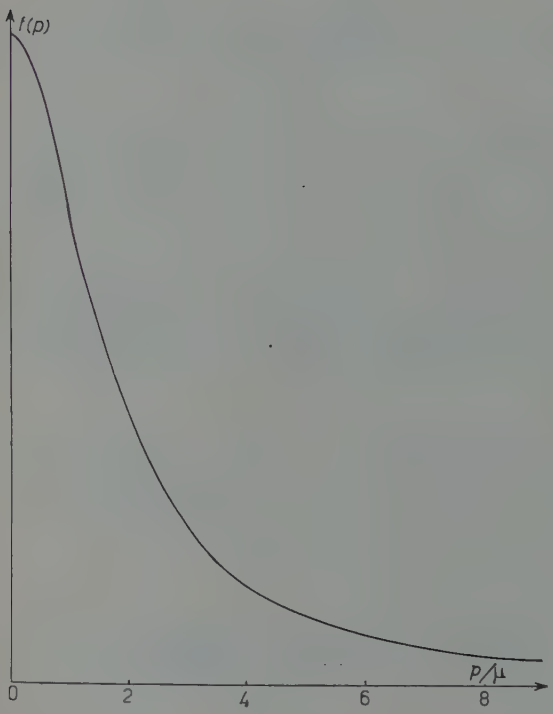

Fig. 1.

If $f_1(p)$ is not orthogonal to the eigenfunction associated with the smaller eigenvalue α, the limiting function

$$f(p) = \lim_{n\to\infty} f_n(p) \tag{18}$$

represents the eigenfunction corresponding to α.

In Fig. 1, we have plotted the function $f_4(p)$.

Kellog's method may be used to determine α by the formula

$$\alpha = \lim_{n\to\infty} \frac{\| F_n \|}{\| F_{n+1} \|} .$$

Setting $n = 3$ and $n = 4$ we obtain:

$$\begin{cases} \alpha_3/\mu^2 = 0.61 , \\ \alpha_4/\mu^2 = 0.61 . \end{cases} \tag{19}$$

We also can define α as the limit of two sequences:

$$\alpha(0) = \lim_{n\to\infty} \frac{f_n(0)}{f_{n+1}(0)} \quad \text{and} \quad \alpha(\infty) = \lim_{n\to\infty} \frac{f_n(\infty)}{f_{n+1}(\infty)} .$$

In practical calculation, we replace the last sequence by $f_n(7)/f_{n+1}(7)$. The results are the following (in units $\mu = 1$):

$$(20)\quad \begin{cases} \text{1-st iteration} & \alpha(0) = 0.825\,, & \alpha(7) = 0.37\,, \\ \text{2-nd iteration} & \alpha(0) = 0.64\,, & \alpha(7) = 0.54\,, \\ \text{3-rd iteration} & \alpha(0) = 0.61\,, & \alpha(7) = 0.56\,. \\ \text{4-th iteration} & \alpha(0) = 0.61\,, & \alpha(7) = 0.59\,. \end{cases}$$

If we compare the results (13), (15), (19) and (20), we remark two interesting features. First, the exact value of α is:

$$\alpha/\mu^2 = 0.60 \pm 0.01\,.$$

Secondly, the best method is that of the trace of the kernel. This shall permit, for the more complicated problem of a deuteron with spin, to reduce the calculations only to this method.

4. – The wave function in the configuration space.

The quantum numbers l, m, n, are conserved in a Fourier transformation [14]. To an expansion of the wave function $\Phi(p)$ in the momentum space corresponds an expansion of its Fourier transform $\chi(x)$ in the configuration space. The radial functions are Bessel transforms to each other. In the particular case of an S wave we obtain:

$$(21)\qquad A_q(r) = \frac{1}{(2\pi)^2}(-1)^q \int_0^\infty A_q(p)\,\frac{J_{2q+1}(pr)}{pr}\,p^3\,\mathrm{d}p\,.$$

The ordinary S wave function corresponds to a summation over q. Passing to the equal time limit ($\beta_r = \pi/2$) we find

$$\psi(r) = \sum_0^\infty A_q(r)\,\mathscr{C}_0^{2q}\left(\frac{\pi}{2}\right).$$

It is easy to evaluate the Gegenbauer polynomial when the argument is $\pi/2$.

---

[14] See G, Appendix III.

The unrenormalized wave function is then given by

$$\psi_R(r) \simeq \int_0^\infty A_0(p) \sum_q \left[h^q(p) \frac{J_{2q+1}(pr)}{pr} \right] p^3 \, \mathrm{d}p \,, \tag{22}$$

where formula (11) for $A_q(p)$ is used.

We have performed the numerical integration in (22) with the approximate function $L(p) f_4(p)$ for $A_0(p)$. The result is plotted in Fig. 2 for the reduced wave function $r\psi_R(r)$.

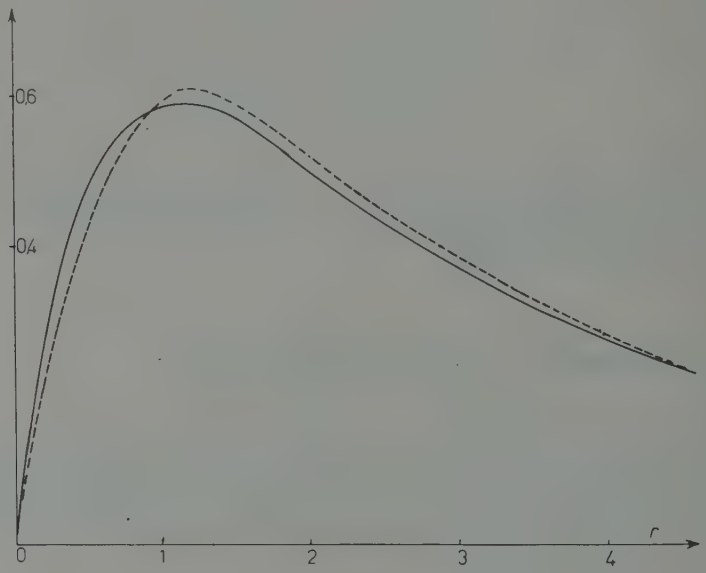

Fig. 2.

At this stage it seems to be interesting to compare this wave function with the Hulthén wave function given by:

$$\psi_H(r) = \frac{\exp[-\gamma r] - \exp[-\beta r]}{r} \,,$$

where γ is the binding energy parameter as defined above and β is adjusted to reproduce the experimental value of the triplet neutron-proton effective range ($\beta \gg \gamma$).

One can easily see, on the integral (22), that the asymptotic form of $\psi_R(r)$ reduces to the ordinary exponential form $\exp[-\gamma r]/r$ as necessary.

The Fig. 2 shows a displacement of the wave function $r\psi(r)$ corresponding to a repulsive effect of the interaction. The probability distribution inside

the range of nuclear forces ($r < \hbar/\mu c$) is reduced by the relativistic treatment. It is about the effect produced by a repulsive core added to an attraction potential ([15,16]). We also can obtain, using a Gartenhaus potential ([17]), a similar effect corresponding to the addition of second and fourth order terms in a fixed source treatment of the two nucleon problem.

With such a wave function we are able to calculate the electron-deuteron scattering, neglecting the D part of the deuteron wave function. We shall find a reduction in the cross-section below its value computed with a non-relativistic deuteron wave function. This agrees with Blankenbecler's results ([18]) where this reduction is estimated to be $(25 \div 30)\%$ for a momentum transfer $q = 3f^{-1}$.

5. – Conclusion.

We have developed a practical method to find a deuteron wave function from the Bethe and Salpeter equation. The problem of solving an infinite set of coupled equations appears, *a priori*, very difficult. Fortunately, the analytic expression of the interaction kernel permits a large decoupling of the equations and leads to classical integral equations solvable by straightforward methods. We then obtain the coupling constant and the radial wave function for the S state in the energy momentum space. We easily deduce the corresponding wave function in the configuration space and compare its equal time limit with the Hulthén wave function.

We already know that nucleon-nucleon scattering experiments require a change of sign for the ^1S phase shift. This particularity can be easily explained by assuming the presence of an infinitely repulsive potential of short range ([19,20]). The relativistic corrections, calculated in the ladder approximation as well in the scattering problem as in the bound state problem, give a result equivalent to that of such a hard core. A complete study would consist to take into account interaction terms of higher order. Nevertheless this approximation is in part compensated by the empirical determination of the coupling constant to have the experimental value for the binding energy.

We think it is not sufficient to consider a spinless deuteron and to take account phenomenologically of the spin and of the ^3S-^3D mixture. The

---

([15]) K. A. Brueckner and K. M. Watson: *Phys. Rev.*, **92**, 1034 (1953).

([16]) J. Bernstein: *Phys. Rev.*, **104**, 249 (1956).

([17]) S. Gartenhaus: *Phys. Rev.*, **100**, 900 (1955).

([18]) 1958 *Annual International Conference on High Energy Physics at CERN* (Ferretti, 1958).

([19]) R. Jastrow: *Phys. Rev.*, **81**, 165 (1951).

([20]) M. M. Lévy: *Phys. Rev.*, **88**, 725 (1952).

calculations for two Dirac particles are in progress; we use the pseudoscalar theory with pseudo-scalar coupling and try to solve the bound state problem for the value $J=1$ of the total angular momentum and an even parity. Because the interaction kernel involves the same functions as in the present case, we can use identical approximations to obtain an explicit form for the $({}^3S_1+{}^3D_1)$ wave function. This calculations shall be the purpose of a subsequent paper.

RIASSUNTO (*)

Si studia il problema del deuterone partendo dall'equazione d'onda relativistica di Bethe e Salpeter È possibile, con alcune approssimazioni, calcolare la costante di accoppiamento corrispondente all'energia di legame misurata sperimentalmente e dare una forma numerica esplicita della funzione d'onda nello spazio dell'energia-impulso. La trasformata di Fourier di questa funzione d'onda, considerata al limite d'intervalli di tempo uguali, si confronta con la funzione d'onda non relativistica di Hulthén utilizzata generalmente per rappresentare il deutone. Le correzioni relativistiche producono un effetto repulsivo analogo a quello d'un nucleo duro, e questo risultato s'appaia a quello già trovato per il problema della diffusione nucleone-nucleone trattato in precedenza.

(*) *Traduzione a cura della Redazione.*

IL NUOVO CIMENTO · Vol. XIV, N. 5 1° Dicembre 1959

On the Mechanism of the Pinch Effect (*).

T. Gotō, M. Sato and T. Uchida

Department of Physics, College of Science and Engineering, Nihon University - Tokyo

(ricevuto il 4 Agosto 1959)

Summary. — Phenomenological analysis of the fast pinch effect is presented and compared with some existing experimental data. It is argued that several results consistent with experiments can be derived from a general basic picture of the fast contracting process, independent of its detailed mechanism. To establish a consistent model of the pinch mechanism, it is therefore necessary to get more detailed experimental information about the dynamical behaviour of the plasma column under various initial conditions. Dimensional considerations are added in the Appendix.

1. – Introduction.

Many theoretical and experimental works have been published on the mechanism of the pinch effect in a high current gas discharge. While it is now obvious that the plasma formed by fast contracting processes is unstable without stabilizing magnetic fields and conducting walls, and new devices have been invented in several countries in order to study further how to stabilize the discharge, the efforts are still being continued to establish an overall picture of the fast pinch effect [1].

Several models have been proposed as a physical picture of the fast con-

(*) The main content of this paper was reported at the Second Atomic Energy Symposium, Tokyo, February 1958.

(1) S. C. Curran *et al.*: *Proc. of the 2nd United Nations International Conference on the Peaceful Uses of Atomic Energy*, P/1460 (Geneva, 1958).

tracting process; for example, the so-called « snow-plow model » by M. ROSENBLUTH ([2,3]), the « shock wave model » by J. E. ALLEN ([4]) and J. D. JUKES ([5]), and the « inertia force theory » by M. A. LEONTOVIČ and S. M. OSOVETS ([6]). Each of these models has explained the process qualitatively well and presented some interesting results. It has been argued then sometimes that their agreement with experiments is the justification of the model itself.

One of these results is that the time of the first maximum contraction depends on the initial conditions of discharge as follows ([3-6]):

$$t_f \propto a_0 p_0^{\frac{1}{2}} (\dot{I})^{-\frac{1}{2}} ,$$

where a_0 is the radius of the discharge tube, p_0 the initial gas pressure, and $\dot{I}$ the rate of the initial current build-up. However, it is easy to show that this relation is obtained by a dimensional consideration, independent of the details of the contraction mechanism, if it is only assumed that the process is pictured as the contraction of a plasma column with a well-defined radius, under the action of the self-magnetic pressure produced by the discharge current. Other quantities of interest, such as the mean contraction velocity and the total energy input to the plasma, can also be derived from dimensional analysis (cf. Appendix).

In this paper, a phenomenological approach different from the above authors was made to derive relations more generally, independently of the detailed mechanism of the contraction process. To make such an analysis, the equation for the current build-up is approximately integrated to obtain the magnetic pressure, which is then used for the pressure balance equation at the current sheet, in accordance with the picture mentioned above. The ohmic resistance is neglected as compared with the inductive one, since we are concerned with a fast process. Several main results are summarized at the end of Section **2**, and they are compared with some existing experimental results in Section **3**. Finally it is argued in Section **4** that more detailed experimental information under various initial conditions will be needed about the dynamical behaviour of the plasma column, in order to establish a consistent model of the pinch mechanism.

([2]) M. ROSENBLUTH: *Los Alamos Scientific Laboratory Report*, LA-1850 (1954).

([3]) S. A. COLGATE: *University of California Radiation Laboratory Report*, UCRL-4895 (1957); O. A. ANDERSON *et al.*: *Proc. of the 3rd International Conference on the Ionization Phenomena in Gases* (Venice, 1957), p. 62.

([4]) J. E. ALLEN: *Proc. Roy. Soc.*, B **70**, 24 (1957).

([5]) J. D. JUKES: A.E.R.E. Gp/R 2293 (1958).

([6]) M. A. LEONTOVIČ and S. M. OSOVETS: *Atomnaya Energija*, **1**, 81 (1956).

2. – Phenomenological analysis of the contraction process.

In this Section, we analyse the contraction process phenomenologically. The main results are contained in eqs. (2.14), (2.18), (2.20) and (2.21), below, which are derived on the basis of some simplifying but reasonable assumptions.

Since the ohmic resistance of the plasma may be neglected after the first stage of the break-down, most of the input energy will be supplied to the gas as the compression work done by the self-magnetic field produced by the discharge current. Owing to the rapid compression process, there is certainly strong possibility of the shock wave to be produced, as assumed and treated by J. E. ALLEN [4] and J. D. JUKES [5], and there is some experimental evidence for it. This compression process may also be treated by the snow-plow shock model of M. ROSENBLUTH (*) [2]. But we shall make a more phenomenological approach which does not contain explicit assumptions about the dynamical behaviour of the discharge column. It is only assumed, as mentioned in the Introduction, that the process may be pictured as the contraction of a plasma column with a well-defined radius under the action of the self-magnetic pressure.

The energy supply to the gas per unit time is expressed, in circuit variables by

$$\mathrm{d}W_M/dt = \tfrac{1}{2}(\mathrm{d}L/\mathrm{d}t)I^2 , \tag{2.1}$$

where L and I are the total inductance and the total current, respectively, and L, I and the capacitance C are related by the following equation:

$$\mathrm{d}^2(LI)/\mathrm{d}t^2 + I/C = 0 . \tag{2.2}$$

Assuming that the change of L is not very large, the solution of eq. (2.2) is obtained by using the W.K.B. approximation:

$$I = I_0(L_0/L)^{\frac{1}{2}} \sin\left(\int_0^t \omega(t')\,\mathrm{d}t'\right), \tag{2.3}$$

where $I_0 = V_0(C/L_0)^{\frac{1}{2}}$, $\omega^2 = 1/LC$, and L_0 and V_0 are the initial inductance and the initial voltage, respectively. When the contraction process is completed

(*) S. KUWABARA (private communication) obtained a solution of the hydromagnetic equations of the conducting cylindrical column being compressed by the pinch magnetic field. It was found that the distance between the converging shock front and the current sheet is rather small and, therefore, the snow-plow model would be a good description of the process.

before the first peak of the current, *i.e.*, when the integrand of eq. (2.3) is small compared with unity, eq. (2.3) may be approximated as

$$I \approx V_0(_0/L)^{\frac{1}{2}} \cdot t/L \,. \tag{2.4}$$

Then the energy supply to the plasma until the first maximum contraction is given by

$$W_M = \int_0^{t_f} (\mathrm{d}W_M/\mathrm{d}t)\,\mathrm{d}t \approx \frac{1}{2}\int_0^{t_f} V_0^2 (L_0/L)^{\frac{1}{2}} (\mathrm{d}L/\mathrm{d}t)(t/L)^2\,\mathrm{d}t \,, \tag{2.5}$$

where we have put

$$L = L_0\,(1 + \varphi(t)) \tag{2.6}$$

and φ is given by

$$\varphi = -\,(\mu l/2\pi L_0)\,1n(a(t)/a_0) \,, \tag{2.7}$$

where it is assumed that the inner radius of the discharge tube is small compared with its length (l). Here $a(t)$ is the radius of the cylindrical plasma column and a_0 is it initial value.

It is assumed that the current flows on the surface of the column since the plasma conductivity is large. (This assumption has minor effect for the following discussion.) The magnetic pressure, acting on the plasma column, is (in MKS units):

$$P_M = \tfrac{1}{2}\,\mu H^2 = (\mu/8\pi^2)(I/a)^2 = (\mu/8\pi^2)(V_0/L_0)^2\,(1+\varphi)^{-\frac{5}{2}}\,t^2/a^2. \tag{2.8}$$

where use has been made of eqs. (2.4) and (2.6).

Now it will be reasonable to assume that this magnetic pressure is balanced by the gas kinetic pressure at the current sheet if the initial gas pressure, p_0, can be neglected:

$$\varrho(a)(\mathrm{d}a/\mathrm{d}t)^2 = P_M \,, \tag{2.9}$$

where $\varrho(a)$ is the mass density just at the inner side of the current sheet and we assume in the following that it is a function of a/a_0 or, by eq. (2.7), of φ, only, and put

$$\varrho(a) = \varrho_0 \Psi^2(a/a_0) = \varrho_0 \Psi^2(\varphi) \,, \tag{2.10}$$

where $\Psi(a/a_0)$ or $\Psi(\varphi)$ includes no circuit variables and is dependent only on the mechanism of the contraction but not on the contraction speed, explicitly. ϱ_0 is the initial value of ϱ.

Then, after some manipulations starting from eq. (2.9), we have

$$(2.11)\quad \int_0^{\varphi} \mathrm{d}\varphi' \Psi(\varphi') \exp\left[-\frac{4\pi L_0}{\mu l}\varphi'\right](1+\varphi')^{\frac{1}{2}} = \frac{\mu l}{2\pi L_0}(\mu/8\pi^2)^{\frac{1}{2}}(V_0/L_0)(t^2(\varphi)/2\sqrt{\varrho_0}a_0^2)\,.$$

Getting $t^2(\varphi)$ from (2.11) and inserting it into eq. (2.5), we obtain

$$(2.12)\quad W_M = \frac{1}{2}(V_0/L_0)(4\pi L_0/\mu l)L_0(8\pi^2/\mu)^{\frac{1}{2}}\sqrt{\varrho_0}a_0^2\int_0^{\varphi_f}\mathrm{d}\varphi(1+\varphi)^{-\frac{3}{2}}f(\varphi)\,.$$

Here the function $f(\varphi)$ is defined by

$$(2.13)\quad f(\varphi) = \int_0^{\varphi}\mathrm{d}\varphi'(1+\varphi')^{\frac{1}{2}}\exp\left[-\frac{4\pi L_0}{\mu l}\varphi'\right]\Psi(\varphi')\,.$$

In terms of $f(\varphi)$, $t^2(\varphi)$ and P_M are written as

$$(2.14)\quad t^2(\varphi) = \frac{4\pi L_0}{\mu l}\sqrt{\varrho_0}a_0^2\sqrt{\frac{8\pi^2}{\mu}}(L_0/V_0)f(\varphi)\,,$$

$$(2.15)\quad P_M = \frac{4\pi L_0}{\mu l}\sqrt{\frac{\mu}{8\pi^2}}(V_0/L_0)\sqrt{\varrho_0}\exp\left[\frac{4\pi L_0}{\mu l}\varphi\right](1+\varphi)^{-\frac{3}{2}}f(\varphi)\,.$$

It may be considered that the supplied energy, W_M, will be suddenly converted into the random thermal energy of the plasma at the state of the maximum contraction. The estimate of the thermalization times for ions and electrons indicates that the randomization will occur within a sufficiently short time for conditions usually met in the pinch experiments. Then, assuming that the magnetic pressure and the gas pressure are nearly balanced at the maximum contraction, $t = t_f$, we get

$$(2.16)\quad P_M = P_G\,,$$

where $P_G = nkT$ and $kT = W_M/3N$ (n: number density, N: total number) or,

$$(2.17)\quad (1/3\pi a_0^2 l)(a_0/a_f)^2 W_M = P_M\,,$$

where a_f is the final constricted radius of the plasma column. Using eqs. (2.12) and (2.15), this is expressed as

$$\int_0^{\varphi_f} \mathrm{d}\varphi g(\varphi) = (3\mu l/4\pi L_0) g(\varphi_f) , \tag{2.18}$$

with $g(\varphi)$ defined by

$$g(\varphi) = (1+\varphi)^{-\frac{5}{2}} f(\varphi) . \tag{2.19}$$

The final contraction velocity of the column will be obtained from $\varrho_f v_f^2 = P_{M,f}$ (eq. (2.9)) and $\varrho_f = (a_0/a_f)^2 \varrho_0$. The result is

$$v_f^2 = \frac{4\pi L_0}{\mu l} \sqrt{\frac{\mu}{8\pi^2}} \frac{1}{\sqrt{\varrho_0}} (V_0/L_0) g(\varphi_f) . \tag{2.20}$$

Finally, from eqs. (2.18) and (2.20), we get

$$(W_M/\tfrac{1}{2}\varrho_0 \pi a_0^2 l v_f^2) \approx 6 , \tag{2.21}$$

where the denominator corresponds to the total kinetic energy of the contracting plasma at t_f when all the particles initially existing in the tube were involved in the contraction.

Summarizing the above analysis, we shall infer that:

i) From eq. (2.18) it is evident that at the final instant φ_f, *viz.* a_f, is constant independently of the initial gas pressure and the applied voltage because φ_f depends only upon the two factors: l/L_0 and $\Psi(\varphi_f)$.

ii) Since φ_f is constant for a given apparatus, it is found easily from eq. (2.14) that the time of the first pinch is proportional to $a_0 p_0^{\frac{1}{4}} V_0^{-\frac{1}{2}}$ or $a_0 p_0^{\frac{1}{4}} I_0^{-\frac{1}{2}}$. This result was alredy obtained by several authors ([3-6]), using the models mentioned earlier, and can be got also by a dimensional analysis (see Appendix).

iii) If eq. (2.21) is confirmed experimentally, it will mean that $P_M \approx P_G$ is justified at the final instant.

3. – Comparison with experimental data.

As noted before, since the inductive resistance is much larger than the ohmic one in a high current pulsed discharge, we can use the current and voltage oscillograms to find the time dependence of the inductance of the

plasma column and hence determine how the radius of the column changes at various stages of the process. By this time, it has been confirmed experimentally that such a method of analysis gives results in fairly good agreement with other measurements, *e.g.*, the magnetic probes ([7]).

The oscillograms taken from references ([8-10]) were analysed about two

TABLE I. – *Dimensions of apparatus and initial conditions of the USSR experiments.*

Length of the cylindrical discharge tube (distance between electrodes)	$l = 100$ cm
Inner radius of the tube (initial radius of the plasma column)	$a_0 = 20$ cm
Radius of return circuit (assumed to be coaxial with the discharge tube)	$b = 23.5$ cm
Initially stored energy in condensor bank	$W_0 = 80$ kJ
Total capacitance	$C = 100$ μF
Initial voltage between electrodes	$V_0 = 40$ kV
Initial total inductance of the circuit	$L_0 = 0.25$ μF
Period of the discharge current	$\tau = 32$ μs
Total resistance of circuit except the tube	$R \leqslant 0.01$ Ω
Rate of current increase at the initial phase of the discharge	$(\mathrm{d}I/\mathrm{d}t)_0 = 1.6 \cdot 10^{11}$ A/s
Enclosed gas	deuterium
Initial gas pressure: Experiment *A*	$p_0 = 0.05$ mm Hg
Experiment *B*	$p_0 = 0.2$ mm Hg

TABLE II. – *Results of the analysis.*

	Exp. *A*	Exp. *B*
Time of the first maximum contraction (t_f)	$4 \cdot 10^{-6}$ s	$6 \cdot 10^{-6}$ s
Initially stored energy	80 kJ	80 kJ
Energy dissipation from condensor bank until t_f	28 kJ	54 kJ
Energy dissipation in the discharge tube	21 kJ	44 kJ
energy stored in magnetic field at $t_f(\frac{1}{2}LI^2)$	8 kJ	17 kJ
energy used for the contraction of plasma column until $t_f(W_M)$	13 kJ	27 kJ
Other loss of energy	7 kJ	10 kJ
Maximum temperature assuming $kT = W_M/3N$	$4 \cdot 10^6$ °K	$2 \cdot 10^6$ °K
$W_M/\frac{1}{2}\varrho_0\pi a_0^2 l v_f^2$	~ 6	~ 6
Radius of the plasma column at $t_f(a_f)$	2 cm	2 cm

([7]) A. M. ANDRIANOV *et al.*: *Proc. on the 2nd United Nations International Conference on the Peaceful Uses of Atomic Energy* (Geneva, 1958), p. 2301.

([8]) I. V. KURCHATOV: *Atomnaya Energiya*, **1**, 65 (1956).

([9]) L. A. ARTSIMOVIČ *et al.*: *Atomnaya Energiya*, **1**, 76 (1956).

([10]) S. YU. LUKYANOV and V. I. SINITSYN: *Atomnaya Energiya*, **1**, 88 (1956).

years ago. Table I shows our estimation of the dimensions of the apparatus and the initial conditions of those experiments. Since no detailed experimental conditions were stated on those oscillograms except for the initial voltage and the initial gas pressure, we had to assume these values as reasonably as possible from the several parts of [8-10]. Referring to papers published in the USSR afterwards, it seem that this table needs no particular correction.

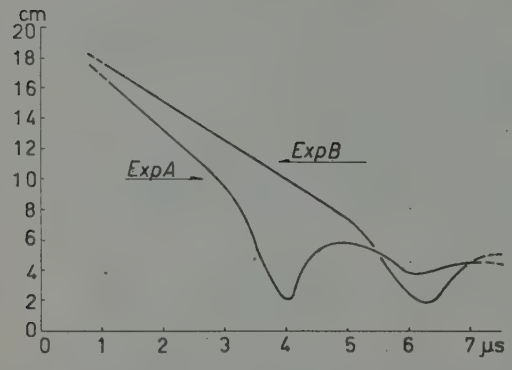

Fig. 1. – Variation of the plasma column radius with time for two experimental examples listed in Table I.

As a result of the analysis, the aspect of the change of the radius with time has been obtained (Fig. 1), and it was found that the final plasma radius is independent of the initial pressure, and the time of the first maximum contraction is proportional to (initial pressure)$^{\frac{1}{2}}$. The results for the energy transfer relation until the first maximum contraction is shown in Table II.

From the last row of Table II, we may say that eq. (2.21) is well satisfied in these two experiments. It is to be noted also that the energy transfer to the plasma, W_M, depends on the initial pressure as $p_0^{\frac{1}{2}}$, in agreement with eq. (2.12). (See also the Appendix).

4. – Concluding remarks.

In this paper, the attempt was made to analyse the fast contracting process in a high current gas discharge phenomenologically, as independently as possible of the concrete models of the contraction mechanism. Only the basic picture was assumed that the cylindrical plasma column having a well-defined radius is involved in the process as a whole, under the action of the self-magnetic field of the discharge current. Summarizing our discussions, we should like to remark the following points:

1) It was tacitly assumed in Sections **2** and **3** that all the particles initially existing in the tube should be included inside the plasma column at any stages of the process. This assumption will be reasonable if the radius of the tube, a_0, is sufficiently large as compared with the ion-neutral collision mean free path, because only ion-neutral collisions will cause considerable momentum change of the neutrals and push them inward. Taking the ion-

neutral collision cross-section as $\sigma \sim 10^{-16}$ cm^2 the minimum density n_0 to satisfy the required condition is given by

$$1/n_0\sigma = a_0 .$$

Then for $a_0 \sim 20$ cm, $n_0 \sim 5 \cdot 10^{14}$ particles/cm^3, corresponding to the initial gas pressure $p_0 \sim 1 \cdot 10^{-2}$ mm Hg, and the examples analysed in Section 3 satisfy this condition.

2) It has been reported in some experiments ([7-11]) that there exists considerable initial time delay for the leaving of the discharge from the tube wall, and the calculation ([3]) is not yet completely successful in accounting for the time delay. But the delay time is short as compared with the total contracting time, and it has been verified that the time of the first maximum contraction is proportional to $(p_0/V_0^2)^{\frac{1}{2}}$ or $p_0/\dot{I}_0^2)^{\frac{1}{2}}$, and this will indicate that our basic picture of the contracting process mentioned before is certainly good. It should be noted, however, that this result is rather a model-independent one, and one cannot draw definite conclusions for or against a particular model from this result, only.

3) It was shown in Section 3 that the final plasma radius a_f is independent of the initial pressure p_0 in the case of the two examples analysed there. It has been shown also in other papers on the fast pinch experiments that a_f is constant for a given apparatus ([11,12]).

These results are consistent with our conclusion in Section 2 that a_f is independent of the initial gas pressure and the applied voltage. As our phenomenological analysis of Section 2 indicates also that a_f depends only on l/L_0 and $\Psi(\varphi_f)$, the relation between a_f and $\Psi(\varphi_f)$ will be obtained by varying the initial parameter l/L_0 experimentally, and this in turn will serve to analyse the contraction mechanism in greater detail. What is actually required is to follow the time dependence of the column radius carefully with various values of l/L_0 as well as p_0 and V_0.

* * *

The authors wish to thank Professor G. Tominaga for first suggesting the analysis of the Soviet pinch data, and to the members of the Nuclear Fusion Group of Nihon University for helpful discussions.

([11]) V. S. Komel'kov: *Žurn. Éxp. Teor. Fiz.*, **35**, 16 (1958).

([12]) N. A. Borzunov, D. V. Orlinskij and S. M. Osovets: *Atomnaya Energija*, **4**, 149 (1958).

Appendix

Dimensional considerations.

With our basic picture mentioned in the text, the motion of the contracting plasma column will be governed by the following three parameters (C.G.S. electromagnetic units are used for I and B):

(i) the mass per unit length of the discharge tube:

$$\pi\varrho_0 a_0^2 = [\mathrm{M/L}]\,; \tag{A.1}$$

(ii) the radius of the tube:

$$a_0 = [\mathrm{L}]\,; \tag{A.2}$$

(iii) the rate of current increase:

$$\dot{I} = [\mathrm{L}^{\frac{1}{2}}\mathrm{M}^{\frac{1}{2}}\,\mathrm{T}^{-2}]\,, \tag{A.3}$$

or the rate of increase of the magnetic field

$$\dot{B} = [\mathrm{L}^{-\frac{1}{2}}\mathrm{M}^{\frac{1}{2}}\,\mathrm{T}^{-2}]\,, \tag{A.3'}$$

where the symbols M, L and T in the brackets indicate the dimensions of mass, length, and time, respectively. The only quantity having the dimension of time made from combinations of eqs.. (A.1)-(A.3) is

$$t_1 = [\mathrm{M/L}]^{\frac{1}{4}}[\mathrm{L}]^{\frac{1}{2}}\dot{I}^{-\frac{1}{2}}\,. \tag{A.4}$$

Therefore,

$$t_1 = (\pi\varrho_0)^{\frac{1}{4}} a_0 \dot{I}^{-\frac{1}{2}} \approx (\text{several})\cdot 10^{-6} n_0^{\frac{1}{2}} a_0 \dot{I}^{-\frac{1}{2}}\ \mathrm{s}\,, \qquad (\dot{I}\ \text{in e.m. units}), \tag{A.5}$$

where $n_0 = \varrho_0/m$ is the initial number density, and the value of the particle mass $m \approx (\text{several})\cdot 10^{-24}$ g was substituted. Eq. (A.5) means the characteristic time of the contraction process under consideration and it can be verified that it gives the right order of magnitude of the contraction time, t_f.

The mean contraction velocity, $\bar{v}$, is given by

$$\bar{v} = a_0/t_1 \approx (mn_0)^{-\frac{1}{4}} I^{\frac{1}{2}}\,, \tag{A.6}$$

which will be of comparable order with the final contraction velocity, v_f.

Then the kinetic energy of an individual ion is

$$\text{(A.7)} \qquad \tfrac{1}{2}m\bar{v}^2 \approx \tfrac{1}{2}m^{\frac{1}{2}}n_0^{-\frac{1}{2}}\dot{I} \approx 10^{-20}n_0^{-\frac{1}{2}}\dot{I} \quad \text{J} \quad (\dot{I}\text{: in e.m.u.}),$$

$$\approx 10^{-1}\, n_0^{-\frac{1}{2}}\dot{I}_A, \quad \text{eV}, \quad (\dot{I}_A\text{: in A/s}),$$

and the total energy used for the compression is

$$\text{(A.8)} \qquad W \approx (\text{volume of the discharge tube})\cdot\tfrac{1}{2}mn_0\bar{v}^2,$$

$$\approx (\text{volume})\cdot 10^{-23}n_0^{-\frac{1}{2}}I_A \quad \text{kJ}.$$

Referring to the values of Table I (volume $\approx 10^5$ cm^3, $\dot{I}_A = 1.6\cdot 10^{11}$, and $n_0 = 2\cdot 10^{15}$ cm^{-3} (for A) and $7\cdot 10^{15}$ cm^{-3} (for B)), it can be seen that eq. (A.8) gives just the nice order of magnitude of W_M, listed in Table II. The dependence of W_M on n_0 (or p_0) is confirmed rather well.

A very analogous consideration would be applicable to other types of the contraction process, as far as our basic picture is guaranteed. As an example, we shall take the case of the « induced-pinch », in which the discharge will be developed by the inductive effect of the axial magnetic field produced by the external coils wound around the discharge tube. (Only the radial compression is considered). In this case $\dot{I}$ of eq. (A.3) should be replaced by $\dot{B}$, (A.3′), and the result corresponding to (A.4) and (A.5) is

$$\text{(A.9)}\ (^*) \qquad \begin{cases} t_1 = [\mathrm{M/L}]^{\frac{1}{4}}\dot{B}^{-\frac{1}{2}} = \varrho_0^{\frac{1}{4}}a_0^{\frac{1}{2}}(\dot{B})^{-\frac{1}{2}}, \\ \quad \approx (\text{several})\cdot 10^{-6}(a_0^{\frac{1}{2}}n_0^{\frac{1}{2}}\dot{B}^{-\frac{1}{2}}) \quad \text{s}, \qquad (\dot{B}\text{: in G/s}), \end{cases}$$

and similar relations as eqs. (A.6)-(A.8) are readily obtained. At present, however, it is still to be confirmed experimentally if and/or under what conditions our basic picture of the contraction process could be applied to this type of discharge.

(*) Eq. (A.5) may be reproduced by putting $\dot{B} = 2\dot{I}/a_0$ in (A.9).

RIASSUNTO (*)

Si presenta l'analisi fenomenologica dell'effetto di contrazione veloce e la si confronta con alcuni dati sperimentali già acquisiti. Si arguisce che parecchi risultati coerenti con gli esperimenti si possono dedurre da una rappresentazione fondamentale del processo di contrazione veloce indipendentemente dal suo meccanismo dettagliato. Allo scopo di stabilire un modello coerente del meccanismo di contrazione, è quindi necessario ottenere informazioni sperimentali più dettagliate intorno al comportamento dinamico del plasma sotto condizioni sperimentali diverse. Si aggiungono nell'Appendice delle considerazioni dimensionali.

(*) *Traduzione a cura della Redazione.*

IL NUOVO CIMENTO Vol. XIV, N. 5 1° Dicembre 1959

On Some Phenomena Related to the Saturation of Rotational Resonances in the Microwave Spectrum of OCS.

A. Battaglia, A. Gozzini and E. Polacco

Istituto di Fisica dell'Università - Pisa

(ricevuto il 6 Agosto 1959)

Summary. — One experiment is described, which shows the interaction between two electromagnetic fields E_1 and E_2 propagating in a gas, their frequencies ν_1 and ν_2 being close to the frequencies $\nu_{J-1,J}$ and $\nu_{J,J+1}$ of two adiacent rotational resonances, and their intensity being sufficient to perturb appreciably the thermal equilibrium. The shape and the intensity of the line $J \to J+1$ is modified by the presence of the saturating field of frequency ν_1. Moreover a new resonance is observed, at a frequency $(E_{J+1} - E_{J-1})/h - \nu_1$. This is interpreted as a two quantum effect, *i.e.* as a transition between the $J-1$ and the $J+1$ levels produced by simultaneous absorption of a photon of frequency ν_1 and a photon of frequency ν_2.

1. – Introduction.

Interaction effects between two electromagnetic fields can be observed everywhere two fields propagate in a medium, whose dielectric properties for one of the waves are appreciably modified by the presence of the other.

In a gas, at low pressure, the population of two rotational states J, $J+1$ is perturbed by the presence of intense microwave radiation of the resonant frequency $\nu_{J,J+1}$. Consequently the refractive index and the absorption coefficient of the gas must change at frequencies close the frequencies $\nu_{J-1,J}$ and $\nu_{J+1,J+2}$ of the other transitions involving the perturbed states.

To study this effect we have examined how the absorption of OCS at frequencies near the resonance between the $J=2$ and $J=3$ states is modified by the saturation of the $J=1$-2 line. We found that the shape, intensity and resonant frequency of the $J=2$-3 line is changed by the presence of a field saturating the $J=1$-2 resonance. Moreover we found an additional resonant absorption when the sum of the frequencies of the two applied fields satisfies the Bohr relation between the $J=1$ and $J=3$ states.

2. – Experimental.

The absorption cell of a video spectrometer containing OCS at low pressure is fed by two klystrons, oscillating at the frequencies ν_1 and ν_2 close to 24 325 MHz and 36 490 MHz respectively. At these frequencies the gas absorbs for transitions between the $J = 1$, $J = 2$ and $J = 2$, $J = 3$ rotational levels of the ground vibrational state $v = 0$.

The two klystrons are frequency modulated, their frequency varying periodically with time; during each period the dependence on time is respectively:

$$\nu_1 = \nu_{12} + k_1 \left(t - \frac{T}{2} + \tau \right),$$

$$\nu_2 = \nu_{23} + k_2 \left(t - \frac{T}{2} \right),$$

where ν_{12} and ν_{23} are the frequencies of the $J = 1$-2 and $J = 2$-3 resonances, T is the period of the modulation, k_1 and k_2 the modulation velocities. By varying the polarization of the klystron reflector, a delay τ can be introduced between the times of the passages of the two frequencies through the resonances ν_{12} and ν_{23}.

The crystal holder is made from a rectangular wave guide cut off for the lower frequency ν_1 and is connected to the end of the absorption cell through a tapered transition, so that only the power of the higher frequency wave ν_2 is detected.

The $J = 2$-3 absorption line is displayed on the trace of a dual beam oscilloscope, whereas the resonance signal of a transmission cavity, tuned to the frequency ν_{12} is displayed on the other trace.

This allows an accurate determination of the value of τ.

The modulation velocities k_1 and k_2 are measured by means of frequency markers.

The maximum power of the ν_1 wave is 30 mW, sufficient to produce appreciable saturation of the $J = 1$-2 line; the power of the other wave is of the order of magnitude of 10^{-4} W.

3. – Results.

For pressures $p > 200$ μHg no observable effect is produced on the absorption of the field E_2 of frequency ν_2 by the presence of the field E_1 of frequency ν_1.

At lower pressures the shape and intensity of the $J = 2$-3 line is modified by the saturating field E_1 and the following phenomena are observed:

a) A new absorption line appears. The frequency and intensity of this line depends upon the value of the parameter τ that characterises the modulation of the ν_1 wave. The line appears on the sweep delayed by $-\tau(k_1/(k_1+k_2))$ from the main line at the frequency ν_{23} (Fig. 1,*a*).

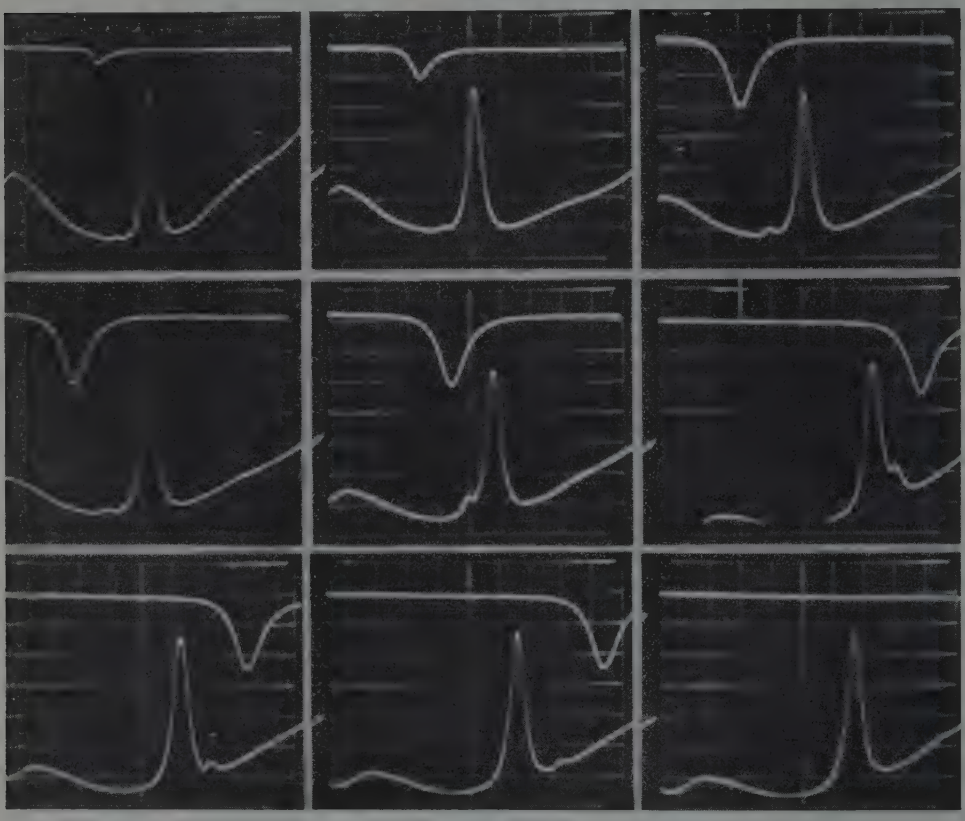

Fig. 1. – The oscillograms shows the dependence of the frequency ν_{2i} of the interaction from the frequency of the perturbing field E_1. In the upper traces is the resonance signal at the freguency ν_{2i} and the normal line at the freguency ν_{23}. In the lower traces is the resonance signal of a high Q cavity tuned at the frequency ν_{12} of the $J=1 \rightarrow 2$ line. For both the traces, one division corresponds to a frequency range of 1.1 MHz ($k_1=k_2=550$ MHz). The gas pressure is 85 μm Hg and the pictures correspond to several values of $\delta\nu = \nu_{2i} - \nu_{23}$. The oscillograms *b*) are at the same value of $\delta\nu$ but at three different powers of the perturbing field E_1, showing the dependence of α_i upon the intensity of the E_1 field.

Therefore the frequencies ν_{2i} and ν_{1i} of the two fields when this resonance occurs satisfy the relation

$$\nu_{1i} + \nu_{2i} = \nu_{12} + \nu_{23} .$$

The extra resonance occurs when the sum of the frequencies of the two fields equals the sum of the two resonant frequencies (*).

Fig. 2. – The lower frequency klystron is alternatively on during a period of the modulation and off during the following period so that the absorption curves in presence and absence of the perturbing field E_1 are superimposed, showing the effect of the E_1 field on the absorption of the ν_2 wave. The oscillograms are taken for several values of $\delta\nu$ at the pressures of 100 (*a*), 65 (*b*) and 40 μm Hg (*c*).

(*) The theory given by Di Giacomo (see following paper), predicts that the maximum of the new resonant absorption occurs when the sum of the two frequencies is very close, but not exactly equal to the sum of the resonant frequencies.

This has been confirmed by further more accurate measurements.

The intensity α_i of the new resonance depends upon the pressure and decreases with the absolute value of $\delta\nu = \nu_{2i} - \nu_{23}$.

At a given pressure, α_i does not depend upon the intensity I_2 of the absorbed wave of frequency ν_2 and, within the limits of the experimental accuracy, is proportional to the intensity I_1 of the saturating field E_1 (Fig. 1,*b*).

The width of the extra resonance depends upon the modulation velocities, resulting proportional to $k_2/(k_1+k_2)$. Therefore the maximum width is obtained when the ν_1 wave is not modulated.

This maximum width is smaller then the width of the normal line.

b) The normal absorption line at the frequency ν_{23} is broadened by the field E_1. The absorption is increased in the wings and decreased at the center of the line (Fig. 2).

This effect strongly depends upon the pressure and the absolute value of $\delta\nu$ and reaches its maximum when $\delta\nu = 0$ $(\nu_{2i} = \nu_{23})$.

When $\nu_{2i} \neq \nu_{23}$ the frequency of the maximum absorption ν_{max} is different from ν_{23}.

Corresponding to $\delta\nu \gtreqless 0$ we have $\nu_{max} \lesseqgtr \nu_{23}$.

However this shift of the resonance frequency is too small to allow quantitative measurements.

4. – Conclusion.

Multiple quantum transitions have been observed by several authors, in connection with molecular beams (1) experiments and magnetic resonance experiments in optically oriented atoms (2), in atomic oxigen (3) and in Mn^{++} (4).

In these experiments new lines at the frequencies $(E_{M+2} - E_M)/2h$ are observed, when the applied radiofrequency field is strong.

These are interpreted as double quantum transitions $(\Delta M = 2)$ that occur between nearly equally spaced levels, by simultaneous absorption of two photons, whose frequency is equal to half of the Bohr frequency for the transition $\Delta M = 2$.

Theoretical work has been done on this subject of multiple quantum transitions, showing that the effect occurs through one (or more) intermediate states at high radiofrequency power (5).

---

(1) V. HUGHES and L. GRABNER: *Phys. Rev.*, **79**, 314 (1950); P. KUSCH: *Phys. Rev.*, **93**, 1022 (1954).

(2) J. BROSSEL, B. CAGNAC and A. KASTLER: *Journ. Phys. et Rad.*, **15**, 6 (1954).

(3) V. HUGHES and J. GEIGHER: *Phys. Rev.*, **99**, 1842 (1955).

(4) P. SOROKIN, L. GELLES and W. SMITH: *Phys. Rev.*, **112**, 1513 (1958).

(5) C. BESSET, J. HOROWITZ, A. MESSIAH and J. WINTER: *Journ. Phys. et Rad.*, **15**, 251 (1954).

In conventional microwave spectroscopy involving, transitions between different rotational states of a molecule, this effect, with only one field, does not occur because the separations of the rotational adjacent levels differ by a large factor. Nevertheless double quantum transitions occur if two different frequencies are applied, provided their sum equal the Bohr frequency for the double transition and each frequency is close to that of the normal transition (6). The line observed in our experiment is the contribution of the E_2 field to the process involving transitions of the molecule between the $J=1$ to the $J=3$ states. This and the other main features of this experiment are explained by the theoretical work of DI GIACOMO (6), where the absorption and dispersion of the gas, at the two frequencies applied and in the experimental conditions described, are calculated. The agreement of the experimental and theoretical results is good, in the limits of the experimental accuracy.

* * *

We wish to thank Professors A. KASTLER and C, TOWNES for many helpful discussions.

(6) A. DI GIACOMO: *Nuovo Cimento*, **14**, 1082 (1959).

RIASSUNTO

Si è studiata la interazione fra due onde elettromagnetiche propagantisi in un gas che presenta due risonanze rotazionali contigue a frequenze prossime a quelle ν_1 e ν_2 delle due onde. La presenza di radiazione di frequenza prossima a quella della risonanza fra due livelli rotazionali $J-1$, J, e di intensità sufficiente a perturbare apprezzabilmente l'equilibrio termico fra le popolazioni dei due livelli, modifica la forma della riga di assorbimento prodotta da transizioni fra i livelli contigui $J, J+1$. Si è osservata inoltre una nuova risonanza alla frequenza $(E_{J+1}-E_{J-1})/h-\nu_1$. Questa è prodotta da transizioni dirette fra i livelli $J-1$, $J+1$, per assorbimento contemporaneo di due fotoni, uno per ciascuna frequenza.

IL NUOVO CIMENTO Vol. XIV, N. 5 1° Dicembre 1959

On some Phenomena Related to the Saturation of Rotational Resonances.

A. Di Giacomo

Istituto di Fisica dell'Università - Pisa
Istituto Nazionale di Fisica Nucleare - Sezione di Pisa

(ricevuto il 6 Agosto 1959)

Summary. — The statistical operator has been calculated for a gas with rotational levels, in the presence of two electromagnetic waves with frequencies in the neighbourhood of two contiguous resonances. The absorption coefficient has been determined for the two waves. The agreement with experiment is good.

1. – Introduction.

It has recently been shown by Gozzini and co-workers [1] that the shape and the intensity of a spectral line due to a transition between two rotational levels $\bar{J}$, $\bar{J}+1$ (transition 2 in Fig. 1), is modified by the presence of an electric field $\boldsymbol{E}_1$, whose frequency ω_1 lies in the neighbourhood of $\bar{\omega}_1$ (see Fig. 1), $\bar{\omega}_1$ being the resonance frequency of the transition $\bar{J}-1$, $\bar{J}$.

The modification depends upon the pressure and the intensity of the applied field E_1^0, which must be high enough to change appreciably the thermal distribution of the levels $\bar{J}-1$, $\bar{J}$.

It has also been shown that, besides the absorption at the frequency $\bar{\omega}_2 = (E_{\bar{J}+1} - E_{\bar{J}})/\hbar$, there is a resonant absorption corresponding to the frequency $\omega = \bar{\omega}_1 + \bar{\omega}_2 - \omega_1$.

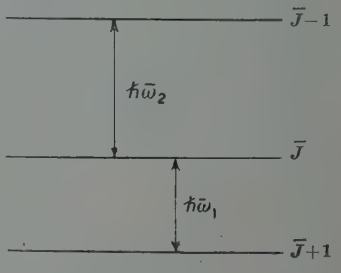

Fig. 1.

[1] A. Battaglia, A. Gozzini and E. Polacco: *Nuovo Cimento*, **14**, 1076 (1959).

We propose in this paper to show that the main features of this experiment can be understood on the basis of the theory of Karplus and Schwinger (2).

In particular we shall calculate the absorption coefficient

$$\alpha_2 = \frac{8\pi}{eE_2^{0^2}} N \boldsymbol{E}_2 \frac{\mathrm{d}}{\mathrm{d}t} \langle \boldsymbol{p} \rangle , \tag{1}$$

for the gas.

Here

$$\boldsymbol{E}_2 = \boldsymbol{E}_2^0 \cos \omega_2 t$$

is the electric field which induces the transition $\bar{J} \to \bar{J}+1$; N is the number of molecules per unit volume; $\langle \boldsymbol{p} \rangle$ is the average-electric dipole moment of the molecules; the bar means average with respect to time.

The average dipole moment $\langle \boldsymbol{p} \rangle$ can be calculated from the density operator ϱ which describes the system by the well known formula (3)

$$\langle \boldsymbol{p} \rangle = \mathrm{Tr}\{\boldsymbol{p}\varrho\} . \tag{2}$$

Our main task is therefore to calculate the density operator ϱ which describes a molecule of the gas in interaction with the other molecules and with the applied electric fields $\boldsymbol{E}_1$ and $\boldsymbol{E}_2$.

2. – Calculations.

Let us consider a gas whose molecules have a rotational spectrum such that at a given temperature T the first few excited levels are almost equally populated.

We shall indicate by H the total Hamiltonian for a molecule in interaction with the fields $\boldsymbol{E}_1$ and $\boldsymbol{E}_2$:

$$H = H_0 - H_1 \cos \omega_1 t - H_2 \cos \omega_2 t \equiv H_0 + H' , \tag{3}$$

where H_0 is the free Hamiltonian, and

$$H_1 = \boldsymbol{p}\boldsymbol{E}_1 , \qquad H_2 = \boldsymbol{p}\boldsymbol{E}_2 .$$

We shall as usual assume that:

---

(2) R. Karplus and J. Schwinger: *Phys. Rev.*, **73**, 1020 (1948).

(3) P. A. M. Dirac: *The Principles of Quantum Mechanics*, (Oxford) p. 130.

i) The pressure is so low that the average distance between two neighbouring molecules is large compared to the range of the molecular forces. The molecules can therefore be treated as free during the time interval between two collisions.

ii) The collision time is very short compared to the period of the incident wave. One can accordingly define the phase of the incident field at the time when the collision occurs.

iii) The collision is « strong », *i.e.* immediately after a collision at time t the statistical operator for the molecules which have collided is of the form

$$\varrho_0(t) = \exp[-H(t)/KT]/\mathrm{Tr}\,\{\exp[-H(t)/KT]\}\,.$$

Let τ be the average time between two collisions, and let $D(t)$ be the difference between $\varrho(t)$ and $\varrho_0(t)$.

It has been shown by KARPLUS and SCHWINGER [2] that under assumptions i), ii), iii), $D(t)$ satisfies the equation

$$\left(\frac{\partial}{\partial t}+\frac{1}{\tau}\right)D(t) = -\frac{i}{\hbar}[H(t), D(t)] - \frac{\partial \varrho_0(t)}{\partial t}\,. \tag{4}$$

We shall solve eq. (4) in a representation where H_0 (with eigenvalues E_J), and the z-component J_z of the angular momentum $\boldsymbol{J}$ are diagonal.

We shall assume the electric fields $\boldsymbol{E}_1$ and $\boldsymbol{E}_2$ to be polarized in the z-direction.

In all practical cases $H'_{JM,J'M'}/KT$ and $H'_{JM,J'M'}/(E_J - E_{J'})$ $(J \neq J')$ are small, of the order of $\hbar/\tau(E_J - E_{J'})$ $(J \neq J')$.

We can according solve eq. (4) by expanding $\partial\varrho_0/\partial t$ in a power series and keeping only first order terms in H'. The result is [2]

$$\left[\frac{\partial \varrho_0}{\partial t}\right]_{JM,J'M'} = \frac{\exp[-E_J/KT] - \exp[-E_{J'}/KT]}{\mathrm{Tr}\,\{\exp[-H_0/KT]\}}\,\frac{p^z_{JM,J'M'}}{E_J - E_{J'}}\cdot$$
$$\cdot\{\omega_1 E_1^0 \sin\omega_1 t + \omega_2 E_2^0 \sin\omega_2 t\} \equiv A_{JM,J'M'}\{\omega_1 E_1^0 \sin\omega_1 t + \omega_2 E_2^0 \sin\omega_2 t\}\,.$$

Inserting this expansion into (4) one gets

$$\left(\frac{\partial}{\partial t}+\frac{1}{\tau}\right)D = -\frac{i}{\hbar}[H, D] - A\{\omega_1 E_1^0 \sin\omega_1 t + \omega_2 E_2^0 \sin\omega_2 t\}\,, \tag{5}$$

or

$$\left(\frac{\partial}{\partial t}+i\omega_{JJ'}+\frac{1}{\tau}\right)D_{JM,J'M'} = \frac{i}{\hbar}[p^z, D]_{JM,J'M'}\{E_1^0 \cos\omega_1 t + E_2^0 \cos\omega_2 t\} -$$
$$- A_{JM,J'M'}\{\omega_1 E_1^0 \sin\omega_1 t + \omega_2 E_2^0 \sin\omega_2 t\}\,, \tag{5'}$$

where

$$\omega_{JJ'} = \frac{E_J - E_{J'}}{\hbar} .$$

A stationary solution of eq. (5) must necessarily be of the form

$$D(t) = \sum_{\varrho\sigma=-\infty}^{+\infty} M^{\varrho\sigma} \exp\left[i\varrho\omega_1 t + i\sigma\omega_2 t\right], \tag{6}$$

where $M^{\varrho\sigma} = [M^{-\varrho-\sigma}]^+$ because of the hermiticity of D, and the $M^{\varrho\sigma}$'s are time independent. The operators $M^{\varrho\sigma}$ correspond to processes which involve absorption or emission of $|\varrho|$ photons with frequency ω_1 and $|\sigma|$ photons with frequency ω_2. Absorption processes correspond to $\varrho, \sigma > 0$, emission processes to $\varrho, \sigma < 0$. From (5) and (6) it follows

$$\left(i\varrho\omega_1 + i\sigma\omega_2 + \frac{1}{\tau}\right) M^{\varrho\sigma} = \frac{i}{2\hbar}\{[H_1, M^{\varrho+1,\sigma} + M^{\varrho-1,\sigma}] + [H_2, M^{\varrho,\sigma+1} + M^{\varrho,\sigma-1}]\} - \tag{7}$$

$$- \frac{i}{\hbar}[H_0, M^{\varrho\sigma}] + \frac{A}{2i}\{\omega_1 E_1^0(\delta_{\varrho,-1}\delta_{\sigma,0} - \delta_{\varrho,1}\delta_{\sigma,0}) + \omega_2 E_2^0(\delta_{\varrho,0}\delta_{\sigma,-1} - \delta_{\varrho,0}\delta_{\sigma,1})\} .$$

Equations (7) can be solved by iteration. If one neglects all the $M^{\varrho\sigma}$'s with $|\varrho| + |\sigma| > 1$, *i.e.* all terms which involve more than one photon, one obtains from (7)

$$\left(i\omega_1 + \frac{1}{\tau}\right) M^{10} = \frac{i}{2\hbar}[H_1, M^{00}] - \frac{i}{\hbar}[H_0, M^{10}] - \frac{A}{2i}\omega_1 E_1^0 , \tag{7a'}$$

$$\left(i\omega_2 + \frac{1}{\tau}\right) M^{01} = \frac{i}{2\hbar}[H_2, M^{00}] - \frac{i}{\hbar}[H_0, M^{01}] - \frac{A}{2i}\omega_2 E_2^0 , \tag{7b'}$$

$$\frac{1}{\tau} M^{00} = \frac{i}{2\hbar}\{[H_1, M^{10} + M^{-10}] + [H_2, M^{01} + M^{0-1}]\} - \frac{i}{\hbar}[H_0, M^{00}] . \tag{7c'}$$

Solving (5′) gives the first order approximation, to M^{10}, M^{01}, M^{00}. Inserting these values into

$$\begin{cases} \left(2i\omega_1 + \frac{1}{\tau}\right) M^{20} = \frac{i}{2\hbar}[H_1, M^{10}] - \frac{i}{\hbar}[H_0, M^{20}] , \\ \left(2i\omega_2 + \frac{1}{\tau}\right) M^{02} = \frac{i}{2\hbar}[H_2, M^{02}] - \frac{i}{\hbar}[H_0, M^{02}] , \\ \left(i\omega_1 + i\omega_2 + \frac{1}{\tau}\right) M^{11} = \frac{i}{2\hbar}\{[H_1, M^{01}] + [H_2, M^{10}]\} - \frac{i}{\hbar}[H_0, M^{11}] , \\ \left(i\omega_1 - i\omega_2 + \frac{1}{\tau}\right) M^{1-1} = \frac{i}{2\hbar}\{[H_1, M^{0-1}] + [H_2, M^{10}]\} - \frac{i}{\hbar}[H_0, M^{1-1}] , \end{cases} \tag{7''}$$

(where all terms with $|\varrho| + |\sigma| > 2$ have been neglected), one gets a first order solution for M^{20}, M^{02}, M^{11}, M^{1-1}. These values can be used to deter-

mine from

$$(7''')\quad \begin{cases} \left(i\omega_1+\dfrac{1}{\tau}\right)M^{10}= \\ =\dfrac{i}{2\hbar}\{[H_1, M^{20}+M^{00}]+[H_2, M^{11}+M^{1-1}]\}-\dfrac{i}{\hbar}[H_0, M^{10}]-\dfrac{A}{2i}\omega_1 E_1^0, \\ \left(i\omega_2+\dfrac{1}{\tau}\right)M^{01}= \\ =\dfrac{i}{2\hbar}\{[H_1, M^{11}+M^{-11}]+[H_2, M^{00}+M^{02}]\}-\dfrac{i}{\hbar}[H_0, M^{01}]-\dfrac{A}{2i}\omega_2 E_2^0, \\ \dfrac{1}{\tau}M^{00}=\dfrac{i}{2\hbar}\{[H_1, M^{10}+M^{-10}]+[H_2, M^{01}+M^{0-1}]\}-\dfrac{i}{\hbar}[H_0, M^{00}], \end{cases}$$

a second order approximation to M^{10}, M^{01}, M^{00}.

The procedure can be continued.

The convergence of this method depends upon the nature of the energy spectrum of H_0.

We shall show in the Appendix that for the rotational levels the procedure does indeed converge, except when one of the transitions involves the ground level.

Using the results proved in the Appendix one gets from (7) a set of linear equations for the matrix elements of $M^{\varrho\sigma}$ in the JM representation (with neglect of terms of order H'/kT)

$$(8)\quad \begin{cases} \dfrac{1}{\tau}M^{00}_{\bar J-1M,\bar J-1M'}=\dfrac{iE_1^0}{2\hbar}(p^z_{\bar J-1M,\bar JM}M^{-10}_{\bar JM,\bar J-1M'}-M^{10}_{\bar J-1M,\bar JM}p^z_{\bar JM',\bar J-1M'}), \\ \dfrac{1}{\tau}M^{00}_{\bar JM,\bar JM'}=\dfrac{iE_1^0}{2\hbar}(p^z_{\bar JM,\bar J-1M}M^{10}_{\bar J-1M,\bar JM'}-M^{-10}_{\bar JM,\bar J-1M}p^z_{\bar J-1M',\bar JM'})+ \\ \qquad+\dfrac{iE_2^0}{2\hbar}(p^z_{\bar JM,\bar J+1M}M^{0-1}_{\bar J+1M,\bar JM'}-M^{01}_{\bar JM,\bar J+1M'}p^z_{\bar J+1M',\bar JM'}), \\ \dfrac{1}{\tau}M^{00}_{\bar J+1M,\bar J+1M'}=\dfrac{iE_2^0}{2\hbar}(p^z_{\bar J+1M,\bar JM}M^{01}_{\bar JM,\bar J+1M'}-M^{0-1}_{\bar J+1M,\bar JM'}p^z_{\bar JM',\bar J+1M'}), \\ \left(i\omega_1-i\bar\omega_1+\dfrac{1}{\tau}\right)M^{10}_{\bar J-1M,\bar JM'}=\dfrac{iE_1^0}{2\hbar}(p^z_{\bar J-1M,\bar JM}M^{00}_{\bar JM,\bar JM'}-M^{00}_{\bar J-1M,\bar J-1M'}p^z_{\bar J-1M',\bar JM'})- \\ \qquad-\dfrac{iE_2^0}{2\hbar}M^{11}_{\bar J-1M,\bar J+1M'}p^z_{\bar J+1M',\bar JM'}-\dfrac{A_{\bar J-1M,\bar JM}}{2i}\omega_1 E_0^1\delta_{MM'}, \\ \left(i\omega_2-i\bar\omega_2+\dfrac{1}{\tau}\right)M^{01}_{\bar JM,\bar J+1M'}=\dfrac{iE_2^0}{2\hbar}(p^z_{\bar JM,\bar J+1M}M^{00}_{\bar J+1M,\bar J+1M'}-M^{00}_{\bar JM,\bar JM'}p^z_{\bar JM',\bar J+1M'})+ \\ \qquad+\dfrac{iE_1^0}{2\hbar}p^z_{\bar JM,\bar J-1M}M^{11}_{\bar J-1M,\bar J+1M'}-\dfrac{1}{2i}A_{\bar JM,\bar J+1M}\omega_2 E_2^0\delta_{MM'}, \\ \left[i\omega_1+i\omega_2-i(\bar\omega_1+\bar\omega_2)+\dfrac{1}{\tau}\right]M^{11}_{\bar J-1M,\bar J+1M'}= \\ \qquad=\dfrac{iE_1^0}{2\hbar}p^z_{\bar J-1M,\bar JM}M^{01}_{\bar JM,J+1M'}-\dfrac{iE_2^0}{2\hbar}M^{10}_{\bar J-1M,\bar JM'}p^z_{\bar JM',\bar J+1M'}. \end{cases}$$

The solution of these equations is:

$$M^{\varrho\sigma}_{\bar{J}M,\bar{J}'M'} = M^{\varrho\sigma}_{\bar{J},\bar{J}'M}\delta_{MM'}\,,$$

(9)
$$M^{10}_{\bar{J}-1,\bar{J}M} = \frac{E_1^0\omega_1}{\Delta_M}\,\frac{\varrho^0_{\bar{J}-1}-\varrho^0_{\bar{J}}}{2\hbar\bar{\omega}_1}\,p^z_{\bar{J}-1,\bar{J}M}\left\{\left(\alpha+\frac{i}{\tau}\right)\left[(\alpha+\beta)^2+\frac{1}{\tau^2}+\gamma_M+\delta_M\right]\cdot\right.$$
$$\cdot\left[\beta^2+\frac{1}{\tau^2}+4\delta_M+\gamma_M\right]-\gamma_M\left(\alpha+\frac{i}{\tau}\right)(2\beta+\alpha)^2-\delta_M(2\alpha+\beta)\cdot$$
$$\left.\cdot\left[\beta^2+\frac{1}{\tau^2}+\gamma_M+4\delta_M\right]+3\gamma_M\delta_M(\alpha+2\beta)\right\}+$$
$$+\frac{E_1^0\omega_2}{\Delta_M}\,\frac{\varrho^0_{\bar{J}}-\varrho^0_{\bar{J}+1}}{2\hbar\bar{\omega}_2}\,p^z_{\bar{J}-1,\bar{J}M}\left\{\left(\alpha+\frac{i}{\tau}\right)3\delta_M\left[(\alpha+\beta)^2+\frac{1}{\tau^2}+\gamma_M+\delta_M\right]-\right.$$
$$-\left(\alpha+\frac{i}{\tau}\right)\delta_M(2\alpha+\beta)(2\beta+\alpha)+\delta_M(2\beta+\alpha)\cdot$$
$$\left.\cdot\left[\alpha^2+\frac{1}{\tau^2}+\delta_M+4\gamma_M\right]-3\delta_M^2(2\alpha+\beta)\right\},$$

where

$$\alpha = \omega_1-\omega_1\,,$$
$$\beta = \omega_2-\bar{\omega}_2\,,$$
$$\gamma_M = \frac{E_1^{02}\,|\,p^z_{\bar{J}-1,\bar{J}M}\,|^2}{4\hbar^2}\,,\qquad \delta_M = \frac{E_2^{02}\,|\,p^z_{\bar{J},\bar{J}+1\,M}\,|^2}{4\hbar^2}\,,$$
$$\delta^0_J = \frac{\exp\left[-E_J/KT\right]}{\mathrm{Tr}\left\{\exp\left[-H_0/KT\right]\right\}}\,,$$
$$\Delta_M = \left[\alpha^2+\frac{1}{\tau^2}+4\gamma_M+\delta_M\right]\left[\beta^2+\frac{1}{\tau^2}+4\delta_M+\gamma_M\right]\left[(\alpha+\beta)^2+\frac{1}{\tau^2}+\gamma_M+\delta_M\right]-$$
$$-\gamma_M(\alpha+2\beta)^2\left[\alpha^2+\frac{1}{\tau^2}+4\gamma_M+\delta_M\right]-\delta_M(2\alpha+\beta)^2\left[\beta^2+\frac{1}{\tau^2}+4\delta_M+\gamma_M\right]-$$
$$-9\gamma_M\delta_M\left[(\alpha+\beta)^2+\frac{1}{\tau^2}+\gamma_M+\delta_M\right]+6\gamma_M\delta_M(\alpha+2\beta)(\beta+2\alpha)\,.$$

One obtains $M^{01}_{\bar{J},\bar{J}+1M}$ from (9) by interchanging

(9′)
$$\alpha \rightleftarrows \beta\,,\qquad E_1^0 \rightleftarrows E_2^0\,,\qquad p^z_{\bar{J}-1,\bar{J}M} \rightleftarrows p^z_{\bar{J},\bar{J}+1M}\,,$$
$$\omega_1 \rightleftarrows \omega_2\,,\qquad \frac{\varrho^0_{\bar{J}-1}-\varrho^0_{\bar{J}}}{\omega_1} \rightleftarrows \frac{\varrho^0_{\bar{J}}-\varrho^0_{\bar{J}+1}}{\bar{\omega}_2}\,.$$

The result for the diagonal matrix elements, M^{00}_{JM}, (which represent the time average of the change of the population of the state JM, due to the electromagnetic waves) is

$$M^{00}_{\bar J+1M,\bar J+1M} = \frac{\delta_M}{\Delta_M}\left[\frac{\varrho^0_{\bar J}-\varrho^0_{\bar J+1}}{\bar\omega_2}\,\omega_2\left\{\delta_M(2\alpha+\beta)^2-\left[(\alpha+\beta)^2+\frac{1}{\tau^2}+\gamma_M+\delta_M\right]\cdot\right.\right.$$
$$\left.\cdot\left[\alpha^2+\frac{1}{\tau^2}+4\gamma_M+\delta_M\right]\right\}+\frac{\varrho^0_{\bar J-1}-\varrho^0_{\bar J}}{\hbar\bar\omega_1}\,\omega_1\left\{-\left[(\alpha+\beta)^2+\frac{1}{\tau^2}+\gamma_M+\delta_M\right]3\gamma_M+\right.$$
$$\left.\left.+\gamma_M(2\alpha+\beta)(2\beta+\alpha)\right\}\right],$$

$$M^{00}_{\bar J-1M,\bar J-1M} = \frac{\gamma_M}{\Delta_M}\left[\frac{\varrho^0_{\bar J-1}-\varrho^0_{\bar J}}{\bar\omega_1}\,\omega_1\left\{\left[(\alpha+\beta)^2+\frac{1}{\tau^2}+\gamma_M+\delta_M\right]\left[\beta^2+\frac{1}{\tau^2}+4\delta_M+\gamma_M\right]-\right.\right.$$
$$\left.-\gamma_M(2\beta+\alpha)^2\right\}+\frac{\varrho^0_{\bar J}-\varrho^0_{\bar J+1}}{\hbar\omega_2}\,\omega_2\left\{3\delta_M\left[(\alpha+\beta)^2+\frac{1}{\tau^2}+\gamma_M+\delta_M\right]-\right.$$
$$\left.\left.-\delta_M(2\beta+\alpha)(2\alpha+\beta)\right\}\right],$$

$$M^{00}_{\bar J M,\bar J M} = -M^{00}_{\bar J-1M,\bar J-1M}-M^{00}_{\bar J+1M,\bar J+1M}\,.$$

Inserting these values for the M's into (6) one gets the statistical matrix ϱ from which the absorption coefficient can be calculated according to eq. (2) The final result is:

$$\alpha_2 = \sum_{M=-\bar J}^{+\bar J}\alpha^{(2)}_M = \sum_{M=-\bar J}^{+\bar J}\frac{4\pi}{c}\,N\,\frac{|p^z_{\bar J,\bar J+1M}|^2}{\Delta_M}\,\omega_2\,\frac{1}{\tau}\cdot$$
$$\cdot\left[\frac{\varrho^0_{\bar J-1}-\varrho^0_{\bar J}}{\hbar\omega_1}\,\omega_1\gamma_M\left\{3\left[(\alpha+\beta)^2+\frac{1}{\tau^2}+\gamma_M+\delta_M\right]-(2\alpha+\beta)(2\beta+\alpha)\right\}+\right.$$
$$\left.+\frac{\varrho^0_{\bar J}-\varrho^0_{\bar J+1}}{\hbar\bar\omega_2}\,\omega_2\left\{\left[(\alpha+\beta)^2+\frac{1}{\tau^2}+\gamma_M+\delta_M\right]\left[\alpha^2+\frac{1}{\tau^2}+4\gamma_M+\delta_M\right]-\delta_M(2\alpha+\beta)^2\right\}\right].$$

The absorption coefficient for the wave $\boldsymbol{E}_1$ is obtained from (10) by the interchanges (9′).

3. – Discussion.

Equation (10) can be easily compared with the experimental results that Gozzini and coworkers obtained for OCS at room temperature. The two transitions involved in that experiment are $J=1\to J=2$ ($\bar\omega_1=2\pi$ 24 325 MHz), $J=2\to J=3$, ($\bar\omega_2=2\pi$ 36 489.25 MHz).

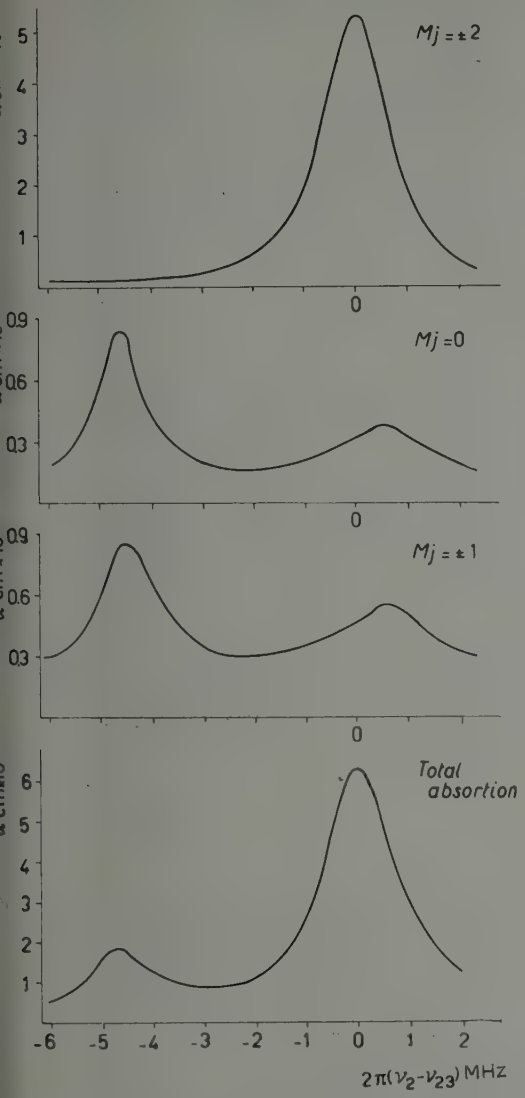

Fig. 2. – Calculated absorption at the frequency ω_2 in the case that the frequency ω_1 of the $\overline{E}_1$ field has a fixed value $\omega_1 = 2\pi\nu_1 = \overline{\omega}_1 - 4$ MHz. The OCS pressure is 65 μ Hg, the power of the $\overline{E}_1$ and $\overline{E}_2$ fields are 30 and 1 mW respectively and the fields propagate in a waveguide of 0.4 cm² cross-section.

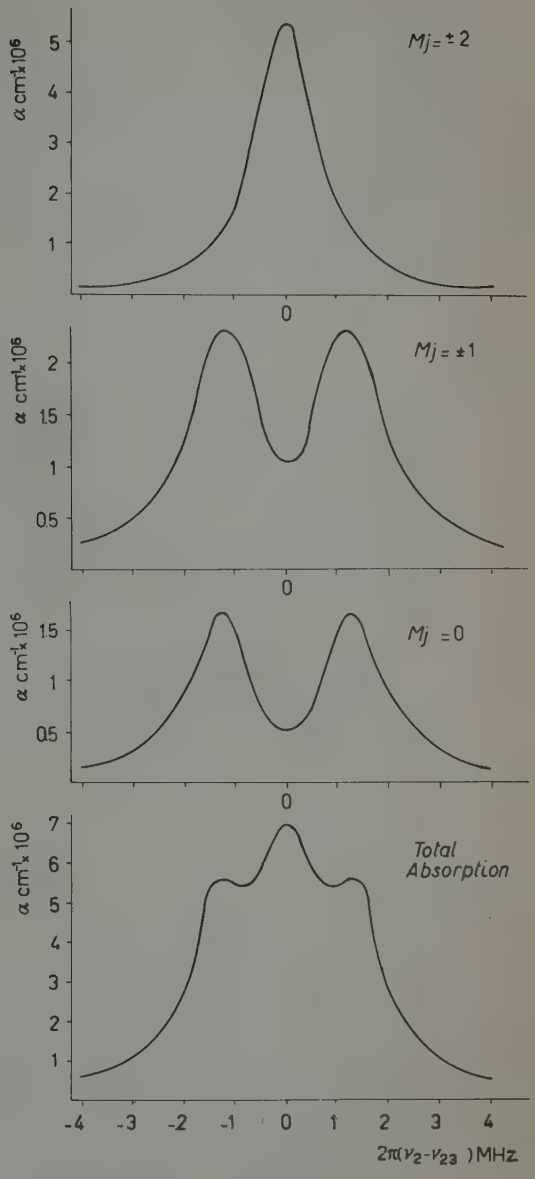

Fig. 3. – Same that in Fig. 2 in the case that the frequency of the $\overline{E}_1$ field is not the same for all the values of ω_2, but the frequencies are related so that $\omega_2 - \overline{\omega}_2 = \omega_1 - \overline{\omega}_1$.

The square modulus of the dipole moment matrix elements has been determined from the experimental data on the absorption of the two lines at low intensities, by means of the van Vleck formula (4).

In Figs. 2 and 3 are plotted the absorption coefficients $\alpha_M^{(2)}$ versus the frequency $\omega_2 - \overline{\omega}_2$ for values of the parameters appropriate to the experimental conditions.

The agreement between the experimental and the theoretical result is good. In particular it should be noted that the theory predicts correctly the resonant absorption at the frequency

$$\omega = \overline{\omega}_1 + \overline{\omega}_2 - \omega_1 .$$

This is essentially due to the terms M^{11}, M^{-1-1}, *i.e.* to those processes which involve the simultaneous absorption or emission of two photons. The theory also predicts a shift of the resonant frequency ω_2 due to the presence of the electric field $\boldsymbol{E}_1$.

This shift is very small and occurs in the opposite direction to the position of the extra resonance.

* * *

The author is indebited to Prof. A. Gozzini for having suggested the problem, and for many helpful discussions.

He whishes also to thank Prof. L. Radicati for his helpful assistance.

Appendix

It is easily seen that in the solution of the first order equations (7′) the only important matrix elements are:

a) The one photon matrix elements $M^{10}_{JM,J'M}$, $M^{01}_{J''M,J''M}$ for which $\omega_1 - \omega_{J'J} \simeq 0$ and $\omega_2 - \omega_{J''J'} \simeq 0$ (resonant matrix elements).

b) The diagonal matrix elements of M^{00} when the right hand side of the equations (7*c*′) which serve to determine them contains one of the resonant terms $M^{10}_{JM,J'M}$, $M^{01}_{JM,J'M}$. Similarly in the equations (7″) the two photon terms are not negligible only when the right hand side of the equations contains a resonant one photon term.

Let us now consider the equation analogous to (7″) for the three photon terms. We want to show that in our case there are no resonant three photon matrix elements depending upon two photon resonant matrix elements. The

(4) J. H. van Vleck and V. F. Weisskopf: *Rev. Mod. Phys.*, **17**, 227 (1945).

energy of a rotational level E_J with angular momentum J is $E_J = E_0 + J(J+1)B$. Therefore one has approximately

$$\omega_1 \simeq \frac{2\bar{J}B}{\hbar}, \qquad \omega_2 \simeq \frac{2(\bar{J}+1)B}{\hbar} \tag{A.1}$$

The condition for the matrix element $M^{\varrho\sigma}_{JM,J'M'}$ to resonate is

$$0 \simeq \varrho\omega_1 + \sigma\omega_2 + \omega_{JJ'}, \tag{A.2}$$

or from (A.1)

$$2\varrho\bar{J} + 2\sigma(\bar{J}+1) = J'(J'+1) - J(J+1). \tag{A.3}$$

Let us now make use of the selection rule for the operator $\boldsymbol{p}$,

$$\Delta J = 0 \pm 1.$$

This implies that the right hand side of the equation (7) which contains $M^{\varrho\sigma}_{JM,J'M'}$ in the left hand side, will contain a resonating matrix element only if one of the numbers

$$\begin{cases} 2(\varrho+1)\bar{J} + 2\sigma(\bar{J}+1), & 2\varrho\bar{J} + 2(\sigma+1)(\bar{J}+1), \\ 2(\varrho-1)\bar{J} + 2\sigma(\bar{J}+1), & 2\varrho\bar{J} + 2(\sigma-1)(\bar{J}+1), \end{cases} \tag{A.4}$$

is equal to one of the numbers

$$(J'+1)(J'+2) - J(J+1), \qquad J'(J'-1) - J(J+1),$$
$$J'(J'+1) - J(J+1), \quad J'(J'+1) - (J+1)(J+2), \quad J'(J'+1) - J(J-1).$$

The condition that also $M^{\varrho\sigma}_{JM,J'M'}$ be a resonant term is, from (A.2) and (A.4), that one of the numbers

$$J'(J'+1) - J(J+1) \begin{cases} +2\bar{J}, \\ -2\bar{J}, \\ +2(\bar{J}+1) \\ -2(\bar{J}+1), \end{cases}$$

equals one of the numbers

$$J'(J'+1) - J(J+1) \begin{cases} +2(J'+1) \\ -2J' \\ +2J \\ -2(J+1). \end{cases}$$

This can be satisfied only if

$$J' = \begin{cases} \bar{J}-1 \\ \bar{J} \\ \bar{J}+1\,, \end{cases} \qquad J = \begin{cases} \bar{J}-1 \\ \bar{J} \\ \bar{J}+1\,. \end{cases}$$

One can easily verify that the condition for $M^{\varrho\sigma}_{JM,J'M'}$ to resonate between two of the levels $\bar{J}-1$, $\bar{J}$, $\bar{J}+1$, implies that one of the numbers

$$\bar{J}(|\varrho|+|\sigma|)\pm\begin{cases} \bar{J} \\ \bar{J}+1 \\ 2\bar{J}+1\,, \end{cases}$$

is equal to

$$|\sigma|(2\bar{J}+1)\,, \tag{A.5}$$

if

$$|\varrho|+|\sigma|>2\,.$$

(A.5) cannot be satisfied by $|\varrho|+|\sigma|=3$ unless $J-1=0$. This proves our statement that in the equations for three-photon matrix elements analogous to eq. (7″), the resonant three-photon matrix elements do not depend upon resonating two-photon terms (if $J\neq 1$). The condition (A.5) also proves the convergence of the iteration procedure, since there are infinitely many values of $|\varrho|+|\sigma|$ for which (A.5) is not satisfied.

RIASSUNTO

Si è calcolato l'operatore statistico per un gas con livelli rotazionali, in presenza di due campi elettromagnetici di frequenze vicine a quelle di due risonanze contigue. Si è determinato il coefficiente di assorbimento per le due onde. L'accordo con l'esperienza è buono.

IL NUOVO CIMENTO Vol. XIV, N. 5 1º Dicembre 1959

Approximation of Velocity-Dependent Potentials by Separable Kernels.

Gy. Targonski (*)

CERN - Geneva

(ricevuto il 5 Settembre 1959)

Summary. — The Schrödinger equation for a two-nucleon problem with velocity-dependent forces contains an integral operator; the kernel of this might be approximated by a separable kernel, then the equation can be easily solved. A method to construct the best separable approximation is given; the goodness of which is expressed in a simple way with the eigenvalues. It turns out that a reasonable approximation is possible if the first eigenvalue of the kernel is non-degenerate and widely separated from the next one. The properties of the approximation remain unchanged in momentum space representation.

Introduction.

Assuming velocity-dependence (« non-locality ») of the nucleon-nucleon force, the Schrödinger equation for the two-nucleon problem is

$$\Delta\psi + [k^2 - U(r)]\psi + \Omega\psi = 0 \,. \tag{1}$$

Here purely central forces are assumed. Ω is an operator which arises through quantization from a classical potential energy term

$$V(\boldsymbol{r}, \boldsymbol{p}) \to V(\boldsymbol{r}, \text{grad}) \,.$$

The exact velocity-dependence, and therefore the exact form of Ω is not known; but Ω is obviously linear and also hermitian [1]. While Ω is unknown,

(*) Ford Research Fellow.

(1) S. Okubo and R. Marshak: *Ann. Phys.*, **4**, 166 (1958).

it is possible to write it in a standard form, *i.e.* as an integral transformation [2] with an hermitian kernel. (1) then takes the form:

$$\Delta\psi + [k^2 - U(r)]\psi + \int_0^\infty K(r, r')\psi(r')\,\mathrm{d}r' = 0 \,. \tag{2}$$

with

$$K(r, r') = K^*(r', r) \,.$$

$U(r)$ represents an ordinary velocity-independent (« local ») force. It is possible to include this term into the integral:

$$K'(r, r') = K(r, r') + \delta(r - r')U(r)$$

but such a step is purely formal and moreover destroys the continuity of the kernel, a property we want to use.

The equation (2) can be treated more easily if the kernel is « separable » [3]:

$$K(r, r') = h(r)\,h^*(r') \,. \tag{3}$$

The following questions (largely of academical interest only) arise:

1) how can one find, for a given $K(r, r')$, the best separable approximation

$$K(r, r') \approx h(r)\,h^*(r') \;?$$

2) How can one give a simple criterion for this best approximation to be also « good », so that it can be used as an approximation to the kernel in (2)?

3) What happens to this approximation if we go over to momentum space representation — the procedure usually applied? [3].

The aim of the present paper is to answer these there questions.

1. – Let be

$$\int_0^\infty\int_0^\infty K(r, r')K^*(r, r')\,\mathrm{d}r\,\mathrm{d}r' = K^2 < \infty \,, \tag{4}$$

---

[2] This fact is tacitly used and can be proven rigorously. See F. RIESZ and B. SZ.-NAGY: *Functional Analysis*, chap. V, no. 90.

[3] Y. YAMAGUCHI: *Phys. Rev.*, **95**, 1628 (1954); Y. YAMAGUCHI and Y. YAMAGUCHI: *Phys. Rev.*, **95**, 1635 (1954).

we want to find a function $h(r)$ such that

$$\int_0^\infty\int_0^\infty |K(r, r') - h(r)h(r')|^2 \,\mathrm{d}r\,\mathrm{d}r'$$

becomes a minimum; thus we define the « best » approximation in the sense of square deviation. It is well known from the theory of integral equations that $K(r, r')$ can be formally expanded into the—not necessarily convergent—series

$$K(r, r') = \sum_{n=1}^{\infty} \lambda_n U_n(r)\, U_n^*(r')\,; \qquad \int_0^\infty |U_n(r)|^2 \,\mathrm{d}r = 1\,, \tag{5}$$

here $U_n(r)$ and λ_n are determined by the eigenvalue equation

$$\int_0^\infty K(r, r')\, U^*(r')\,\mathrm{d}r' = \lambda U(r)\,. \tag{6}$$

The expansion (5) will converge in the sense of square deviation; if moreover the eigenvalues are all positive, or all negative, (5) will also converge in the strict sense. (Definite kernel.) The sequence $\{|\lambda_n|\}$ is bounded

$$|\lambda_1| \geqslant |\lambda_2| \geqslant \ldots \geqslant |\lambda_n| \geqslant \ldots \tag{7}$$

and if there is an infinity of different eigenvalues (non-degenerate kernel), then

$$\lambda_n \to 0\,. \tag{8}$$

To find the best separable approximation, we start from the relation valid for every $h(r)$

$$\left(\int_0^\infty h(r)h^*(r)\,\mathrm{d}r - \lambda_1\right)^2 \geqslant 0\,,$$

i.e.

$$\left[\int_0^\infty (h(r)h^*(r))\,\mathrm{d}r\right]^2 - 2\lambda_1 \int_0^\infty h(r)h^*(r)\,\mathrm{d}r \geqslant -\lambda_1^2\,, \tag{9}$$

the first term on the l.h.s. can be written as

$$\int_0^\infty\int_0^\infty h(r)h^*(r)\; h(r')h^*(r')\,\mathrm{d}r\,\mathrm{d}r'\,;$$

the second term can be replaced, without upsetting the inequality, by the algebraically larger term

$$-2\int_0^\infty\int_0^\infty K(r, r')h(r)h^*(r')\,\mathrm{d}r\,\mathrm{d}r';$$

this follows from the Ritz variation principle which states

$$\left|\int_0^\infty h(r)\left[\int_0^\infty K(r, r')h^*(r')\,\mathrm{d}r'\right]\mathrm{d}r\right| \leqslant \left|\lambda_1\int_0^\infty h(r)\,h^*(r)\,\mathrm{d}r\right|. \tag{10}$$

Carrying out these alterations, (9) can be written as

$$\int_0^\infty\int_0^\infty h(r)h^*(r)h(r')h^*(r')\,\mathrm{d}r\,\mathrm{d}r' - 2\int_0^\infty\int_0^\infty h(r)h^*(r')K(r, r')\,\mathrm{d}r\,\mathrm{d}r' \geqslant -\lambda_1^2. \tag{11}$$

From (6) it can be easily verified that

$$-\lambda_1^2 = -2\lambda_1\int_0^\infty\int_0^\infty K(r, r')\,U_1(r)\,U_1^*(r')\,\mathrm{d}r\,\mathrm{d}r' + \cdot$$
$$+\lambda_1^2\cdot\int_0^\infty\int_0^\infty U_1(r)\,U_1^*(r)\,U_1(r')\,U_1^*(r')\,\mathrm{d}r\,\mathrm{d}r'. \tag{12}$$

Finally we substitute $-\lambda_1^2$ from (12) into (11) and add

$$K^2 = \int_0^\infty\int_0^\infty K(r, r')K^*(r, r')\,\mathrm{d}r\,\mathrm{d}r'$$

to both sides; thus we obtain

$$\int_0^\infty\int_0^\infty |K(r, r') - h(r)h^*(r')|^2\,\mathrm{d}r\,\mathrm{d}r' \geqslant \int_0^\infty\int_0^\infty |K(r, r') - \lambda_1 U_1(r)\,U_1^*(r')|^2\,\mathrm{d}r\,\mathrm{d}r'. \tag{13}$$

Thus we have found the following result:

The best separable approximation is given by

$$h(r)\,h^*(r') = \lambda_1 U_1(r)\,U_1^*(r'): \tag{14}$$

here λ_1 is the eigenvalue with maximum modulus of $K(r, r')$ and $U_1(r)$ one of the corresponding eigenfunctions (4).

2. – The question now arises, how good this best approximation is. As a measure for this we introduce the ratio (see (4))

$$R_K = \frac{1}{K^2} \int_0^\infty \int_0^\infty | K(r, r') - \lambda_1 U_1(r) U_1^*(r') |^2 \, dr \, dr' . \tag{15}$$

The calculation yields, as an immediate consequence of (5)

$$R_K = \frac{\sum_{n=2}^{\infty} \lambda_n^2}{\sum_{n=1}^{\infty} \lambda_n^2} = 1 - \frac{\lambda_1^2}{\sum_{n=1}^{\infty} \lambda_n^2} . \tag{16}$$

Obviously R_K will be very small if $|\lambda_1|$ is very much larger (5) than the other eigenvalues.

From (16)

$$0 \leqslant R_K < 1 \tag{17}$$

follows. Thus we have two extreme cases: $R_K = 0$ implies $\lambda_2 = \lambda_3 = \ldots = 0$, *i.e.* if we have only one eigenvalue, the approximation becomes exact and (5) yields

$$K(r, r') = \lambda_1 U_1(r) U_1^*(r')$$

(strictly separable kernel). It is important to notice that in the sequence

$$|\lambda_1| \geqslant |\lambda_2| \geqslant |\lambda_3| \geqslant \ldots$$

each eigenvalue figures as often as its multiplicity indicates. Thus (18) implies also that λ_1 is a non-degenerate eigenvalue.

The other extreme case $R_K \approx 1$, occurs if the largest eigenvalues are closely spaced and particularly if the first eigenvalue has a degeneracy of high order.

(4) This result can be regarded as a special case of a general theorem of E. Schmidt. See *Math. Ann.*, **65**, 370 (1908).

(5) It must be noted that we call « largest » the eigenvalue with maximum modulus; in a physical situation the eigenvalues are bound states with negative energy and thus our largest eigenvalue will correspond to the ground level.

To summarize: *An hermitian kernel can be approximately factorized if its largest eigenvalue is non-degenerate and widely separated from the others; while a high order degeneracy of the largest eigenvalues makes such an approximate factorization impossible.*

A simple example is the approximate factorization of the real symmetric kernel

$$K(r, r') = \begin{cases} r + r' & \text{if} \quad 0 \leqslant r \leqslant 1, \quad 0 \leqslant r' \leqslant 1 \\ 0 & \text{otherwise} . \end{cases}$$

We have here

$$\lambda_1 = \frac{1}{2} + \frac{1}{\sqrt{3}}, \qquad U_1(r) = \frac{1 + \sqrt{3}\, r}{\sqrt{2 + \sqrt{3}}},$$

$$\lambda_2 = \frac{1}{2} - \frac{1}{\sqrt{3}}, \qquad U_2(r) = \frac{1 - \sqrt{3}\, r}{\sqrt{2 - \sqrt{3}}}.$$

There are no other eigenvalues. The best approximation is

$$K(r, r') \approx \frac{(\frac{1}{2} + 1/\sqrt{3})}{2 + \sqrt{3}} (1 + \sqrt{3}\, r)(1 + \sqrt{3}\, r') ,$$

with

$$R_K = \frac{(\frac{1}{2} - 1/\sqrt{3})^2}{(\frac{1}{2} + 1/\sqrt{3})^2 + (\frac{1}{2} - 1/\sqrt{3})^2} \approx 0.005 ,$$

a good approximation.

3. – If the assumed nucleon-nucleon force is purely non-local (6), *i.e.* in (2)

$$U(r) = 0 ,$$

it is of advantage to treat the problem in momentum space representation. Then the integro-differential equation (2) becomes the pure integral equation

$$(p^2 + k^2)\tilde{\psi} + \int_0^\infty \tilde{K}(p, p')\, \tilde{\psi}(p')\, \mathrm{d}p' = 0 . \tag{19}$$

If, moreover, $K(p, p')$ is approximated by a separable kernel, (19) can be solved at once (3).

(6) As pointed out in the introduction, this is formally always the case, but then we are forced to include a δ-function into the kernel, destroying its most useful properties.

The connection between co-ordinate and momentum space is given by

$$(20)\qquad \begin{cases} \tilde{\psi}(p) = \dfrac{1}{\sqrt{2\pi}} \displaystyle\int_0^\infty \exp[pri]\psi(r)\,\mathrm{d}r\,, \\ \psi(r) = \dfrac{1}{\sqrt{2\pi}} \displaystyle\int_0^\infty \exp[-pri]\tilde{\psi}(p)\,\mathrm{d}p\,. \end{cases}$$

We are going to show that the best separable approximation remains the best if we go over to momentum space and vice versa. Moreover the value of R_K remains unchanged.

Transforming (2) into momentum space (taking into account $U(r) = 0$), we have

$$(21)\qquad (p^2 + k^2)\tilde{\psi}(p) + \frac{1}{\sqrt{2\pi}} \int_0^\infty \int_0^\infty K(r, r') \exp[pri]\psi(r')\,\mathrm{d}r'\,\mathrm{d}r\,,$$

or, expressing $\psi(r')$ from (20)

$$(22)\qquad (p^2 + k^2)\tilde{\psi}(p) + \frac{1}{2\pi} \int_0^\infty \int_0^\infty \int_0^\infty K(r, r') \exp[pri - p'r'i]\tilde{\psi}(p')\,\mathrm{d}p'\,\mathrm{d}r'\,\mathrm{d}r\,.$$

Comparing with (19) we find

$$(23)\qquad \tilde{K}(p, p') = \int_0^\infty \int_0^\infty K(r, r') \exp[(pr - p'r')i]\,\mathrm{d}r\,\mathrm{d}r'\,.$$

(23) shows the following facts: Since $K(r, r')$ is hermitian, so is $K(p, p')$. If K is separable, $\tilde{K}$ is also separable. In particular, if

$$K(r, r') = h(r)\,h^*(r')$$

then

$$\tilde{K}(p, p') = h(p)\,h^*(p')$$

with

$$(24)\qquad \tilde{h}(p) = \frac{1}{\sqrt{2\pi}} \int_0^\infty h(r) \exp[pri]\,\mathrm{d}r\,.$$

We have to show that if $h(r)$ is a best separable approximation, the best similar approximation in momentum space is given by (24). Substituting (5) into (23), we have

$$\widetilde{K}(p, p') = \sum_{n=1}^{\infty} \frac{\lambda_n}{2\pi} \int_0^{\infty} U_n(r) \exp[pri]\,\mathrm{d}r \int_0^{\infty} U_n^*(r') \exp[-p'r'i]\,\mathrm{d}r' = \tag{25}$$

$$= \sum_{n=1}^{\infty} \lambda_n \widetilde{U}_n(p)\, \widetilde{U}_n^*(p') .$$

From this, the eigenvalue equation

$$\int_0^{\infty} K(p, p')\, \widetilde{U}_n^*(p')\,\mathrm{d}p' = \lambda_n \widetilde{U}_n(p) , \tag{26}$$

follows. $U_1(r)$ is the first eigenfunction of K and therefore $\lambda_1 U_1(r) U_1^*(r')$ the best separable approximation to K, (26) indicates that $\widetilde{U}_1(p)$ is the first eigenfunction of $\widetilde{K}$ and thus $\lambda_1 \widetilde{U}_1(p) \widetilde{U}_1^*(p')$ the best separable approximation to $\widetilde{K}$.

Finally (26) shows that the eigenvalues are not changed by transforming into momentum space. We can now define $R_{\widetilde{K}}$ in exact analogy to R_K (see (15)) and since both depend only on the—unchanged—eigenvalues, we have

$$R_K = R_{\widetilde{K}} .$$

With other words: the goodness of approximation is the same both in co-ordinate and in momentum space. The proof for a transformation from momentum space to co-ordinate space proceeds on exactly the same lines.

We conclude with the remark that all the statements are still true, if the kernel (and therefore the wave function) depends on $\boldsymbol{r}$ (and not on $|\boldsymbol{r}| = r$ only). The proofs remain exactly the same, but the integrations have to be understood over three variables. As pointed out earlier, the question of finding the best separable approximation to a given kernel is largely academical; besides, the best approximation to the kernel does not necessarily guarantee the best approximation to the wave function. It is therefore interesting to point to a well-known result of Chew (7) who derives from a Schwinger's variational principle results for the S-matrix corresponding to those described in this paper.

---

(7) G. F. Chew: *Phys. Rev.*, **93**, 341 (1954).

* * *

The author wishes to thank Professors C. J. BAKKER and M. FIERZ for hospitality during the Summer 1959 at the Theoretical Study Division, CERN, Geneva. A Ford Research Fellowship is also gratefully acknowledged.

RIASSUNTO (*)

L'equazione di Schrödinger per un problema di due nucleoni con forze dipendenti dalla velocità contiene un operatore integrale; il nocciolo di questo si può approssimare con un nocciolo separabile: in tal caso l'equazione può essere facilmente risolta. Per costruire la migliore approssimazione separabile, si mostra un metodo, la bontà del quale è espressa in maniera semplice con gli autovalori. Da ciò risulta che è possibile una approssimazione ragionevole se il primo autovalore del nocciolo è non degenere e largamente separato dal successivo. Le proprietà dell'approssimazione restano immutate nella rappresentazione nello spazio degli impulsi.

(*) *Traduzione a cura della Redazione.*

IL NUOVO CIMENTO Vol. XIV, N. 5 1° Dicembre 1959

A Remark on the Unitarity Property of the Scattering Operator.

T. Kato and S. T. Kuroda

Department of Physics, University of Tokyo - Tokyo

(ricevuto il 7 Settembre 1959)

Summary. — An example of a scattering system with the following properties is constructed: 1) the unperturbed Hamiltonian possesses no bound states, 2) the wave operators exist and 3) the scattering operator is not unitary.

In a previous paper (1), one of the authors considered the mathematical problem related to the wave and scattering operators. There the proof of the unitary property of the scattering operator required more stringent assumptions on the scattering potential than the one required for the existence of the wave operators. The purpose of the present note is to show that the existence of the wave operators does not in general imply the unitary property of the scattering operator. To this end we consider a *mathematical model* of the system of two particles moving in the one-dimensional space. There is no difficulty in replacing the one-dimensional space by the three-dimensional.

Let E_2 be the two-dimensional Euclidean space and $\mathfrak{H} = L^2(E_2)$ the Hilbert space consisting of all complex-valued absolutely square integrable functions defined on E_2 (2). We assume that the total Hamiltonian H of the system is given by

$$H = -\frac{\partial^2}{\partial x_1^2} - \frac{\partial^2}{\partial x_2^2} + V(x_2) + K\,, \tag{1}$$

(1) S. T. Kuroda: *Nuovo Cimento*, **12**, 431 (1959).

(2) Notations such as E_1, $L_2(E_1)$, $L^2(0, \infty)$ etc., will be used in a similar sense. For those notions in the theory of Hilbert space which are used in the following, see (1) and the literature cited in (1).

where the potential $V(x_2)$ for the second particle is a real-valued function such that $\int_{-\infty}^{\infty}|V(x)|\,\mathrm{d}x<\infty$ and $\int_{-\infty}^{\infty}|V(x)|^2\,\mathrm{d}x<\infty$. Moreover, we assume that the Hamiltonian of the second particle

$$H_{12}=-\frac{\mathrm{d}^2}{\mathrm{d}x_2^2}+V(x_2)\,,$$

considered as an operator in $L^2(E_1)$, has one and only one negative eigenvalue. (The square well potential with suitable width and depth provides such an example.) The interaction K is a self-adjoint integral operator of rank 1, that is, K has a kernel of the form $c\varphi(x_1, x_2)\overline{\varphi(\xi_1, \xi_2)}$, where φ is a fixed function of $\mathfrak{H}$ and c is a real number; thus we can write $Ku=c(u, \varphi)\varphi$. We set

$$H_0=-\frac{\partial^2}{\partial x_1^2}-\frac{\partial^2}{\partial x_2^2}\,,\qquad H_1=H_0+V(x_2)\,,$$

and regard H_0 as the unperturbed Hamiltonian (which is by no means unique). All the derivatives are taken in a generalized sense (*i.e.* in the sense of « strong derivatives »), so that H_0, H_1 and H are self-adjoint ([3]). Then we have the following result, to the verification of which the remainder of this note is devoted.

The wave operators $W_{\pm}(H, H_0)=s-\lim \exp[itH]\exp[-itH_0]$ *exist. If* K *is suitably chosen, however, the scattering operator* ([4]) $S=W_+(H, H_0)^* W_-(H, H_0)$ *is not unitary (or equivalently, the relation* $\mathfrak{R}(W_+(H, H_0))\neq\mathfrak{R}(W_-(H, H_0))$ *holds* ([5])).

It follows from the assumptions on $V(x_2)$ that the spectrum of H_{12} consists of one simple (*i.e.* non-degenerate) negative eigenvalue λ and a simple, absolutely continuous part extending from 0 to $+\infty$ ([6]). Furthermore, if we put $H_{02}=-\mathrm{d}^2/\mathrm{d}x_2^2$ (operating in $L^2(E_1)$), then $W_{\pm}(H_{12}, H_{02})$ exist and have a common range which consists of all functions of $L_2(E_1)$ orthogonal to the eigenfunction $u_0(x_2)$ of H_{12} corresponding to λ (see ([1]), Theorem 5.1). Let $\mathfrak{H}_1$ be a subspace of $\mathfrak{H}=L^2(E_2)$ consisting of all functions of the form $u(x_1)u_0(x_2)$,

---

([3]) T. Kato: *Trans. Amer. Math. Soc.*, **70**, 195 (1951).

([4]) It is doubtful from the physical point of view whether this S may be called the scattering operator, but our main interest lies in the mathematical fact stated here.

([5]) See ([1]). $\mathfrak{R}(A)$ denotes the range of an operator A.

([6]) Since H_{12} is an ordinary differential operator, this is a consequence of the theory of eigenfunction expansions. See, *e.g.*, ([7]), especially §§ 5.2 and 5.3.

([7]) E. C. Titchmarsh: *Eigenfunction Expansions Associated with Second-Order Differential Equations* (Oxford, 1946).

where $u(x_1)$ is an arbitrary function of $L^2(E_1)$. Then, on the basis of the fact mentioned above, we can conclude that

i) $\mathfrak{H}_1$ and $\mathfrak{H}_2 = \mathfrak{H} \ominus \mathfrak{H}_1$ reduce H_1. The part of H_1 in $\mathfrak{H}_1$ has a simple absolutely continuous spectrum extending from λ to $+\infty$ and that in $\mathfrak{H}_2$ has an infinitely degenerate absolutely continuous spectrum extending from 0 to $+\infty$.

ii) $W_\pm(H_1, H_0)$ exist and their ranges are identical with $\mathfrak{H}_2$ [8].

Since K is of rank 1, we see that $W_\pm(H, H_1)$ exist and have common range, so that $S_1 = W_+(H, H_1)^* W_-(H, H_1)$ is unitary. (See [1] or [9]. Note that H_1 is absolutely continuous.) Therefore, by the « transitivity » of $W_\pm$ (see [1], Theorem 3.2) we see that $W_\pm(H, H_0) = W_\pm(H, H_1) W_\pm(H_1, H_0)$ exist and that $S = W_+(H_1, H_0)^* W_+(H, H_1)^* W_- (H, H_1) W_-(H_1, H_0) = W_+(H_1, H_0)^* S_1 W_-(H_1, H_0)$. Since $\mathfrak{R}(W_\pm(H_1, H_0)) = \mathfrak{H}_2$, the last relation shows that S *is unitary if and only if*

$$S_1 \mathfrak{H}_2 = \mathfrak{H}_2 . \tag{2}$$

We shall now show that (2) is violated by a suitable choice of K. To this end we pick out subspaces $\mathfrak{M}_1$ and $\mathfrak{M}_2$ of $\mathfrak{H}_1$ and $\mathfrak{H}_2$, respectively, such that $\mathfrak{M}_1$ and $\mathfrak{M}_2$ reduce H_1 and the parts of H_1 in $\mathfrak{M}_1$ and $\mathfrak{M}_2$ have simple, absolutely continuous spectra extending from 0 to $+\infty$. (This is possible because of the property i) mentioned above. $\mathfrak{M}_1$ is uniquely determined by the above requirements.) Let $\varphi \in \mathfrak{M}_1 \oplus \mathfrak{M}_2 = \mathfrak{M}$ and define K by the formula $Ku = (u, \varphi)\varphi$. Since K is then equal to 0 in $\mathfrak{H} \ominus \mathfrak{M}$ and H_1 is reduced by $\mathfrak{M}$ and $\mathfrak{H} \ominus \mathfrak{M}$, it is easily seen that $W_\pm(H, H_1)$ and consequently S_1 are reduced by $\mathfrak{M}$ and $\mathfrak{H} \ominus \mathfrak{M}$ and that their parts in $\mathfrak{H} \ominus \mathfrak{M}$ are equal to the identity. Thus it is sufficient to consider the problem only in $\mathfrak{M}$ and to verify the relation $S_1 \mathfrak{M}_2 \neq \mathfrak{M}_2$, because $S_1 \mathfrak{M}_2 \neq \mathfrak{M}_2$ implies $S_1 \mathfrak{H}_2 = S_1 \mathfrak{M}_2 \oplus S_1(\mathfrak{H}_2 \ominus \mathfrak{M}_2) = S_1 \mathfrak{M}_2 \oplus (\mathfrak{H}_2 \ominus \mathfrak{M}_2) \neq \mathfrak{H}_2$.

Let now $\mathfrak{M}'$ be the Hilbert space consisting of all pairs $\{f_1(k), f_2(k)\}$ such that $f_1, f_2 \in L^2(0, \infty)$ with the inner product defined by $(\{f_1, f_2\}, \{g_1, g_2\}) = -(f_1, g_1) + (f_2, g_2)$, where $(f, g) = \int_0^\infty f(k)\overline{g(k)}\,dk$. Then every $u \in \mathfrak{M}$ can be represented by a vector of $\mathfrak{M}'$; more precisely, there exists a unitary transformation $u \to Uu = \{f_1(k), f_2(k)\}$ from $\mathfrak{M}$ onto $\mathfrak{M}'$ such that $f_2 = 0$ if and only if $u \in \mathfrak{M}_1$, $f_1 = 0$ if and only if $u \in \mathfrak{M}_2$ and $UH_1u = \{kf_1(k), kf_2(k)\}$ if $u \in \mathfrak{M} \cap \mathfrak{D}(H_1)$ ($\mathfrak{D}(A)$ denotes the domain of an operator A). In view of this unitary equivalence of $\mathfrak{M}$ and $\mathfrak{M}'$, we see that our problem is reduced to the following one:

---

[8] A mathematical proof of these facts, which is carried out by using the theory of the tensor product of Hilbert spaces, will be given in the Appendix.

[9] T. KATO: *Journ. Math. Soc. Japan*, **9**, 239 (1957).

Let H_1' be a multiplicative operator $H_1'\{f_1, f_2\} = \{kf_1, kf_2\}$ in $\mathfrak{M}'$ with the maximal domain, K' a self-adjoint operator in $\mathfrak{M}'$ with rank 1 and $H' = H_1' + K'$. Determine K' in such a way that $S_1'\mathfrak{M}_2' \neq \mathfrak{M}_2'$, where $\mathfrak{M}_2' = U\mathfrak{M}_2$ and $S_1' = W_+(H', H_1')^* W_-(H', H_1')$.

$\mathfrak{M}'$ is expressed as a direct sum $\mathfrak{M}' = \mathfrak{N}_1 \oplus \mathfrak{N}_2$, where $\mathfrak{N}_1$ and $\mathfrak{N}_2$ are subspaces of $\mathfrak{M}'$ consisting of all pairs such that $f_1(k) = f_2(k)$ and $f_1(k) = -f_2(k)$, respectively. Each $\{f_1, f_2\} \in \mathfrak{M}'$ is then expressed as

$$\text{(3)} \qquad \begin{cases} \{f_1, f_2\} = \{\hat{f}_1, \hat{f}_1\} + \{\hat{f}_2, -\hat{f}_2\}, \\ \text{where} \\ \hat{f}_1(k) = \tfrac{1}{2}\{f_1(k) + f_2(k)\} \quad \text{and} \quad \hat{f}_2(k) = \tfrac{1}{2}\{f_1(k) - f_2(k)\}. \end{cases}$$

Now put $\varphi = \{\psi(k), \psi(k)\}$, $\psi \in L^2(0, \infty)$ and $K'u = (u, \varphi)\varphi$, $u \in \mathfrak{M}'$. Since K' is then equal to 0 in $\mathfrak{N}_2$ and H_1' is reduced by $\mathfrak{N}_1$ and $\mathfrak{N}_2$, S_1' is reduced by $\mathfrak{N}_1$ and $\mathfrak{N}_2$ and its part in $\mathfrak{N}_2$ is equal to the identity. To determine the form of S_1' in $\mathfrak{N}_1$ we note that S_1' is a unitary operator which commutes with H_1' (see [1], Corollary to Theorem 3.1) and that H_1' has a simple spectrum in $\mathfrak{N}_1$. Hence we see easily that S_1' is expressible in the form

$$\text{(4)} \qquad S_1'\{f_1, f_2\} = \{\exp[i\theta(k)]\hat{f}_1(k), \exp[i\theta(k)]\hat{f}_1(k)\} + \{\hat{f}_2, -\hat{f}_2\},$$

where $\theta(k)$ is a real-valued measurable function defined on $(0, \infty)$. Now let $\{f_1, f_2\} \in \mathfrak{M}_2'$, so that $f_1 = 0$. Then, from (3) and (4) it follows that

$$S_1'\{0, f_2(k)\} = \{\tfrac{1}{2}(\exp[i\theta(k)] - 1)f_2(k), \tfrac{1}{2}(\exp[i\theta(k)] + 1)f_2(k)\}.$$

Using the explicit expression of $\theta(k)$ given in Kato [9], however, a simple consideration shows that $\exp[i\theta(k)]$ is not identically equal to 1 if $\psi \neq 0$ as an element of L^2. Hence, $S_1'\{0, f_2\} \notin \mathfrak{M}_2'$ for some $\{0, f_2\} \in \mathfrak{M}_2'$. This shows that $S_1'\mathfrak{M}_2' \neq \mathfrak{M}_2'$, as we wished to show.

Appendix

Proof of i) and ii).

Let $\mathfrak{H}^{(i)}$, $i = 1, 2$, be two copies of the Hilbert space $L^2(E_1)$ consisting of all square integrable functions $u(x_i)$ of one variable x_i. The Hilbert space $\mathfrak{H} = L^2(E_2)$ may be regarded as the tensor product (direct product) of $\mathfrak{H}^{(1)}$ and $\mathfrak{H}^{(2)}$: each $u \in \mathfrak{H}$ can be written as $u(x_1, x_2) = \sum_{k=1}^{\infty} u_1^{(k)}(x_1)\, u_2^{(k)}(x_2)$, $u_i^{(k)} \in \mathfrak{H}^{(i)}$.

(The sum is convergent in the sense of $\mathfrak{H}$.) We write $u_1(x_1)u_2(x_2) = u_1 \otimes u_2$ and denote by $\mathfrak{H}'$ the linear manifold of $\mathfrak{H}$ consisting of all linear combinations of elements of the form $u_1 \otimes u_2$. Then $\|u_1 \otimes u_2\| = \|u_1\| \, \|u_2\|$ and $\mathfrak{H}'$ is dense in $\mathfrak{H}$. We also write $\mathfrak{H} = \mathfrak{H}^{(1)} \otimes \mathfrak{H}^{(2)}$. The abstract definition of the tensor product is given, *e.g.*, in SCHATTEN ([10]).

The tensor product $A_1 \otimes A_2$ of bounded operators A_i in $\mathfrak{H}^{(i)}$, $i = 1, 2$, is defined as follows. For each $u \in \mathfrak{H}'$, $u = \sum_{k=1}^{n} u_1^{(k)} \otimes u_2^{(k)}$, we put $(A_1 \otimes A_2)u = \sum_{k=1}^{n} A_1 u_1^{(k)} \otimes A_2 u_2^{(k)}$. This defines a bounded linear operator $(A_1 \otimes A_2)'$ from $\mathfrak{H}'$ into $\mathfrak{H}$ ([10]). $A_1 \otimes A_2$ is the unique bounded extension of $(A_1 \otimes A_2)'$ on $\mathfrak{H}$. When A_i is unbounded, the definition of the tensor product is not so simple, but we shall only use the following special case. Let A_1 be a self-adjoint operator in $\mathfrak{H}_1$ and I_2 the identity in $\mathfrak{H}_2$. Define a symmetric operator A_1' as follows. $D(A_1')$ is the aggregate of all linear combinations of $u_1 \otimes u_2$ with $u_1 \in D(A_1)$ and $A_1'(u_1 \otimes u_2) = A_1 u_1 \otimes u_2$ for such a $u_1 \otimes u_2$. Then $(A_1' \pm i)(u_1 \otimes u_2) = (A_1 \pm i)u_1 \otimes u_2$ ranges over all $u_1 \otimes u_2$, $u_i \in \mathfrak{H}^{(i)}$, when u_1 and u_2 range over all $D(A_1)$ and $\mathfrak{H}^{(2)}$, respectively. Hence $\mathfrak{R}(A_1' \pm i)$ is dense in $\mathfrak{H}$, which shows that A_1' is essentially self-adjoint. The tensor product $A_1 \otimes I_2$ is defined as the unique self-adjoint extension of A_1'. (If A_1 is bounded, this definition coincides with the previous one.) Let $E_1(\lambda)$, $-\infty < \lambda < +\infty$, be the resolution of the identity corresponding to A_1: $A_1 = \int \lambda \, \mathrm{d}E_1(\lambda)$. A simple consideration then shows that $E(\lambda) = E_1(\lambda) \otimes I_2$ forms a resolution of the identity in $\mathfrak{H}$ and $A_1 \otimes I_2 = \int \lambda \, \mathrm{d}E(\lambda)$. For a self-adjoint operator A_2 in $\mathfrak{H}_2$, $I_1 \otimes A_2$ is defined similarly.

Let now $A_i = \int \lambda \, \mathrm{d}E_i(\lambda)$ be a self-adjoint operator in $\mathfrak{H}_i$, $E^{(1)}(\lambda) = E_1(\lambda) \otimes I_2$ and $E^{(2)}(\lambda) = I_1 \otimes E_2(\lambda)$. Obviously we have $E^{(1)}(\lambda) E^{(2)}(\mu) = E^{(2)}(\mu) E^{(1)}(\lambda)$. Hence, there exists a self-adjoint operator B in $\mathfrak{H}$ and real-valued functions $f(\lambda)$ and $g(\lambda)$ such that $A_1 \otimes I_2 = f(B)$ and $I_1 \otimes A_2 = g(B)$ (see, *e.g.*, RIESZ and SZ.-NAGY ([11]), § 130). From this we see that $A_1 \otimes I_2 + I_1 \otimes A_2$ is essentially self-adjoint and $A = (f + g)(B) = (A_1 \otimes I_2 + I_1 \otimes A_2)^{\sim}$ ($^{\sim}$ denotes the closure of an operator). We then obtain

$$\begin{aligned} \exp[itA] &= \exp[itf(B)] \exp[itg(B)] \\ &= \exp[it(A_1 \otimes I_2)] \exp[it(I_1 \otimes A_2)] \\ &= \exp[itA_1] \otimes \exp[itA_2] . \end{aligned} \tag{5}$$

We now apply these formulas to our problem. Let H_0, H_1 and H_{12} be as defined before, $H_{0i} = -\mathrm{d}^2/\mathrm{d}x_i^2$, $i = 1, 2$, and $H_1' = (H_{01} \otimes I_2 + I_1 \otimes H_{12})^{\sim}$. We show that $H_1' = H_1$ ([12]) Let D be the set of all $u \in \mathfrak{H}$ of the form $u(x_1, x_2) = P(x_1, x_2) \exp[-(x_1^2 + x_2^2)]$, where P is a polynomial. Then we have $u \in \mathfrak{D}(H_1') \cap \mathfrak{D}(H_1)$ and $H_1' u = H_1 u$ for each $u \in \mathfrak{D}$. In other words, H_1' is a

---

([10]) R. SCHATTEN: *A Theory of Cross Spaces*, « Ann. Math. Studies » (Princeton, 1950).

([11]) F. RIESZ and B. VON SZ.-NAGY: *Functional Analysis* (New York, 1955).

([12]) A detailed consideration shows that $H_1 = H_{01} \otimes I_2 + I_2 \otimes H_{12}$, but this is not needed in the sequel.

self-adjoint extension of the restriction $H_{1|D}$ of H_1 to D. On the other hand, it is known that $H_{1|D}$ is essentially self-adjoint ([3]) and hence $H_{1|D}$ has a unique self-adjoint extension. This implies that $H_1' = H_1$. By virtue of (5) we then have $\exp[itH_1] = [\exp[itH_{01}] \otimes \exp[itH_{12}]$. In the same way we also have $\exp[-itH_0] = \exp[-itH_{01}] \otimes \exp[-itH_{02}]$. Since H_0, H_{01} and H_{02} are absolutely continuous, we see from this that $W_{\pm}(H_1, H_0)$ exist and

$$W_{\pm}(H_1, H_0) = I_1 \otimes W_{\pm}(H_{12}, H_{02}) . \tag{6}$$

As is easily seen, (6) gives $\mathfrak{R} = \mathfrak{R}(W_{\pm}(H_1, H_0)) = \mathfrak{H}^{(1)} \otimes \mathfrak{R}(W_{\pm}(H_{12}, H_{02}))$. Since $\mathfrak{R}(W_{\pm}(H_{12}, H_{02}))$ is the orthogonal complement of the (one-dimensional) eigenspace $\{u_0\}$ of H_{12} ([1]), $\mathfrak{R}$ is the orthogonal complement of $\mathfrak{H}^{(1)} \otimes \{u_0\} = \mathfrak{H}_1$, where $\mathfrak{H}_1$ is as in i). Thus we proved i) and ii) except the assertion on the spectrum of the part of H_1 in $\mathfrak{H}_1$. But this assertion follows immediately from the relation $H_1(u_1 \otimes u_0) = H_{01}u_1 \otimes u_0 + u_1 \otimes H_{12}u_0 = (H_{01} + \lambda)u_1 \otimes u_0$, $u_1 \in \mathfrak{D}(H_{01})$.

RIASSUNTO (*)

Si costruisce un esempio di un sistema disperdente avente le seguenti proprietà: 1) i suoi gli Hamiltoniani non perturbati non hanno stati limiti; 2) esistono gli operatori d'onda; 3) l'operatore di scattering non è unitario.

(*) *Traduzione a cura della Redazione.*

IL NUOVO CIMENTO Vol. XIV, N. 5 1° Dicembre 1959

Quantization of the Two-Component Fermion Theory.

M. Tonin

Istituto di Fisica dell'Università - Padova
Istituto Nazionale di Fisica Nucleare - Sezione di Padova

(ricevuto il 7 Settembre 1959)

Summary. — In this work the two-component fermion field, which has been recently studied by L. M. Brown, satisfying a second order Pauli wave equation has been quantized. Anticommutation rules for the two-component spinors describing the fermion field have been found which are particularly simple. At last, the possibility of extending to this case Wick's theorem has been shown, and therefore rules of calculation for the Feynman diagrams are obtained, which are strictly closed to the rules for the quantum electrodynamics of Klein-Gordon particles.

1. – Introduction.

The Pauli second order equation for two-component spinors has been invoked by Feynman and Gell-Mann (1) to justify the $V-A$ theory of the Fermi interaction. This equation is strictly equivalent to the better known four-component Dirac equation at least as long as we remain in the domain of electromagnetism. For this reason we can construct the theory of $\frac{1}{2}$ spin particles with electromagnetic interaction as a two-component fermion theory.

One theory of this type has been recently developed and put into lagrangian form by L. M. Brown (2). From his theory it results that, if we use for

(1) R. P. Feynman and M. Gell-Mann: *Phys. Rev.*, **109**, 193 (1958).
(2) L. M. Brown: *Phys. Rev.*, **111**, 957 (1958).

the γ's of Dirac the representation [3]

$$\gamma_\mu = \begin{pmatrix} 0 & \sigma_\mu \\ \bar{\sigma}_\mu & 0 \end{pmatrix},$$

with $\sigma_\mu = (1, \boldsymbol{\sigma})$ and $\bar{\sigma}_\mu = (1, -\boldsymbol{\sigma})$ and we put $\Psi = \begin{pmatrix} \Omega \\ \Psi \end{pmatrix}$, the Dirac equation satisfied by the four-component Ψ, can be broken into two equations with two components:

(1) $$\Pi^+ \Omega = m\Psi ,$$

(2) $$\Pi^- \Psi = m\Omega .$$

Replacing (2) in (1) and (1) in (2), we obtain the equations

(3) $$\Pi^+ \Pi^- \Psi = m^2 \Psi ,$$

(4) $$\Pi^- \Pi^+ \Omega = m^2 \Omega .$$

These are equivalent to the system (1), (2) and therefore to the Dirac equation. We can thus consider (3) and (4) as fundamental equatio (*i.e.* as the Euleron equations of a convenient Lagrangian) and (2) as the supplementary condition which connects Ω to Ψ.

The lagrangian density that gives the equations (3), (4) is:

(5) $$\mathscr{L} = m^{-1} (\Pi^+ \Omega)^\dagger (\Pi^- \Psi) - m\Omega^\dagger \Psi .$$

For a free field this lagrangian becomes:

(5′) $$\mathscr{L} = m^{-1} (\partial^+ \Omega)^\dagger (\partial^- \Psi) - m\Omega^\dagger \Psi$$

---

[3] Here and in the following we shall use, when possible, the same notations used in ref. [2]. In particular, we shall employ the metric $g_{00} = 1$, $g_{kk} = -1$ and we shall put

$$\Pi_\mu = i \frac{\partial}{\partial x_\mu} - A_\mu ,$$

A_μ being the electromagnetic potential, and

$$q^- = q_\mu \sigma_\mu ; \qquad q^+ = q_\mu \bar{\sigma}_\mu ,$$

q_μ being a generic four-vector. Moreover we use the units $\hbar = c = 1$.

and gives us the equations

$$\partial^+\partial^-\Psi = -m^2\Psi \tag{3'}$$

$$\partial^-\partial^+\Omega = -m^2\Omega \tag{4'}$$

while (1), (2), reduce to:

$$i\partial^+\Omega = m\Psi\,, \tag{1'}$$

$$i\partial^-\Psi = m\Omega\,. \tag{2'}$$

In order to clarify the meaning of the density of Lagrangian (5') let us spend a few words in connecting (5') to the Dirac lagrangian density which, when written in two-component form, is:

$$\mathscr{L} = i\Omega^\dagger\partial^+\Omega + i\Psi^\dagger\partial^-\Psi - m\Omega^\dagger\Psi - m\Psi^\dagger\Omega\,. \tag{6}$$

The appearance of four two-component spinors in (6) is redundant.

By using the equations (2'), we can eliminate two of these spinors; if we eliminate $\Omega^\dagger$, Ω we have the following lagrangian density:

$$\mathscr{L} = \frac{i}{m^2}\Psi^\dagger\overleftarrow{\partial^-}(\Box + m^2)\Psi\,, \tag{7}$$

which has been studied by KIBBLE and POLKINGHORNE [4]. An alternative possibility is the elimination of $\Psi^\dagger$ and Ω and in this case we obtain automatically (except for a divergence) the Brown's lagrangian density.

The Lagrangian (7) contains higher order derivatives of the field functions and therefore it cannot be studied and in particular quantized with the usual techniques. The more convenient way to study (7), is to linearize it and, to do this linearization, and if we want to exclude (6) which is a trivial one, we must extend (7) to the case of four-components and linearize it in a convenient way and then introduce a supplementary condition for the states, in order to exclude the superfluous components [4].

Another possibility which eliminates the supplementary condition consists in interpreting the four-component generalization of (7) as describing an isodoublet of fermions [5].

Moreover a second order lagrangian density such as

$$\mathscr{L} = -\frac{1}{m^2}\Psi^\dagger(\Box + m^2)\Psi\,,$$

---

[4] T. W. KIBBLE and J. C. POLKINGHORNE: *Nuovo Cimento*, **8**, 74 (1958).
[5] G. MARX: *Nucl. Phys.*, **9**, 337 (1958-59).

as KIBBLE and POLKINGHORNE have shown [4], presents some difficulties because in this case an indefinite metric must be used.

On the contrary, Brown's lagrangian density (5′) can be treated and quantized with the standard methods and no difficulty of indefinite metric does arise.

The aim of the present work is just to carry out in detail this quantization.

2. – Anticommutation rules.

The anticommutation rules between Ψ, $\Omega^\dagger$ are simply

$$[\Psi(z), \Omega^\dagger(y)]_+ = im\,\Delta(z-y)\,, \tag{8}$$

$$[\Psi(z), \Psi(y)]_+ = [\Omega^\dagger(z), \Omega^\dagger y)]_+ = 0\,. \tag{9}$$

These can be derived by the Peierl's method as follows:

If we write the two different variations of the Lagrangian (5′):

$$\delta_{R(z)}\mathscr{L}(x) = \varepsilon\,\delta^4(x-z)\,R(x)\,, \tag{10}$$

$$\delta_{Q(y)}\mathscr{L}(x) = \varepsilon\,\delta^4(x-y)\,Q(x)\,, \tag{11}$$

$R(z)$ and $Q(y)$ satisfy the following commutation relations:

$$[R(z), Q(y)]_- = i\{\delta_{R(z)}Q(y) - \delta_{Q(y)}R(z)\}\,,$$

where we have used the conventional notations $\delta_{R(z)}A(x)$ $[\delta_{Q(y)}A(x)]$ to represent the variation of the generic operator $A(x)$ due to the variation (10) [(11)] of the lagrangian.

Now we put

$$R(z) = u^\dagger\cdot\Psi(z)\,,$$

$$Q(y) = \Omega^\dagger(y)\cdot v\,,$$

$u^\dagger$ and v being constant spinors which anticommute with Ψ and $\Omega^\dagger$ and with each other.

The Euler equation of the varied field

$$\Psi'(z) = \Psi(z) + \varepsilon\,\delta_{Q(y)}\Psi(z)$$

is therefore

$$\Box\,\Psi'(z) + m^2\Psi'(z) = m\varepsilon\,\delta^4(y-z)v\,.$$

Thus

$$(\Box + m^2)\,\delta_{Q(y)}\Psi(z) = m\,\delta^4(y-z)v$$

or

$$(\Box + m^2)\,\delta_{Q(y)} R(z) = mu^\dagger\,\delta^4(y-z)v\,. \tag{12}$$

We also must have

$$\delta_{Q(y)} R(z) = 0 \qquad \text{for} \quad y_0 > z_0\,. \tag{13}$$

From (12) and from the condition (13), it follows

$$\delta_{Q(y)} R(z) = mu^\dagger\,\Delta_R(z-y)v = mu^\dagger\,\Delta_A(y-z)v\,.$$

Similarly we can demonstrate:

$$\delta_{R(z)} Q(y) = mu^\dagger\,\Delta_R(y-z)v = mu^\dagger\,\Delta_A(z-y)v\,.$$

Then it results

$$[R(z), Q(y)]_- = u^\dagger\,[\Psi(z), \Omega^\dagger(y)]_+ v = \\ = miu^\dagger\,[\Delta_A(z-y) - \Delta_R(z-y)]v = miu^\dagger\,\Delta(z-y)v\,,$$

which proves (8). $\Delta(x)$, $\Delta_A(x)$, $\Delta_R(x)$ are the usual invariant Green functions for mass m. In the same way we can demonstrate (9).

Now we must note that, because the lagrangian density does not contain $\Psi^\dagger$, Ω, it does not contain any information about the anticommutation rules between Ψ, Ω; $\Psi^\dagger$, Ψ; $\Omega^\dagger$, Ω; $\Psi^\dagger$, $\Omega^\dagger$. It follows that no incompatibility can exist between the anticommutation rules that we have found and the relations (1′) and (2′). These therefore can be admitted also quantum-mechanically for the operators Ψ and Ω and used to define the anticommutation rules between Ψ, Ω; $\Psi^\dagger$, Ψ etc.

3. – Plane wave decomposition.

With standard methods we can immediately obtain the plane wave decomposition of the $\Psi(x)$ and $\Omega(x)$ fields. It results:

$$\begin{cases} \Psi(x) = \dfrac{1}{(2\pi)^{\frac{3}{2}}}\displaystyle\int \frac{\mathrm{d}^3p}{\sqrt{2\varepsilon}}\,[a_+(\boldsymbol{p})\sqrt{q_-}\,u_+(\boldsymbol{p}) + a_-(\boldsymbol{p})\sqrt{q_+}\,u_-(\boldsymbol{p})]\exp[-ipx] + \\ \qquad + \dfrac{1}{(2\pi)^{\frac{3}{2}}}\displaystyle\int \frac{\mathrm{d}^3p}{\sqrt{2\varepsilon}}\,[b^*_+(\boldsymbol{p})\sqrt{q_-}\,u_+(\boldsymbol{p}) + b^*_-(\boldsymbol{p})\sqrt{q_+}\,u_-(\boldsymbol{p})]\exp[ipx]\,. \\ \Omega(x) = \dfrac{1}{(2\pi)^{\frac{3}{2}}}\displaystyle\int \frac{\mathrm{d}^3p}{\sqrt{2\varepsilon}}\,[a_+(\boldsymbol{p})\sqrt{q_+}\,u_+(\boldsymbol{p}) + a_-(\boldsymbol{p})\sqrt{q_-}\,u_-(\boldsymbol{p})]\exp[-ipx] - \\ \qquad - \dfrac{1}{(2\pi)^{\frac{3}{2}}}\displaystyle\int \frac{\mathrm{d}^3p}{\sqrt{2\varepsilon}}\,[b^*_+(\boldsymbol{p})\sqrt{q_+}\,u_+(\boldsymbol{p}) + b^*_-(\boldsymbol{p})\sqrt{q_-}\,u_-(\boldsymbol{p})]\exp[ipx]\,, \end{cases} \tag{14}$$

$u_{\pm}(\boldsymbol{p})$ are spinors, normalized to unity, defined by the relations

$$\tfrac{1}{2}(1 \pm \boldsymbol{\sigma}\cdot\boldsymbol{p})\, u_{\pm}(\boldsymbol{p}) = u_{\pm}(\boldsymbol{p}) ,$$

$$\tfrac{1}{2}(1 \pm \boldsymbol{\sigma}\cdot\overline{|\boldsymbol{p}|^2})\, u_{\mp}(\boldsymbol{p}) = 0 .$$

To deduce (14) use has also been made of the relation (2′) and we have employed the notations

$$p_0 = \varepsilon = +\sqrt{\boldsymbol{p}^2 + m^2} ,$$

$$q_{\pm} = \varepsilon \pm |\boldsymbol{p}| .$$

The anticommutation rules (8), (9), in terms of the operators $a_r(\boldsymbol{p})$, $b_r(\boldsymbol{p})$ $(r = +, -)$, are given by:

$$\text{(15)} \qquad \begin{cases} [a_r(\boldsymbol{p}), a^*_{r'}(\boldsymbol{p}')]_+ = [b_r(\boldsymbol{p}), b^*_{r'}(\boldsymbol{p}')]_+ = \delta_{rr'}\,\delta^3(\boldsymbol{p}-\boldsymbol{p}') \\ [a_r(\boldsymbol{p}), a^*_{r'}(\boldsymbol{p}')]_+ = [b_r(\boldsymbol{p}), b_{r'}(\boldsymbol{p}')]_+ = [a_r(\boldsymbol{p}), b_{r'}(\boldsymbol{p})]_+ = 0 \end{cases}$$

and the four—momentum P_μ and the charge Q have the following expressions:

$$\text{(16)} \qquad \begin{cases} P_\mu = \int \mathrm{d}^3p \cdot p_\mu \sum_r (a^*_r(\boldsymbol{p})\, a_r(\boldsymbol{p}) + b^*_r(\boldsymbol{p})\, b_r(\boldsymbol{p})) , \\ Q = e\int \mathrm{d}^3p \sum_r (a^*_r(\boldsymbol{p})\, a_r(\boldsymbol{p}) - b^*_r(\boldsymbol{p})\, b_r(\boldsymbol{p})) . \end{cases}$$

Eq. (15) and (16) enable us to interpret $a_r(\boldsymbol{p})$, $a^*_r(\boldsymbol{p})$, $b_r(\boldsymbol{p})$, $b^*_r(\boldsymbol{p})$ as operators of creation and destruction of particles and antiparticles respectively.

4. – Quantum electrodynamics.

The considerations developed so far were referred to the free fermion field. Now we will study the interaction with the electromagnetic field in order to obtain the rules of calculation for the processes between charged fermions and photons. We shall therefore proceed in the usual way *i.e.* going first to the interaction representation and writing the perturbative expansion of the S-matrix, and then extending to the present case Wick's theorem to go from the chronological products to the normal one.

Let us call $\psi(x)$, $\omega(x)$, $a_\mu(x)$ the fields $\Psi(x)$, $\Omega(x)$, $A_\mu(x)$ in the interaction

representation

$$(17)\qquad \begin{cases} \psi(x) = P\left[\exp\left[-i\int_{-\infty}^{\tau} H(\tau')\,\mathrm{d}\tau'\right]\right]\cdot\Psi(x)\cdot P\left[\exp\left[-i\int_{-\infty}^{\tau} H(\tau')\,\mathrm{d}\tau'\right]\right], \\ \omega(x) = P\left[\exp\left[-i\int_{-\infty}^{\tau} H(\tau')\,\mathrm{d}\tau'\right]\right]\cdot\Omega(x)\cdot P\left[\exp\left[-i\int_{-\infty}^{\tau} H(\tau')\,\mathrm{d}\tau'\right]\right], \\ a_\mu(x) = P\left[\exp\left[-i\int_{-\infty}^{\tau} H(\tau')\,\mathrm{d}\tau'\right]\right]\cdot A_\mu(x)\cdot P\left[\exp\left[-i\int_{-\infty}^{\tau} H(\tau')\,\mathrm{d}\tau'\right]\right], \end{cases}$$

P being the symbol of the chronological product. $\psi(x)$, $\omega(x)$, $a_\mu(x)$ satisfy the free fields equations and so we can extend to them the anticommutation rules that we have found previously

$$(18)\qquad \begin{cases} [\psi(x), \omega^+(y)]_+ = mi\,\Delta(x-y) \\ [\psi(x), \psi(y)]_+ = [\omega^+(x), \omega^+(y)]_+ = 0 \end{cases}$$

and also

$$(19)\qquad [a_\mu(x), a_\nu(y)]_- = -i\,g_{\mu\nu}D(x-y)\,.$$

We can easily verify that, to let (17) satisfy the free field equations, $H(\tau)$ must have the following expression:

$$(20)\qquad H(\tau) = -\int_{\sigma(\tau)}[\psi^+(x)\,a^-(x)\,\psi(x) + \omega^+(x)\,a^+(x)\,\omega(x)]\,\mathrm{d}\sigma\,,$$

and therefore the n-order term of the S-matrix is given by

$$(21)\qquad S^{(n)} = \frac{1}{m^n}\,\frac{(-1)^n}{n!}\cdot$$

$$\cdot\int \mathrm{d}^4x_1 \ldots \int \mathrm{d}^4x_n P[\omega^+(x_n)\,g_{\mu_n}(n)\,\psi(x_n)\ldots\omega^+(x_1)\,g_{\mu_1}(1)\,\psi(x_1)]\cdot P[a_{\mu_n}(x_n)\ldots a_{\mu_1}(x_1)]^*,$$

with

$$g_{\mu_s}(s) = [-\overleftarrow{\partial}_s^+\sigma_{\mu_s} + \overline{\sigma}_{\mu_s}\overrightarrow{\partial}_s^-]\,.$$

To the chronological products appearing in (21) we can apply the ordering

theorem (6) but in the case of the first chronological product a precaution must be taken. This ordered product, in opposition to the usual case, includes differential operators that, when it is written in normal form, operate backwards on the contraction factors

$$C(i,j)=[-\theta(x_i-x_j)\,\Delta^{(-)}(x_j-x_i)+\theta(x_j-x_i)\,\Delta^{(+)}(x_j-x_i)]=-\Delta_c(x_i-x_j). \quad (22)$$ (7)

but only on the $\Delta^{(+)}$-functions and not on the step functions $\theta(i,j)$. In the following we shall use the symbol $C(i,j)$ to mean this fact, *i.e.* that the differential operators $g_{\mu_s}(s)$ operate only on the Δ functions and not on the function $\theta(i,j)$. Otherwise we shall use the simbol $\Delta_c(i,j)$. Therefore we have that the term (8)

$$(-1)^{j-1}\,\omega^{\dagger}(x_{r_1})g(r_1)\,C(r_1,r_2)g(r_2)\,C(r_2,r_3)\ldots g(r_s)\,\psi(x_{r_s}) \quad (23)$$

(and the terms in the normal expansion of the chronological product are always products of terms similar to (23)) is equal to

$$(-1)^{s-1}\,\omega^{\dagger}(x_{r_1})g(r_1)\,\Delta_c(r_2,r_1)g(r_2)\,\Delta_c(r_3,r_2)\ldots g(r_3)\,\psi(x_{r_s})$$

plus a sum of terms which contain factors of the type

$$\bar{\sigma}\,\delta^4(r_i,r_i+1)\sigma\,.$$

Strictly (see Appendix I) we have the following relation (9)

$$g[1]\,C[1,2]\,g[2]\,C[2,3]\ldots g[s]=\sum_{q=0}^{N}\sum_{\text{permutations}}A^{s}_{t_1,\ldots,t_q} \quad (24)$$

with

$$N=\begin{cases}\dfrac{s}{2} & \text{for } s \text{ even},,\\[2ex] \dfrac{s-1}{2} & \text{for } s \text{ odd},\end{cases}$$

where $A^{s}_{t_1,\ldots,t_q}$ is what we obtain from the first member of (24) substituting $g[t_i]\,C[t_i,t_i+1]\,g[t_i+1]$ with $\bar{\sigma}\,\delta^4[t_i,t_i+1]\sigma$ for $i=1\ldots q$ and the remaining $C[t_j,t_j+1]$ with $\Delta_c[t_j,t_j+1]$.

(6) See, for instance, J. M. Jauch and F. Rohrlich: *The Theory of Photons and Electrons* (Cambridge, Mass., 1955), p. 445.

(7) Concerning the notations employed see ref. (6) loc.

(8) For simplicity we left out in the operators g_μ and σ_μ, $\bar{\sigma}_\mu$ the vector index.

(9) We shall use the notations $g[i]=g(r_i)$, $C[i,j]=C(r_i,r_j)$ and so on.

Now to the generic term

$$\int \mathrm{d}^4 x_i \int \mathrm{d}^4 x_j \ldots \bar{\sigma}_{\mu_i} \delta^4(i, j) \sigma_{\mu_j} \ldots ,$$

which appears in the normal form expansion of (21), when (24) is used, we sum the analogous term

$$\int \mathrm{d}^4 x_i \int \mathrm{d}^4 x_j \ldots \bar{\sigma}_{\mu_j} \delta^4(j, i) \sigma_{\mu_i} \ldots$$

which also appears in this expansion and perform the integration over x_j. So we obtain the term:

$$\int \mathrm{d}^4 x_i \ldots [\bar{\sigma}_{\mu_i} \sigma_{\mu_j} + \bar{\sigma}_{\mu_j} \sigma_{\mu_i}] \ldots .$$

In this way we have a convenient expansion of (21) the terms of which can be easily interpreted in graphical form.

To this regard we only observe that to the factors

$$[\bar{\sigma}_\mu \sigma_\nu + \bar{\sigma}_\nu \sigma_\mu] = 2 g_{\mu\nu}$$

correspond vertices with emission or absorption of two photons. Also we note that the terms which correspond to the diagrams

(I)

arise from the sum of one and two (and not two and four) « different » terms respectively (« different » according to the usual convention which let us cancel the $1/n!$ factor in (21)), so that the diagrams of the type (I) are weighted with a $\frac{1}{2}$ factor. A similar situation arises also in the quantum electrodynamics of Klein-Gordon spin zero particles.

Conversely we can write down the S-matrix element which corresponds to a given diagram of order n [10]. In the momentum space we have the rules expressed in the Table.

---

[10] We assume that to determine the order of a diagram, the two photon vertices must be counted double.

These rules give us the S-matrix element aside from a multiplicative factor which is

$$(-1)^l \delta_p \frac{1}{2^\alpha} e^n i^{n-m}$$

where l is the number of closed fermion loops, δ_p is the signature of the permutation of the final electrons, α is the number of parts of diagram (I) and m is the number of two photon vertices and e is the electric charge.

Component of a diagram	Factor in S-matrix element
Internal photon line	$i(2\pi)^{-4} g_{\mu\nu} \frac{1}{k^2}$
Internal fermion line	$i(2\pi)^{-4} \frac{1}{p^2 - m^2}$
One photon vertex	$(2\pi)^4 \delta^4(p - p' \pm k)[p^+\sigma_\mu + \bar{\sigma}_\mu p'^-]$
Two photon vertex	$(2\pi)^4 \delta^4(p - p' \pm k \pm k')\, 2g_{\mu\nu}$
Ingoing and outgoing photon line	$\frac{(2\pi)^{-\frac{3}{2}}}{\sqrt{2\lvert k_0\rvert}} e_\mu(\boldsymbol{k})$; $\frac{(2\pi)^{-\frac{3}{2}}}{\sqrt{2\lvert k_0\rvert}} e_\mu(\boldsymbol{k})$
Ingoing and outgoing particle line	$(2\pi)^{-\frac{3}{2}} \sqrt{\frac{q_\mp}{2m\varepsilon}}\, u_\pm(\boldsymbol{p})$; $(2\pi)^{-\frac{3}{2}} \sqrt{\frac{q_\mp}{2m\varepsilon}}\, u^\dagger_\pm(\boldsymbol{p})$
Ingoing and outgoing antiparticle line	$-(2\pi)^{-\frac{3}{2}} \sqrt{\frac{q_\pm}{2m\varepsilon}}\, u^\dagger_\pm(\boldsymbol{p})$; $(2\pi)^{-\frac{3}{2}} \sqrt{\frac{q_\mp}{2m\varepsilon}}\, u_\pm(\boldsymbol{p})$

The so obtained results agree with and confirm the calculational methods described in Brown's paper (2). Moreover in pratical calculations the « backwards rule » contained in the quoted paper can be advantageously used.

Finally we observe that we are so led to a new formalism for the quantum electrodynamics which, although equivalent to the usual one can be interesting in many cases. First of all it is quite close to the Klein-Gordon particles formalism and this analogy can be convenient in some problems. In any case the calculations based on such a formalism often appear simpler.

* * *

I wish to express my deep gratitude to Prof. L. M. Brown for having suggested this work and for guidance and valuable advice. I am also very grateful to Prof. N. Dallaporta for his kind interest and encouragement and to Prof. C. Ceolin and Dr. A. Schroeder for useful discussions and advices.

Appendix

The relation (24) can be demonstrated by induction. For $s = 2$ we have

$$g[1]\,C[1,2]g[2] = -g[1]\,\Delta_c[1,2]g[2] + f[1,2]$$

with

$$f[1,2] = \bar{\sigma}(\partial^-_{[1]}\theta[1,2])\,(\partial^+_{[2]}\Delta[1,2])\,\sigma + \bar{\sigma}\,\partial^-_{[1]}[\Delta[1,2]\,(\partial^+_{[2]}\theta[1,2])]\sigma - \\ -\{\bar{\sigma}\,(\overleftarrow{\partial}^-_{[1]}\theta[1,2])\,\Delta[1,2]\bar{\sigma}\partial^-_{[2]} + \partial^+_{[1]}\sigma(\partial^+_{[2]}\theta[1,2])\Delta[1,2]\sigma\}.$$

We are nov interested in the integral

$$\int \mathrm{d}^4x_i \int \mathrm{d}^4x_j \ldots f(x_i - x_j) \ldots \tag{1A}$$

We can assume that the space-like hypersurface on which the initial conditions of $\Delta(x)$ are defined, is the hyperplane $t = 0$.

With this assumpion we can easily see that the contributions to the integral (1A) of the second and third term of $f(x_i - x_j)$ vanish and the contribution of the first term is

$$\int \mathrm{d}^4x_i \int \mathrm{d}^4x_j \ldots \bar{\sigma}_{\mu_i}\,\delta^4(x_i - x_j)\sigma_{\mu_j}\,.$$

This proves (24) for $s = 2$.

Let us admit (24) for $s = k$ and demonstrate it for $s = k+1$. We observe that

$$A^k_{t_1,\ldots,t_q}\,C[k,k+1]g[k+1] = \begin{cases} A^{k+1}_{t_1,\ldots,t_q}, & \text{if } t_q = k-1, \\ A^{k+1}_{t_1,\ldots,t_q} + A^{k+1}_{t_1,\ldots,t_q,k}\,. & \text{if } t_q < k-1. \end{cases}$$

Therefore it results

$$g[1]\,C[1,2]g[2] \ldots g[k]\,C[k,k+1]g[k+1] = \\ = \sum_{q=0}^{N} \sum_{\text{permutations}} A^k_{t_1,\ldots t_q}\,C[k,k+1]g\,[k+1] = \sum_{q'=0}^{N'} \sum_{\text{permutations}} A^{k+1}_{t_1,\ldots t_{q'}},$$

whith

$$N' = \begin{cases} \frac{k}{2}, & \text{for } k \text{ even}, \\ \frac{k+1}{2}, & \text{for } k \text{ odd}. \end{cases}$$

RIASSUNTO

In questo lavoro si è quantizzato il campo fermionico a due componenti soddisfacente a un'equazione d'onda tipo Pauli del secondo ordine, che è stato recentemente studiato da L. M. Brown. Si sono trovate regole di anticommutazione particolarmente semplici per gli spinori a due componenti descriventi il campo fermionico. Infine si è indicata la possibilità di estendere al caso considerato il teorema di Wick e quindi si sono ottenute le regole di calcolo dei diagrammi di Feynmann: queste risultano come c'è da aspettarsi, strettamente analoghe a quelle che si hanno nell'elettrodinamica quantistica delle particelle di Klein-Gordon.

IL NUOVO CIMENTO Vol. XIV, N. 5 1° Dicembre 1959

(n, d) Reactions with 14 MeV Neutrons on ^{27}Al, ^{40}Ca, ^{55}Mn, ^{63}Cu, ^{103}Rh.

L. Colli

Istituto di Scienze Fisiche dell'Università - Milano
Laboratori CISE - Milano

F. Cvelbar (*), S. Micheletti and M. Pignanelli

Istituto di Scienze Fisiche dell'Università - Milano
Istituto Nazionale di Fisica Nucleare - Sezione di Milano

(ricevuto l'8 Settembre 1959)

Summary. — Energy spectra of the deuterons from the (n, d) reaction on the elements ^{27}Al, ^{40}Ca, ^{55}Mn, ^{63}Cu and ^{103}Rh are presented. Deuteron peaks corresponding to the fundamental level as well as to some excited levels of residual nuclei are brought into evidence. In Mn and Rh, the existence of gross-structure is shown.

1. – Introduction.

The study of nuclear reactions where a mechanism of the direct interaction type is evident has aroused great interest in the last few years.

This is due to the fact that the character of these reactions is strictly determined by the properties of the state which the nucleons involved in the reaction occupy in the nucleus, and can therefore furnish information on the state of these nucleons, and hence on the nuclear structure.

One group of this type are the (n, d) reactions believed to take place through a direct process called pick-up. This process is the inverse of the

(*) On leave of absence from the Jozef Stefan Institute, Ljubljana.

well known stripping process for which a theory vas evolved by BUTLER [1], which is also applied to the pick-up reactions.

In this pick-up theory, a hypothesis is laid whereby the incident neutron interacts with the protons at the surface of the nucleus, and a proton is captured by the neutron to form a deuteron. No reaction is held to take place between the incident neutron and the entire nucleus. The simplicity of the properties of a reaction that obeys this hypothesis permits an easy and clear comparison with experimental results. In the case where the residual nucleus is left in its fundamental state, it is certain that the less-bound proton has been expelled so that we can study the properties of the state occupied by the last proton. If the spectrum of the deuterons shows peaks corresponding to excited levels of the residual nucleus, then from the relative intensity of these peaks we can deduce the reduced width for the emission of a proton that belongs to those states of the nucleus involved in the reaction.

A complete study can only be accomplished when the angular distribution of the various peaks presented by the spectra is known: the comment that we can now make on our measurements, restricted to the forward direction, is therefore only preliminary.

We have begun a systematic study of (n, d) reactions induced by 14 MeV neutrons. So far we have studied the nuclei of ^{27}Al, ^{31}P, ^{32}S, ^{40}Ca, ^{55}Mn, ^{63}Cu and ^{103}Rh. The results on ^{31}P and ^{32}S were published in a previous work [2]. In this work, the spectra of the deuterons obtained from the other elements are presented.

2. – Description of apparatus.

The 14 MeV neutrons were obtained from the d+t reaction induced by deuterons accelerated at 160 keV by the accelerator of the Milan Section of the INFN.

The deuteron detector is the same instrument described in some previous works [3,4], and is essentially a telescope constituted by two proportional counters, a scintillation counter in coincidence, and a proportional counter in anticoincidence. Taking advantage of the different energy loss per cm in the proportional counter, it is possible by means of an electronic circuit to distinguish

---

[1] S. T. BUTLER: *Nuclear Stripping Reactions* (1957).

[2] L. COLLI, F. CVELBAR, S. MICHELETTI and M. PIGNANELLI: *Nuovo Cimento*, **13**, 868 (1959).

[3] G. MARCAZZAN, A. M. SONA and M. PIGNANELLI: *Nuovo Cimento*, **10**, 155 (1958).

[4] L. COLLI, F. CVELBAR, S. MICHELETTI and M. PIGNANELLI: *Nuovo Cimento*, **14**, 81 (1959).

between the pulses due to deuterons and those due to protons. The deuterons are detected at an emission angle of 0° to 30° with the incident neutrons direction.

The targets of the elements under study have variable thicknesses between 10 mg/cm² and 36.5 mg/cm² The energy resolution of the detector is about 5%. To this value is to be added, case by case, the energy dispersion due to the self-absorption in the target.

The energy scale was determined by means of the recoil deuterons emitted by a thin radiator of deuterized paraffin.

An accurate energy scale was also obtained from the spectrum of the reaction ^{27}Al(n, d)^{26}Mg which gives rise to three well-defined peaks corresponding to the fundamental level and to two excited states of known energy. The two scales agree within an accuracy of $\pm 2\%$.

3. – Experimental results.

^{27}Al(n, d)^{26}Mg. – The spectrum of the deuterons emitted by Aluminum, presented in Fig. 1 shows three well-resolved peaks corresponding to the fundamental state and to the known excited levels of the nucleus ^{26}Mg at 1.83 MeV and 2.97 MeV ([5]).

From our spectrum it is noted that the cross-section for (n, d) reaction is rather small in comparison with the other nuclei studied, and that the three peaks shown have the same intensity.

From the assignations made on the basis of the shell model we can estimate a $\Delta l_{\min} = 2$ for the transition to the fundamental state. The nucleus ^{27}Al should in fact contain the last 5 protons in the $d\,\frac{3}{2}$ level. From the conservation of the total angular momentum and with the spin of both the initial and the final states being known ([5]), it is in fact deduced that $\Delta l = 2$ is the least value of Δl required in the transition to the fundamental state corresponding to the capture of a $d\,\frac{3}{2}$ proton. Therefore it may be expected that the peak corresponding to the fundamental level does not show its maximum intensity at small angles, as in the case of the present measurement, since the angular distribution with $\Delta l = 2$ shows its maximum at larger angles. However, from the measurements of the angular distribution of the spectrum of protons + deuterons emitted by Al ([6]), we can easily deduce from the shape of the spectra that even at larger angles, the contribution of this peak of

([5]) P. M. Endt and C. M. Braams: *Rev. Mod. Phys.*, **29**, 683 (1957).
([6]) P. V. March and W. T. Morton: *Phil. Mag.*, **3**, 1256 (1958).

deuterons is not much more important than in the forward direction. The total cross-section for this level is therefore small.

A similar reasoning is true for the other two levels.

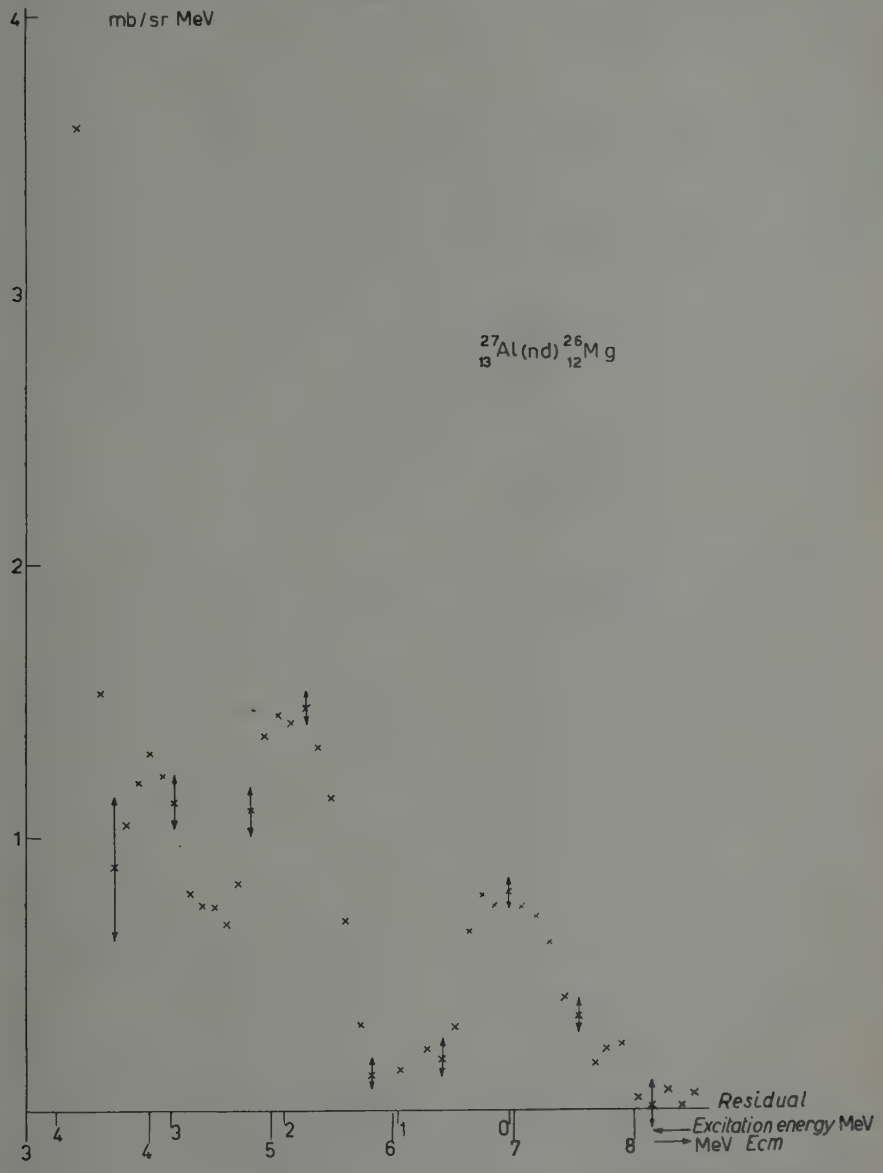

Fig. 1. – Spectrum of deuterons from the reaction $^{27}Al(n, d)^{26}Mg$.

It is therefore concluded that for these three states of the ^{26}Mg nucleus, the reduced width for the emission of a proton is small in comparison with that obtained for other nuclei .

^{40}Ca(n, d)^{39}K. – The spectrum of Ca (Fig. 2) shows the peak corresponding to the fundamental level and, beginning at 2.5 MeV excitation energy of the residual nucleus ^{39}K, a steep rise, evidently corresponding to the beginning

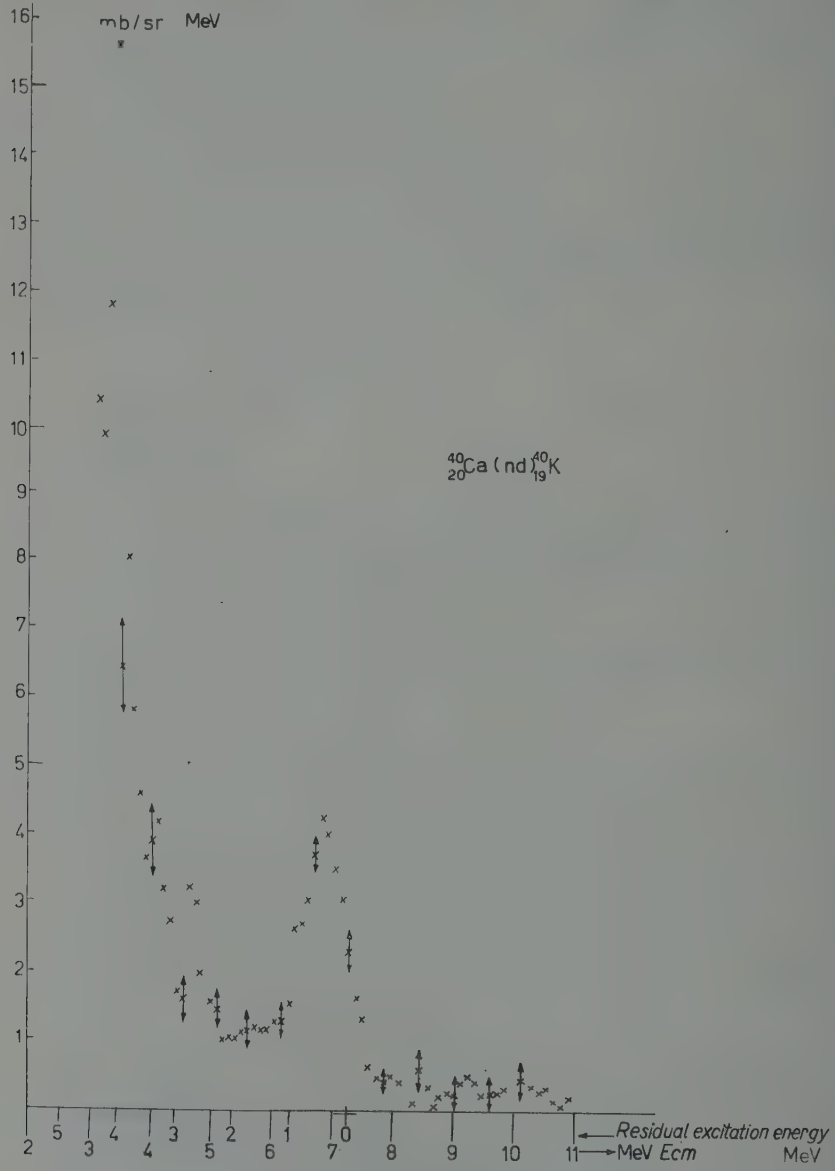

Fig. 2. – Spectrum of deuterons from the reaction ^{40}Ca(n, d)^{39}K.

of a series of excited levels of ^{39}K (2.53, 2.82, 3.02, 3.60). It is interesting to note the much greater intensity that this part of low energy has in comparison with the peak corresponding to the fundamental level, in spite of the

Coulomb barrier which should appreciably reduce the intensity at these low energies.

Following the description of the reaction (n, d) by means of the pick-up effect, it is possible to conclude that one or more levels of ^{39}K above 2.63 MeV of excitation have a greater reduced width in comparison with that belonging to the fundamental state.

Taking into account the description of the mechanism of (n, d) given by Butler's theory, we may presume that the reduced width pertaining to the transition from the fundamental state of the initial nucleus to an excited state of the final nucleus is particularly large when this level is obtained by removing a proton from one of the deep shells in the nucleus. In the case under consideration, the shell immediately beneath the last filled shell of ^{40}Ca consists of two S protons. The protons extracted from this shell should have an angular momentum $l = 0$, and therefore a great probability of being emitted forward, whereas those extracted from the last shell $d\frac{3}{2}$ having a $l = 2$ would not have their maximum in the forward direction. Lacking knowledge of the angular distribution of these deuterons, we cannot at this stage give a definite interpretation to this measurement.

^{55}Mn(n, d)^{54}Cr. – According to the values of the binding energies given by WAPSTRA, the deuterons that leave the residual nucleus in its fundamental state have and energy of 7.7 MeV. At this energy there is very small intensity for the spectrum of ^{55}Mn(n, d)^{54}Cr shown in Fig. 3. On the basis of the shell model, the last proton belongs to an $f\frac{7}{2}$ shell. This results in an angular distribution of the deuterons of the (n, d) corresponding to $l = 3$, hence with and intensity in the forward direction that sbould be practically zero. A peak at 0.90 MeV of excitation energy is then visible, which is in good agreement with the position of an excitation level of ^{54}Cr found by means of the reaction ^{53}Cr(d,p)^{54}Cr(7).

The peak at excitation energy 1.8 MeV shows a level hitherto unknown.

Towards low energies a rapid increase of intensity is obtained, with perhaps an indication of a peak at 3 MeV.

Two levels, respectively at 1.2 and 2.6 MeV, found by means of the reaction ^{53}Cr(d, p)^{54}Cr, do not give an appreciable contribution here.

It is interesting to note that the two reactions (d, p) and (n, d) which give the same residual nucleus do not always show the same levels of this one. This can be easily explained if one takes into consideration that the reaction

(7) F. A. EL BEDEWI and S. TADROS: *II United Nations Intern. Conf. on the Peaceful Uses of Atomic Energy*, A/conf/14/P/1482 (1958).

(d, p), as has been shown by some authors ([8-9]), has a greater probability, for levels or groups of levels of the residual nucleus which probably correspond to the excitation of a state of single particle obtained by adding a neutron, whereas in the reaction (n, d) there is a greater probability with respect to levels obtained

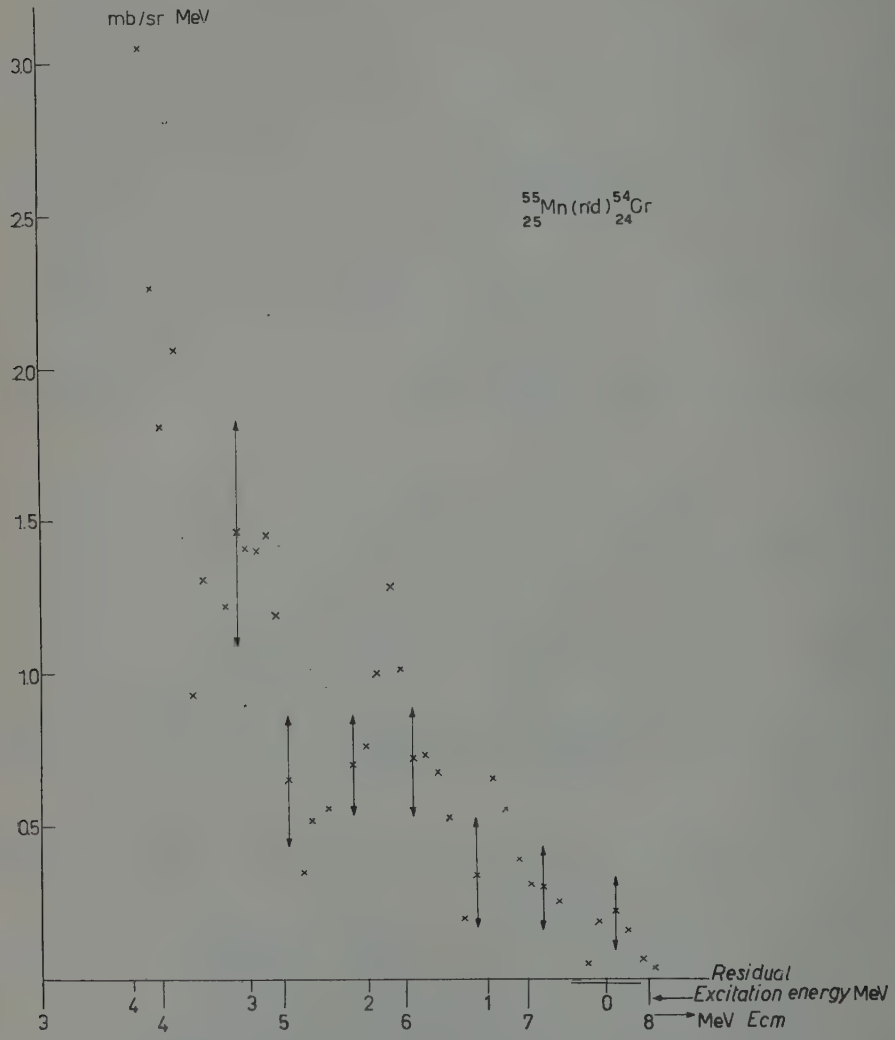

Fig. 3. – Spectrum of deuterons from the reaction $^{55}Mn(n, d)^{54}Cr$.

([8]) L. COLLI and S. MICHELETTI: *Nuovo Cimento*, **6**, 1001 (1957).

([9]) J. P. SCHIFFER, L. L. LEE jr., J. L. YNTEMA and B. ZEIDMAN: *Compt. Rend. du Congrès Intern. de Phys. Nucl., Paris, Juillet 1958* (Paris, 1959), p. 536; J. P. SCHIFFER and L. L. LEE jr.: *Phys. Rev.*, **109**, 2098 (1958).

by subtracting a proton, that is levels of single hole that will evidently be different.

It is particularly interesting to note how the resolved peaks of Mn apparently give rise to a gross structure around an excitation energy of 2 MeV.

This spectrum, together with that of Rh given further on, shows evidently the existence of a gross structure even for this type of reaction, which are similar to those found in the spectra of (d, p) and (n, p) reactions ([4-8-9]).

^{63}Cu(n, d)^{62}Ni. – The spectrum of the deuterons from ^{63}Cu(n, d)^{62}Ni again presents the peak corresponding to the rather intense fundamental level, while a peak corresponding to the excitation energy 1.17 MeV of ^{62}Ni is hardly

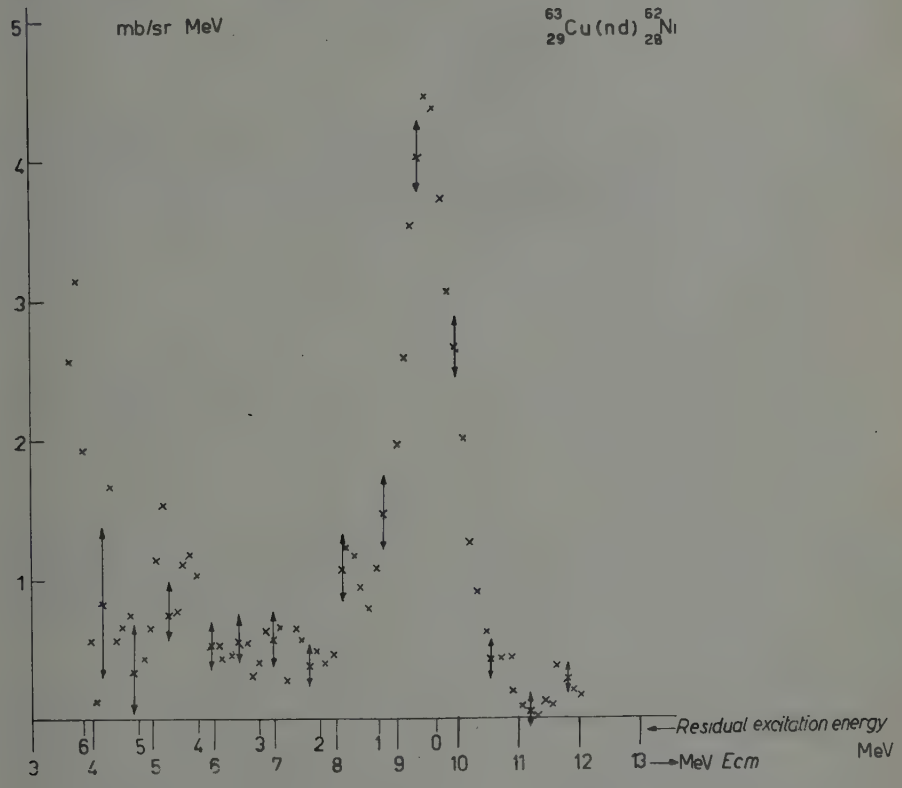

Fig. 4. – Spectrum of deuterons from the reaction ^{63}Cu(n, d)^{62}Ni.

visible. The little hump at 2.5 MeV may possibly contain the well-known Ni levels at 2.05 and 2.3 MeV.

^{63}Cu has only one proton on the $p\frac{3}{2}$ level besides a core which closes at the magic number 28 with the subshell $f\frac{7}{2}$: The fact that there is a strong contribution corresponding to this last proton is therefore significant. On the

other hand, a contribution of far less importance is to be expected from the other protons, both because of the angular distribution (refer to discussion on Mn) as for the fact that the 8 protons $f\frac{7}{2}$ are more bound to each other.

^{103}Rh(n, d)^{102}Ru. – For this nucleus we had to use a rather thick target. The energy resolution is therefore worse than in the other cases.

This interesting spectrum shows clearly enough two gross structures with the respective maxima at 0 MeV and 3 MeV on the scale of the excitation energy

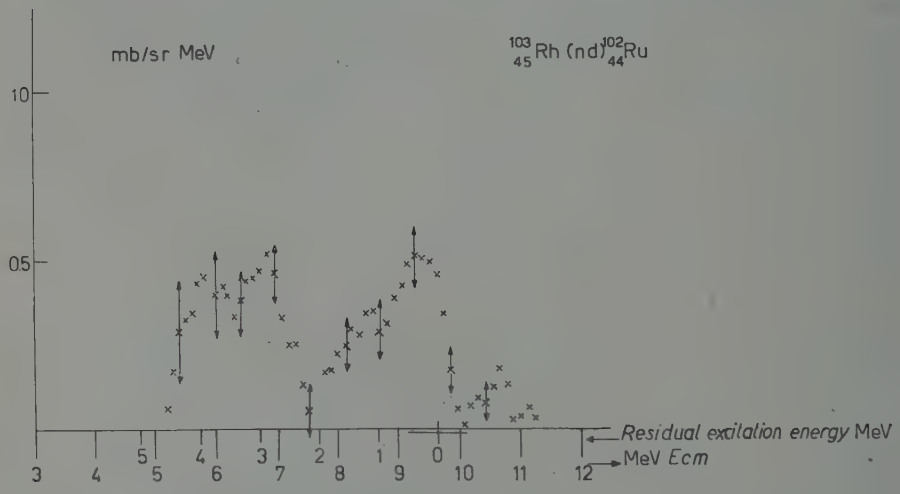

Fig. 5. – Spectrum of deuterons from the reaction ^{103}Rh(n, d)^{102}Ru.

of the residual nucleus ^{102}Ru. As two levels of this nucleus are known, namely at 0.47 and 1.1 MeV, it is certain that the levels are sufficiently dense even at few MeV of excitation energy, so much so that we can be sure that the two humps (gross structures) contain several levels.

These two humps of the deuteron spectrum of Rh explain now the reason for the existence of the two humps in the spectrum of the particle which in the spectra (n, p)+(n, d) ([10,11]) were believed to be exclusively protons. These humps are entirely to be attributed to the deuterons, as is shown by their position in energy and by their intensity. The reaction being of the pick-up

---

([10]) L. COLLI, U. FACCHINI, I. IORI, G. MARCAZZAN, A. SONA and M. PIGNANELLI: *Nuovo Cimento*, **7**, 400 (1958).

([11]) G. BROWN, G. C. MORRISON, H. MUIRHEAD and W. T. MORTON: *Phil. Mag.*, **2**, 785 (1957).

type, these hump are, with every probability, to be attributed to the levels of a single hole.

* * *

The authors gladly thank Prof. L. ROSENFELD for very interesting discussions and Prof. P. CALDIROLA and Prof. C. SALVETTI for their continuous interest and encouragement.

RIASSUNTO

Sono presentati gli spettri di energia dei deutoni emessi dagli elementi ^{27}Al, ^{40}Ca, ^{55}Mn, ^{63}Cu e ^{103}Rh a seguito del bombardamento con neutroni da 14 MeV. Sono stati trovati picchi di deutoni corrispondenti sia allo stato fondamentale che agli stati eccitati del nucleo residuo. Nel Mn e nel Rh è mostrata l'esistenza di larghe strutture negli spettri.

IL NUOVO CIMENTO Vol. XIV, N. 5 1° Dicembre 1959

The Logical Foundations of Invariance Principles in Physics - I.

E. Fabri

Istituto di Fisica dell'Università - Pisa
Istituto Nazionale di Fisica Nucleare - Sezione di Pisa

(ricevuto il 18 Settembre 1959)

Summary. — The logical foundations of invariance principles in physics are discussed with the aim of clarifying the physical meaning of the main concepts and operations involved. Care is taken to avoid the use of coordinate systems, which are likely to lead to misunderstandings in the most critical points. The group character of the reference changes is studied, and its relation with the assumption of a postulate of equivalence is shown. The physical consequences of the conclusions of this work for the most usual laws of invariance will be discussed in a subsequent paper.

1. – Introduction.

The existence of laws of invariance under suitable transformations has been recognized since long time in many physical phenomena. We may go back to Galilei for the first exact formulation of the invariance of the laws of mechanics for two reference frames moving with a translational uniform motion relative to each other; it must also be noted that Galilei's recognition of this law was not a purely theoretical one, since he based upon it his argument concerning the unobservability of earth's motion through mechanical experiments. Nevertheless, the fruitfulness and importance of Galilei's discovery were not fully recognized at that time, and during a long time—perhaps because of Newton's authority, and of his « absolute space »—the principles of invariance did not receive much attention from physicists. It was only for the work of the great mathematicians of last century (such as Hamilton, Gauss, Riemann, Klein, Lie, and others) that the general theory of invariants assumed a systematic form through the introduction of the concept of *group of transformations*. But to see a physical application of the new ideas we must arrive to this century, with Einstein's most fundamental contribution in the

theory of relativity, and with the work of WIGNER, WEYL, etc., in quantum mechanics.

At present the use of the groups of transformations and the search for principles of invariance are essential tools for the theoretical physicist in particle and field theory: it is well known that the recent discovery of non-conservation of parity in weak interactions has been one of the most stimulating of last years, and that many discussions have arosen about the physical interpretation of such a result. Should we infer that God can distinguish right from left, or that the neutrino possesses a « helicity »? In this case, should we expect two neutrinos with opposite helicities to exist? How is it possible that parity does not conserve? Is not parity conservation a principle of the same kind as the principle of relativity? These are some of the questions put forward by parity non-conservation; apart from the answers they may receive, the only fact that they have been asked proves that the whole of the principles of invariance is by no means a definitely clarified matter.

In this paper I will expose some results obtained by treating the whole matter from a viewpoint rather different from the usual one: indeed, I will try to study the problems that will arise, by going back to the physical meaning of the concepts involved, while doing a most cautious use of the formal apparatus (co-ordinates, transformation equations, etc.). This is because I think that many confusions and obscurities often encountered in dealing with this matter originate in the use of a formal apparatus whose interpretation is often not unique.

I would like to emphasize this point, since the current opinion is rather different: it is usually assumed that a formal treatment of an invariance law is the best one can desire, or, at least, the best one can obtain in many cases. Moreover, it is a common practice to devise new invariance laws and to study their consequences on a merely formal ground, paying no attention to their operational meaning. The reason for doing so is obvious: it is easy (at least by principle) to draw formal consequences from a law which has been given a definite mathematical form, whereas it is much more difficult to express that law in an operationally meaningful form. One could also observe that the latter is too strict a requirement, and not fully necessary if the law—though it has been given only a formal expression—is capable of giving predictions that can be checked by experiments; I cannot give a logical confutation of this viewpoint, but I am afraid that it lets too much freedom in our search for a good law of invariance. On the contrary, I believe that by strictly adhering to an operational viewpoint, many laws could be discarded, among the ever growing number that are proposed.

Having this program in mind, it is easily understood why the first part of this paper is a purely logical treatment of the matter. Though a logical analysis cannot, in my opinion, give itself the solution of our physical problems,

it is necessary in order to prepare the instruments and to clearly define the matter with which physicists will work. In the following, therefore, a general formulation of the principles and the deduction of some logical results will be given. No physical conclusion will be drawn in this part, the discussion of the consequences of its results for the physical world being deferred to Part II.

In Section **2** some fundamental definitions are stated, such as the ones of reference frame, of description, etc., with special emphasis on the distinction between the physical aspects and the abstract ones, as represented by the widespread concept of co-ordinate system. Throughout Part I the use of co-ordinates is avoided, because of the reasons explained above: it is thus shown that co-ordinates are not necessary in order to state such fundamental results as the invariance properties of physical laws (though they may be of much use in practical applications).

Section **3** is devoted to the discussion of the relation between different reference frames: the concept of « coherent » reference frames is introduced there. The same matter is more fully developed in Section **4**, where some notations are introduced and some statements are expressed through the methods of symbolic logic. This is done with the main purpose of giving a more synthetic expression to some definitions and theorems relating to facts and descriptions, as well as the connection thereof. The most important concepts introduced are the « truth » of a fact and the « reliability » of a description.

Section **5** deals with the main subject of this paper, *i.e.* « the general principle of equivalence ». A general expression is given there to the idea that two different reference frames should be in some way equivalent as to the description of physical world. By this way we can express a general symmetry of physical laws, as formulated in restricted fields by the various invariance laws introduced till now. No assumption is made as to the validity of the principle, but it is always shown its connection to invariance requirements for physical laws. The main point in this connection—to be developed further in Part II—is the rule stating that no invariance law can be given a physical meaning if one cannot find a reference change associated with it.

While this work was in progress, the author had the opportunity of reading a manuscript by V. BARGMANN, A. S. WIGHTMAN and E. P. WIGNER, circulated at the Varenna Summer School of Physics, 1958 (after referred to as BWW), where many points are discussed which are in a strict connection with the matter being dealt with here. The viewpoint held by BWW is in many respects similar to the author's, but there are also some important differences, which are discussed in Section **6** (1).

Section **7** is a short conclusion, where the programm of Part II is sketched.

(1) For a treatment on the same lines of BWW's see also R. HAGEDORN: *Suppl. Nuovo Cimento*, **12**, 73 (1959).

2. – The logical elements of a physical description (2).

In setting up a logical basis for a theory of the laws of invariance, the first point to be discussed is that of « *reference frame* » (shortly, RF). It is meant here in its most general acception: by RF I will mean the whole complex of *objects* which are necessary and sufficient for setting up a « *description* » of the physical phenomena which are of interest.

Some words of comment will be needed to the foregoing sentence. First, I would observe that the definition or RF is founded upon the undefined word « description »; but to this I shall return later. Secondly, it must be stressed that the principal aim of the given definition of RF is to point out that it must be an assembly of physical objects, and not an abstract thing: it must be clearly distinguished between the RF on one hand and a « *co-ordinate system* » (shortly, CS) on the other. A CS must always rest on a RF, since by CS I will mean a set of rules whereby to find, in the given RF, some numerical elements that will be used as a part of the description of the physical situation one is examining. On the contrary, a RF may, by principle, always stay by itself, without any CS attached to it, or it may have more. In the first case, we are in a situation like that one has when working with synthetic geometry (which, contrasted with analytic geometry, makes no use of co-ordinates): this is quite possible, though in practice it is much easier in many cases to use a suitable CS. In the latter case, if one has to do with several CS's in one RF, the problem arises of establishing *transformation rules* for the co-ordinates of the various systems. But it is clear that no physical question can arise in solving such problem, so that I will not enter here into further details.

It would remain now to explain what is meant by *description* of a physical situation or phenomenon. I think, however, that the common sense usage of the word is good enough for the present purpose, whereas a discussion of it would bring us away from our main subject. It is only to be noted that a description is a matter of language, *i.e.* it is to be meant as a succession of words, symbols (numerical, geometrical, etc.), and that after that it has to meet some requirements of *adequacy* (faithfulness, completeness, etc.), with which we will never the concerned in the following. Another distinction must be made, however, between a description having a *sense* and its having a *deno-*

(2) For a better understanding of the topics of this section the reader could refer to MORRIS' book: *Segni, linguaggio e comportamento* (Milano, 1949). A discussion of the theory of equivalent descriptions is found in H. REICHENBACH: *I fondamenti filosofici della meccanica quantistica* (Torino, 1954), though the aim of Reichenbach's treatment is quite different from the present one.

tation. Roughly speaking, a description will be said to have a sense when it may be interpreted as a description of a *fact*, no matter if it is a *real* (or *true*) fact, or not; a description will be said to have a denotation if the fact described is *real* (or at least realizable). I will not attempt to give a more precise definition of what is meant by sense and by denotation: it will be enough for us to point out that the sensedness of a description may be verified by examining its conformity to some formal rules not to be specified here, but without any reference to experimental proof; on the contrary, we can assert that a description denotes only by showing that the fact described actually happens (or might happen, if suitable conditions would be satisfied).

In the foregoing analysis, the concept of description was founded upon that of *fact*, which we must briefly analyze. Without entering the deep-seated intricacies of this subject, I will only stress that a fact must be—in opposition to the linguistic, conventional character of a description—a part of what we usually call *the real world*, *i.e.* it must have an objective character, irrespective of the many different appearances it may exhibit to various observers in different RF's. It must still be observed that a fact—in our acception—may not be real, without losing its objectiveness. For instance, if I say: « two positively charged particles attract each other » this is the (shortened) description of a fact, but the fact is not real nor realizable. What really matters is that, even in this case, the reality or irreality of the fact cannot depend on the RF or on the language used. All physicists in the world agree that two positively charged particles cannot attract each other, and this is what is needed, for we may say that the above description refers to a fact, though it is not real. Of course, the description has a sense, but no denotation.

3. – The connection between two different RF's.

We are now faced with a question, arising from our assumption that several RF's may be equally suited for studying physical phenomena. That is, we must now discuss the relation between the descriptions of the same fact from two different RF's, or, alternatively, between two facts that are described in the same way from both RF's. To begin with, I will make the following assumptions:

a) given a fact, it may be described as well from a RF, R_1, as from another, R_2;

b) given a description, if it has a sense for R_1, the same happens for R_2, and *vice versa*.

If *a*) and *b*) are verified, R_1 and R_2 will be said to be *coherent*.

Before going further, a discussion is needed of some underlying ideas, whereon assumptions *a*) and *b*) above are strongly dependent. First of all, at least from a practical point of view, assumption *a*) will be not verified if R_1 and R_2 are too far away in space or in time, and in many other cases too; in other words, assumption *a*) puts a restriction on the class of RF's to be considered, and possibly also on the class of facts. As to assumption *b*), it obviously implies that the languages used in connection with both RF's are the same, *i.e.* a communication must be possible about the possible experiments in R_1 and in R_2. Moreover, we must be able to state that in R_1 and in R_2 we are describing *the same* fact. But in order to verify the sameness of descriptions as well as that of facts, some communication rules and invariance principles are to be known in advance: is it not this a vicious circle?

The argument above is quite right, of course, but the existence of a circularity causes no trouble if we pay due attention to the constructive aspect of the process outlined. In fact, the whole existence of a scientific language requires that a previous agreement exist about certain facts and laws, the agreement growing wider and deeper as long as the language gets refined, thus permitting to describe new facts; these then cause an extension and a greater functionality of the language, etc. In Part II we will see some instances of such process: but this same paper could be written because a partial agreement already exists about its subject and a sufficiently effective language is available; on the other hand, it may hope to be of some usefulness although the agreement is not complete and the language not perfect.

It is readily seen that coherence is a transitive relation: thus we may speak of a class of coherent RF's. In the following we will always be concerned with such a class (which is by no means unique). No explicit reference will be made to the coherence of RF's nor to the sensedness of a description; both facts, however, will always be assumed.

4. – Formal restatement of the relation between RF's.

We will introduce the following notations:

— $\delta_R F$ for the description in the RF R of the fact F;

— $\varphi_R D$ for the fact whose description in the RF R is D.

Of course:

$$\delta_R \varphi_R D = D \,, \tag{1}$$

$$\varphi_R \delta_R F = F \,, \tag{2}$$

i.e. the operators δ_R and φ_R are inverse to each other. This is a restatment of the one-one correspondence existing in any RF between a fact and its description.

If two RF's are taken into account we may put, for a given F:

$$\begin{cases} D_1 = \delta_{R_1} F , \\ D_2 = \delta_{R_2} F , \end{cases} \tag{3}$$

therefrom:

$$\begin{cases} D_1 = \delta_{R_1} \varphi_{R_2} D_2 , \\ D_2 = \delta_{R_2} \varphi_{R_1} D_1 , \end{cases} \tag{4}$$

and if we define $\tau_{R_1 R_2}$ as a shorthand notation for $\delta_{R_1} \varphi_{R_2}$:

$$\begin{cases} D_1 = \tau_{R_1 R_2} D_2 , \\ D_2 = \tau_{R_2 R_1} D_1 . \end{cases} \tag{5}$$

Obviously $\tau_{R_1 R_2}$ and $\tau_{R_2 R_1}$ are reciprocal of each other; eqs. (5) state that the descriptions of the same fact from two different RF's are in a one-one correspondence, depending only on the two RF's. In other words, a reference change defines a one-one mapping of the space of descriptions onto itself, so that such descriptions correspond that belong to the same fact before and after the change. Just on the same lines we may fix a description D, and put:

$$\begin{cases} F_1 = \varphi_{R_1} D , \\ F_2 = \varphi_{R_2} D , \end{cases} \tag{6}$$

and then:

$$\begin{cases} F_1 = \varphi_{R_1} \delta_{R_2} F_2 , \\ F_2 = \varphi_{R_2} \delta_{R_1} F_1 . \end{cases} \tag{7}$$

Putting $\theta_{R_1 R_2}$ as a shorthand for $\varphi_{R_1} \delta_{R_2}$, we have:

$$\begin{cases} F_1 = \theta_{R_1 R_2} F_2 , \\ F_2 = \theta_{R_2 R_1} F_1 , \end{cases} \tag{8}$$

where $\theta_{R_1 R_2}$ and $\theta_{R_2 R_1}$ are inverse to each other, thus expressing that a one-one correspondence exists between two facts, whose descriptions from two RF's

are the same. In other words: a reference change defines a one-one mapping of the space of facts onto itself, so that such facts correspond, that have the same description before and after the change.

We want now to go somewhat farther into the study of the transformations τ and θ. In particular, it is very interesting for us to see whether the τ's and the θ's possess group characters, in a sense to be explained later.

Of course, we can always define a product of two τ's, as follows:

$$\tau_{R_1 R_3} = \tau_{R_1 R_2} \tau_{R_2 R_3} ,$$

and the same for the θ's, but this is not enough. No meaning could be assigned to an expression like $\tau_{R_1 R_2} \tau_{R_1 R_3}$—as it would be necessary if the τ's are to form a group—unless it is possible to find an R_4 such that $\tau_{R_1 R_3} = \tau_{R_2 R_4}$. Then, indeed, we would have:

$$\tau_{R_1 R_2} \tau_{R_1 R_3} = \tau_{R_1 R_2} \tau_{R_2 R_4} = \tau_{R_1 R_4} .$$

So, in order that the τ's form a group, the following should be true: given three RF's: R_1, R_2, R_3, there always exists an R_4 such that $\tau_{R_1 R_3} = \tau_{R_2 R_4}$. But I cannot see how this could be proved in the general case.

The same applies to the θ's too; but we shall see later that in a very important case the group property for the τ's and the θ's can be proved.

In the foregoing definitions of operators δ, φ, τ, θ, a remarkable symmetry was exhibited between facts and descriptions. I will now show that the symmetry is destroyed if « truth » is taken into account. Only in next section will we be able to recover the symmetry by introducing a new principle, which is the main object of our investigations.

In order to express that a fact is *true* I will adopt a functional notation:

$$\Phi(F) .$$

Of course, the truth of a fact is quite independent of the RF, as we have already pointed out. $\Phi(F)$ may be read: « the fact F is true »; or else: « F belongs to the class Φ (of true facts) ». If F is true, a description of it will be said *reliable*. We may then put by definition:

$$\Delta_R(D) \equiv \Phi(\varphi_R D) , \tag{9}$$

to be read: « D is reliable in the FR R if and only if the fact of which D is the description in R, is true ».

From (9) one can easily deduce ([3]):

$$(10) \qquad (R)\Delta_R(\delta_R F) = \Phi(F)\,,$$

to be read: « if F is true, then for all R its description in R is reliable, and *vice versa* ». It will be noted that (9) and (10) are not symmetrical; this is due to the appearance on the subscript R to Δ, which is not needed to Φ. While it is obvious that it should be so, we may attempt to restore the symmetry by a new postulate. This will be discussed in the next section.

5. – The general principle of equivalence.

The concepts and notations developed in the preceding sections are of a rather general character, and their validity may hardly be questioned (at least as long as one tries to avoid highly involved philosophical questions). We cannot, however, content ourselves with a framework which is too general to be useful for our purposes: we must find the way to give a general formulation to the intuitive idea that something like an « equivalence » of the various RF's should exist. We are also prepared to find some limits to our requirement: it will be a matter of experience how far the equivalence of RF's can be extended. At present it will be better to give an exact definition of our ideas, and to draw all consequences we will be able to do; in Part II physical conditions, experimental proofs, etc., will be discussed as fully as necessary.

When we say that two RF's are equivalent, we usually mean that the physical laws hold equally true in both RF's, *i.e.* that if certain relations exist among the physical quantities relating to a given phenomenon in the first RF, it will be possible to find another phenomenon for which the same relations hold, with the same values for the quantities involved, in the second RF. By using our terminology, we may say: *two RF's are equivalent if and only if any description which is reliable in one, is reliable in the other too.* Formally

---

([3]) The proof may run as follows: substituting $\delta_R F$ for D into (9) we have:

$$(*) \qquad \Delta_R(\delta_R F) \equiv \Phi(\varphi_R \delta_R F)\,,$$

which, using (2) becomes:

$$(**) \qquad \Delta_R(\delta_R F) \equiv \Phi(F)\,.$$

Since the second member of (**) does not depend on R, we may apply to the first member the universal quantifier (R) (to be read: « for all R ... »), thus arriving to (10).

that means:

$$(11) \qquad (D)\{\Delta_{R_1}(D) \equiv \Delta_{R_2}(D)\} .$$

We are now in a position to state the *general principle of equivalence*, as follows: *all coherent RF's are equivalent to one another.* In formulae:

$$(12) \qquad (R_1)(R_2)(D)\{\Delta_{R_1}(D) \equiv \Delta_{R_2}(D)\} .$$

Hence we may deduce that the subscript R in Δ is superfluous: if the general principle of equivalence is assumed, the class of reliable descriptions becomes independent of the RF. We will then be able to simply speak of « a description being reliable », and write:

$$\Delta(D) .$$

From (9) we can deduce:

$$(13) \qquad \Delta(D) \equiv (R)\Phi(\varphi_R D) ,$$

whereas (10) becomes:

$$(14) \qquad \Phi(F) \equiv (R)\Delta(\delta_R F) ,$$

thus showing again a perfect symmetry between facts and descriptions.

Let us take again into account the problem we left unsolved in last section, concerning operators τ (and θ). Now it will be possible to show that such operators do form a group, and to investigate some properties thereof. Remember that what is to be proved is: « given three RF's, R_1, R_2, R_3, there always exists and R_4 such that $\tau_{R_1 R_3} = \tau_{R_2 R_4}$ ».

Last sentence may be expressed as follows:

$$(15) \qquad (\exists R_4)\{\tau_{R_1 R_3} = \tau_{R_2 R_4}\} .$$

Expression (15) may be interpreted as the description in RF R_2 of a fact; what is to be shown is that such fact is true. But it is certainly so if we take $R_2 = R_1$, as the R_4 we are looking for is then R_3. For any other R_2 we have to verify a fact whose description is reliable if referred to R_1: for our general principle of equivalence such fact must also be true, wichever R_2 be (4).

We can easily deduce from what we have just shown, that if we fix a RF: R, the class of transformations $\tau_{RR'}$ (all R') exhausts the class of all τ's. In

(4) A formal proof of this theorem would require some refinements in the forma system we have sketched, and this is beyond our present concern.

order to complete the proof that such class is a group, it only remains to show that the only R' for which $\tau_{RR'}$ is the identity, is R itself. But this is implied in the definition of RF. If we could have, indeed, a RF R' such that the description in it of any fact always coincides with that we give in R, there could be no way of distinguishing between the two RF's; they should then be looked upon as the same.

As a consequence of the foregoing arguments we can now express the relation among facts, descriptions and RF's in many different forms. After noting that the same arguments above might have been repeated for the operators θ too, I will no longer dwell upon this point, since it will be of little use later. Instead, I would like to point out that our preceding results enable us to speak of the τ-group independently of any previously chosen RF; on the contrary, *we can interpret an operator of the group as building up a mapping of the class of coherent RF's onto itself*, so that all properties of all possible changes of RF can be studied with reference only to our group. In particular, an important result is obtained if we try to express the general principle of equivalence as a property of the group.

We may transform (12) through (9):

$$(R_1)(R_2)(D)\{\Delta_{R_1}(D) \equiv \Phi(\varphi_{R_2} D)\} .$$

Instead of φ_{R_2} we may write:

$$\varphi_{R_1}\delta_{R_1}\varphi_{R_2} = \varphi_{R_1}\tau_{R_1R_2} ,$$

and we get:

$$(R_1)(R_2)(D)\{\Delta_{R_1}(D) \equiv \Phi(\varphi_{R_1}\tau_{R_1R_2} D)\} ,$$

wherefrom, using (9) again:

$$(R_1)(R_2)(D)\{\Delta_{R_1}(D) \equiv \Delta_{R_1}(\tau_{R_1R_2} D)\} .$$

This may also be written:

$$(R_1)(\tau)(D)\{\Delta_{R_1}(D) \equiv \Delta_{R_1}(\tau D)\} ,$$

having made use of our result that $\tau_{R_1R_2}$ for all R_2 spans the whole group of τ's. Then we may suppress the subscript R_1 to Δ, and finally get:

$$(\tau)(D)\{\Delta(D) \equiv \Delta(\tau D)\} . \tag{16}$$

Eq. (16) is of a most fundamental importance, since it expresses that the group τ transforms a reliable description into a new reliable description. Hence we may infer that *any reliability criterion for a description must be invariant under group* τ. It is not difficult to see that a reliability criterion is nothing but a physical law, so that we have justified the requisite according to which physical laws must be invariant under reference changes, giving a more precise meaning thereto.

6. – Comparison with BWW's treatment.

The first point to be noted in BWW's paper is the definition of two kinds of identity, concerning physical systems: *bodily* and *subjective*. There is a close parallelism between this distinction and my emphasis on the relation between *facts* and *descriptions*, though BWW prefer to speak about « observers » and « systems », whereas I have found better to use the terms « reference frame » and « fact ». The difference may be of some philosophical relevance, but it brings little or no consequence for the main problem wherein we are interested.

The second, more important point is about what takes the place of our « description » in BWW's treatment. Since these authors were primarily interested in a quantum theory, they have directly used the quantum formalism: a « description » in quantum language becomes a Hilbert space, some rays and/or vectors in it, and possibly some operators. We shall see later how this correspondence can be traced into the postulates of the two theories. But the reason for our most abstract treatment must now be discussed.

One could think that an abstract treatment may be preferable for the only reason that it gives a unified account of both classical and quantum theories. But this is not the strongest reason: what has been said in the introduction against the formal treatment forces to a unique choice. If we want to avoid co-ordinate systems and all the ensuing apparatus, we are only left with such general and abstract tools as « descriptions », « facts », etc. One instance of the different attitude one is led to assume whether the abstract viewpoint is adhered to, or not, may be seen in the discussion about the meaning of « relativity group ».

If a formal view is adopted, a reference change is nothing but a co-ordinate transformation, and thus fully characterized by the transformation law. It follows therefrom, as an obvious consequence, that the set of all reference changes is a group. In the preceding treatment we have seen, on the other hand, that the group property could not be proved until a relativity principle was not assumed. This is because the explicit use of reference frames as dis-

tinct physical objects did not enable us to speak of a reference change in itself, abstracted from its objects. This is quite possible when co-ordinates are used, as we are naturally led to identify the co-ordinate (mathematical) spaces of all reference frames, so that no difficulty arises in defining the product of two reference changes.

Another proof that this is a critical point may be seen in the use made by BWW of the phrase: « ... does not depend on both inertial frames A and B but only on their relation to each other », which is explained later by saying that by this relation is meant the transformation between CS's. This transformation is thought of as a purely mathematical fact, and this enables to overcome the difficulty. In our treatment, on the other hand, the result that the relativity group is independent of the RF is achieved only in Section **5**, after introducing the principle of equivalence. Of course, the two ways of proceeding are equivalent as far as the final results are concerned; but I think that the abstract treatment gives due relevance to the intervention of the principles of equivalence, whereas in the formal treatment it must be introduced too early, thus rendering more difficult its full appreciation.

We can now examine BWW's postulates and find how they are to be translated if the abstract viewpoint is adopted. Postulates I and II are not relevant for our discussion, as these fix the type of description to be used (the quantum one). Postulate III, concerning the identity of results for two observers dealing with bodily the same system, and measuring bodily the same observable, should be interpreted as an essential part of the definition of bodily identity. Postulate IV may be divided into two postulates: IV′ states that all RF's are coherent, while IV″ is exactly equivalent to our formula (12), *i.e.* the first expression of the general principle of equivalence. After postulate IV BWW introduce a ray correspondence which is directly related to our operator τ. We have already seen that BWW assume that the τ's have the group property; they also state that the independence of the τ-group from the RF can be proved starting from their postulate I-IV, but do not give the proof, which has been given in Section **5**.

The last point to be noted in BWW's paper is the discussion of the active and passive interpretation of reference changes. The main point of the discussion is fully appreciated and clearly expressed by BWW: the passive point of view requires the use of a transformed measuring apparatus, which is quite difficult to conceive in some cases (it is usual to make in this connection the example of time reversal; but what about charge conjugation?). The active point of view enables us to circumvent the difficulty, thus proving very useful in the actual use of invariance principles; but this is true only if a formal treatment (in the sense explained above) is adopted. If an operational viewpoint is followed, we are forced to assume that a reflected (or a rotated, or more generally a transformed) system can be realized, whatever the original

system may be: we can consider as such a system the measuring apparatus itself, and thus we are faced again with the same difficulty the active point of view had to overcome.

An objection to this argument could be raised: after the passive point of view we have not only two *systems*, but two *observers* as well, and very often it is rather difficult to « transform » an observer. It is for this reason that I have preferred not to speak about observers, but only about reference frames: as far as physics, and not psychology, are concerned, a reference frame (or a measuring apparatus, which is much the same) is all what is needed. By this way we can avoid such psychological difficulties as are frequently encountered when dealing with reference changes, the most conspicuous example of which is given by the problem of the physical realizability of time reversal (5).

7. – Concluding remarks.

In the foregoing the general principle of equivalence was formulated, and some direct consequences deduced therefrom; the next point to be discussed should be the truth of the principle and the role it can play in physics (in particular, in elementary particle physics). We should be prepared to find that our principle will be of no absolute validity; in such case we would not have to deal with the whole group τ, but with a sub-group of it, corresponding to the restricted class of RF's to be considered equivalent to one another. Actually, many of these subgroups (and perhaps all of them) are already known and have been thoroughly studied since a more or less long time; thus, the only thing to be done is a review of such subgroups with the aim of identifying the associated class of RF's (whenever one can be found). Then, for each subgroup we will be able to decide, on the ground of experience, whether an equivalence principle holds true or not.

The analysis, sketched hereupon, of the various subgroups of the general group, will not be undertaken here: it will be the subject of the second part of this paper. I would like to conclude this general introduction to the matter of invariance principles by re-asserting the fundamental rule that will be followed in applying our results: no one of the many subgroups known so far will be considered physically meaningful, if it will not be possible to find a corresponding class of RF's (in the sense explained in the foregoing). It will appear that new problems arise when the rule is applied to some of the most

(5) For a discussion of this point see: E. Fabri: *Nuovo Cimento*, **13**, 326 (1959).

usual subgroups; it is hoped that a deeper insight into the meaning of the principles of invariance in physics will be reached when all these problems will receive an adequate consideration.

* * *

The author acknowledges Prof. L. RADICATI for his kind interest in this work.

RIASSUNTO

Si discutono i fondamenti logici dei principi di invarianza della fisica, allo scopo di chiarire il significato fisico dei concetti e delle operazioni principali che vi intervengono. In questo studio si è accuratamente evitato di usare coordinate di qualsiasi specie, per non incorrere in equivoci o confusioni nei punti più delicati. Si studia anche il carattere di gruppo dei cambiamenti di riferimento, per mostrarne la relazione con i postulati di equivalenza. In un prossimo articolo verranno esposte le conseguenze fisiche che dalle conclusioni di questo lavoro derivano per le più comuni leggi di invarianza.

IL NUOVO CIMENTO Vol. XIV, N. 5 1° Dicembre 1959

Parity Non-Conservation in Pion Production.

D. Lurié and E. A. Power (*)

CERN - Geneva

(ricevuto il 23 Settembre 1959)

Summary. — In this note we calculate using the method of Weizsäcker-Williams the pion production asymmetry in the scattering of pions on oriented nucleons due to a possible parity violation in the pion-nucleon interaction. One gets an upper bound for the asymmetry using the upper bounds for the parity violation in pion-nucleon scattering calculated by Fubini and Walecka in the assumption of the maximum parity violation in K-production. The result obtained is not inconsistent with the result of a recent pion production experimental results.

Recent experiments (1) to detect an asymmetry proportional to $\bar{\sigma} \cdot \boldsymbol{k}_\pi$ and thus a parity non-conserving effect in meson production in oriented nucleon collisions have shown little evidence for such an effect. Fubini and Walecka (2) have investigated the effect of a possible parity violation in the strong K-hyperon-nucleon interaction on low energy pion-nucleon scattering. They have shown that the possible parity-mixing parameters in pion-nucleon scattering are largest in the $J=\frac{1}{2}$ channel in which they are linear in the meson momentum but that they do not exceed a few percent even with maximum parity violation in the K-hyperon-interaction. The upper limits are $|\varepsilon_{31}| < (q/\mu)\times 1\%$, $|\varepsilon_{11}| < 2(q/\mu)\times 1\%$, where $\varepsilon_{2T,2J}$ is the mixing parameter in the J, T channel. Fubini and Walecka conclude that parity violation effects are expected to be small in low energy pion physics. In this note we make an approximation to the asymmetry possible in meson production in nucleon-

(*) On leave of absence from the Dept. of Mathematics, University College, London.

(1) A. Roberts: *Proc. of CERN Conference on High Energy Physics* (1958), p. 221; D. G. Davis, R. C. Hanna, F. F. Heymann and C. Whitehead: private communication; to be published shortly.

(2) S. Fubini and D. Walecka: *Phys. Rev.*, in print.

nucleon collisions, using a crude form of the Weizsäcker-Williams method to relate the production asymmetry to the mixing parameters in pion-nucleon scattering.

The analysis of FUBINI and WALECKA gives a transition matrix

$$M = f_1 + f_2 \cos\theta + i f_2 \boldsymbol{\sigma}\cdot\hat{\boldsymbol{n}} + g\,\boldsymbol{\sigma}\cdot(\hat{\boldsymbol{q}}_1 + \hat{\boldsymbol{q}}_2) \tag{1}$$

where $\hat{\boldsymbol{n}}$ is the normal to the scattering plane and $\boldsymbol{q}_1$ and $\boldsymbol{q}_2$ are the initial and final meson momenta. f_1 and f_2 are the parity conserving amplitudes while g is the parity non-conserving amplitude given by

$$g_{J=\frac{1}{2}} = \varepsilon_{J=\frac{1}{2}} \frac{(\exp[2i\delta_1] - \exp[2i\delta_0])}{2iq}, \tag{2}$$

in the $J = \frac{1}{2}$ channel. δ_0 and δ_1 are the s- and p-wave phase shifts. It is assumed that the parity mixing effect is small so that only the off-diagonal elements in the S-matrix are changed, and these linearly in ε.

To use the Weizsäcker-Williams approach we first compute the cross-section for meson scattering on a polarized nucleon. It is given by

$$\frac{\mathrm{d}\sigma}{\mathrm{d}\Omega} = |f_1|^2 + |f_2|^2 + (f_2^* f_1 + f_1^* f_2)\cos\theta + \tag{3}$$
$$+ 2\,\mathrm{Re}\,[(f_1^* + f_2^*\cos\theta) g \sin\theta \sin\varphi - i f_2^* f_1 \sin\theta\cos\varphi] + 2|g|^2(1+\cos\theta),$$

where the nucleon is oriented in the y-direction and the pion wave is incident along the z-direction. Bearing in mind the experiment of DAVIS *et al.* [1], we consider the case of π^0 production at 90° in the laboratory due to polarized neutrons of about 490 MeV incident on protons. (The cross-section for π^0 production is much larger for np than for nn at this energy). For laboratory π^0's of 140 MeV, $\theta \doteq 142°$ in the moving frame. The asymmetry can be related to the cross-sections for elastic scattering of π^0's and charge-exchange scattering of π^-'s on polarized neutrons at this angle. If we make the plausible assumption that the dominant production channel is through the $J = \frac{3}{2}$, $T = \frac{3}{2}$ state [3], we retain in (1) the parity conserving amplitude corresponding to this channel only and obtain

$$\lambda = \frac{\sigma_{\mathrm{prod}}^{\parallel} - \sigma_{\mathrm{prod}}^{\perp\perp}}{\sigma_{\mathrm{prod}}^{\parallel} + \sigma_{\mathrm{prod}}^{\perp\perp}} = \frac{\int N(q)\,\mathrm{Re}\,[(f_1^* + f_2^*\cos\theta)\sin\theta\,(2g^{\frac{3}{2}} - g^{\frac{1}{2}})]\,\mathrm{d}q}{\int N(q)[\,|f_1|^2 + |f_2|^2 + (f_2^* f_1 + f_1^* f_2)\cos\theta]\,\mathrm{d}q}, \tag{4}$$

[3] S. MANDELSTAM: *Proc. Roy. Soc.*, **244**, 491 (1958).
[4] W. HEITLER: *Proc. Roy. Irish Acad.*, A **49**, 101 (1943).

$N(q)$ is the number of Weizsäcker-Williams neutral pions of momentum q in the meson cloud (4) and g^T the parity non-conserving amplitude in the isotopic T-state. Expanding the amplitudes in partial waves, *e.g.*

$$g = \sum_{l=1}^{\infty} (g_{l+} - g_{l-}) P'_l(\cos\theta) ,$$

we keep the $l=1$, $J=\frac{3}{2}$ terms for f and the $l=0$, 1, $J=\frac{1}{2}$ terms for g. Taking the Fermi-type phase shifts, so that all angles are small except δ_{33} we obtain

$$\lambda = \frac{\int A(\theta) N(q) [\varepsilon_{11}(\delta_1 - \delta_{11}) - 2\varepsilon_{31}(\delta_3 - \delta_{31})] \sin 2\delta_{33} \, dq}{\int B(\theta) N(q) \sin^2 \delta_{33} \, dq} , \tag{5}$$

where $A(\theta)$ and $B(\theta)$ are known functions in Legendre polynomials. One sees that for Fermi type phase shifts $(\delta_1 - \delta_{11}) > 0$, $(\delta_3 - \delta_{31}) < 0$ and the asymmetry will be largest when ε_{11} and ε_{31} have the same sign. Taking the maximum allowed ε's of reference (2) we can estimate the integrals over q rather crudely, hoping that, since λ is a ratio of cross-sections, the detailed form of $N(q)$ will be unimportant. The asymmetry not only depends on the relative sign of the ε's but is also rather sensitive to the small phases and therefore cannot be estimated very precisely. It is, however, possible to give an upper bound to λ; this is all that is feasible in any case, since only the bounds of the ε's are known. This upper bound to λ varies between 0.3% and 1% depending on the phase shift taken. The small bound to λ is obtained from the CHIU and LOMON (5) phases $\delta_1 - \delta_{11} \doteq 11°$ and $\delta_3 - \delta_{31} \doteq 8°$; the larger from the Bethe de-Hoffman (6) phase shifts.

Such upper bounds imply that the pion production experimental results of the U.C.L.-Harwell group at CERN are not inconsistent with maximum parity violation in K-hyperon interactions (*). At the lower bias of the experiments, mesons of considerably lower energy are included and these would give a lower upper bound to λ due to the smaller phases and mixing parameters in (5). On the other hand, the computation is less reliable at such lower energies. Of course in low energy nuclear processes, the experimental upper limit on the parity non-conserving amplitude is much smaller ($\sim 4 \cdot 10^{-5}$).

---

(5) H. Y. CHIU and E. L. LOMON: *Ann. Phys.*, **6**, 50 (1959).

(6) H. A. BETHE and F. DE HOFFMANN: *Mesons and Fields*, vol. **2** (Evanston. Ill., 1955).

(*) It should also be noted that the latest Berkeley results show no evidence for parity non-conservation in Σ production.

* * *

It is a pleasure to thank the Harwell-U.C.L. group at CERN for discussions on their experiments and to Dr. FUBINI and members of the Theoretical division for helpful comments. We would like to thank Professor BAKKER for the hospitality accorded to us at CERN.

RIASSUNTO

Si calcola col metodo di Weizsäcker-Williams l'asimmetria di produzione di pioni nell'urto di nucleoni orientati dovuta a una eventuale violazione di parità nell'interazione pione nucleone. Si ottiene un limite superior nell'asimmetria usando i limiti superiori sulla violazione di parità in scattering pione nucleone calcolati da Fubini e Walecka nell'ipotesi di massima violazione di parità nella produzione di K. Il risultato ottenuto non è inconsistente con quello di un recente esperimento per rivelare un tale effetto.

IL NUOVO CIMENTO Vol. XIV, N. 5 1° Dicembre 1959

Photoneutrons from K and Ca.

V. Emma and C. Milone

Istituto di Fisica dell'Università - Catania
Centro Siciliano di Fisica Nucleare - Catania

R. Rinzivillo

Istituto Nazionale di Fisica Nucleare - Sottosezione di Napoli

(ricevuto il 24 Settembre 1959)

Summary. — Photoneutrons from Ca and K irradiated with 31 MeV bremsstrahlung are studied by means of nuclear plates. Neutrons emitted at 90° from Ca and 60°, 90° and 120° from K are recorded. The spectra show that at least $\sim 50\%$ of the neutrons above 2 MeV are due to direct process. For Ca and also for K, a second resonance seems to exist about 10 MeV above the threshold. At 31 MeV photoneutron yields for Ca and K (neutron/mole·roentgen) at $\theta \sim 90°$ and for $E_n > 2$ MeV are about the same: $(Y_{Ca}/Y_K) \sim 1.1$.

1. – Introduction.

Systematic study of the photoneutrons has shown the following relationship between neutron spectra and atomic mass number [1]: the spectra become harder, as the mass number decreases.

For heavier nuclei the direct process accounts for about 10% of the emitted photoneutrons. The direct process contribution rises to about 25% for the Al(γ, n) reaction and is prevalent in the O(γ, n) reaction [2].

---

[1] G. Cortini, C. Milone, T. Papa and R. Rinzivillo: *Nuovo Cimento*, **14**, 54, (1959).

[2] C. Milone: *Phys. Rev. Lett.*, **3**, 43 (1959); C. Milone and A. Rubbino: *Nuovo Cimento*, **13**, 1035 (1959).

However, the particular behaviour of the spectrum depends on the particular nucleus investigated (3).

In a previous work we have reported the first results on the energy spectrum of photoneutrons from Ca (4).

A comparison of the experimental spectrum with that given by the evaporation theory, taken for Ca a « nuclear temperature » $T = 1.1$ MeV, shows a relevant contribution of the direct process even in the low energy region: $E_n = (3 \div 4)$ MeV (4).

The nucleus $^{40}_{20}$Ca differs from the most abundant isotope of K ($^{39}_{19}$K = 95 %), only by a proton that fills up the closed proton shell of ^{40}Ca; the neutron shell is closed in both nuclei. Neutron binding energies are nearly 13.2 MeV for ^{39}K, and 16 MeV for ^{40}Ca.

In the present work results on photoneutron spectra from Ca are given with improved statistics and are compared with photoneutron spectra from K.

2. – Experimental procedure.

A spherical target, 3 cm in diameter, of natural K has been irradiated with the collimated bremsstrahlung beam of the B.B. Betatron of Turin. The irradiation was made at $E_{\gamma max} = 31$ MeV.

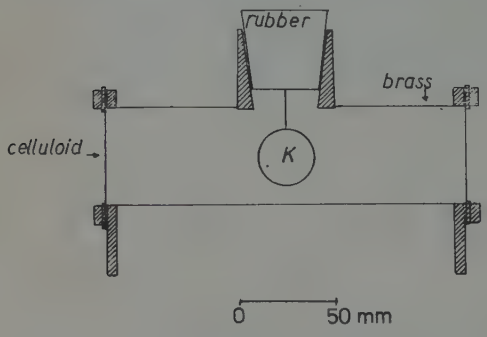

Fig. 1. – Vessel containing the K target.

The photoneutrons, emitted at the laboratory angles of $\theta = 60°$, 90° and 120° with respect to the photon beam, have been recorded by means of proton recoil tracks in Ilford L 4 plates 1 in. × 3 in., 400 μm thick. The distance between the center of the plates and the center of the target was ~ 17 cm. The plates were screened against spurious neutrons coming from the betatron as in a previous work (3).

In order to avoid oxidation the K target was prepared (*) in fused paraffin and was contained in the vessel shown in Fig. 1 during irradiation.

(3) G. CORTINI, C. MILONE, A. RUBBINO and F. FERRERO: *Nuovo Cimento*, **9**, 85 (1958).

(4) A. AGODI, S. CAVALLARO, G. CORTINI, V. EMMA, C. MILONE, R. RINZIVILLO, A. RUBBINO and A. FERRERO: *Compt. Rend., Congrès International de Physique Nucleare*. Paris, 7-12 Juillet 1958 (Paris, 1959) p. 625.

(*) Our thanks are due to Dr. S. PRIVITERA of the C.S.F.N. for his kind help during the preparation of the K target.

The contribution of photoneutrons produced in the celluloid window was negligeable.

For the Ca target (a cilinder 20 mm high and of 29 mm diameter) a thin layer of glicerine was sufficient to prevent oxidation. Photoneutrons emitted at 90° were recorded.

The diameter of the γ beam on the K and Ca targets was 35 mm.

The plates were scanned and the proton recoil tracks were analysed according to the previously described method ([3]). The background was determined by means of an irradiation without the target. The L4 plates have been found more suitable than the C 2 plates used in our previous experiment.

Fig. 2 shows two tracks nearly parallel to the emulsion surface obtained in C 2 and L 4 plates 400 μm thick exposed directly to a γ-ray beam of $E_{\gamma\,max} = 30$ MeV. The irradiation dose was 2 roentgens.

The tracks are due to protons from (γ, p) processes in the emulsion. The two plates were processed in the same conditions and the two tracks were photographed under the same conditions included depth in the emulsion.

From Fig. 2 it is apparent that in L 4 plates the contrast between the tracks and the background is much improved.

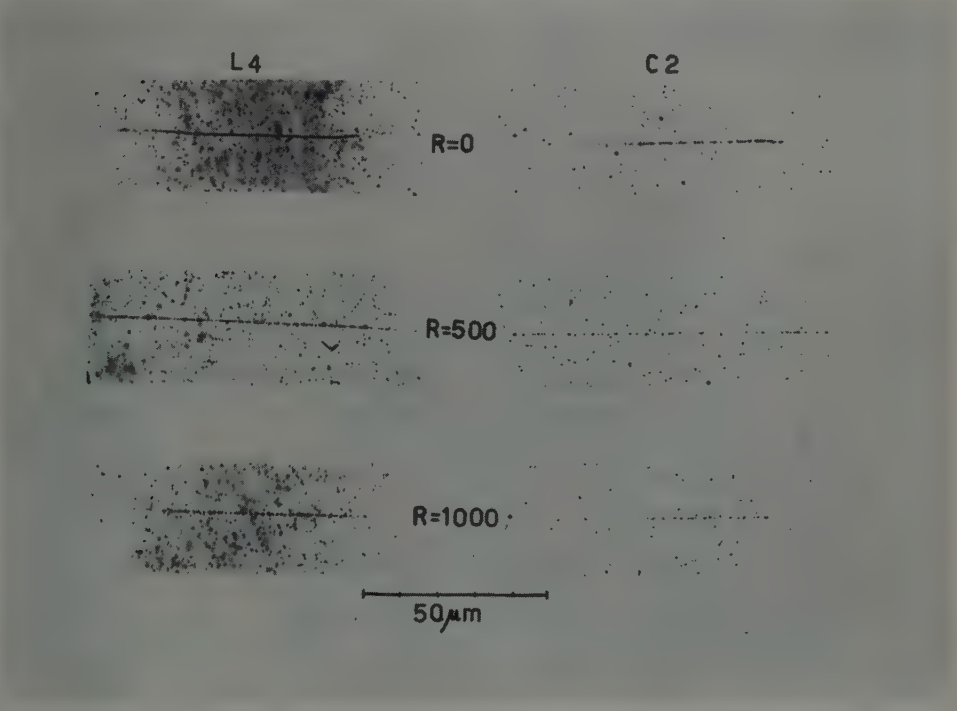

Fig. 2. – Proton tracks in C 2 and L 4 plates, 400 μm thick.

3. – Results.

Data on exposure and scanning are summarized in Table I.

TABLE I.

Scatterer	Ca		K				Background		
Weight of the target (g)	19		12				—		
Dose (roentgen)	3 722	3 690	6 027				2 100		
$E_{\gamma max}$ (MeV)	30	30	31				31		
(γ, n) threshold (MeV)	~ 16		13.2±0.2 (5)				—		
θ	90°	90°	60°	90°	90°	120°	60°	90°	120°
Plates	C 2; 200	L 4	L 4	L 4	C 2; 400	L 4		L 4	
Scanned volume (mm^3)	620	184	189	180+ 177 (*)	180	209	96	48	84
Number of observed tracks $\Delta\beta \leqslant 15°$, $\Delta\varphi \leqslant 15°$ $E_n < 5$ MeV	682	181	300	277	139	177	3	—	2
$\Delta\beta \leqslant 15°$, $\Delta\varphi \leqslant 30°$ $E_n > 5$ MeV	262	86	184	193	107	116	—	—	1

All L 4 plates are 400 μm thick.

(*) The mean distance of the 177 mm^3 of scanned volume was 20 cm instead of 17 cm.

The neutron spectra are deduced from the recoil proton spectra, taking into account the scattering of neutrons by hydrogen atoms in the emulsion. The correction $E_n = E_p \cos^2 \alpha$ was introduced only for $\alpha > 10°$, following the method previously described (3).

Only little corrections are due:

i) to the probability of escape of recoil proton tracks from the emulsion;

ii) to the neutron absorption in the target, in the window of the vessel containing the K target (Fig. 1) and in a 3 mm thick Pb plate that

(5) *Rev. Mod. Phys.*, **26**, 425 (1954).

screened the nuclear plates against the low energy photons diffused by the target.

The energy spectrum of the photoneutrons from Ca emitted at $\theta = 90°$ is shown in Fig. 3.

Fig. 4, 5 and 6 show the energy spectra of the photoneutrons from K emitted at $\theta = 90°$, 60° and 120° respectively.

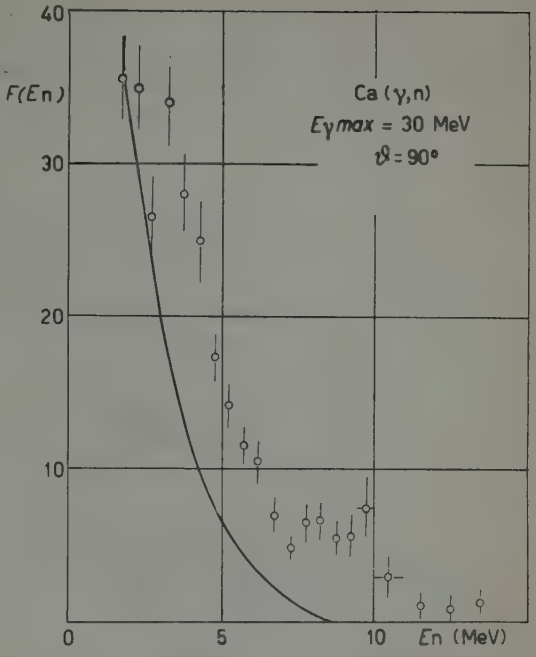

Fig. 3. – Photoneutron spectrum from Ca at $\theta \sim 90°$. $F(E_n)$ (arbitrary units) = neutron number/ΔE_n.

4. – Discussion and conclusions.

In Fig. 3 to 6, together with the experimental spectra are reported evaporation theoretical curves:

$$F(E_n) = \text{const} \cdot E_n \cdot \exp(-E_n/T)$$

calculated using the nuclear temperature $T = 1.1$ MeV deduced from the Gugelot experiment (6) on the (p, n) reaction.

The theoretical curves are normalized at the lowest sides of the experimental spectra.

For a discussion on the evaporation theoretical curves see the reference (1).

The comparison shows that for neutron energy greater than 2 MeV there are relevant contributions of neutrons exceeding the theoretical values both in Ca and in K cases.

TABLE II.

Element	Ca				K									
θ angle	90°				60°			90°				120°		
E_n (MeV)	>1.5	> 2	2÷5	> 5	> 2	2÷5	> 5	> 1.5	> 2	2÷5	> 5	> 2	2÷5	> 5
F (neutron fraction)	0.52	0.59	0.46	0.75	0.56	0.32	0.83	0.48	0.53	0.38	0.82	0.56	0.36	0.82

(6) P. C. GUGELOT: *Phys. Rev.*, **81**, 51 (1951).

The amount of neutrons exceeding the theoretical values divided by the total neutron number is shown in the Table II (neutron fraction F) for various neutron energy regions.

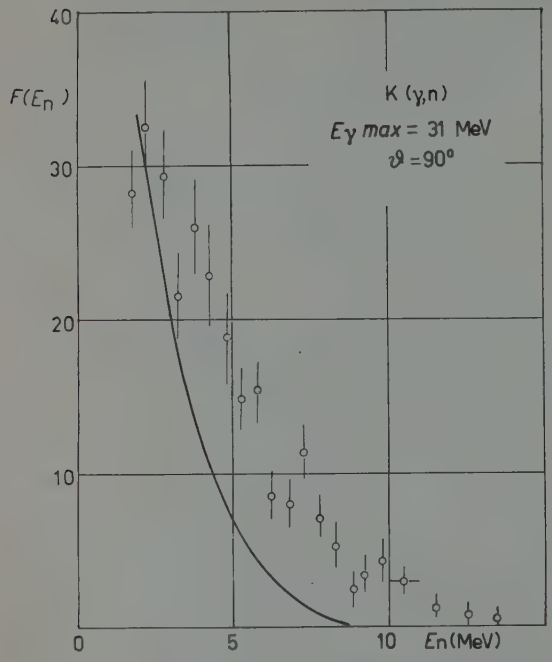

Fig. 4. – Photoneutron spectrum from K at $\theta \sim 90°$.

The fraction F represents a lower limit for the contribution of the neutrons whose emission may be attribuetd to the direct process.

Table II shows that the contribution from the direct process above 2 MeV of neutron energy is much more relevant than the 10% found for the heavier nuclei ([3,7-9]).

If the transitions to the ground state only were relevant in the direct process a maximum in the photoneutron spectrum might be expected around $E_n = E_{\sigma max} - E_b$, $E_{\sigma max}$ being the photon energy correspondent to the maximum of the (γ, n) cross-section and E_b the binding energy of the neutron in the target nucleus.

The contribution from transitions to excited states of the residual nucleus flattens this maximum because the neutrons are distributed towards the lower energy side.

Thus the experimental neutron spectrum at neutron energy of 2 MeV, where the evaporation theoretical spectrum has been normalized to the experimental one, may contain some neutrons not due to evaporation. If this is the case, the fraction F given in Table II will be higher.

For Ca, for which $E_{\sigma max} \approx 20$ MeV and $E_b \approx 16$ MeV, a maximum in the spectrum for neutrons emitted through the direct process may be expected at neutron energy around 4 MeV. The maximum at neutron energy around 9.5 MeV found in the experimental spectrum may be interpreted as a surface

(7) G. A. PRICE: *Phys. Rev.*, **93**, 1279 (1954).
(8) M. E. TOMS and W. E. STHEPHENS: *Phys. Rev.*, **108**, 77 (1957).
(9) S. CAVALLARO, V. EMMA, C. MILONE and A. RUBBINO: *Nuovo Cimento*, **9**, 736 (1957).

direct process ([10]) in correspondence of a second resonance in the region around $E_\gamma = (25 \div 26)$ MeV.

For K, being $E_{\sigma max} = 18.5$ MeV ([11]), a maximum may be expected around 5.5 MeV; for higher energies the energy spectrum at $\theta = 90°$ seems to show

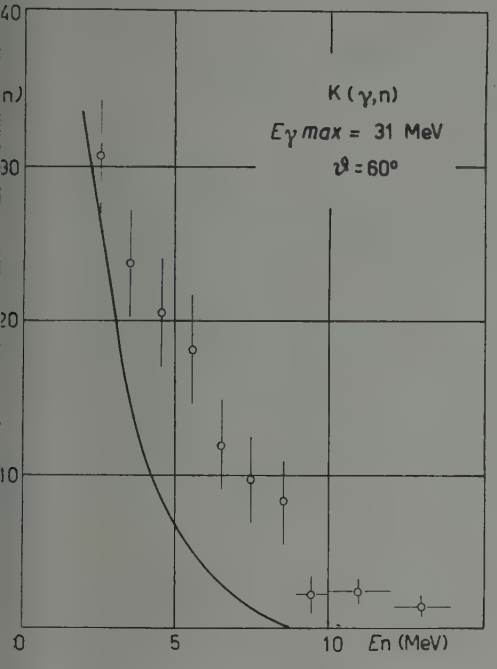

Fig. 5. - Photoneutron spectrum from K at $\theta \sim 60°$.

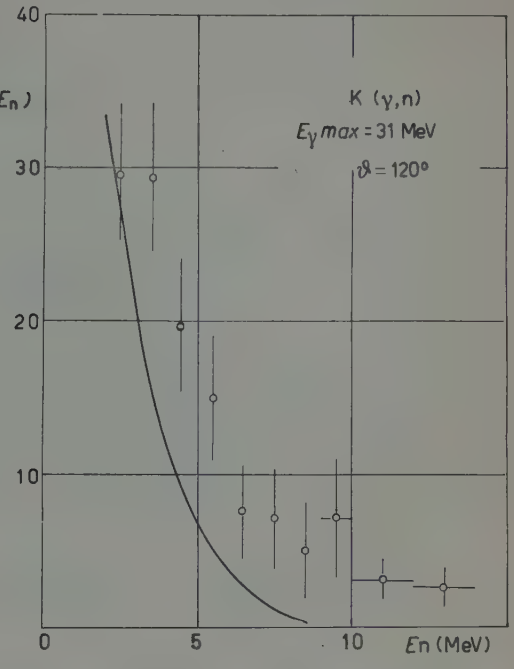

Fig. 6. – Photoneutron spectrum from K at $\theta \sim 120°$.

a behaviour quite similar to that of Ca. The interpretation might also be the same.

The photoneutron yelds (neutron-mole·roentgen) for $\theta \sim 90°$ and $E_n 2 >$ MeV, are about the same for Ca and K.

Our experimental figure is $(Y_{Ca}/Y_K)_{\theta=90°} \sim 1.1$.

For K the yeld at $\theta = 60°$ is about twice both yelds at 90° and 120°, so that the angular distribution is anisotropic and is peaked forward.

* * *

Our best thanks are due to Prof. R. RICAMO and Prof. G. WATAGHIN for having put at our disposal the means for performing this research.

([10]) A. AGODI, E. EBERLE and L. SERTORIO: *Nuovo Cimento*, **13**, 1279, (1959).

([11]) M. D. DE SOUZA SANTOS, J. GOLDEMBERG, R. R. PIERONI, E. SILVA, O. A. BORELLO, S. S. VILLAÇA and J. L. LOPES: *An. Acad. Brasil Cience*, **27**, 437 (1955)

We are also very grateful to Prof. R. RICAMO, G. CORTINI, R. MALVANO and A. AGODI for helpful discussions.

RIASSUNTO

Si studia mediante emulsioni nucleari lo spettro dei fotoneutroni emessi dal potassio e dal calcio in seguito al bombardamento con bremsstrahlung di 31 MeV. Vengono rilevati i neutroni emessi con angolo $\theta \sim 90°$ per il calcio e $\theta \sim 60°$, $90°$, $120°$ per il potassio. Si trova che in entrambi i casi almeno il 50% dei fotoneutroni di energia superiore a 2 MeV sono emessi in seguito a processi diretti. Nel caso del calcio lo spettro indica l'esistenza di una seconda risonanza nella sezione d'urto col massimo a circa 10 MeV sopra la soglia. Un andamento circa simile sembra probabile anche nel caso del potassio. Le rese a 31 MeV (neutroni/mole·roentgen) a $\theta \sim 90°$ e per $E_n > 2$ MeV per Ca e K risultano circa eguali: $(Y_{Ca}/Y_K) \sim 1.1$.

IL NUOVO CIMENTO Vol. XIV, N. 5 1° Dicembre 1959

Causality Complementarity and S-Matrix Formalism in a Non-Local Relativistic Theory of Fields.

G. WATAGHIN

Istituto di Fisica dell'Università - Torino

(ricevuto il 24 Settembre 1959)

Summary. — A new formalism of a non local theory is suggested permitting to substitute the description of point-interactions and point particles by interactions taking place in certain 4-dimensional domains and by an approximate description of propagation of fields representing extended physical particles. The conditions of relativistic invariance and of macroscopic causality result compatible with the above limitations because the interactions can be described by the S-matrix in p-space and studied independently from the propagation problem.

1. – Introductory remarks.

One of the fundamental assumptions of a non local field theory can be stated as follows: in a representation in which the co-ordinates x_μ are diagonal:

$$\langle x' | x_\mu | x'' \rangle = x'_\mu \, \delta^4(x' - x'') , \tag{1}$$

the direct interaction between fields (of the type $e\bar{\psi}\gamma_\mu \psi A''$) cannot be represented by a diagonal matrix:

$$f(x') \, \delta^4(x' - x'') .$$

As is well known, this situation can be found in cases in which the interaction hamiltonian depends explicitly on (1) and on the relative momentum operators $\langle x' | p_\mu | x'' \rangle$, or cut-off operators are introduced in the elements of the S-matrix.

The indirect interactions in a field theory are non local because of the possibility of creation of new particles (1).

We shall consider also as a fundamental hypothesis of a non-local theory the assumption of the existence of new universal limitations of all interactions between fields depending on the relativistic cut-off operators and on the value of a fundamental length l (where *e.g.* $l \sim M_p^{-1}$ and M_p is the proton mass.) This limitations can be expressed by the introduction of the cut-off in the S-matrix in a way as to take into account simultaneously the elimination of divergencies and the reduction of the contribution of states of high relative momenta in collision problems and in self energy problems (the « high » momenta $|\boldsymbol{p}| > M_p$ being measured in the CM system). The description of this situation in the space time of relative co-ordinates $\eta_\mu = x_\mu - x_\mu^{CM}$ canonically conjugated to the relative momenta can be stated conveniently in the CM reference frame by saying that the 4-dimensional domain D_l of relative coordinates η_μ, in which the interaction takes place, is defined by the universal relativistic cut-off operators, and, in the CM frame, has dimensions of the order of l^4.

Since, as a general rule, the interactions we are considering here lead to several possible channels of created particles, the results of the interaction in the domain D_l can be described only statistically. One can ascribe to each channel or to a subset of eigenvalues referring to outgoing particles only a certain probability.

This statistical nature of the interaction in D_l is well illustrated in cases of multiple production in high energy collisions and in the nucleon antinucleon annihilation processes.

The experimental data show that if the momenta of ingoing particles in CM system are $> M_p$ the creation of pairs of particles and the multiple meson production become important. This induces us to deny the possibility of measurements of η_μ and postulate that inside D_l the causal propagation of the field amplitudes cannot be followed, and space-time intervals cannot be measured (2).

The difficulties encountered in the usual formulation of a non-local field theory are due essentially to the apparent *incompatibility* of the two following fundamental assumptions:

1) *The causal* description of propagation laws derived from linear differential equations and expressed by *causal* Green functions.

2) The assumption that *statistical* laws govern the creation and destruction of particles and exchange of momenta, charges, spin, etc., in finite 4-dimensional domains of interactions D_l specified above.

---

(1) M. A. Braun: *Žurn. Èksp. Teor. Fiz.*, **37**, 816 (1959).

(2) G. Wataghin: *Lectures in Theoretical Physics at the University of Colorado*, Boulder, 1958 (New York, 1959), p. 219.

Indeed the linear equations and the conditions of local commutativity refer to the probability amplitude of a free « physical particle » having an extended structure. But an experimental control of causality inside D_l with $|\Delta x|_{\text{CM}} < l$ gives rise to the creation of new particles which is acausal because of 2).

We suggest in the following a solution of the above difficulties based on the adoption of two different mathematical formalisms for the two problems:

1) The propagation in space-time of a physical particle in a region where interactions with other physical particles are negligible. This propagation can be described approximately by probability amplitudes obeying linear differential equations and boundary conditions for free particles.

2) The interaction of two or more physical particles with exchange of momenta, spins, etc., which can be described by the S-matrix formalism in the momentum space.

The two mathematical formalisms must be referred to two different sets of variables and are compatible and *complementary* in the sense of Bohr's principle. In the case of a collision process of a given group of ingoing and outgoing physical particles it is possible to separate the problem of the motion of the centre of momenta (CM) of the incident particles from the description of the interaction by means of an S-matrix. Indeed the translational invariance leads to the conservation laws of momenta and to the conclusion that in the CM reference frame in which $\sum_r \boldsymbol{p}_{\text{CM}}^{(r)} = \boldsymbol{P}_{\text{CM}} = 0$, the CM space co-ordinates $\boldsymbol{x}_{\text{CM}} = \text{const.}$ are constant in time. But the description of the interaction and of the cross-sections cannot depend on $\boldsymbol{x}_{\text{CM}}$ and on time t_{CM} corresponding to the centre of the interaction domain D_l and thus it can depend only on other parameters as the relative momenta: $\boldsymbol{p}^{(r)} - \boldsymbol{P} = (\boldsymbol{p}^{(r)})_{\text{CM}}$ and $p_0^{(r)} - P_0$ and naturally also $p_\mu^{(r)}$, P_μ, spin and isotopic spin variables and relative co-ordinates $\eta_\mu = x_\mu - x_\mu^{(\text{CM})}$. Similar considerations can be applied to the description of a physical particle.

Therefore since the relative co-ordinates in D_l are not observable and the applicability of differential equations in D_l is beyond our possibility of control, we shall postulate that « short range » interactions must be described in the momentum space and no use will be made of the unobservable η_μ variables. One can for instance deduce the form of the S-matrix starting from a problem of diagonalization of the total hamiltonian operator expressed in p-variables. Following Heisenberg's discussion of the S-matrix method one can solve in this way two classes of problems: the self energy problem and the stationary description of a collision process.

The question of the existence of finite domains of interaction D_l, which are also domains of uncertainty for space and time measurements, is con-

nected with the atomic structure of the measuring devices and of the reference frames. The Lorentz transformation will be used below with the following limitations. The coefficients l^{ν}_{μ} of the homogeneous L.T. in p-space ($p'_{\mu} = l^{\nu}_{\mu} p_{\nu}$) are defined, as usually, as c-numbers on the basis of the invariance of the fundamental quadratic form $p_{\nu}p^{\nu} = p_0^2 - p_1^2 - p_2^2 - p_3^2$. We assume also that l^{ν}_{μ} can be measured with an arbitrary precision. In the Lorentz transformation of co-ordinates: $x_{\varrho} = L^{\sigma}_{\varrho} x'_{\sigma} + \alpha_{\varrho}$, the terms α_{ϱ} cannot be known with an arbitrary precision ($\Delta\alpha_{\varrho} \geqslant l$), so that also x_{ϱ} and x'_{σ} are affected all with an error $\Delta x_{\varrho} \geqslant l$, $\Delta x'_{\sigma} \geqslant l$. The question of measurability of the coefficient L^{ν}_{μ} in a representation in which the x_{ϱ} are diagonal, lies outside the scope of the present note. The above assumptions and the choice of $l = M_{\mathrm{p}}^{-1}$ are depending on the hypothesis that in the Universe do not exist stable elementary particles of a mass essentially greater than the nucleon mass.

As a consequence of cut-off's introduced in the S-matrix the causal propagators (Green's functions) of physical particles have no singularity on the light cone.

2. – The mathematical formalism.

The method of introduction of relativistic form factors in the S-matrix was already indicated in earlier papers ([3]). It can be illustrated on the example of a collision process in which the 4-momenta of the two incident physical particles $p^{(i)}_{1\mu} p^{(i)}_{2\mu}$ ($\mu = 0, 1, 2, 3$) and of the $(n+2)$ outgoing physical particles $p^{(\varrho)}_{1\mu} p^{(\varrho)}_{2\mu} k_{1\mu} k_{2\mu} \ldots k_{\mu\mu}$ are given.

Indicating by $P_{\mu} = p^{(i)}_{1\mu} + p^{(i)}_{2\mu}$ the total energy momentum 4-vector and by u_{μ} the velocity vector of the CM system: $u_{\mu} = (1/m) P_{\mu}$, where $P_{\mu} P^{\mu} = m^2 > 0$, we introduce the folllwing invariant projections of a 4-vector k_{μ}:

$$
(2) \qquad \begin{cases} I_t(k_{\mu}) = k_{\mu} u^{\mu}, \\ I_s(k_{\mu}) = \sqrt{I_t^2 - k_{\mu} k^{\mu}}, \\ (k_{\mu} k^{\mu} = k_0^2 - k_1^2 - k_2^2 - k_3^2), \end{cases}
$$

$I_t(k_{\mu})$ is the projection on the time axis of the CM frame, and $I_s(k_{\mu})$ is the projection on the space of the CM system. In the CM system one has:

$$
u^{\mu} = (1, 0, 0, 0), \qquad I_t = k_0,
$$

$$
I_s = \sqrt{k_1^2 + k_2^2 + k_3^2} = |\boldsymbol{k}|.
$$

([3]) (*a*) G. WATAGHIN: *Bras. Acad. Sciences, Symposium on Cosmic Ray*, 1941 (Rio de Janeiro, Acad. Bras. de Ciencias, 1943); (*b*) *Phys. Rev.*, **74**, 975 (1948); (*c*) *Lectures at the 1958 Summer Theor. Phys.* (New York, 1959). (*d*) *Nuovo Cimento*, **5**, 689 (1957).

The fundamental assumption of the proposed non-local theory consists in the statement that the introduction of cut-off operators in the invariant interaction lagrangian or directly in the elements of the transition matrix must be done by means of invariant form-factors which, in the momentum representation, are universal functions $G_s^{\pm}(I_s)\, G_t^{\pm}(I_t)$ of the projections $I_s(k_\mu l)$, $I_t(k_\mu l)$. Following provisional choice of $G_s^{\pm}$ and $G_t^{\pm}$ is suggested by the criterium of mathematical simplicity, by the claim of macroscopic causality and by some experimental results.

We shall consider as a universal rule, the prescription that in a field theory (with Dirac's 2-nd quantization) to each creation operator a_k of a particle in a given eigenstate of momentum k_μ must be associated the operator

$$(3) \qquad G^{+}(k_\mu) = G_s^{+}\, G_t^{+} = (1 - il\, I_s)^{-3}(1 - il\, I_t)^{-1} = \frac{M_p^4}{(|\boldsymbol{k}| + i\, M_p)^3 (k_0 + i\, M_p)},$$

and to each absorption operator a_k must be associated:

$$(4) \qquad G^{-}(k_\mu) = G_s^{-} G_t^{-} = (1 + ilI_s)^{-3}(1 + il\, I_t)^{-1} = M_p^4 (|\boldsymbol{k}| - i M_p)^{-3}(k_0 - i M_p)^{-1},$$

where we put $\hbar = 1$, $c = 1$ and the universal constant: $l = M_p^{-1}$. Obviously after the introduction of these operators the hamiltonian remains hermitian and the invariance properties of the S-matrix are not altered although the dependence on the four-vector u_μ signifies that each sector of the S-matrix is modified in a special and generally different way. The Fourier transforms of the set of cut-off functions $G_s^{\pm}$, $G_t^{\pm}$ correspond to the limitation of the interaction (or of the scattering process) to a small 4-dimensional domain D_l having an extension $\sim l^4$.

These Fourier transforms can be interpreted in terms of the relative coordinates $\eta_\mu = x_\mu - x_\mu^{(\mathrm{CM})}$ [4]. Then one finds that the Fourier transform of G^{+-} vanishes for $\eta_0 < 0$ and is $= \mathrm{const} \exp[-(\eta_0/l)]$, if $\eta_0 > 0$, whereas G_t^{-} vanishes if $\eta_0 > 0$ and is $\sim \exp[\eta_0/l]$ if $\eta_0 < 0$. Thus operators $G_t^{\pm}$ are the natural non local generalization of $\delta^{\pm}(k_0)$.

All $G^{\pm}$ are normalized by the conditions:

$$\lim_{l \to 0} G^{\pm} = 1 \qquad \text{and} \qquad \lim_{|\boldsymbol{k}| \to 0} G^{\pm} = 1 .$$

$G^{+}G^{-}(k_\mu)$ can be interpreted as a statistical weight of the state k_μ.

One must expect that the correct choice of the universal cut-off will depend on the solution of the elementary particles problem of the type suggested by

---

(4) G. WATAGHIN: *Nuovo Cimento*, **5**, 689 (1957).

HEISENBERG (5). I think that only after the solution of the problems of mass-values and coupling constants there will be a sure criterium for the choice of a specific form of G^+G^-.

It is certainly possible to introduce such cut-offs in the non-linear interaction lagrangian used by HEISENBERG, without using the actual differential equations of Heisenberg and limiting the solution to the determination of the S-matrix by means of a « hamiltonian » in p-space.

The following features of the present day local quantum theory of fields will be maintained in the non-local formalism:

1) The second quantization of the uncoupled fields depending on the usual « free » hamiltonian H_0. The bare-particle masses are introduced in H_0 for particles having a rest mass $\neq 0$, but the exact values are not needed in the formalism before the introduction of the interactions. (The interference and diffraction-phenomena depend on $\lambda = |\boldsymbol{k}|^{-1}$). Further calculations can be made with sufficient approximation assuming that the bare masses have small mass differences $\Delta m/m \ll 1$ relative to the experimental values of the dressed physical particles(See (1)). In this approximation it is possible to interprete the observed mass differences of the type $m_{\pi^+} - m_{\pi^0}$ in terms of interactions.

2) The time independent and $\boldsymbol{x}$-independent interaction hamiltonian H' is supposed to be hermitian and to be a sum of terms representing linear and non-linear interactions of all kind of fields in p-space.

These terms contain the creation and destruction operators of particles in states which are eigen-states of the energy-momentum operator. This interaction hamiltonian H' will obviously depend only on the momentum variables and on internal parameters like spin, isospin..., also after the introduction of the cut-off operators $G_s^{\pm}$ and $G_t^{\mp}$. But we shall suppose it does not depend on the co-ordinates x_μ or η_μ (these last parameters must be eliminated by integration if one starts from the hamiltonian density).

3) The non-local S-matrix formalism requires a separate treatment of each group of terms representing a collision process with given ingoing physical particles or a self-energy problem of a physical particle.

In both cases one can determine in a covariant way, a subset of terms of the S-matrix referring to such a special process, in which the total energy momentum vector P_μ is conserved, and the momentum $\boldsymbol{P}$ is constant in every transition. Then one can solve *e.g.* the Heisenberg-Schrödinger eigen-value problem of the total hamiltonian $H = H_0 + H'$ in the CM system and in the

---

(5) H. P. DURR, W. HEISENBERG, H. MITTER, S. SCHLIEDER and K. YAMAZAKI: *Zeits. f. Naturfor.*, **14**, 441 (1959).

representation in which the eigen-function ψ is a sum of eigenstates of the free hamiltonian:

$$\psi = \sum \alpha(\boldsymbol{k}\sigma, \boldsymbol{k}'\sigma', \ldots) \, | \boldsymbol{k}\sigma, \boldsymbol{k}'\sigma', \ldots \rangle \,, \tag{5}$$

where the parameters $\sigma, \sigma', \ldots$ represent the internal parameters (spin, isotopic spin, ...) and the occupation number of the state. In the CM reference frame:

$$\begin{cases} (H_0 + H')\,\psi = W\psi \,, \\ \boldsymbol{P} = 0, \qquad W = P_0 \,, \\ (W - \sum E_{p\varrho})\,\alpha(p\varrho, \ldots) = \sum \langle p\varrho, \ldots | H' | \boldsymbol{k}\sigma, \ldots \rangle \, \alpha(\boldsymbol{k}\sigma, \ldots) \,. \end{cases} \tag{6}$$

From the necessarily approximate solution of these equations *e.g.* by the Tamm-Dankov method, one can deduce the subset of the S-matrix elements representing the special process we have chosen to consider.

In order to eliminate divergencies a cut-off must be introduced in (6), in $H = H_0 + H'$ taking into account that the choice of the CM system constitutes a fundamental assumption, permitting to give a definite meaning also to the cut-off operators $G_s^{\pm} G_t^{\pm}$, appearing in the formalism associated with the operators of creation or destruction or with positive and negative frequencies respectively.

In scattering problems usually we know the incident physical particles and we don't know in which special state they react. So in the S-matrix some projection operators must be introduced from the physical state to the particular state of bare particles we want to examine. Indeed the particles react as bare particles and they propagate as dressed physical particles. So that in the final states of bare particles appearing in the S-matrix one must consider an operator which transforms the bare particle state (which is unstable) into the physical state of an outgoing dressed particles.

One can see easily that the above cut-off method satisfies the claim of macroscopic causality. Indeed the propagators obtainable from the above S-matrix and referred to the outgoing particles have only positive frequency components corresponding to the future cone and they vanish for negative time. The inverse situation happens for ingoing particles, having propagators with negative frequency components. As was shown in [2] the cut off's depending on $G_s^{\pm}$ satisfy the above condition insofar as in the complex P_0 plane the usual prescription about the path of integration for causal propagators of Stueckelberg and Feynman can be fulfilled. In the $G_t^{\pm}$ cut-off operators the new poles lie always outside the integration contour and the same conclusion is valid. Moreover it can be shown that the eventual overlapping of domains of interaction between many

neighbour-particles can never give rise to a signal propagating with a speed $> c$ because of the special choice of the time-formfactors.

As a concluding remark, one can say that in the above non-local theory the causality refers to the propagation of amplitudes of probability of physical particles obeying linear differential equations. But the sources of the fields, where the physical particles are created, are extended in finite 4-dimensional domains D_l and the same is true for the domains of arrival where a physical particle annihilates or interacts.

The main problem of the future theory remains the determination of the mass values, of the coupling constants and of the interactions between about 30 types of elementary particles. Some important features of the interactions in high energy collisions appear in the observations of the high energy jets in cosmic rays. The anisotropy of the momentum distribution in the CM system of the created particles makes plausible the assumption that the non-linear hamiltonian responsible for the multiple production depends explicitly on a new invariant $I_a(k_\mu)$:

$$I_a = k_\mu v^\mu ,$$

where in the two-body collision the 4-vector v_μ is:

$$v_\mu = \frac{p_{1\mu}^{(i)} - p_{2\mu}^{(i)}}{\sqrt{(p_{1\mu}^{(i)} - p_{2\mu}^{(i)})(p_1^{(i)\mu} - p_2^{(i)\mu})}} .$$

If the p_1-axis is parallel to the relative velocity in the CM frame of the initial nucleons, and if the two incident particles have identical masses, then the components of v_μ in the CM system are: (0, 1, 0, 0) and the invariant $I_a(k_\mu)$ is the projection $(k_1)_{\mathrm{CM}}$ of the 4-vector k_μ on the axis of the jet.

Appendix (*)

If one considers the total hamiltonian H as the 4-th component of the operator P^μ having eigenvalues: $P'_0 = W$, $P'_1 P'_2 P'_3$, then for each « sector » of the S-matrix these eigenvalues are well defined and the vector $u_\mu = (1/m)P'_\mu$ of the corresponding CM frame is given. The equation (6) can be written in the invariant form

$$(P_\mu u^\mu)\psi = (P'_\mu u^\mu)\psi \ ; \tag{8}$$

(*) Added in proofs.

ψ is a covariant function of the invariant projections of the momenta K_μ on the axis of the CM system (this being of the type of I_t, I_s, I_a). The operator $P_\mu u^\mu$ corresponds to $i\hbar(\partial/\partial\tau) = i\hbar u_\mu(\partial/\partial x_\mu)$, here τ is the proper time of the CM frame.

The introduction of the cut-offs (3) and (4) into a causal propagator for outgoing or ingoing physical particles can be done in the following way. One modifies the Feynman-Stueckelberg propagator for external bosons:

$$\int_{C^+} \frac{G^+(k_\mu)\exp\left[-ik_\mu x^\mu\right]}{k^2 - m^2}\,\mathrm{d}^4k\,, \tag{9}$$

where for $x_0 > 0$, $G^+(k_\mu)$ and the C^+ contour must be taken (and for $x_0 < 0 \to G^-(k_\mu)$ and C^-), and where one keeps the usual rules of integration in the complex k_0 plane.

The calculations show that, *e.g.* in the case of vanishing rest mass the propagator has no singularities on the light cone.

The macroscopic causality follows from the fact that particles created in the domain D_t give rise only to outgoing external waves at times $x_0 > 0$ and those absorbed in D_t are connected only with ingoing waves at $x_0 < 0$.

The above non-local formalism brings many new features in the theory. The commutation rules in the x-space are modified. If one introduces representations of physical particles, field operators representing two such particles do not commute because all particles interact. The application of the gravitational theory must be limited to macroscopic domains, etc.

RIASSUNTO

Si propone una nuova formulazione della teoria non locale dei campi che sostituisce le interazioni in un punto con interazioni aventi luogo in un dominio quadridimensionale di coordinate relative. Le condizioni di invarianza relativistica e di causalità macroscopica risultano compatibili con le limitazioni imposte dai fattori di forma perchè le interazioni fra i campi possono essere descritte da una matrice S nello spazio degli impulsi e dell'energia indipendentemente dallo studio del problema della propagazione nello spazio-tempo.

A Direct Consequence Arising from the Relativistic Handling of an « Uniform » Field.

I. Gottlieb

Faculté des Sciences Mathématiques et Physiques - Université de Jassy - Jassy

(ricevuto l'11 Giugno 1959)

1. – Considering the metrics from the relativistic theory of gravitation, Schwarzschild's metrics can be written as follows:

$$ds^2 = c^2\left(1-\frac{\lambda}{r}\right)dt^2 - \frac{dr^2}{1-\lambda/r} - r^2(d\theta^2+\sin^2\theta\,d\varphi^2) =$$

$$= c^2\left(1-\frac{2}{c^2}\frac{M}{r}\right)dt^2 - \frac{dr^2}{1-(2/c^2)(M/r)} - r^2(d\theta^2+\sin^2\theta\,d\varphi^2)\,,$$

or generally

$$ds^2 = c^2\left[1-\frac{2W(r)}{c^2}\right]dt^2 - \frac{dr^2}{1-2W(r)/c^2} - r^2(d\theta^2+\sin^2\theta\,d\varphi^2)\,. \tag{1}$$

We are allowed to consider the metrics (1) as a generalization of Schwarzschild's metrics, $W(r)$ being the potential energy of the mass unit, whilst, only the corrective term $2W/c^2$ differs from the Minkowski metric.

The interesting results given by this generalization are very well known [1,3].

We shall try to obtain a similar correction by using a different metric, namely:

$$ds^2 = F(x)\,dt^2 - G(x)\,dx^2 - dy^2 - dz^2\,. \tag{2}$$

This metric corresponds from the classical point of view, to a symmetry towards any straight line, parallel to the Ox axis. As we have to deal only with the statical case, this field corresponds to a classical uniform field at the exterior of masses or charges which create it.

---

[1] T. T. Vescan: *Compt. Rend.*, **245**, 2014 (1957); **247**, 2301 (1958).

[2] T. T. Vescan: *Revue de Physique.* Acad. RPR Buc., **2**, no. 2, 175 (1957).

[3] T. T. Vescan: *Analele Stiint. ale Univ. « Al. I. Cuza » Iasi,* (serie noua) Secţiunea I, **3**, fasc. 1-2, 257 (1957).

Einstein's equations, $R_{ik} = 0$, are reducing to a single one

$$F'' - \frac{F''}{2}\left(\frac{F'}{F} + \frac{G'}{G}\right) = 0 .$$

We may choose an additional condition, namely we shall impose to the determinant of the fundamental form to be constant (4)

$$|g_{ik}| = FG = c^2 = \text{const} .$$

This condition could always be realized by an arbitrary transformation $x = \psi(x')$, which does not alter the general form of the metric (2). The calculations are the same as in the case of spherical symmetry (5).

In this case the metric (2) becomes

$$ds^2 = c^2(1 - \beta x)\, dt^2 - \frac{dx^2}{1 - \beta x} - dy^2 - dz^2 , \tag{3}$$

where β is a constant of integration.

From the metric (3) comes out as a fact that, from the classical point of view, we have to deal with an uniform field, because the corresponding term βx, in respect to Minkowski's metric, is, up to a constant factor, the classical potential of an uniform field.

The trajectory of a particle will be a geodesic of the metric given by (3) which satisfies the equations

$$\begin{cases} \ddot{x} + \dfrac{\beta}{2(1 - \beta x)}\dot{x}^2 - \dfrac{c^2\beta}{2}(1 - \beta x) & \dot{t}^2 = 0 , \\ & \ddot{y} = 0 , \\ & z = 0 , \\ \ddot{t} - \dfrac{\beta}{1 - \beta x} & \dot{x}\dot{t} = 0 . \end{cases} \tag{4}$$

We shall choose the initial conditions

$$x_0 = y_0 = z_0 = 0; \qquad \left(\frac{dx}{dt}\right)_0 = \left(\frac{dy}{dt}\right)_0 = 0; \qquad \left(\frac{dz}{dt}\right)_0 = v_0 . \qquad \text{for } t = 0: \tag{5}$$

Integrating we find

$$\begin{cases} x = \dfrac{1}{\beta}\operatorname{tgh}^2\dfrac{\beta ct}{2} , \\ y = 0 , \\ z = \dfrac{2v_0}{\beta c}\operatorname{tgh}\dfrac{\beta ct}{2} . \end{cases} \tag{6}$$

(4) M. Nuyens: *Etude syntetique des champs massiques à symétrie sphérique* (Bruxelles, 1925).
(5) Th. de Donder: *La gravifique Einsteinienne* (Paris, 1921), p. 87 and 167-168.

The trajectory will be

$$z^2 = \frac{4v_0^2}{\beta c^2} x \,, \tag{7}$$

namely a « parabola » which is the same as in the non relativistic case but which differs from that concerning the laws of motion (6). These laws can be reduced to what is practically the classical form, by expanding in a series the tgh $\beta ct/2$ term.

We may integrate the equation (4) considering s the independent variable. In this case the initial conditions will be

$$x_0 = y_0 = z_0 = 0; \qquad \left(\frac{\mathrm{d}x}{\mathrm{d}s}\right)_0 = \left(\frac{\mathrm{d}y}{\mathrm{d}s}\right)_0 = 0; \qquad \left(\frac{\mathrm{d}z}{\mathrm{d}s}\right)_0 = u_0 \,, \qquad \text{for } s = 0 \,. \tag{8}$$

Therefore we obtain

$$\begin{cases} x = \dfrac{\beta}{2}(1 + u_0^2)\dfrac{s^2}{2} \,, \\ y = 0 \,, \\ z = u_0 s \,, \end{cases} \tag{9}$$

and the equation of the trajectory will have the following form:

$$z^2 = \frac{4u_0^2}{\beta(1 + u_0^2)} x \,. \tag{10}$$

Identifying both equations (7) and (10), we again obtain the well known relativistic relation

$$u_0 = \frac{v_0}{c\sqrt{1 - v_0^2/c^2}} \,. \tag{11}$$

In the non relativistic case, the equation of motion in the z direction is

$$z = v_0 \cdot t_1 \,. \tag{12}$$

Taking into account both (6.3) and (12), as a direct result arises that, covering a known distance, the particle retards concerning the duration (for $\beta ct/2 \ll 1$)

$$\Delta t = t_1 - t \approx -\frac{\beta^2 c^2 t^3}{3} \,. \tag{13}$$

In addition to this, owing to the fact that $\lim_{t \to \infty} \mathrm{tgh}\, \beta ct/2 = 1$, the particle will strive to the point

$$\begin{cases} x = \dfrac{1}{\beta} \,, \\ y = 0 \,, \\ z = \dfrac{2v_0}{\beta c} \,, \end{cases} \tag{14}$$

(which is a singular point on a singular plane of the four-dimensional world, because there $1-\beta x=0$), without reaching it for ever. Therefore, in fact, we don't obtain the whole « parabola ».

If $\beta x \ll 1$, we are allowed to make some semirelativistic remarks. We can evaluate the force components by classical means calculating the acceleration from the laws of motion (6). Then we obtain:

$$(15) \qquad \begin{cases} F_x = \dfrac{m\beta c^2}{2}(1-4\beta x+3\beta^2 x^2)\,, \\ F_y = 0\,, \\ F_z = -\dfrac{m\beta^2 c^2}{2} z(1-\beta x)\,, \end{cases}$$

where the last term is a hamper force.

2. – It would be a mistake to apply these results to gravitation, because the metric (3) which from the classical point of view means an uniform gravitational field, occurs only on a small area of the earth surface and the corrections are, therefore, far behind the limit of observation.

On the contrary, we obtain appreciable corrections considering the movement of an electrical charge e, an electron for instance, through the sheets of a condenser which, from the classical point of view, means an uniform field.

The potential energy of the electric charge, evaluated in the classical manner, for the mass unit will be:

$$(16) \qquad W = \frac{eE}{m_0} x\,.$$

Taking into account the previous results, the correction, compared with the Minkowski metric, will be

$$(17) \qquad \beta = \frac{2eE}{m_0 c^2}\,.$$

The condition $\beta x \ll 1$, for the electron, in electrostatic units will be

$$(18) \qquad Ex \ll 10^3\,.$$

To satisfy this condition, we shall consider a field $E=10^{-2}$ e.s.u. $=3$V/cm. In this case $\beta \approx 10^{-5}$ cm^{-1}. Using the formula (13) to evaluate the retardation, we must have $t \ll 10^{-5}$ s. If $t=10^{-7}$ s, the correction (13) is $\Delta t \approx 3\cdot 10^{-11}$ s, which affects only the fourth decimal; in the same time, however, the electron deviates in the direction of x by 10 cm approximately.

3. – Extending the relation (17) to an area in which βx is nearly equal to unity, the electron appears to have the value $x_\infty = c^2 m_0/2eE$ if $t \to \infty$. If the distance between the sheets of a condenser is l and the potential V then $E=V/l$ and

$$x_\infty = \frac{c^2 m_0 l}{2eV}\,.$$

An electron with initial velocity which moves in the Oz direction will hit the sheet only if $l < x_\infty$. We should obtain the effect of asymptotic stop if $x_\infty < l$, which means

$$\frac{x_\infty}{l} = \frac{c^2 m_0}{2eV} < 1 ,$$

which will give us

$$V > \frac{c^2 m_0}{2e} \approx 10^3 \text{ u.e.s.} = 3 \cdot 10^5 \text{ V} . \tag{19}$$

The electron approaching x_∞ will accumulate the energy of $3 \cdot 10^5$ eV. But this is very near to that required by the transformation of the electron, namely $5.11 \cdot 10^5$ eV. Probably, this effect can hardly be expected, this level never being reached. At any rate, to this extent when $m_0 c^2 = 0.511$ MeV the phenomena appear to be far too complicated and only pure relativistic considerations are quite inadequate to explain all aspects of these complex phenomena.

IL NUOVO CIMENTO Vol. XIV, N. 5 1° Dicembre 1959

On the Photodisintegration of Three-Particle Nuclei.

C. Rossetti

Istituto di Fisica dell'Università - Torino
Istituto Nazionale di Fisica Nucleare - Sezione di Torino

(ricevuto il 20 Giugno 1959)

The two-body photodisintegration cross section of a three-particle nucleus is very sensitive to its size. This will be proved in the following, by studying the behaviour of the total cross section as function of the energy just above the threshold. We have therefore the good chance of obtaining a new information upon the size of ^{3}He and ^{3}H, when the corresponding measurements will be carried out.

The photodisintegration differential cross section for the proceses $^3\mathrm{He}(\gamma, \mathrm{p})\mathrm{d}$ and $^3\mathrm{H}(\gamma, \mathrm{n})\mathrm{d}$ reads as usual

$$\mathrm{d}\sigma = \frac{1}{4}\sum \frac{2\pi}{\hbar} |\langle f|H_{\mathrm{int}}|i\rangle|^2 \frac{\varrho_f}{N}, \tag{1}$$

where the sum runs over the final and the initial spin states and the polarisation directions of the incoming photon. $\frac{1}{4}$ is the statistical weight of the four possible initial states (2 nucleon spin states $\times$ 2 polarisation directions of the photon) which are equally probable; ϱ_f is the density of final states and N is the number of incident photons per unit time and unit area.

For incoming photons with energy $\hbar\omega \leqslant 100$ MeV, one may use for the matrix element $\langle f|H_{\mathrm{int}}|i\rangle$ the electric dipole approximation since, as one can easily verify, the magnetic transitions give no contribution [1].

Eq. (1) reduces to:

$$\mathrm{d}\sigma = \frac{e^2}{\hbar c}\,\frac{2M}{3\hbar^2}\,\frac{\hbar\omega}{k_q} I^2 \sin^2\theta \frac{\mathrm{d}\Omega}{4\pi}, \tag{2}$$

where $\hbar\boldsymbol{k}_q$ is the momentum of the free nucleon in the C.M. system of the remaining deuteron, θ is the angle between $\boldsymbol{k}_q$ and the direction of the incoming photon and

$$I = A\int_0^\infty q\,u_1(q)\,\mathrm{d}q \int_0^\infty r^2\,\varphi_d(r)\,\varphi_s(r, q)\,\mathrm{d}r\,. \tag{3}$$

---

[1] See for instance M. Verde: *Helv. Phys. Acta*, **23**, 453 (1950).

A is a numerical constant, $\varphi_i(r, q)$ and $\varphi_d(r)$ are the spacial wave functions of the three-body nucleus and of the deuteron respectively, and $u_1(q)$ denotes the spacial p wave function of the free nucleon (2) *i.e.* $u_1(q) = (\sin k_q q)/k_q q - \cos k_q q$. In order to obtain a first quantitative information about the cross sections, we have adopted for the deuteron's wave function the usual form $\exp[-\alpha r_{23}]/r_{23}$ and for the three-body one the wave function given by IRWING (3) $\exp[-\beta(r^2+q^2)^{\frac{1}{2}}]$. The parameters $1/\alpha = 4.315 \cdot 10^{-13}$ cm and $\sqrt{2}/\beta = 1.462 \cdot 10^{-13}$ cm are usually considered as the radii of the deuteron and triton (or ^{3}He) respectively. The integral (3) becomes

$$I = B\sqrt{\alpha}\beta^3 \int_0^\infty \int_0^\infty r q^2 \exp\left[-\gamma r - \beta\sqrt{r^2+q^2}\right] \left\{ \frac{\sin k_q q}{k_q q} - \cos k_q q \right\} \mathrm{d}r\,\mathrm{d}q\,, \tag{4}$$

where B is a numerical constant and $\gamma = 2\alpha/\sqrt{3}$. Assuming as new variables ϱ and φ defined by

$$r = \varrho \cos\varphi\,, \qquad 0 \leqslant \varrho \leqslant \infty,$$

$$q = \varrho \sin\varphi\,, \qquad 0 \leqslant \varphi \leqslant \pi/2,$$

one can easily carry out the integration with respect to ϱ obtaining for the differential cross section the expression

$$\mathrm{d}\sigma = C \frac{e^2}{\hbar c} \frac{M}{\hbar^2} \frac{\alpha}{\beta^3} \hbar\omega k_q^3 \{R(\eta^2)\}^2 \sin^2\theta \frac{\mathrm{d}\Omega}{4\pi}\,, \tag{5}$$

where C is a numerical constant and

$$R(\eta^2) = \int_0^{\pi/2} \frac{\cos\varphi \sin^4\varphi(\mu\cos\varphi + 1)\{5(\mu\cos\varphi+1)^2 - 3\eta^2\sin^2\varphi\}}{\{(\mu\cos\varphi+1)^2 + \eta^2\sin^2\varphi\}^5} \mathrm{d}\varphi\,; \tag{6}$$

$$\eta = k_q/\beta; \qquad \mu = \gamma/\beta.$$

After integrating (5) with respect to Ω one obtains immediately the total cross section:

$$\sigma = \frac{2C}{3} \frac{e^2}{\hbar c} \frac{M}{\hbar^2} \frac{\alpha}{\beta^3} \hbar\omega k_q^3 \{R(\eta^2)\}^2\,. \tag{7}$$

One observes here that σ is very much influenced by the size of the triton, since in eq. (7) it appears that the factor α/β^3 and $R(\eta^2)$ is not strongly varying with respect to the factor α/β^3. The cross section as a function of the relative energy $\varepsilon = 3\hbar^2 k_q^2/4M$ of the emitted nucleon with respect to the C.M. system of the remaining deuteron, reads

$$\sigma = 1.7\{R(\eta^2)\}^2 \frac{\varepsilon + \varepsilon_s}{\mathrm{MeV}} (\varepsilon/\mathrm{MeV})^{\frac{3}{2}} \cdot 10^{-28}\ \mathrm{cm}^2\,, \tag{8}$$

(2) Experimental information about the phase shifts confirms that the effect of the nuclear force in the final state is practically negligible for low energies.
See R. S. CHRISTIAN and J. GAMMEL: *Phys. Rev.*, **91**, 100 (1953).

(3) J. IRWING: *Phil. Mag.*, **42**, 338 (1953).

and has been evalued numerically for several values of the energy. In eq. (8) ε_s is the threshold of the process:

$$\varepsilon_s = 5.49 \text{ MeV for the process } {}^3\text{He}(\gamma, \text{p})\text{d} ;$$

$$\varepsilon_s = 6.26 \text{ MeV for the process } {}^3\text{H}(\gamma, \text{n})\text{d} .$$

The ratio between the total cross section for the process ^{3}He(γ, p)d as resulting from our calculations and that for the process d(γ, p)n ([4]), has been plotted in the Fig. 1. We know that the deuteron cross-section shows a maximum of nearly 2.5 mbar, for an incident photon energy of 2.2 MeV over the threshold; for the process ^{3}He(γ, p)d according to our calculations we get the maximum of nearly 1.8 mbar for an incident photon energy of 11 MeV over the threshold ([5]).

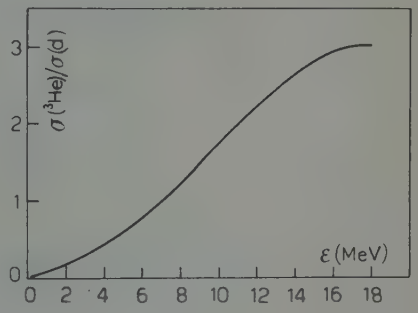

Fig. 1.

In order to reach further information about the photodisintegration processes in question, we are now carrying out calculations referring to the integrals $\int\sigma(E)\,\mathrm{d}E$ and $\int\{\sigma(E)/E\}\,\mathrm{d}E$ with a more accurate wave function for the ground state of the three-body nucleus ([6]). These numbers are not affected, as the $\sigma(E)$, from our scarce knowledge of the three body continuum eigenstates.

* * *

I wish to thank Prof. M. VERDE for suggesting this problem and for many useful discussions.

([4]) See for instance: L. HULTHÉN and M. SUGAWARA: *Handb. d. Phys.*, **39** (Berlin, 1957).

([5]) M. VERDE [see ref. ([1])], using a different tipe of wave function for the three bodies, obtained a much lower value for the maximum (which came out about 0.5 mbar for the same energy). This is a connection with the assumption of a smaller value for the size of the three-particle nuclei.

([6]) See, for instance, E. M. GELBARD: *Phys. Rev.*, **100**, 1531 (1955).

IL NUOVO CIMENTO Vol. XIV, N. 5 1° Dicembre 1959

On the Collective Model Wave Functions.

Z. Jankovic (*)

Faculty of Science and Institute « Rudjer Bošković » - Zagreb

(ricevuto il 12 Ottobre 1959)

Vibrational modes of collective excitations have not been explored so thoroughly up to now as the rotational modes, the reason lying perhaps in the insufficient knowledge of the respective wave functions.

Therefore we take A. Bohr's collective Hamiltonian (1)

$$(1) \qquad H = -\frac{\hbar^2}{2B}\frac{1}{\beta^4}\frac{\partial}{\partial\beta}\beta^4\frac{\partial}{\partial\beta} - \frac{\hbar^2}{2B\beta^2}\frac{1}{\sin 3\gamma}\frac{\partial}{\partial\gamma}\sin 3\gamma\frac{\partial}{\partial\gamma} + \frac{\hbar^2}{2}\sum_{k=1}^{3}\frac{Q_k^2}{J_k} + \frac{1}{2}C\beta^2 ,$$

and try to determine solutions of the parts of separated Schrödinger equation

$$(2a) \qquad \left\{-\frac{\hbar^2}{2B}\left[\frac{1}{\beta^4}\frac{\mathrm{d}}{\mathrm{d}\beta}\beta^4\frac{\mathrm{d}}{\mathrm{d}\beta} - \frac{\Lambda}{\beta^2}\right] + \frac{1}{2}C\beta^2 - E\right\} f(\beta) = 0 ,$$

$$(2b) \qquad \left\{-\frac{1}{\sin 3\gamma}\frac{\partial}{\partial\gamma}\sin 3\gamma\frac{\partial}{\partial\gamma} - \Lambda + \frac{1}{4}\sum_{k=1}^{3}\frac{Q_k^2}{\sin^2\left(\gamma - k(2\pi/3)\right)}\right\}\Phi(\gamma, \vartheta_i) = 0 ,$$

Λ being the separation parameter.

The first differential equation (2a) can easily be transformed in a special confluent hypergeometric differential equation

$$(3) \qquad zy''(\nu, s : z) + (s + 1 - z)y'(\nu, s : z) + \nu y(\nu, s : z) = 0 ,$$

and one gets, from the known properties of its solutions (2), the orthonormalized β

(*) Present address: Centre d'Etudes Nucléaires de Saclay.

(1) A. Bohr: *Mat. Fys. Medd. Dan. Vid. Selsk.*, **26**, no. 14 (1952); A. Bohr and B. R. Mottelson: *Mat. Fys. Medd. Dan. Vid. Selsk.*, **27**, no. 16 (1953).

(2) Z. Jankovic: *Rad JAZU* (Zagreb, in press).

part of the wave function in the form

$$(4)\quad f_{n_\beta,\lambda}(\beta) = \sqrt{\frac{2}{n_\beta!}\,\Gamma(n_\beta+\lambda+\tfrac{5}{2})}\,\sqrt[4]{\left(\frac{B\omega}{\hbar}\right)^{5+2\lambda}}\,\beta^\lambda \exp\left(-\frac{B\omega}{2\hbar}\beta^2\right)\Psi\left(n_\beta,\ \lambda+\frac{3}{2};\frac{B\omega}{\hbar}\beta^2\right),$$

with n_β and λ positive integers or zero, Ψ being then a confluent hypergeometric polynomial (proportional to generalized Laguerre polynomial) and

$$(5)\quad \int_0^\infty f_{n_\beta,\lambda}\, f_{n'_\beta,\lambda}\, \beta^4\, \mathrm{d}\beta = \delta_{n_\beta n'_\beta}\,.$$

In the same time we determine the quantized energy

$$(6)\quad E = \hbar\omega(\lambda + 2n_\beta + \tfrac{5}{2})\,, \qquad \omega = \sqrt{\frac{C}{B}}\,,$$

and the unique allowed shape for the separation parameter Λ

$$(7)\quad \Lambda = \lambda(\lambda+3)\,.$$

The other differential equation (2*b*) is more difficult to be solved, because it is not possible to decouple the rotational degrees of freedom from the γ vibrations and we apply the following constructive method for finding its explicit solutions. Because of the known symmetry properties of the collective wave function ([1]) we can start with

$$(8)\quad \Phi^I_M(\gamma,\vartheta_i) = \sum_{K=1\ (-1)^I}^{\leq I} g_K(\gamma)\,[D^I_{M,K}(\vartheta_i) + (-1)^I D^I_{M,-K}(\vartheta_i)]\,, \qquad K \text{ even}.$$

Inserting the expression (8) in the equation (2*b*), we get a sum composed of members, where the same combinations of D functions as in (8) are multiplied by factors composed of a bilinear form in g_K functions and $\sin^{-2}[\gamma - k(2\pi/3)]$ added to a part containing first and second derivatives in γ. D functions being independent, these factors have to vanish separately and we get in this way coupled second order linear homogeneous differential equations for unknown functions $g_K(\gamma)$. As these functions have to be periodic in γ (with 2π), finite everywhere and with a definite parity, we represent them by trigonometric polynomials (in $\sin n\gamma$ for odd and $\cos n\gamma$ for even parity respectively). Expressing all coefficients in differential equations with trigonometric functions of multiples of γ and inserting, the trigonometric polynomials we arrive to systems of homogeneous linear equations for coefficients of polynomials by equating to zero the factors of every trigonometric function in the obtained relations. The form (7) for Λ is a necessary condition for obtaining non-trivial solutions and only even or odd subscript coefficients appear. By this procedure it is left open and should be decided by calculation for which Λ (*i.e.* λ) values the obtained linear homogeneous equations have non-trivial solutions. Remarks concerning λ as a « seniority » number could provide an indication ([3]).

([3]) G. Rakavy: *Nucl. Phys.*, **4**, 289 (1957); D. R. Bes: *Nucl. Phys.*, **10**, 373 (1959).

The procedure is trivial for $I=0$ and $I=3$ cases containing only one differential equation which solutions are Legendre polynomials ($\lambda=3n$) $P_n(\cos 3\gamma)$ and associated Legendre functions of the first kind ($\lambda=3n$) $\sin 3\gamma P_n^{(1)}(\cos 3\gamma)$ respectively. As an example we quote a first few solutions for $I=2$ case.

(9)

λ	$2g_0$	$\sqrt{2}g_2$
1	$a_0 \cos\gamma$	$a_0 \sin\gamma$
2	$a_2 \cos 2\gamma$	$-a_2 \sin 2\gamma$
3	no polynomial solution	
4	$a_2(\cos 2\gamma + 3\cos 4\gamma)$	$a_2(-\sin 2\gamma + 3\sin 4\gamma)$
5	$a_1(\cos\gamma + 3\cos 5\gamma)$	$a_1(\sin\gamma - 3\sin 5\gamma)$
6	no polynomial solution .	

Calculations have been made for $I=4$ and $I=5$ cases too.

Naturally, the systems of linear homogeneous equations become more and more complicated with increasing number of unknown g functions and λ values. The only remaining constant in g functions is determined from the requirement of normalization of the total wave function and the known orthonormalization of the D functions.

For a slightly generalized Hamiltonian [4]

$$H = -\frac{\hbar^2}{2B_\beta}\left(\frac{1}{\beta^4}\frac{\partial}{\partial\beta}\beta^4\frac{\partial}{\partial\beta}\right) - \frac{\hbar^2}{2B_\gamma}\left(\frac{1}{\sin 3\gamma}\frac{\partial}{\partial\gamma}\sin 3\gamma\frac{\partial}{\partial\gamma} - \frac{Q_3^2}{4\sin^2\gamma}\right) + \frac{Q_1^2}{2J_1} + \frac{Q_2^2}{2J_2} + V(\beta,\gamma)\,, \tag{10}$$

with the restriction to small γ values range the approximate separation of the rotational and γ and β vibrational degrees of freedom is possible for separable potential energy and we get Schrödinger equation separated in three differential equations corresponding to ϑ_i, β and γ variables. The leading terms in potential energy expansion for small $\beta-\beta_0$ and $\gamma-\gamma_0$ values range being quadratic, the corresponding differential equations can be solved for equilibrium values β_0, γ_0 (equal or different from zero) by transforming them into the special confluent hypergeometric differential equation (3), *i.e.* in the same manner as the $f(\beta)$ wave function (4) has been determined.

Detailed results and explicit calculations will be contained in a separate paper to be published soon.

* * *

The author wishes to express his appreciation for the arrangements which made possible his stay at Centre d'Etudes Nucléaires de Saclay and is very much indebted to Prof. J. THIRION for hospitality in the Section des Réactions Nucléaires à Moyenne Energie. A grant from the Institute « Rudjer Bošković », Zagreb is gratefully acknowledged.

---

(4) B. L. BIRBRAIR, L. K. PEKER and L. A. SLIV: *Žu. Éksp. Teor. Fiz.*, **36**, 803 (1959).

IL NUOVO CIMENTO Vol. XIV, N. 5 1° Dicembre 1959

Analyticity, Unitarity and Resonances.

B. Bosco

Istituto di Fisica dell'Università - Torino
Istituto Nazionale di Fisica Nucleare - Sezione di Torino

(ricevuto il 30 Ottobre 1959)

In a recent paper [1] R. Omnes has shown for the matrix element $M(E)$ (E being the energy of the reaction:

$$\sum_i a_i \rightleftarrows b_1 + b_2$$

the interesting property expressed by the following relation

$$(1) \quad M(E) = M^*(E^*)\, S(E) \quad \text{for } \operatorname{Im} E < 0,$$

where $S(E)$ is the scattering matrix for the b particles. Equation (1) tells us that, for $\operatorname{Im}(E) < 0$, $M(E)$ has generally the same poles as the scattering matrix $S(E)$. Since, as is well known, a resonance in the b particles scattering corresponds to a pole of the S matrix in the lower half-plane, equation (1) allows one to transfer a known and very general property of the matrix S to the matrix $M(E)$.

The proof given by Omnes of eq. (1) is based directly on the explicit solution [2] of the dispersive equation for the matrix element $M(E)$:

$$(2) \quad M(E) = f(E) + \frac{1}{\pi}\int_0^\infty \frac{M(E')h^*(E')\,\mathrm{d}E'}{E' - E - i\varepsilon},$$

where $f(E)$ is a function of E depending on the particular reaction (that in Omnes paper is supposed analytic) and $h(E) = e^{i\delta}\sin\delta$, δ being the phase shift for the b particles scattering.

In the present note we wish to show that equation (1) can be derived under the following general assumptions:

a) analyticity of matrix element $M(E)$ for $\operatorname{Im}(E) \geqslant 0$ (in a region about which we shall discuss later);

b) unitarity of the S matrix.

Indeed let us analyse what conclusions we can draw about $M(E)$ from *a*) and *b*).

Let us begin from *b*).

Fubini, Nambu and Wataghin [3]

---

(1) R. Omnes: preprint.

(2) R. Omnes: *Nuovo Cimento*, **8**, 316 (1958).

(3) S. Fubini, Y. Nambu and V. Wataghin: *Phys. Rev.*, **111**, 329 (1958). This theorem is a generalization of a theorem previously stated by by Aizu, Fermi and Watson on the pion-photoproduction matrix elements.

have shown under very general conditions that the unitarity of S the matrix implies for $M(E)$ the form:

$$M(E) = \varrho(E)\, e^{i\delta}\,, \tag{3}$$

where $\varrho(E)$ is a real function of E.

We now make use of a). Let us suppose $M(E)$ to be an analytic function in a region D of the upper half E plane which has a segment l of the real axis as a part of its boundary. Then by (3) we can say that

$$\mathrm{Im}\,[M(E)e^{-i\delta}] \to 0 \quad \text{when} \quad \mathrm{Im}\,E \to 0^{+},$$

Therefore we may apply the Riemann-Schwarz « principle of reflection » (4) to the function $M(E)e^{-i\delta}$ which gives at once the equation (1) for the region D' which is the reflexion in l of the region D.

Clearly the assumptions a) and b), or if one likes, the assumption a) and eq. (3) are much less restrictive than eq. (2).

In particular the very fact that, as it turns out in the proof, if eq. (1) is needed to be valid in a limited region D' one has only to prove the analyticity in the limited « reflected » region D, it seems rather remarkable and may be of practical importance.

* * *

The author is very grateful to Prof. S. FUBINI for criticism and to Dr. R. OMNES for sending to him a preprint prior to publication.

(4) E. C. TITCHMARSH: *Theory of Functions*, 2nd ed. (Oxford, 1952), p. 155.

IL NUOVO CIMENTO Vol. XIV, N. 5 1° Dicembre 1959

Experimental Evidence for the Decay Mode $\Sigma^+ \to p + \gamma$ (*).

G. Quareni and A. Quareni Vignudelli

Istituto di Fisica dell'Università - Bologna
Istituto Nazionale di Fisica Nucleare - Sezione di Bologna

G. Dascola and S. Mora

Istituto di Fisica dell'Università - Parma

(ricevuto il 7 Novembre 1959)

We found in photographic emulsion three events, which give a remarkable evidence for a new decay mode of the positive Σ-hyperon. These three events belong to a collection of ~15000 K^--captures at rest. They are very similar to each other; one of them is represented in the Fig. 1 and their common characteristics are as follows:

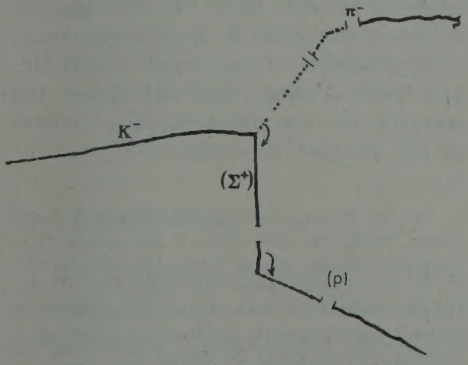

Fig. 1. – Sketch of the event no. 2.

a) the capture of a K^- at rest makes a star composed with a thin prong and a heavy prong (Σ^+);

b) the thin prong is due to a π^--meson (the particle is captured at rest);

c) the heavy particle (Σ^+) seems to arrive at the end of its range and produces only an heavy prong ~3000 μm long (p).

The data referring to the three events appear in the Table I.

The errors of the ranges include the straggling and the uncertainty of the emulsion thickness.

Each mass was measured by combining ionization, multiple scattering and range measurements. Comparisons were made with other identified particles, K^--mesons, protons, hyperons and singly charged hyperfragments, having the same dip angle.

The last few microns of the (Σ^+) tracks were considered in order to define the (Σ^+)(p) angles.

The observed experimental picture is exactly the one that is to be expected if the decay mode $\Sigma^+ \to p + \gamma$ exists. The kinetic energies of the particles (p), as deduced from their ranges assuming them to be protons, are very near the expected value of the kinetic energy of the proton,

(*) Presentato a Pavia.

TABLE I.

no.	T_{π^-} (MeV)	π^--capture	(Σ^+)		T_{Σ^+} (MeV)	(p)		T_p (MeV)	$(\Sigma^+)(p)$ angle see Fig. 1	$\pi^-(\Sigma^+)$ angle see Fig. 1
			Range (μm)	Mass (MeV/c^2)		Range (μm)	Mass (MeV/c^2)			
1	38.8	1 prong	540	1215^{+830}_{-400}	11.0	3130 ± 180	960 ± 310	26.9 ± 0.9	42°	208°
2	51.4	0 prong Auger el.	4200	1150 ± 200	35.4	3000 ± 60	1060 ± 225	26.3 ± 0.3	103°	131°
3	40.0	2 prongs	700	1200^{+920}_{-440}	13.0	3150 ± 200	785^{+460}_{-240}	27.1 ± 1.0	154°	99°

which would be emitted in the photon decay ($T = 26.5$ MeV), the differences being compatible with the experimental errors. The mass measurements restrict the possibilities to identify the particles (Σ^+) and (p) among the different elementary barions; mesons and nuclei are probably to be excluded.

Besides the type of the observed stars is very simple and it justifies our confidence that the heavy prong is a positive hyperon, since such stars are to be reasonably attributed to the elementary process $K^- + p \to \Sigma^+ + \pi^-$.

Assuming the three events to be photon decays and taking into account the number of the Σ^+, we have so far recognized in the same emulsion, it results that the branching ratio $p + \gamma / p + \pi^0$ is of the order of 1%.

We are now trying to detect the γ-rays associated with the decays; the search is still in progress also in order to give a better estimate of the branching ratio.

However other possible interpretations have been considered such as, for istance, an one prong Σ^- capture instead of the Σ^+ decay, or the decay in fligh $\Sigma^+ \to p + \pi^0$, even if the measured angles $(\Sigma^+)(p)$ in the event 1 and 2 are not compatible with kinematics. Actually it is possible to fit together the experimental figure with a chain of well known fenomena, but they should take place under such circumstancies that their occurence is to be considered very improbable.

On the other hand the proposed new decay mode, besides making the interpretation of the experimental data very simple, satisfies with the branching ratios, which have been recently calculated under different assumptions [1].

* * *

The authors of the Bologna group wish to inform that the first partial evidence was given by the Parma group.

The authors thank Prof. MORPURGO and Prof. PUPPI, who stimulated the research for the different decay modes of the charged hyperons.

[1] M. KAWAGUCHI and N. NISHIJMA: *Progr. Theor. Phys.*, **15**, 182 (1956); C. ISO and K. KAWAGUCHI: *Progr. Theor. Phys.*, **16**, 177 (1956); R. R. BEHERENDS: *Phys. Rev.*, **111**, 1691 (1958). [In this paper (foot note 4) an event is reported, which was interpreted by M. GOLDHABER as a possible photon decay of the Σ^+].

Direttore responsabile: G. POLVANI Tipografia Compositori - Bologna

Questo Fascicolo è stato licenziato dai torchi il 21-XII-1959